RECONSTRUCTING HOLOCENE INDIAN SUMMER MONSOON VARIABILITY USING HIGH RESOLUTION SEDIMENTS FROM THE SOUTHEASTERN TIBET

Melanie Marie Perello

Submitted to the faculty of the University Graduate School
in partial fulfillment of the requirements
for the degree
Doctor of Philosophy
in the Department of Earth Sciences,
Indiana University

December 2020

Accepted by the Graduate Faculty of Indiana University, in partial fulfillment of the requirements for the degree of Doctor of Philosophy.

Doctoral Committee

_____
Broxton Bird, Ph.D., Chair

_____
Gabriel Filippelli, Ph.D.

August 27, 2019

_____
William Gilhooly, Ph.D.

_____
Lixin Wang, Ph.D.

_____
Jeffrey Wilson, Ph.D.

DEDICATION

I want to dedicate this work to my mother, Maria Louise Perello (1955-2015). My mother encouraged me to take every opportunity to explore the world and to try new things, including taking the big leap to start this doctorate. She is dearly missed, but her faith and love lives on.

ACKNOWLEDGEMENT

I first would like to acknowledge all of the support that I have received from my advisor, Dr. Broxton Bird. I am thankful for field assistance and support for this project provided by the Institute for Tibetan Plateau Research. I appreciate the opportunity to be a part of this exciting work and will remember these experiences for my entire life. It has been a tremendous privilege to visit Tibet and meet the amazing people that live and work there.

I want to thank all of my family for their tremendous support of me throughout my education. I would not be able to have completed this degree without their help, particularly Dad and his first-class pet sitting services.

I want to thank all of the faculty, staff and my fellow students in the Department of Earth Sciences, especially my committee, Cheryl Montgomery and Cathy Chouinard, for their support. Appreciation for research assistance to Dr. John Southon and the W.M Keck Carbon Cycle AMS Laboratory, Dr. Mark Abbott and his students in at the University of Pittsburgh, and Dr. Byron Steinman at the Large Lakes Observatory. I am especially grateful for Dr. Pratigya Polissar and Sam Phelps for all of their help with preparing and running our leaf-wax samples at Lamont Doherty Earth Observatory. Thank you for making me feel welcome and supporting this research.

I wish to acknowledge that funding for this project was provided by the National Science Foundation (Award #1405072).

Melanie Marie Perello

RECONSTRUCTING HOLOCENE INDIAN SUMMER MONSOON VARIABILITY USING HIGH RESOLUTION SEDIMENTS FROM THE SOUTHEASTERN TIBET

The Indian summer monsoon (ISM) is the dominant hydrometeorological phenomenon that provides the majority of precipitation to southern Asia and southeastern Tibet specifically. Reliable projections of ISM rainfall are critical for water management and hinge on our understanding of the drivers of the monsoon system and how these drivers will be impacted by climate change. Because instrumental climate records are limited in space and time, natural climate archives are required to understand how the ISM varied in the past in response to changes in climatic boundary climate conditions. Lake sediments are high-resolution natural paleoclimate archive that are widely distributed across the Tibetan Plateau, making them useful for investigating long-term precipitation trends and their response to climatic boundary conditions. To investigate changes in monsoon intensity during the Holocene, three lakes were sampled along an east-west transect in southeastern Tibet: Galang Co, Nir'Pa Co, and Cuobu. Paleoclimate records from each lake were developed using isotopic (leaf wax hydrogen isotopes; δ^2H), sedimentological, and geochemical proxies of precipitation and lake levels. Sediments were sampled at high temporal frequencies, with most proxies resolved at decadal scales, to capture multi-decadal to millennial-scale variability in monsoon intensity and local hydroclimate conditions. The ISM was strongest in the early Holocene as evidenced by leaf-wax *n*-alkane δ^2H at both Cuobu and Galang Co corresponding with Cuobu's higher lake levels and effective moisture. Monsoon intensity declined at Cuobu and Galang Co around 6 ka which corresponds to reduced riverine sediment influxes at Cuobu and deeper lake levels at Galang Co. The antiphase relationship between lake levels and monsoon intensity at Galang Co is attributed to air temperatures and effective moisture, with a warmer and drier local hydroclimate driving early Holocene low lake levels. The late Holocene ISM was more variable with wet and dry periods, as seen in the Nir'Pa Co lake level and leaf wax *n*-alkane δ^2H record. These records demonstrate coherent drivers of synoptic and local hydroclimate that account for Holocene ISM expression across the southeastern Tibetan Plateau, indicating possible drivers of future monsoon expression under climate change.

Broxton Bird, Ph.D., Chair

TABLE OF CONTENTS

LIST OF TABLES

LIST OF FIGURES

1. INTRODUCTION

The Indian summer monsoon (ISM) is one of the largest and most crucial hydrometeorological systems in the world, with over 40% of the world's population living in its domain (Gadgil et al., 2004). The ISM serves as the dominant source of growing season precipitation on the Tibetan Plateau and surrounding region (termed the Third Pole; Qui, 2008), delivering ~80% of South Asia's precipitation (Sinha et al., 2015). Major rivers with headwaters in the plateau, including the Ganges, Indus, Sutlej, and Brahmaputra, flow south through the Himalayas (Harris, 2006). The ISM is closely connected with other major climate systems including the East Asian Monsoon (EAM) and the Western Pacific Monsoon (Salinger et al., 2014). Concerns over future dependability of ISM precipitation underscores the need to understand natural variability of the monsoon and respective climatic drivers, including the increasing role of anthropogenic influences. Natural variability combined with changing global climatic conditions paints a bleak picture of a monsoon system that will be less dependable with less precipitation which is devastating in a region that struggles with food deficits and inadequate potable water availability (Bollasina et al., 2011; Niyogi et al., 2010; Sinha et al., 2015; Tiwari and Joshi, 2012; Vrese et al., 2016). Projections of future monsoon rainfall are reliant on accurate and precise modeling of the integration of natural variability and climate change, based on both paleoclimate records and modern observations. Despite the importance of the ISM and a plethora of paleoclimate records, considerable knowledge gaps remain concerning how monsoon intensity has varied both temporally and spatially, indicating a need for more studies of climate in the region.

1.1 Indian Summer Monsoon & Regional Climate

The ISM, also referred to as the South Asian or summer Asian monsoon, is the dominant precipitation source for Southeastern Asia each summer (June-September). The monsoon is driven in part by the temperature gradient between sea surface temperatures (SSTs) and land, including the large arid land mass of the Tibetan Plateau (Molnar et al., 2010). Other recognized forces behind monsoon intensity include the migration of the Intertropical Convergence Zone (ITCZ), solar insolation, and larger climate systems, such as the El Niño-Southern Oscillation (Haug et al., 2001). The

modern extent of the monsoon is centered over the Indian subcontinent but expands north through the eastern Tibetan Plateau, west towards Pakistan and the tip of the Arabian Peninsula, and east in Bangladesh and western Myanmar. Isotopic signature of the monsoon is evident over a much larger area extending to the Arabian Peninsula (Fleitmann et al., 2003), Eastern China (Dykoski et al., 2005), and the Tanggula Mountains in central Tibet, China (Tian et al., 2001).

1.1.1 Seasonal Monsoon & Intra-Annual Variability

The onset of the monsoon season is dictated by temperature gradients between the Indian Ocean and the dry, arid Tibetan Plateau along with the seasonal migration of the Intertropical Convergence Zone (ITCZ) and the orographic effects of the mountainous terrain (Chen et al., 2014; Gadgil, 2003). The maximum northern position of the ITCZ is reached during the summer months, which corresponds with the onset of the monsoon rainfalls and the respective strength of the monsoon (Fleitmann et al., 2007). The elevation of the TP plays a significant role in the intensity of the seasonal monsoons (Harris, 2006; Wu et al., 2007). A low-pressure system pulls in warm, humid air from the Indian Ocean, producing intense precipitation of the southern slopes of the Himalayas with moderate rainfall further inland (Harris, 2006). Intra-annual variability of the monsoon consists of active and break periods in rainfall that are attributed to tropical convergence zones and intra-seasonal oscillations (Goswami and Mohan, 2001). Monsoon seasons can vary year to year in intensities, rainfall amounts, and in timing of the onset and the length of the monsoon season. Failures of the monsoon, characterized by drought conditions during the monsoon season, have been attributed to reduced wind strength and cooler temperatures (Cook et al., 2010).

Multiple drivers of these inter-annual changes in monsoon intensity have been identified through modern observations and supplemented with paleoclimate records. Ocean-atmosphere conditions in the Indian Ocean and tropical Pacific Ocean are considered to be key drivers of inter-annual variability in the ISM rainfall. Previous research indicates that the ENSO moderates the ISM by reducing the length of the rainy season resulting in decreased rainfall (Cook et al., 2010; Gadgil et al., 2004; Goswami and Xavier, 2005; Thompson, 2000). El Niño events have the greatest influence on the

ISM rainfall by cooling the air over the Indian subcontinent and weakening easterly trade winds along with increasing atmospheric subsidence and convection (Kumar et al., 2006; Yeh et al., 2009) and are associated with monsoon failures and drought conditions (Cook et al., 2010; Thompson, 2000); with La Nina conditions resulting in a stronger monsoon due to stronger easterly trade winds. The EQUINOO (Equatorial Indian Ocean Oscillation) when overlapping with ENSO conditions can also affect monsoon rainfall with positive (negative) phases being associated with stronger (weaker) monsoons (Surendran et al., 2015). Both the Indian Ocean Dipole (IOD) and the Pacific Ocean Dipole (POD) have a positive correlation with ISM rainfall, although research on how these climate forcings influence the monsoon on longer time-scales is still ongoing (Ashok et al., 2001).

The ITCZ, where winds and precipitation converge in a latitudinal zone, is another crucial driver of the summer monsoon (Fleitmann et al., 2007). The summer position of the ITCZ drives how far inland precipitation falls, with a more northerly trajectory linked to higher rainfall amounts. The winter position of the ITCZ, which reaches its southern-most position in January, drives a winter monsoon system. The winter monsoon has an inverse relationship with the summer monsoon, with heavier snowfalls in Eurasia correlating with decreased summer monsoon rainfall (Blanford, 1884; Walker, 1910), but analyses suggest that this relationship is most apparent in extreme anomalies rather than an annual trend (Bamzai and Shukla, 1999).

1.1.2 Historical Monsoon Variability

Decadal monsoon variability is affected by the same drivers of inter-annual variability: Indian and Pacific Ocean and atmosphere conditions. Modern records have shown a strengthening of the relationship between monsoon rainfall and the Indian Ocean post-1976 AD due to warming SSTs (Clark et al., 2000). The short instrumental record, however, prevents much analysis on longer time scales. As such there is a substantial need for understanding how the monsoon has varied on longer time scales using paleoclimate records. These paleoclimate records have identified long-term and abrupt changes to the monsoon in connection with the ITCZ, solar insolation, and ENSO

conditions (Bird et al., 2010; Cook et al., 2010; Dykoski et al., 2005; Fleitmann et al., 2007).

The short instrumental (1930s to present) and historical records in the ISM region necessitate the need for developing paleoclimate records from natural archives, such as lake sediments, to interpret long-term changes. Centennial and decadal-resolved records are particularly sparse in the ISM region (Bird et al., 2017; Bird et al., 2014), which limits the understanding of monsoon variability on shorter-time scales. Existing studies of the ISM have demonstrated long-term millennial changes in the ISM since the early Holocene where the monsoon was strongest, before transitioning to a weaker monsoon in the Middle Holocene (5-3 ka) that persists today (Chen et al., 2014; Djamali et al., 2010; Seki et al., 2009). However, the timing of the weakening of the monsoon is not consistent between records, which suggests that the timing of changes in ISM rainfall may be spatially-dependent. Higher-resolution records have demonstrated that even within periods described by long-term records as either strong or weak monsoons, there can be significant variability on shorter-time scales (Bird et al., 2014). Consideration of the ISM response to climate events is important as there has not been agreement between global responses to the MCA and LIA and the responses seen in the ISM region which may be critical in understanding how climate forcings differ in this region (Bird et al., 2017; Mann et al., 2009; Sinha et al., 2015).

Large-scale interpretations of regional climate are made possible with comparisons of paleoclimate records from a variety of deposits and environments using proxies or indicators of natural climate conditions. Paleoclimatology relies on proxies, or indicators, of past climate conditions that are preserved in natural archives including marine and freshwater sediments, ice caps, tree rings, and speleothems. Lakes are a critical, sensitive terrestrial archive for both within lake processes (*i.e.* water quality, lake level) and watershed environmental conditions (*i.e.* climate, land use). Lakes are well distributed across biomes and elevations and most have high sedimentation rates, making them sensitive to climate conditions on shorter-time scales and at higher spatial frequencies than most natural archives. Lake-specific sedimentation rates can provide information on varying time-scales, from seasonal to decadal. Sediments record information about conditions within the lake and the surrounding watershed with typical

proxies including geochemistry and isotopes, sedimentology, and biological fossils. The diverse proxies found in lake sediments can be used to interpret local, regional, and global climate-processes. Dating of these sediments makes it possible to interpret temporal changes in climate and compare records from other lakes and archives (Bird et al., 2017; Bird et al., 2014). In most lakes, sediments are continuously deposited, with rare hiatuses associated with extreme dry conditions (Fleitmann et al., 2003), and well preserved making them a useful archives of regional climate and watershed specific responses. In the Tibetan Plateau, lakes are a valuable archive for paleoclimate due to the high density of lakes in the region while other archives, such as tree rings, are less prevalent in the region.

Precipitation is not as well constrained as temperature in paleoclimate records, because it is less spatially homogenous than temperature, with precipitation levels varying significantly with location. Indicators of precipitation and other measures of the hydrological cycle, such as evaporation, are recorded in lake sediments through multiple proxies, including isotopes, biological indicators, and directly through physical evidence of changing lake levels. This project utilizes both ^{18}O and ^{2}H isotopes, with a focus on ^{2}H extracted from leaf-wax *n*-alkanes, to interpret hydrologic changes including precipitation and evaporation during the summer monsoon. The correlation between $\delta^{2}H$ and $\delta^{18}O$ reflects global and local meteorological water lines (GMWL and LMWL; Craig, 1961). Deuterium excess ($d = \delta^{2}H - 8 \times \delta^{18}O$) is a measure of the deviation between the expected linear relationship of $\delta^{18}O$ and $\delta^{2}H$ (GMWL: $\delta^{2}H = 8.0 \times \delta^{18}O + 10\%$), which varies spatially and reflects local fractionation processes (Dansgaard, 1964). Both $\delta^{18}O$ and $\delta^{2}H$ values are impacted by temperature, elevation and amount effects, with amount effects playing the largest role in monsoon isotopic expression (Tian et al., 2003; Vuille et al. 2005).

Isotopic records combined with other sedimentological proxies are crucial for interpretations of how the ISM has varied throughout the Holocene. The ISM was strongest during the early Holocene, during a period known as the Holocene Climate Optimum (10.5-6.5 ka), but began to weaken during the middle Holocene (~5.2 ka; e.g., (Campo and Gasse, 1993; Chen et al., 2014; Djamali et al., 2010). In the paleoclimate record from Paru Co, a lake sampled in this study, maximum ISM rainfall in the study

region was between 10.1 – 5.2 ka, after which conditions became drier (Bird et al., 2014). The timing of this transition to a weaker monsoon differed between isotopic and sedimentological proxies, which suggests that monsoon isotopic signatures reflect regional synoptic conditions while the sedimentology reflects local watershed responses. The monsoon continued to weaken into the late Holocene, where two climate events occurred: the Medieval Climate Anomaly (MCA: 950-1250 AD), and the Little Ice Age (LIA: 1400-1700 AD; Mann et al., 2009). Existing records are not in agreement about how these climate events influenced monsoon precipitation. Some records found a moderate strengthening of the monsoon during the MCA, but no response to the LIA (Bird et al., 2017; Sinha et al., 2015).

1.2 Precipitation & Isotopes

Hydrogen and oxygen isotopes are useful for studying both relative volume and trajectories of precipitation across terrestrial landscapes and have been used in many studies of the Asian monsoons. Isotopic measurements of hydrogen (δ^2H) and oxygen ($\delta^{18}O$) are strongly influenced by moisture source and climate, including temperature and the amount of precipitation (Gat, 1996; Tian et al. 2018). Modern isotopic observations have found that the ISM extends across the Indian subcontinent, west to the Brahmaputra Valley, and north towards the Tanggula Mountains, where both the tropical and temperate air masses converge and the northernmost extent of the summer ITCZ lies (Tian et al., 2001). Monsoon precipitation from the Indian Ocean and Indian subcontinent reaches the Tibetan Plateau in two primary directions: from the Bay of Bengal through the Brahmaputra Valley and across the subcontinent towards the Himalayan slopes, providing a significant orographic effect on northern India. Summer rainfall travels through the southeast corner of the plateau and is then redistributed to the north and west, reaching the central and western plateau through the Nyainqêntanglha Mountains. Mean annual precipitation in the Tibetan Plateau ranges from 172 to 650 mm with driest conditions in the western plateau and at higher altitudes (Tian et al., 2001; Tian et al., 2003).

Isotopic analyses of modern precipitation have generally found there is little variation between the global and local meteoric water lines during the monsoon,

reflecting a low evaporation signal (Breitenbach et al., 2010; Tian et al., 2001). Isotopic measurements of $\delta^{18}O$ and $\delta^{2}H$ in northeastern India near the Bay of Bengal during the monsoon range from 0.8 to -18.8 ‰ and 18.5 to -144.4 ‰, respectively (Breitenbach et al., 2010). Monsoon rainfall on the Tibetan Plateau has been found to have consistently lower $\delta^{18}O$ values between -5‰ to -20‰ (Tian et al., 2003). Winter precipitation, in contrast to summer monsoon rainfall, has been observed to be more enriched due to continental recycling and different moisture sources signal (Breitenbach et al., 2010; Tian et al., 2003). $\delta^{18}O$ and $\delta^{2}H$ values are more affected by amount effects than temperature in the monsoon region in contrast to areas on the plateau that are dominated by continental precipitation sources (Thompson, 2000; Tian et al., 2003). Modeling of different forcings, suggest that temperature, transportation, and distillation processes (*i.e.,* rainout and depletion) all affect the isotopic signature of monsoon rainfall (Vuille et al., 2005).

New techniques have allowed for the measurement of hydrogen isotopes incorporated into organic biological compounds, such as lipids produced by terrestrial and aquatic vegetation, producing new isotopic proxies (Aichner et al., 2010; Eglington and Eglington, 2008; Polissar and D'Andrea, 2013; Sachse et al., 2012). These new proxies allow for isotopic measurements of precipitation in lake systems that do not have carbonate sediments which was not possible previously. With the southeastern Tibetan Plateau dominated by non-carbonate lakes, this project is utilizing terrestrial and aquatic leaf-wax *n*-alkanes to measure hydrogen isotopic variability in the ISM region. These results will be verified with carbonate $\delta^{18}O$ measurements where carbonate sediments are available. Both terrestrial and aquatic plants incorporate hydrogen atoms from their respective water sources and use them in the synthesis of lipids and other biological compounds. Studies have found that these organic biological compounds, including *n*-alkanes, alkanoic acids, and fatty acids, provide an indirect measurement of the isotopic composition of precipitation at the time of synthesis (Aichner et al., 2010; Feakins et al., 2016; Hou, 2008; Nichols, 2010).

Interpretations of these isotopic measurements should consider the influences of regional climate, local hydrology (*i.e.,* evaporation and condensation), and plant physiology (*i.e.,* photosynthetic pathways and water uptake) on isotopic fractionation

(Hou, 2008). Plant physiology significantly affects δ^2H_{wax} values and is reflective of the δ^2H of xylem water in plants, which is directly sourced from soil water (Feakins et al., 2016). δ^2H_{wax} has been demonstrated to follow the same spatial trends as δ^2H of precipitation and lake water, but is highly fractionated from those isotopic values (Hou, 2008). Site specific characteristics also influence δ^2H_{wax} including a negative correlation with elevation and continentally (Feakins et al., 2016). Consideration of both regional and site-specific influences on precipitation isotopes is necessary to make interpretations of how monsoon and other precipitation systems vary spatially and temporally.

Both $\delta^{18}O$ and δ^2H values have been shown to decrease through the monsoon season which has been interpreted more as either a reflection of the source waters (Breitenbach et al., 2010) or an amount effect (Clark and Fritz, 1997; Datta et al., 1991; Kurita et al., 2009; Tian et al., 2003; Vuille et al., 2005; Zhang et al., 2006). The surface waters of the Bay of Bengal, the water source for summer rainfall, undergoes significant isotopic variation throughout the monsoon season due to large fluxes of river runoff (Breitenbach et al., 2010). The amount effect has been observed through an inverse relationship between annual precipitation accumulation and $\delta^{18}O$ values in both precipitation studies and ice core records (Thompson, 2000; Tian et al., 2003). Studies have found that the extent of the isotopic signatures of the monsoon has varied throughout the Holocene, reaching as far as the Near East (Djamali et al., 2010), the Arabian Peninsula (Fleitmann et al., 2003; Fleitmann et al., 2007) and caves in southern China (Dykoski et al., 2005; Maher, 2008). However, more records are needed to understand how isotopic measurements vary across different time scales (Thompson, 2000; Tian et al., 2003; Yao et al., 2000), as some paleoclimate records show that isotopic trends have varied significantly through the Holocene (Fleitmann et al., 2003; Zhang et al., 2008).

1.3 Modern Monsoon & Climate Change

Modern weather monitoring in the Tibetan Plateau (TP) began around the 1930s and, currently, there are 97 monitoring stations above 2,000 m and an additional 100 at lower altitudes (Liu et al., 2000). Analysis of modern temperature records have shown that most of the plateau has experienced significant warming since the 1950s, with the

eastern plateau warming slower than other regions (Gou et al., 2007; Liu et al., 2000; You et al., 2008). Calculated evapotranspiration (ET) in the region has decreased in all seasons between the 1960s and 2000 (Shenbin et al., 2006). During that same period (1961-2000), precipitation for the region increased, particularly for the eastern Tibet, but declined in western Tibet (Xu et al., 2008). The growing season has increased throughout the region with an associated decline in the number of days with frost or ice (You et al., 2008). Temperature reconstructions from ice cores and glaciers have also shown a recent warming trend (Thompson et al., 1989; Thompson et al., 1993; Yao et al., 1995). Warming conditions in the TP have been linked with human-induced changing climate (Anmin et al., 2006).

Recent warming on the plateau exceeds the average for the Northern Hemisphere, indicating that this region is particularly vulnerable to changing climate (Liu et al., 1998; Liu et al., 2000). Since the region contains abundant glaciers and permafrost, it is commonly referred to as *The Third Pole Environment* (Qui, 2008). Yet with warming temperatures, the Tibetan Plateau is already experiencing changing conditions, including glacial retreat, melting permafrost, and an altered hydrological cycle (Yang et al., 2011; Yao et al., 2007). Glacial retreat is widespread through the plateau (Tang et al., 1998; Yao et al., 2012) and is a significant concern as a water storage loss. Glacial retreat has been increasing since the 1960s when measurements first began and is connected to a roughly 5% increase in river discharge (Yao et al., 2007). In addition to glaciers, Tibet also has areas of discontinuous and sporadic permafrost. Permafrost melting has increased in relation to warmer soil temperatures connected to an overall warming region (Cheng and Wu, 2007). Soil temperatures are increasing at a faster rate than air temperatures, making the whole region more susceptible to changing climate (Zhao et al., 2004). Climate change has been recognized to have a greater impact at higher altitudes with alpine regions exhibiting greater sensitivity (Yao et al., 2000).

Reviews of meteorological observations of the monsoon system has shown that the monsoon has underwent significant changes throughout the 20th and early 21st centuries. Monsoon intensity has decreased since the mid-20th century although the total precipitation has increased slightly (Bollasina et al., 2011). Simultaneous with decreasing monsoon intensity, the monsoon season has also been shortening, with the monsoon onset

occurring later (Mondal et al., 2014). A hypothesis for weakening monsoon intensity is that increasing volumes of aerosols in the region are impacting monsoon intensity (Bollasina et al., 2011; Sinha et al., 2015). The anthropogenic aerosols in the region, referred to as Asian Dust, are linked to the burning of wood and fossil fuels due to intensive industrialization and population growth. Another consideration is the increased importance of sea surface temperatures (SSTs) in the Indian and Pacific Oceans, which corresponds to warmer SSTs post-1976 AD (Clark et al., 2000).

The future of the ISM is of great scientific interest and is particularly important in the context of the human communities in the region. The Tibetan Plateau has been inhabited for the past 15,000-20,000 years (Barton, 2016), with most communities dependent on subsistence agriculture and nomadic shepherding. Subsistence and nomadic agriculture are highly dependent on monsoon rainfall and its effects on the short growing season in the plateau, which will be substantially affected by monsoon variability. Models of future impacts of changing climate predict reduced rainfall, delayed onset and higher frequency of dry periods within the monsoon season (Ashfaq et al., 2009). Higher Indian Ocean temperatures are expected to produce more extreme storm events and unpredictability in the monsoon precipitation (Kumar et al., 2006). The future monsoon is also expected to be strongly impacted by anthropogenic processes, including agricultural intensification and aerosol emissions (Bollasina et al., 2011; Niyogi et al., 2010; Sinha et al., 2015; Vrese et al., 2016). With over 40% of the world's population reliant on this rainfall, the social and economic ramifications of dry periods are potentially devastating (Gadgil et al., 2004).

1.4 Geological Setting

The Tibetan Plateau (77°E to 105°E and 25°N to 40°N) encompasses the Tibetan Autonomous Region and the southern edge of Qinghai province in southwest China along with areas within Nepal and northern India. The plateau itself has a mean elevation greater than 5,000 m (ASL) and includes an area of approximately 2,500,000 km^2 (Harris, 2006; Liu et al., 2000). Commonly called the *Roof of the World,* the plateau is highly mountainous and has steep surficial relief. The plateau is bordered by the Inner Himalayan Range to the south, the Kunlun Range to the north, and Qilian Range to the

northeast. This region was formed through orogenic processes resulting from a continental collision (convergent boundary) between the Indo-Australian and Eurasian plates that began approximately 50 Mya (Yin and Harrison, 2000; Zhiseheng et al., 2001). Terrestrial and marine sediment analyses have shown that the Asian monsoons developed in phase with uplift of the plateau (Zhiseheng et al., 2001).

Modern dominant geomorphic processes revolve around glaciers, fluvial systems, and mass movements. The Tibetan Plateau is often referred to as the Third Pole Environment due to its high concentration of glaciers and ice caps (Xu et al., 2008). Glacial melt and snowmelt in the spring and early summer are a critical part of the region's hydroclimate by providing base flow to rivers (Yao et al., 2007). Fluvial systems in the region move a massive volume of sediment and dissolved materials with rivers from this region are responsible for over a quarter of all dissolved matter deposited to the oceans (Palmer and Edmond, 1992). These morphological processes may be impacted by future climate conditions, with reduced glaciation and more intense rainfall which will affect fluvial systems and mass movements.

1.5 Records of Holocene ISM Intensity

Existing Holocene climate records for the summer monsoon have been developed from ice cores, speleothems, and lake and bog sediments (Dykoski et al., 2005; Herzschuh et al., 2009; Liu et al., 1998; Mügler et al., 2008; Shao et al., 2010; Shi et al., 2001; Yanhong et al., 2006). Predicting how continued greenhouse gas emission induced warming will impact rainfall from the ISM requires high frequency resolved climate records. However, the majority of these proxies are at a low-resolution, often on centennial or millennial timescales, which can overlook climate variability on shorter time scales that are more relevant to human communities. Only three long-term records from the region were resolved at a decadal level: Mawmluh Cave (Berkelhammer et al., 2012), Tianmen Cave (Cai et al., 2012), and Nam Co (Zhu et al., 2008). An important consideration in the study of the ISM throughout the Holocene is how the monsoon rainfall and lake level has varied spatially. There is not a cohesive understanding of whether or not the monsoon extent has varied extensively during the Holocene and, if so,

what drives the spatial extent. That is why assessment of paleoclimate records in southeastern Tibet can provide more information on spatial trends.

Most studies of Holocene climate divide the period into the early (11 – 6.5 ka), middle (6.5 – 2.5 ka), and late (2.5 ka – present) Holocene for their interpretations, with most studies focusing on either the early or late Holocene. The early Holocene was characterized by a strong monsoon, with higher rainfall interpreted in lake, ice, and cave records (Campo and Gasse, 1993; Chen et al., 2014; Djamali et al., 2010; Seki et al., 2009). The Holocene Climate Optimum (10.5-6.5 ka) was a period marked with wet and warm conditions across South Asia, with a strong Indian summer and East Asian monsoon (Seki et al., 2009). The middle Holocene was more varied, with most studies agreeing that the monsoon started to weaken during this period (Campo and Gasse, 1993; Chen et al., 2014; Djamali et al., 2010). Many studies of forcings for the changing monsoon in the early and middle Holocene focus on changes in solar insolation and the migration of the ITCZ (Bird et al., 2014; Cai et al., 2012; Chen et al., 2014; Fleitmann et al., 2007). Decreasing levels of solar insolation over the Holocene coincides with millennial scale decreases in monsoon intensity (Bird et al., 2014; Cai et al., 2012; Fleitmann et al., 2007). One record from the Chinese Loess Plateau suggests a connection between Bond Events in the North Atlantic Oscillation (NAO) and dry conditions on the plateau (Porter and Weijian, 2006), but there is not widespread agreement on this hypothesis between records. The ITCZ is also considered to play a role in the strength of the monsoon, with studies suggesting that a northern ITCZ coincided with stronger monsoon rainfalls in the early Holocene (Chen et al., 2014; Fleitmann et al., 2007). The ITCZ migrated further south during the middle Holocene at the same time as declines in solar insolation, however it is difficult to distinguish which driver played a more significant role in the weakening of the monsoon during this time period.

Specific records vary on when the monsoon weakened during the middle Holocene with dates ranging from 5 – 3 ka (Bird et al., 2014; Cai et al., 2012; Herzschuh et al., 2006; Hong et al., 2003; Xuefeng et al., 2006; Yanhong et al., 2006; Zhu et al., 2008). There are two conflicting hypotheses about how the transition between a strong and weak monsoon occurred. The first hypothesis is that there was an abrupt decrease in monsoon rainfall that occurred sometime between 5 – 4.5 ka (Morrill et al., 2003). The

second, more prominent, hypothesis is that the monsoon weakened gradually simultaneous with decreasing solar insolation (Dykoski et al., 2005; Fleitmann et al., 2003; Gupta et al., 2003; Ivanochko et al., 2005; Wang et al., 2005). Hiatuses in some records, such as the speleothems in Mawmluh Cave around ~3.8 ka and Qunf Cave around ~2.7 ka, suggest dry conditions with insufficient moisture to continue carbonate deposition (Berkelhammer et al., 2012; Fleitmann et al., 2003). The timing of the transition to a drier climate and weaker monsoon varies between sites which may also reflect a spatial influence on the distribution of ISM moisture. One study in the near-east demonstrated that the decline of the monsoon during the middle Holocene led to major forest cover changes, which might have indicated a reduction in the influence of the monsoon on that area (Djamali et al., 2010).

The late Holocene ISM has generally been described as weak, due to lower solar insolation and a more southerly ITCZ (Chen et al., 2014). High-resolution records for the ISM during the late Holocene are less prevalent than those for the early Holocene, due to insufficient material with many hiatuses present in paleoclimate record (Berkelhammer et al., 2012; Fleitmann et al., 2003). A key driver for variability throughout the Holocene, particularly the late Holocene, is the connection between Indian-Pacific Ocean SSTs and the ENSO (El Niño Southern Oscillation) system. El Niño conditions reduce ISM strength and La Niña conditions result in stronger monsoons, relationships that have been established in other published records (Cook et al., 2010; Thompson, 2000). The Dasoupu ice core made strong correlations between drought conditions, indicated by increased dust and chloride concentrations, and El Niño events in the late Holocene (1790-1796 AD, 1876-1877 AD; Thompson, 2000). In another study, Cook et al. (2010) identified large droughts, megadroughts, from tree rings with several events correlating with El Niños (1790-1796 AD, 1876-1877 AD, 1918-1919 AD). The effects of the ENSO system are moderated by the distribution of Indian and Pacific Ocean SSTs (Cook et al., 2010). The Medieval Climate Anomaly (MCA) and the Little Ice Age (LIA) were two major climate events during the late Holocene that have been found in numerous Northern Hemisphere paleoclimate records, with the MCA being a period of anomalous warmth and increased precipitation and the LIA being a period of colder temperatures and reduced precipitation (Mann et al., 2009). Records from the ISM region have not

shown the same relationships between precipitation and the MCA and LIA as other Northern Hemisphere records, emphasizing a need to further understand how these events influenced monsoon intensity (Bird et al., 2017; Sinha et al., 2006; Sinha et al., 2015; Zhang et al., 2008). The modern late Holocene was also characterized by the industrialization-induced warming period that is exhibited in paleoclimate records including ice cores and lake sediments (Thompson, 2000; Wang et al., 2011). Some records have also shown that the 20th century warming period is also connected to a weaker monsoon, with lower lake levels and more frequent droughts (Cook et al., 2010; Wang et al., 2011).

The MCA was marked by warmer temperatures (positive temperature anomalies) with persistent La Niña conditions in the tropical Pacific (Mann et al., 2009), however some modeling has contradicted this observation (González-Rouco et al., 2011). Warming was estimated to have exceeded early-20th century warming across the Northern Hemisphere including the North Atlantic, the Eurasian Arctic, Northern Africa, and North America (Goosse et al., 2012; Mann et al., 2009). Theoretical modeling of the temperature increases in MCA have suggested an integrated forcing with weak increases in solar radiation producing altered atmospheric-ocean circulations including northern migration of the Gulf Stream and Kuroshio currents (Goosse et al., 2012; Servonnat et al., 2010). The LIA is characterized by cooling across the Northern Hemisphere, but isolated warming in some areas in North America and Eurasia (Mann et al., 2009). Theorized forcing for the LIA are reduced solar radiation and increased atmospheric volcanic aerosols (Servonnat et al., 2010; Yan et al., 2015). How the Asian monsoons responded to these events is not fully understood. Select records suggest that the MCA may have resulted in a slight increase in ISM precipitation, which may be attributed to the La Niña state in the Pacific, and a weak response to the LIA (Bird et al., 2017; Sinha et al., 2015), which may have coincided with a southern migration and contraction of the ITCZ (Yan et al., 2015).

Many paleoclimate records of the ISM emphasize millennial trends in hydroclimate, but finer resolution records have demonstrated that there are centennial and decadal-scale variabilities that are superimposed onto the long-term trends. Sedimentology at Paru Co, for example, demonstrated that during the strong monsoon in

the early Holocene, there were five distinct high and low lake stands (Bird et al., 2014). These events, described on centennial time scales, are an important indication that broader, millennial trends miss finer variability in monsoon rainfall. Other records have also demonstrated that greater rainfall variability exists through the Holocene, but is superimposed on the long-term trends (Fleitmann et al., 2007). Finer resolution records are also crucial in understanding how the hydroclimate system responds to specific events, such as the MCA and LIA (Bird et al., 2017).

1.6 Research Questions & Site Selection

In this dissertation, I address some of this uncertainty of Holocene ISM expression by providing new, high-resolution lake sediment records from the southern Tibetan Plateau (TP), where precipitation is predominately from the ISM (Tian et al., 2001). Three small lakes were sampled along an east-west transect across the southeastern to south-central TP: Galang Co, Nir'Pa Co, and Cuobu. All three lakes have relatively small watersheds that showed no evidence of recent glaciation or human-disturbance, reducing non-climatic watershed influences on the sediment records. The plant communities at each site are dependent on monsoon precipitation during their growing season, allowing for the use of leaf-wax *n*-alkane proxies for assessing hydrogen isotopes. Both Cuobu and Nir'Pa Co are high-elevation lakes that were selected for understanding higher, temporal variability in local and synoptic hydroclimate variability in the south-central and southeastern TP respectively. Galang Co is a relatively low-elevation lake in a heavily vegetated watershed, selected to determine whether ISM expression is consistent between high and low elevation sites.

Sediment cores from these three lakes are used to address the primary objectives of this project which include understanding 1) long-term ISM variability throughout the Holocene and what time-scales are appropriate for understanding hydroclimate variability, 2) timing of transitions between stronger and weaker monsoon conditions during the middle Holocene, and 3) how the ISM has responded to specific climatic events, such as the MCA and LIA. Each record consists of proxies that demonstrate changes in precipitation, lake levels, and watershed conditions throughout the Holocene (11.7 ka – present). These proxies were selected to address the primary objectives of this

project, as described earlier, and to test my hypotheses. With current climate models predicting an increase in droughts and delayed onset of the monsoon season, the reliability of the ISM for water during the growing season in this region is under threat. This project improves future climate modeling of the region by providing multiple decadally-resolved records of lake levels and precipitation across the eastern plateau during the past 10,000 years. Expanding the knowledge of the ISM region's climate history is crucial for understanding how the monsoon may vary in the future and how those variabilities might impact the human communities dependent on that system.

1.7 References

Aichner, B., Herzchuh, U., Wilkes, H., Vieth, A. and Böhner, J. 2010. δD values of n-alkanes in Tibetan lake sediments and aquatic macrophytes – A surface sediment study and application to a 16-ka record from Lake Koucha. Organic Geochemistry 41, 779-790.

Anmin, D., Guoxiong, W., Qiong, Z. and Yimin, L. 2006. New proofs of the recent climate warming over the Tibetan Plateau as a result of the increasing greenhouse gases emissions. Chinese Science Bulletin 51(11), 1396-1400.

Ashfaq, M., Shi, Y., Tung, W., Trapp, R., Gao, X., Pal, J. and Diffenbaugh, N. 2009. Suppression of south Asian summer monsoon precipitation in the 21st century. Geophysical Research Letters 36, L01704.

Ashok, K., Guan, Z. and Yamagata, T. 2001. Impact of the Indian Ocean Dipole on the Relationship between the Indian Summer Monsoon Rainfall and ENSO. Geophysical Research Letters 28(23), 4499-4502.

Bamzai, A. and Shukla, J. 1999. Relation between Eurasian snow cover, snow depth, and the Indian summer monsoon: An observational study. Journal of Climate 12, 3117-3132.

Barton, L. 2016. The cultural context of biological adaptation to high elevation Tibet. Archaelogical Research in Asia 5, 4-11.

Berkelhammer, M., Sinha, A., Stott, L., Cheng, H., Pausata, F. and Yoshimura, K. (2012) Climates, Landscapes, and Civilizations, pp. 75-87, Geophysical Monograms AGU, Washington D.C.

Bird, B., Kirby, M., Howat, I. and Tulaczyk, S. 2010. Geophysical evidence for Holocene lake-level change in southern California (Dry Lake). Boreas 39, 131-144.

Bird, B., Lei, Y., Perello, M., Polissar, P., Yao, T., Finney, B., Bain, D., Pompeani, D. and Thompson, L. 2017. Late Holocene Indian summer monsoon variability revealed from a 3,300-year-long lake sediment record from Nir'pa Co, southeastern Tibet. The Holocene 27(4), 541-552.

Bird, B., Polissar, P., Lei, Y., Thompson, L., Yao, T., Finney, B., Bain, D., Pompeani, D. and Steinman, B. 2014. A Tibetan lake sediment record of Holocene Indian summer monsoon variability. Earth and Planetary Science Letters 399, 92-102.

Blanford, H. 1884. On the connexion of the Himalayan snowfall with dry winds and seasons of droughts in India. Proceedings of the Royal Society of London 37, 3-22.

Bollasina, M.A., Ming, Y. and Ramaswamy, V. 2011. Anthropogenic Aerosols and the Weakening of the South Asian Summer Monsoon. Science 334, 502-505.

Breitenbach, S., Adkins, J., Meyer, H., Marwan, N., KK Kumar and Haug, G. 2010. Strong influence of water vapor source dynamics on stable isotopes in precipitation observed in Southern Meghalaya, NE India. Earth and Planetary Science Letters 292, 212-220.

Cai, Y., Zhang, H., Cheng, H., An, Z., Edwards, R., Wang, X., Tan, L., Liang, F., Wang, J. and Kelly, M. 2012. The Holocene Indian monsoon variability over the southern Tibetan Plateau and its teleconnections. Earth Planetary Science Letters 335-336, 135-144.

Campo, E.V. and Gasse, F. 1993. Pollen- and diatom-inferred climatic and hydrological changes in Sumxi Co Basin (Western Tibet) since 13,000 yr B.P. Quaternary Research 39, 300-313.

Chen, F., Chen, X., Chen, J., Zhou, A., Wu, D., Tang, L., Zhang, X., Huang, X. and Yu, J. 2014. Holocene vegetation history, precipitation changes and Indian Summer Monsoon evolution documented from sediments of Xingyun Lake, south-west China. Journal of Quaternary Science 29(7), 661-674.

Cheng, G. and Wu, T. 2007. Responses of permafrost to climate change and their environmental significance, Qinghai-Tibetan Plateau. Journal of Geophysical Research 112, F02S03.

Clark, C., Cole, J. and Webster, P. 2000. Indian Ocean SST and Indian summer rainfall: Predictive relationships and their decadal variability. Journal of Climate 13, 2503-2519.

Clark, I. and Fritz, P. (1997) Environmental isotopes of hydrogeology, Lewis Publishers.

Cook, E., Anchukaitis, K., Buckley, B., D'Arrigo, R., Jacoby, G. and Wright, W. 2010. Asian monsoon failure and megadrought during the last millennium. Science 328, 486-489.

Dansgaard, W. 1964. Stable isotopes in precipitation. Tellus 14, 436-468.

Datta, P., Tyagi, S. and Chandrasekharan, H. 1991. Factors controlling stable isotope composition of rainfall of New Delhi, India. Journal of Hydrology 128, 223-236.

Djamali, M., Akhani, H., Andrieu-Ponel, V., Braconnot, P., Brewer, S., Beaulieu, J.d., Fleitmann, D., Fluery, J., Gasse, F., Guibal, F., Jackson, S., Lézine, A., Médail, F., Ponel, P., Roberts, N. and Stevens, L. 2010. Indian summer monsoon variations could have affected the early-Holocene woodland expansion in the Near East. The Holocene 20, 813-820.

Dykoski, C., Edwards, R., Cheng, H., Yaun, D., Cai, Y., Zhang, M., Lin, Y., Qing, J., An, Z. and Revenaugh, J. 2005. A high-resolution, absolute-dated Holocene and deglacial Asian monsoon record from Dongge Cave, China. Earth and Planetary Science Letters 233, 71-86.

Eglington, T. and Eglington, G. 2008. Molecular proxies for paleoclimatology. Earth and Planetary Science Letters 275, 1-16.

Feakins, S., Bentley, L., Salinas, N., Shenkin, A., Blonder, B., Goldsmith, G., Ponton, C., Arvin, L., Wu, M., Peters, T., West, A., Martin, R., Enquist, B., Asner, J. and Malhi, Y. 2016. Plant leaf wax biomarkers capture gradients in hydrogen isotopes of precipitation from the Andes and Amazon. Geochimica et Cosmochimica Acta 182, 155-172.

Fleitmann, D., Burns, S., Mudelsee, M., Neff, U., Kramers, J., Mangini, A. and Matter, A. 2003. Holocene forcing of the Indian Monsoon recorded from a stalagmite from Southern Oman. Science 300, 1737-1739.

Fleitmann, D., Burns, S.J., Mangini, A., Mudelsee, M., Kramers, J., Villa, I., Neff, U., Al-Subbary, A.A., Buettner, A., Hippler, D. and Matter, A. 2007. Holocene ITCZ and Indian monsoon dynamics recorded in stalagmites from Oman and Yemen (Socotra). Quaternary Science Reviews 26, 170-188.

Gadgil, S. 2003. The Indian monsoon and its variability. Annual Review of Earth and Planetary Sciences 31, 429-467.

Gadgil, S., Vinayachandran, P., Francis, P. and Gadgil, S. 2004. Extremes of the Indian summer monsoon rainfall, ENSO, and equatorial Indian Ocean oscillation. Geophysical Research Letters 31, L12213.

Gat, J. 1996. Oxygen and hydrogen isotopes in the hydrologic cycle. Annual Review of Earth and Planetary Sciences 24, 225–262.

González-Rouco, F.J., Fernández-Donado, L., Raible, C.C., Barriopedro, D., Luterbacher, J., Jungclaus, J.H., Swingedouw, D., Servonnat, J., Zorita, E., Wagner, S. and Ammann, C.M. 2011. Medieval Climate Anomaly to Little Ice Age transition as simulated by current climate models. PAGES news 19(1), 7-8.

Goosse, H., Crespin, E., Dubinka, S., Loutre, M., Mann, M., Renssen, H., Sallaz-Damaz, Y. and Shindell, D. 2012. The role of forcing and internal dynamics in explaining the “Medieval Climate Anomaly”. Climate Dynamics 39, 2847-2866.

Goswami, B. and Mohan, R.A. 2001. Intraseasonal oscillations and Interannual variability of the Indian summer monsoon. Journal of Climate 14, 1180-1198.

Goswami, B. and Xavier, P. 2005. ENSO control on the south Asian monsoon through the length of the rainy season. Geophysical Research Letters 32, L18717.

Gou, X., Chen, F., Jacoby, G., Cook, E., Yang, M., Peng, J. and Zhang, Y. 2007. Rapid tree growth with respect to the last 400 years in response to climate warming, northeastern Tibetan Plateau. International Journal of Climatology 27(11), 1497-1503.

Gupta, A., Anderson, D. and Overpeck, J. 2003. Abrupt changes in the Asian southwest monsoon during the Holocene and their links to the North Atlantic Ocean. Nature 421, 354-357.

Harris, N. 2006. The elevation history of the Tibetan Plateau and its implications for the Asian monsoon. Palaeogeography, Palaeoclimatology, Palaeoecology 241, 4-15.

Haug, G.H., Hughen, K.A., Sigman, D.M., Peterson, L.C. and Ro, U. 2001. Southward Migration of the Intertropical Convergence Zone Through the Holocene. Science 293, 1304-1308.

Herzschuh, U., Kramer, A., Mischke, S. and Zhang, C. 2009. Quantitative climate and vegetation trends since the late glacial on the northeastern Tibetan Plateau deduced from Koucha Lake pollen spectra. Quaternary Research 71, 162-171.

Herzschuh, U., Winter, K., Wunnemann, B. and Li, S. 2006. A general cooling trend on the central Tibetan Plateau throughout the Holocene recorded by the Lake Zigetang pollen spectra. Quaternary International 154-155, 113-121.

Hong, Y., Hong, B., Lin, Q., Zhu, Y., Shibata, Y., Hirota, M., Uchida, M., Leng, X., Jiang, H., Xua, H., Wang, H. and Yi, L. 2003. Correlation between Indian Ocean summer monsoon and North Atlantic climate during the Holocene. Earth and Planetary Science Letters 211, 371-380.

Hou, J., D'Andrea, W.J., and Huang, Y. 2008. Can sedimentary leaf waxes record D/H ratios of continental precipitation? Field, model, and experimental assessments. Geochimica et Cosmochimica Acta 72, 3503-3517.

Ivanochko, T., Ganeshram, R., Brummer, G., Brummer, A., Ganssen, G., Jung, S., Moreton, S. and Kroon, D. 2005. Variations in tropical convection as an amplifier of global climate change at the millennial scale. Earth and Planetary Science Letters 235, 302-314.

Kumar, K., Sahai, A., Kumar, K., Patwardhan, S., Mishra, P., Revadekar, J., Kamala, K. and Pant, G. 2006. High-resolution climate change scenarios for India for the 21st century. Current Science 90(3), 334-345.

Kurita, N., Ichiyanagi, K., Matsumoto, J., Yamanaka, M. and Ohata, T. 2009. The relationship between the isotopic composition of precipitation and the

precipitation amount in the tropical regions. Journal of Geophysical Exploration 102, 113-122.

Liu, K., Yao, T. and Thompson, L. 1998. A pollen record of Holocene climatic changes from the Dunde ice cap, Qinghai-Tibetan Plateau. Geology 26(2), 135-138.

Liu, Z., Kutzbach, J. and Wu, L. 2000. Modeling Climate Shift of El Nino Variability in the Holocen. Geophysical Research Letters 27(15), 2265-2268.

Maher, B. 2008. Holocene variability of the East Asian summer monsoon from Chinese cave records: a re-assessment. The Holocene 18(6), 861–866.

Mann, M., Zhang, Z., Rutherford, S., Bradley, R., Hughes, M., Shindell, D., Ammann, C., Faluvegi, G. and Ni, F. 2009. Global signatures and dynamical origins of the Little Ice Age and Medieval Climate Anomaly. Science 326, 1256-1260.

Molnar, P., Boos, W.R. and Battisti, D.S. 2010. Orographic Controls on Climate and Paleoclimate of Asia: Thermal and Mechanical Roles for the Tibetan Plateau. Annual Review of Earth and Planetary Sciences 38, 77-102.

Mondal, P., Jain, M., Robertson, A., Galford, G., Small, C. and DeFries, R. 2014. Winter crop sensitivity to inter-annual climate variability in central India. Climate Change 126, 61-76.

Morrill, C., Overpeck, J. and Cole, J. 2003. A synthesis of abrupt changes in the Asian summer monsoon since the last deglaciation. Holocene 13, 465-476.

Mügler, I., Sasche, D., Werner, M., Xu, B., Wu, G., Yao, T. and Gleixner, G. 2008. Effect of lake evaporation on δD values of lacustrine n-alkanes: A comparison of Nam Co (Tibetan Plateau) and Holzmaar (Germany). Organic Geochemistry 39, 711-729.

Nichols, J. 2010. Procedures for extraction and purification of leaf wax biomarkers from peats. Mires and Peat 7-13, 1-7.

Niyogi, D., Kishtawal, C., Tripathi, S. and Govindaraju, R. 2010. Observational evidence that agricultural intensification and land use change may be reducing the Indian summer monsoon rainfall. Water Resources Research 46, W03533.

Palmer, M. and Edmond, J. 1992. Controls over the strontium isotope composition over river water. Geochimica et Cosmochimica Acta 56, 2099-2111.

Polissar, P. and D'Andrea, W. 2013. Uncertainty in paleohydrologic reconstructions from molecular D values. Geochimica et Cosmochimica Acta 129(146-156).

Porter, S. and Weijian, Z. 2006. Synchronism of Holocene East Asian monsoon variations and North Atlantic drift-ice tracers. Quaternary Research 65, 443-449.

Qui, J. (2008). The Third Pole. Nature 454, 393-396.

Sachse, D., Billault, I., Bowen, G., Chikaraishi, Y., Dawson, T., Feakins, S., Freeman, K., Magill, C., McInerney, F., Meer, M.v.d., Polissar, P., Robins, R., Sachs, J., Schmidt, H., Sessions, A., White, J., West, J. and Kahmen, A. 2012. Molecular paleohydrology: interpretating the hydrogen-isotopic composition of lipid markers from photosynthesizing organisms. Annual Review of the Earth and Planetary Sciences 40, 221-249.

Salinger, M., Shrestha, M., Ailikun, Wang, S., McGregor, J. and Dong, W. (2014) Security, Society and Sustainability. Manton, M. and Stevenson, L. (eds), pp. 17-57, Springer.

Seki, O., Meyers, P.A., Kawamura, K., Zheng, Y. and Zhou, W. 2009. Hydrogen isotopic ratios of plant wax n-alkanes in a peat bog deposited in northeast China during the last 16 kyr. Organic Geochemistry 40(6), 671-677.

Servonnat, J., Yiou, P., Khodri, M., Swingedouw, D. and Denvil, S. 2010. Influence of solar variability, CO2 and orbital forcing between 1000 and 1850 AD in the IPSLCM4 model. Climate of the Past 6, 445-460.

Shao, X., Xu, Y., Yin, Z., Liang, E., Zhu, H. and Wang, S. 2010. Climatic implications of a 3585-year tree-ring width chronology from the northeastern Qinghai-Tibetan Plateau. Quaternary Science Reviews 29, 2111-2122.

Shenbin, C., Yunfeng, L. and Thomas, A. 2006. Climatic change on the Tibetan Plateau: Potential evapotranspiration trends from 1961-2000. Climatic Change 76(3), 291-319.

Shi, Y., Yu, G., Liu, X., Li, B. and Yao, T. 2001. Reconstruction of the 30-40 ka BP enhanced Indian monsoon climate based on geological records from the Tibetan Plateau. Paleogeography, Paleoclimatology, and Palaeoecology 169, 69-83.

Sinha, A., Cannariato, K., Stott, L., Cheng, H., Edwards, R., Yadava, M., Ranesh, R. and Singh, I. 2006. A 900-year (600 to 1500 A.D.) record of the Indian summer

monsoon precipitation from the core of the monsoon zone of India. Geophysical Research Letters 34, L16707.

Sinha, A., Kathayat, G., Cheng, H., Breitenbach, S., Berkelhammer, M., Mudelsee, M., Biswas, J. and Edwards, R. 2015. Trends and oscillations in the Indian summer monsoon rainfall over the last two millennia. Nature Communications 6, 6309.

Surendran, S., Gadgil, S., Francis, P. and Rajeevan, M. 2015. Prediction of Indian rainfall during the summer monsoon season on the basis of links with equatorial Pacific and Indian Ocean climate indices. Environmental Research Letters 10, 094004.

Tang, M., Cheng, G. and Lin, Z. (1998) Contemporary Climatic Variations over the Qinghai-Xizang (Tibet) Plateau and Their Influences on Environments, Guangdong Science and Technology Press, Guangzhou.

Thompson, Mosley-Thompson, E., Davis, M., Bolzan, J., Dai, J., Klein, L., Yao, T., Wu, X., Xie, Z. and Gundestrip, N. 1989. Holocene-Late Pleistocene climatic ice core records from Qinghai-Tibetan Plateau. Science 246, 474-477.

Thompson, L. 2000. Ice core evidence for climate change in the tropics: Implications for our future. Quaternary Science Reviews 19, 19-35.

Thompson, L., Mosley-Thompson, E., Davis, M., Lin, N., Yao, T., Dyurgerov, M. and Dai, J. 1993.'Recent warming': ice core evidence from tropical ice cores, with emphasis on central Asia. Global Planet Change 7, 145-156.

Tian, L., Masson-Delmotte, V., Stievenard, M., Yao, T. and Jouzel, J. 2001. Tibetan Plateau summer monsoon northward extent revealed by measurements of water stable isotopes. Journal of Geophysical Research 106(22), 28081-28088.

Tian, L., Yao, T., Schuster, P., White, J., Ichiyanga, K., Pendall, E., Pu, J. and Yu, W. 2003. Oxygen-18 concentrations in recent precipitation and ice cores on the Tibetan Plateau. Journal of Geophysical Research 108(9), 4293.

Tian, C., Wang, L., Kaseke, K. F. and Bird, B. W. 2018. Stable isotope compositions (δ2H, δ18O and δ17O) of rainfall and snowfall in the central United States. Scientific Reports 8, 6712.

Tiwari, P. and Joshi, B. 2012. Natural and socio-economic factors affecting food security in the Himalayas. Food Security 4, 195-207.

Vrese, P.D., Hagemann, S. and Claussen, M. 2016. Asian irrigation, African rain: remote impacts of irrigation. Geophysical Research Letters 43, 3737-3745.

Vuille, M., Werner, M., Bradley, R. and Keimig, F. 2005. Stable isotopes in precipitation in the Asian monsoon region. Journal of Geophysical Research 110, D23108.

Walker, G. 1910. Correlations in seasonal variations in weather. Memo Indian Meteorology Department 21, 22-45.

Wang, R., Yang, X., Langdon, P. and Zhang, E. 2011. Limnological responses to warming on the Xizang Plateau, Tibet, over the past 200 years. Journal of Paleolimnology 45, 257-271.

Wang, Y., Cheng, H., Edwards, R., He, Y., Kong, X., An, Z., Wu, J., Shen, C. and Dorale, J. 2005. The Holocene Asian monsoon: links to solar change and North Atlantic climate. Science 308, 854-857.

Wu, G., Liu, Y., Zhang, Q., Duan, A., Wang, T., Wan, R., Liu, X., Li, W., Wang, Z. and Liang, X. 2007. The influence of mechanical and thermal forcing by the Tibetan Plateau on Asian climate. Journal of Hydrometeorology 8, 770-789.

Xu, Z., Gong, T. and Li, J. 2008. Decadal trend of climate in the Tibetan Plateau – regional temperature and precipitation. Hydrological Processes 22(16), 3056-3065.

Xuefeng, Y., Weijian, Z., Franzen, L., Feng, X., Peng, C. and Jull, A. 2006. High-resolution peat records for Holocene monsoon history in the eastern Tibetan Plateau. Science of China: Series D Earth Sciences 49, 615-621.

Yan, H., Wei, W., Soon, W., An, Z., Zhou, W., Liu, Z., Wang, Y. and Carter, R. 2015. Dynamics of the intertropical convergence zone over the western Pacific during the Little Ice Age. Nature Geoscience 8, 315-320.

Yang, K., Ye, B., Zhou, D., Wu, B., Foken, T., Qin, J. and Zhou, Z. 2011. Response of hydrological cycle to recent climate changes in the Tibetan Plateau. Climatic Change 109(3), 517-534.

Yanhong, W., Lücke, A., Zhangdong, J., Sumin, W., Schlesler, G., Battarbee, R. and Weilan, X. 2006. Holocene climate development on the central Tibetan Plateau:

A sedimentary record from Cuoe Lake. Paleogeography, Paleoclimatology, and Palaeoecology 234, 328-340.

Yao, T., Liu, X., Wang, N. and Shi, Y. 2000. Amplitude of climatic changes in Qinhai-Tibetan Plateau. Chinese Science Bulletin 45(13), 1236-1243.

Yao, T., Pu, J., Lu, A., Wang, Y. and Yu, W. 2007. Recent glacial retreat and its impact on the hydrological processes on the Tibetan Plateau, China, and surrounding regions. Arctic, Antarctic, and Alpine Research 39(4), 642-650.

Yao, T., Thompson, L., Mosley-Thompson, E. and Yang, Z. 1995. Recent warming as recorded in the Qinghai-Tibet cryosphere. Annals of Glaciology 21, 196-200.

Yao, T., Thompson, L., Yang, W., Yu, W., Gao, Y., Guo, X., Yang, X., Duan, K., Zhao, H., Xu, B., Pu, J., Lu, A., Xiang, Y., Kattel, D. and Joswiak, D. 2012. Different glacial status with atmospheric circulations in Tibetan Plateau and surroundings. Nature Climate Change 2, 663-667.

Yeh, S., Kug, J., Dewitte, B., Kwon, M., Kirtman, B. and Jin, F. 2009. El Niño in a changing climate. Nature 461, 511-514.

Yin, A. and Harrison, T. 2000. Geologic evolution of the Himalayan-Tibetan orogen. Annual Review of Earth and Planetary Sciences 28, 211-280.

You, Q., Kang, S., Aguilar, E. and Yan, Y. 2008. Changes in daily climate extremes in the eastern and central Tibetan Plateau during 1961-2005. Journal of Geophysical Research 113, D07101.

Zhang, P., Cheng, H., Edwards, R., Chen, F., Wang, Y., Yang, X., Liu, J., Tan, M., Wang, X., Liu, J., An, C., Dai, Z., Zhou, J., Zhang, D., Jia, J. and Johnson, K. 2008. A test of climate, sun and culture relationships from an 1810-year Chinese cave record. Science 322, 940-942.

Zhang, X., Jin, H. and Sun, W. 2006. Stable isotopic variations in precipitation in Southwest China. Advanced Atmospheric Science 23(4), 649-658.

Zhao, L., Ping, C., Yang, D., Cheng, G., Ding, Y. and Liu, S. 2004. Changes of climate and seasonally frozen ground over the past 30 years in Qinghai-Xizang (Tibetan) Plateau, China. Global and Planetary Change 43, 19-31.

Zhiseheng, A., Kutzbach, J., Prell, W. and Porter, S. 2001. Evolution of Asian monsoons and phased uplift of Himalaya-Tibetan plateau since late Miocene times. Nature 411, 62-66.

Zhu, L., Wu, Y., Wang, J., Lin, X., Ju, J., Xie, M., Li, M., Mäusbacher, R., Antje, S. and Daut, G. 2008. Environmental changes since 8.4 ka reflected in the lacustrine core sediments from Nam Co, central Tibetan Plateau. The Holocene 18, 831-839.

2. RECONSTRUCTING LATE HOLOCENE HYDROCLIMATE VARIABILITY USING SHORT AND LONG CHAIN *n*-ALKANE HYDROGEN ISOTOPES, NIR'PA CO TIBET

2.1 Introduction

The Indian summer monsoon (ISM) is the primary precipitation source for the Tibetan Plateau and the adjacent region, which is referred to as the Third Pole Environment (Qui, 2008). Paleoclimate records from this region generally agree that ISM precipitation declined throughout the Holocene after having reached a broad maximum during the early Holocene (11.7 – 7 ka; Berkelhammer et al., 2012; Bird et al., 2014). Between 7 and 5 ka, the ISM weakened, reaching a minimum during the late Holocene around 3.5 ka. The late Holocene (3.5 ka to modern) has been described as an arid period relative to the early Holocene, with reduced monsoon precipitation and hiatuses in some archives (*i.e.,* Berkelhammer et al., 2012; Fleitmann et al., 2003*)*. The Medieval Climate Anomaly (MCA: 950-1250 AD) and the Little Ice Age (LIA: 1275-1700 AD) are two events during the late Holocene that produced temperature and precipitation anomalies across the northern hemisphere with the onset of these events attributed to volcanic aerosols, sea ice temperature feedbacks, and solar radiation (González-Rouco et al., 2011; Mann et al., 2009; Miller et al., 2012; Polissar et al., 2006). As a result, the spatiotemporal expression of late Holocene climate events, including the MCA and the LIA, are not as well represented in the paleoclimate record as other early and middle Holocene events. There are questions about whether the MCA or LIA had an impact on ISM precipitation and the extent of that impact, due to limited records from this period on the Tibetan Plateau.

Previous results from Nir'Pa Co, a small alpine lake on the southeastern Tibetan Plateau, suggested that hydroclimate in this region and the ISM more broadly was driven by Pacific sea surface temperatures (SSTs), with warmer air temperatures on the Tibetan Plateau corresponding to warmer western Pacific SSTs and greater ISM intensity, with most of the late Holocene characterized by pronounced drought between 2.3 and 1.3 ka, evidenced by high sand content indicating shallow lake conditions, which is bracketed by wetter intervals (Bird et al., 2017). Higher silt and sand during the MCA and LIA

respectively both suggest that the monsoon was relatively stronger and weaker during these events, but is superimposed on a broader trend towards a stronger monsoon from 1.2 to 0.2 ka. The sedimentology record suggests that the MCA and LIA were minor hydroclimatic events compared to the drought between 2.3 and 1.3 ka (Bird et al., 2017). This period was characterized with a decrease in lithics and an increase in sand suggesting shallow lake conditions and reduce monsoon rainfall. These drought conditions corresponded with colder temperatures (Herzschuh et al., 2006) and drier conditions at other sites in the Tibetan Plateau (Gu et al., 1993) and was attributed to an El-Niño state in the Pacific.

Climate forcings that contributed to the weaker monsoon during the late Holocene has also been attributed to the southward migration of the intertropical convergence zone (ITCZ), reduced solar radiation, and a shift towards El Niño-like conditions characterized by anomalous warming in the eastern Pacific and cooling in the western Pacific (Bird et al., 2017; Fleitmann et al., 2003). The MCA and LIA events, which were driven by volcanic aerosols, sea ice temperature feedbacks, and solar radiation (González-Rouco et al., 2011; Mann et al., 2009; Miller et al., 2012; Polissar et al., 2006), produced La Niña conditions (anti-phase of the El Niño) during the MCA while El Niño conditions characterized the LIA (Mann et al., 2009). An El Niño-state in the Pacific has also been attributed to a weaker monsoon from 2.3 and 1.3 ka when drought conditions were evident at Nir'Pa Co (Bird et al., 2017). Yet questions remain about ISM fluctuations during the late Holocene and the role of larger climate drivers of monsoon expression. One point of contention is when the strong relationship between the ISM and the El Niño-Southern Oscillation (ENSO) was established, with some records suggesting that the relationship between ISM precipitation and Indo-Pacific SSTs developed around the middle of the Holocene when the ITCZ shifted southwards (Bird et al., 2017; Bird et al., 2014). Another question is how ENSO conditions were expressed during the MCA and LIA and what role this played on the strength of ISM precipitation on the Tibetan Plateau. New hydroclimate records spanning the late Holocene from the Tibetan Plateau are needed to address these questions.

To assess ISM precipitation variability during the late Holocene, this study uses a multi-proxy approach that integrates hydrogen isotopes (δ^2H) of long- and short-chain *n*-

alkanes from sedimentary aquatic and terrestrial and leaf waxes with previously published geochemical and sedimentological data from Nir'pa Co (Bird et al., 2014; Mügler et al., 2008; Polissar and D'Andrea, 2014). The short-chain *n*-alkanes were specifically used to investigate the isotopic variability of Nir'pa Co's lake water, which incorporates isotopic variability associated with ISM precipitation and the local precipitation:evaporation (P:E) balance, while long-chain n-alkane δ^2H variability was used to investigate synoptic scale ISM variability. By subtracting long- and short-chain n-alkane δ^2H values from each other, I additionally derived an independent record of local P/E variability. When integrated with the previously published geochemical and sedimentological results, these new biogeochemical data provide a more robust and comprehensive perspective of late Holocene ISM variability at local and synoptic scales and their interrelationships. The 3.4 ka record of the isotopic composition of short vs. long-chain *n*-alkanes from Nir'Pa Co is compared with paleoclimate archives from around the Third Pole Environment and the broader Pacific region. This study addresses 1) how the monsoon at Nir'Pa Co is expressed across the late Holocene with an emphasis on the response to the weak monsoon from 2.2 to 1.2 ka as well as the MCA and LIA, 2) whether the isotopic expression of the monsoon at Nir'Pa Co agrees with the sedimentology record, and 3) whether monsoon expression is driven by SSTs in the Indo-Pacific.

2.2 Study Area

Nir'pa Co is a small (0.1 km^2), high elevation (4775 m a.s.l) alpine lake in the Nyainqêntanglha Mountains on southeastern Tibet (29.734° N, 92.386° E; Fig. 2.1). The lake has an ephemeral inlet on the northwestern shore with a small outflow on the southwestern shore. The lake's bathymetry consists of a deep central basin (max. water depth = 15 m) and shallow shelves (water depth = ~1 m) on the northwestern and southeastern edges of the lake near the inlet and outlet, respectively (Fig. 2.3). With an ephemeral outlet, the lake is highly sensitive to evaporation as a closed lake system. The lake vegetation includes macrophytes, such as algae and grasses, in the shallow shelf while the deep basin is unvegetated. The surrounding watershed is sparsely vegetated

with C3 and C4 small flowering plants and mosses during the summer season, but vegetation is dormant during the cold winters.

Nir'pa Co's watershed consists of steep mountains (5120 m a.s.l.) and a narrow (1.5 km), glacially carved u-shaped valley (4815 a.s.l.) that extends for over 5 km (Fig. 2.2). The lake is positioned at the southeastern end of the valley and is dammed by a terminal moraine. The regional geomorphology is dominated by past glacial activity, but glaciers have been absent for the duration of the Holocene (Li et al., 1991). The regional climate is dominated by the ISM which accounts for 96% of total annual precipitation (total annual precipitation: 514 mm; May-September precipitation: 495 mm) with moderate summers and cold winters (mean annual temperature: 9.6°C; monthly average temperature range: 0.6-17.3°C; Fig. 2.4). Ice cover is present during the winter months (December-February), preventing evaporation during this time. Precipitation and temperature data were collected from the Lhasa station (Lhasa: 3650 m a.s.l.; 120 km from Nir'Pa Co; 29.667° N, 91.133° E).

2.3 Methods

2.3.1 Sample Collection

A 90-cm surface core (A-11) was collected in May 2011 from the deepest part of the Nir'pa Co's basin (water depth = 17.5 m) using an Aquatic Research hammer corer. Two additional cores, A-15 and B-15, were collected in June 2015 using a piston surface corer. Representative samples of the terrestrial and aquatic vegetation communities were collected from within the lake and around its immediate watershed in June 2015.

2.3.2 Chronology

An age model for Nir'Pa Co A-11 was produced using a combination of ^{210}Pb, ^{137}Cs, and ^{14}C (Bird et al., 2017). Ten samples from the top portion of the core underwent direct gamma counting to measure ^{210}Pb, ^{214}Pb, and ^{137}Cs (Appleby and Oldfield, 1978). Two radiocarbon (^{14}C) dates were measured using accelerator mass spectrometry (AMS) at the Keck AMS Laboratory, University of California Irvine. Both samples consisted of charcoal fragments that were collected from a wet sieve at 63 um, manually cleaned, and

chemically pretreated with an acid-base-acid wash using 1 N HCl and 1 N NaOH (Olsson, 1986). Radiocarbon dates were calibrated using the IntCal 0.914c data set with the CALIB 6.0 program (Stuiver and Reimer, 1993). All dates for this core are reported as median probability age and 2σ error in calendar years before present (BP; 0 = 1950 CE).

2.3.3 Lipid Extraction & δ^2H Analysis

Forty-two samples from the A-11 core were analyzed for *n*-alkane hydrogen (δ^2H) isotopes at the Lamont-Doherty Earth Observatory Organic Geochemistry Lab, Columbia University. Sediment samples were dried and homogenized before undergoing total lipid extraction (TLE) using a 9:1 dichloromethane to methanol solvent on a Dionex ASE-350. The TLE then underwent separation on a silica column (70-230 mesh, 60A) with hexane solvent to isolate the aliphatic fraction. The aliphatic fraction underwent silver nitrate column (10 % $AgNO_3$) chromatography separation with hexane as a solvent to isolate *n*-alkanes.

The distributions and concentrations of *n*-alkanes in each sample were determined using an Agilent Technologies 7890A gas chromatography mass spectrometer (GCMS). Short chain *n*-alkanes (nC23) are produced by both submerged and emergent aquatic macrophytes (Ficken et al., 2000; Seki et al., 2009) while long chain *n*-alkanes (nC29 and nC31) are produced by terrestrial vascular plants (Meyers, 2003). Intermediate *n*-alkanes (nC25 and nC27) can reflect a mixture of aquatic and terrestrial vegetation sources, but are also produced by aquatic (nC25) and terrestrial vascular (nC27) vegetation.

Several indices were used to assess the sources and distributions of *n*-alkanes. The average chain length (ACL) and carbon preference index (CPI) were calculated to assess changes in the distribution of *n*-alkanes (Diefendorf et al., 2015; Marzi et al., 1993). Higher ACL and CPI values indicate terrestrial vegetation inputs in lake sediments while lower values are indicative of aquatic vegetation (Mügler et al., 2008). The aquatic vegetation index (P_{aq}) was calculated to assess the concentration of low and mid-chain *n*-alkanes (aquatic inputs) versus longer chains (terrestrial inputs; Ficken et al., 2000). Higher P_{aq} index values indicate greater aquatic productivity (Ficken et al., 2000; Seki et al., 2009).

$$\mathrm{ACL} = \frac{25[C25] + 27[C27] + 29[C29] + 31[C31] + 33[C33] + 35[C35] + 37[C37]}{[C25] + [C27] + [C29] + [C31] + [C33] + [C35] + [C37]}$$

$$CPI = \frac{([C23] + [C25] + [C27] + [C29] + [C31] + [C33] + [C35]) + ([C25] + [C27] + [C29] + [C31] + [C33] + [C35] + [C37])}{2\,X\,([\mathrm{C24}] + [\mathrm{C26}] + [\mathrm{C28}] + [\mathrm{C30}] + [\mathrm{C32}] + [\mathrm{C34}] + [\mathrm{C36}])}$$

$$Paq = \frac{[C23] + [C25]}{[C23] + [C25] + [C29] + [C31]}$$

δ^2H *n*-alkane isotopic measurements were made using a Thermo Scientific Trace Ultra GCMS (GC column: 30m, 0.25mm, 14.2 psi, 60°C) and Delta V Plus IRMS (isotope ratio mass spectrometer). Both an isotopic (Mix A7) and a lab standard were run with replicate sample injections. Reported values are reported in standard delta notation with per mil (‰) units relative to the VSMOW (Vienna Standard Mean Ocean Water) scale after being corrected using MATLAB. Isotopic variability between replicate measurements ranged between 2.9-3.4% (Polissar and D'Andrea, 2014).

2.3.4 Effective Moisture

nC23 is derived from aquatic plants, which incorporate hydrogen atoms directly from lake water, thereby reflecting its isotopic composition, but with some degree of offset (Mügler et al., 2008; Seki et al., 2009). nC31 is derived from terrestrial plants, which incorporate hydrogen atoms from soil water that is derived directly from precipitation (Xia et al., 2008). The δ^2H for nC31 therefore reflects variations in the isotopic composition of precipitation, while δ^2H for nC23 reflects changes in lake water isotopic compositions that incorporate evaporation and changes in lake volume as well as changes in the isotopic composition of the precipitation that fed the lake. The large difference in hydrogen isotope values between terrestrial (nC31) and aquatic vegetation (nC23) is driven by the enrichment of δ^2H in lake water due to high evaporation of the system (Guenther et al., 2013) and fractionation during biosynthesis, with aquatic plants exhibiting a large, negative fractionation (Mügler et al., 2008). The subtraction of

normalized isotopic measurements of nC31 from nC23 hence removes isotopic variability in the lake water δ^2H attributable to changes in precipitation δ^2H and those factors that influence it (moisture source, distance from source, temperature, etc.), thereby providing an estimation the ratio of precipitation to evaporation (Mügler et al., 2008). Higher $\Delta\delta^2H_{C23\text{-}C31}$ values indicate greater evaporation relative to precipitation and vice versa for lower values.

2.4 Results

2.4.1 Sedimentology

The sedimentology of the A-11 core consisted of homogenous, fine grained sediments that were reddish-brown with slightly darker bands around 30 and 60 cm. Organic fragments including charcoal and grass were dispersed throughout the core (Bird et al., 2017).

2.4.2 Short vs. Long-chain n-alkanes

Concentrations of *n*-alkanes varied significantly between the modern sediments and the early part of the record (~3.4 ka; Fig. 2.5 and Table 2.1). The full dataset is in Appendix 1, Table A 1.1. Throughout the record, short chain leaf waxes were more abundant (nC23-nC25: 1.07 – 1.36 x 10^8 ng/100 µl) than long chain alkanes in the record (nC27-nC31: 9.04x10^7 – 1.0x10^8 ng/100 µl). Noticeably *n*-alkanes were higher during the MCA (950-1250 AD) and decreased during the LIA (1275-1700 AD).

ACL values ranged between 27.9 and 28.66 while CPI values ranged from 4.05 to 4.55 over the last 3.4 ka (Fig. 2.5F-G). Both the ACL and CPI were consistently low between 3.4-2.25 ka (average: ACL: 28.2, CPI: 4.2) and increased from 2.25-1.25 ka (average: ACL: 28.3, CPI: 4.3). ACL decreased sharply at the beginning of the LIA (~610 BP; ACL: 27.9).

P_{aq} ranged between 0.41 and 0.53, which shows that the contribution of aquatic vegetation was high for most of the sediment record, but peaked at the beginning of the LIA (~610 BP; P_{aq} = 0.53; Fig. 2.5G). Aquatic vegetation steadily decreased after that peak and has remained lower in the modern sediments (300 yrs. BP to present).

2.4.3 Leaf Wax δ^2H

Hydrogen isotopic measurements (δ^2H) for C23, C25, C27, C29, and C31 *n*-alkanes extracted from the Nir'Pa Co sediments ranged from -287‰ to -237‰ for the last 3.4 ka (Fig. 2.6: A-E). δ^2H shows high variability throughout the record for all chain lengths. All *n*-alkanes were higher at the beginning of the record (nC23-nC31: -270.5‰ to -247.2‰) and subsequently decreased by 6 to 8.6‰. δ^2H remained lower until ~2750 BP when δ^2H for all *n*-alkanes increased with nC23 and nC25 showing the greatest enrichment (5.3 and 6.7‰, respectively). Isotope values plateaued until they decreased again during the MCA with the lowest values occurring at the beginning of the LIA (620 BP: -280 to -253‰). The isotopic responses during the LIA were lower. Modern *n*-alkane sediment δ^2H values are highest, with values ranging between -267.4 to -243.5‰ (300 yrs. BP to present).

2.4.4 Effective Moisture

$\Delta\delta^2H_{C23\text{-}C31}$ represents the hydrogen isotopic difference between nC23 and nC31 *n*-alkanes (Fig. 2.6F). $\Delta\delta^2H_{C23\text{-}C31}$ ranged between -7.7 to 5.6‰ with high variability throughout the record. $\Delta\delta^2H_{C23\text{-}C31}$ was positive between 3 and 1.2 ka and in the modern part of the record. $\Delta\delta^2H_{C23\text{-}C31}$ was negative in the earliest part of the record from 3.3 and 3 ka and between 1 ka and 250 BP, which includes the MCA and LIA, with the lowest $\Delta\delta^2H_{C23\text{-}C31}$ values at 600 BP (-7.7%).

2.5 Discussion

2.5.1 Localized Hydroclimate at Nir'Pa Co

The previously published geochemical and sedimentological results from Nir'Pa Co suggested relatively wet conditions between 3.4 and 2.4 ka, an abrupt transition into and out of a pronounced dry interval at 2.4 and 1.3 ka, respectively, and a return to relatively wet conditions from 1.2 ka to the present (Bird et al., 2017). The new δ^2H results from Nir'Pa Co support this interpretation, but provide important additional information about the nature of local hydroclimate conditions and its relationship with

synoptic-scale ISM variability during the late Holocene. Here, I use the $\Delta\delta^2H_{C23\text{-}C31}$ time series as an indicator of local hydroclimate conditions at Nir'Pa Co and compare it with established lithics and percent sand time series from the lake. The Nir'Pa Co record indicates that the ISM varied significantly over the late Holocene, transitioning between strong and weak phases that influenced the local hydroclimate as inferred by δ^2H measurements and $\Delta\delta^2H_{C23\text{-}C31}$. Local hydroclimate conditions are indicated by short-chain *n*-alkanes and $\Delta\delta^2H_{C23\text{-}C31}$ while synoptic hydroclimate is inferred by long-chain *n*-alkanes. At Nir'Pa Co δ^2H_{C23}, which incorporates both monsoon intensity and evaporation from lake water, is used to infer local hydroclimate while $\Delta\delta^2H_{C23\text{-}C31}$ represents the hydrologic balance between precipitation and evaporation. The δ^2H record is compared with the sedimentology record at Nir'Pa Co (Bird et al., 2017), with high sand content inferred as low lake level, attributed to the increased proximity of the core site to the littoral zone of the lake. While the modern monsoon is relatively weaker than at any other point in the Holocene, with enriched δ^2H_{C23} and high terrestrial vegetation inputs, there are two earlier periods that show significant variability in the local hydroclimate record at Nir'Pa Co: the LIA and 2.4 to 1.3 ka, with the former characterized as a relatively strong monsoon and the latter as weak monsoon (Fig. 2.7).

The event between 2.4 to 1.3 ka showed an extended significant impact on hydroclimate at Nir'Pa Co. During this period, $\Delta\delta^2H_{C23\text{-}C31}$ values are high which indicates higher evaporation at Nir'Pa Co. Low lake level conditions during this weak monsoon period are indicated by high terrestrial vegetation inputs, exhibited with more abundant longer-chain *n*-alkanes and low P_{aq} values. Observations for increased %sand during this period supports a low lake level interpretation and support the conclusion of arid conditions at Nir'Pa Co from 2.4 to 1.3 ka. Comparing the lake level signal of percent sand to the δ^2H_{C23} and results, it is apparent that while the response of δ^2H to changes in monsoon intensity is gradual the transition from low to high sand content are more abrupt. The sudden influx of sand could be an indication of the lake reaching a threshold where the stand is low enough to expose the shelf on the northeastern edge of the lake, with a minimum decrease of one meter in water level to expose the shelf.

$\Delta\delta^2H_{C23\text{-}C31}$ decreases across the MCA suggesting that evaporation was declining across this period. In contrast, the LIA (675-250 BP) showed significant variability in

δ^2H_{C23} with the lowest values at the beginning of the LIA and an increase at the end of the event. Evaporation was low throughout the LIA as indicated by $\Delta\delta^2H_{C23\text{-}C31}$. More abundant short-chain *n*-alkanes and high P_{aq} values indicate that aquatic vegetation input has been high at Nir'Pa Co for most of the late Holocene, but there is a significant increase during the LIA which corresponds with the decrease in δ^2H_{C23} (Fig. 2.7D). The positive correlation between aquatic productivity and strong monsoon conditions could be interpreted as a lake level signal with a deeper lake producing a greater area for submerged and emergent plant habitat. Comparing with the sand record at Nir'Pa Co (Fig. 2.7E; Bird et al., 2017), the MCA and LIA can be interpreted as a period with highly fluctuating lake levels, with deeper lake conditions towards the beginning of the LIA. The combined lake level and isotopic record suggest that there was little impact of the MCA on local hydroclimate at Nir'Pa Co, while the LIA had a larger, but more variable impact.

2.5.2 Local and Synoptic Hydroclimate Relationships at Nir'Pa Co

Long-chain *n*-alkane δ^2H closely reflects the isotopic expression of precipitation (Xia et al., 2008) and, therefore, is used to assess synoptic or regional scale expression of the ISM. Monsoon intensities inferred by δ^2H_{C31} exhibit the same broad trends as local hydroclimate $\Delta\delta^2H_{C23\text{-}C31}$ with wetter conditions at Nir'Pa Co from 3.4 to 2.4 ka and 1.3 ka to present. Synoptic ISM variability at Nir'Pa Co agrees with the weak monsoon interpretation from 2.4 to 1.3 ka and is also evident in the local hydroclimate proxies with high sand and terrestrial vegetation. The LIA is evident with a strong monsoon at the beginning of the event around 610 BP in conjunction with low $\Delta\delta^2H_{C23\text{-}C31}$ and high aquatic vegetation. There is minimal evidence of any impact of the MCA on monsoon intensity on a synoptic scale, although the increase in silt and lithics suggests a local hydroclimate response with deeper lake conditions. The combination of local and synoptic hydroclimate records at Nir'Pa Co indicate that the drought event from 2.4 to 1.3 ka was consistently expressed at local and synoptic scales, while the LIA showed a small increase in monsoon strength while the MCA was not clearly expressed.

2.5.3 Regional Paleoclimate

Late Holocene records of ISM variability on the Tibetan Plateau are generally coherent with the interpretation of hydroclimate variability at Nir'Pa Co. For example, local hydroclimate at Paru Co, located only 7.5 km northwest of Nir'Pa Co, shows a deeper lake from 3.4 to 2.5 ka and 1.3 ka to present, with an intermittent shallow lake from 2.5 ka to 1.3 ka which corresponds with lake level interpretations at Nir'Pa Co (Fig. 2.7F-G; Bird et al., 2014). Lake level at Paru Co is inferred by percent sand and principal component analysis of grain size data variability. Higher lake levels at Paru Co between 3.3 – 2.5 ka and 1.3 ka to present with an intermittent period of lower lake levels are consistent with a deeper lake at Nir'Pa Co from 3.4 to 2.4 ka and 1.3 ka to present and a shallow lake from 2.4 to 1.3 ka. Another lake on the Tibetan Plateau, Seling Co, 370 km northwest of NPC, shows high $\delta^{18}O$ between 2.2 and 1.2 ka, suggesting increased evaporation during this time that is consistent with the low stands at NPC and Paru Co (Gasse et al., 1996; Gu et al., 1993). Like NPC and Paru Co, the Seling Co $\delta^{18}O$ record also shows no significant departures during either the MCA or LIA, suggesting these events minimally impacted local hydroclimate.

ISM precipitation on the plateau corresponds to shifts between cooler and warmer air temperatures as evidenced by the Lake Zigetang pollen index record from the central plateau, east of Seling Co (Herzschuh et al., 2006). The late Holocene was characterized by a more alpine steppe biome with greater dominance of Cyperaceae and similar cold hardy vegetation. This pattern was emphasized with a significant cooling between 2 and 1.5 ka that reflects the aridity evident in other plateau records. There is a paucity of high-resolution temperature reconstructions from the Tibetan Plateau making it difficult to assess evaporation rates especially during the winter months. The Lake Zigetang pollen record corresponds to summer climate and can't provide information about how winter climate has varied throughout the late Holocene, with warmer winter temperatures decreasing ice cover that could increase evaporation in the lake.

Synoptic variability in the ISM is indicated by leaf-wax *n*-alkane isotopic variability at Paru Co (Fig. 2.7G). The broad trend of long-chain *n*-alkane $\delta^{2}H$ (C27 and C29) of Paru Co shows that synoptic monsoon response was weak between 2.3 and 1.2 ka and relatively strong during the MCA which coincides with the higher-resolution

δ^2H_{C31} record at Nir'Pa Co. Synoptic record of ISM precipitation in the Dunde ice core in the north-central Tibetan Plateau, shows a more consistent strong monsoon during the MCA and LIA inferred by lower $\delta^{18}O$ (Thompson et al., 2006). Comparing the synoptic and local hydroclimate records across the Tibetan Plateau there is general agreement between local and synoptic proxies with the exception of the stronger monsoon intensity during the MCA and LIA in the Dunde ice core. A possible explanation for this difference is that the Dunde ice core record is not influenced by any biosynthesis fractionation compared to the leaf-wax *n*-alkane records at Nir'Pa Co and Paru Co.

2.5.4 Forcing Mechanisms

Evaluating the mechanisms that drove hydroclimate variability on the plateau require the consideration of paleoclimate records from beyond the Tibetan Plateau (Fig. 2.8). The Dongge speleothem record in southeastern China is influenced mainly by the East Asian Monsoon, but has also been theorized to be affected by the ISM due to its location on the margins between the two systems (Fig. 2.8C; Dykoski et al., 2005). Noticeably, Dongge Cave shows a much drier late Holocene with wetter conditions during the modern with less variability than at Nir'Pa Co.

Qunf Cave in Southern Oman is an ISM record that is located at the furthest western extent of the monsoon and the northern point of the ITCZ (Fig. 2.8D; Fleitmann et al., 2003; Fleitmann et al., 2007). The isotopic record of precipitation is less variable and drier than at Nir'Pa Co in the early part of the late Holocene with a steady decline in precipitation across the Holocene which is inferred as the southward migration of the ITCZ. Precipitation increases around the MCA and LIA before declining again. The long hiatus at Qunf Cave between 2.7 and 1.4 ka is attributed to a significant decline in the monsoon that halted deposition and agrees with reduced ISM precipitation on the plateau. A *Globigerina bulloides* foraminifera record (Fig. 2.8E) from the Arabian Sea suggest increased (decreased) upwelling in conjunction with higher (Battarbee et al., 2001) monsoon precipitation on land (Gupta et al., 2003). Upwelling is inferred in that record as an increase in wind strength from the monsoon, with upwelling remaining low for most of the late Holocene, decreasing and remaining stagnant between 2.2 to 1 ka before increasing during the MCA.

Marine and lake sediment records from the Pacific and Indian Oceans inferred to represent El Nino-Southern Oscillation variability provide a possible explanation of how sea surface temperatures and wind patterns drive monsoon rainfall across the plateau. The sand record at El Junco Crater Lake, in the Galapagos Islands, has been argued to indicate higher frequency of El Niño events (Fig. 2.8F; Conroy et al., 2008). Deeper lake level at El Junco defined by high sand influxes and lower C to N ratios occurred from 2 to 1.5 ka when the Asian monsoon was at its weakest points. A transition to El Niño conditions during the late Holocene also coincided with a southward migration of the ITCZ as evidenced in Qunf Cave (Fleitmann et al., 2003) and the Cariaco Basin (Haug et al., 2001). Laguna Pallcacocha sedimentology record from the Ecuadorian Andes exhibits higher frequency of El Niño conditions during the mid-late Holocene, but does not show the same extreme response or temporal duration of these events as El Junco likely influenced by its inland and higher elevation site (Fig. 2.8G; Moy et al., 2002).

Eastern Pacific SSTs were estimated from the ratio of Mg to Ca from *Globigerina bulloides* foraminifera collected in a sediment core near the Baja Peninsula of Mexico (Fig. 2.8H; Marchitto et al., 2010). Warmer temperatures in the eastern Pacific are indicative of an El Niño state while cooler temperatures indicate La Niña conditions, resulting in higher and lower rainfall respectively on the western coast of North and South America. The sparse record does suggest warmer conditions between 1.5 to 1 ka, when the Asian monsoon was weaker. SSTs in the tropical western Pacific are interpreted as cooler (warmer) temperatures indicate El Niño (La Niña) conditions (Fig. 2.8I; Stott et al., 2004). Surface waters were cooler for most of the late Holocene, with warmer temperatures during the MCA suggesting La Niña conditions during this period. Indian Ocean SSTs also indicate warmer temperatures between 2 and 1.2 ka and cooler temperatures during the MCA and LIA indicating La Niña and El Niño conditions respectively (Fig. 2.8J; Tiwari et al., 2006). The increased prevalence of El Niño conditions during the late Holocene has been attributed to declining solar insolation and warmer ocean upwelling resulting in decreased ISM precipitation intensity (Marchitto et al., 2010).

2.6 Conclusions

The leaf wax record at Nir'Pa Co demonstrates that there has been high variability in the ISM throughout the late Holocene with a pronounced weakening of the monsoon between 2.4 to 1.3 ka and a minimal hydroclimate response to the LIA. The modern monsoon is at its weakest point in the Holocene evidenced by high terrestrial vegetation inputs, enriched δ^2H, and greater evaporation at Nir'Pa Co. Comparisons between the isotopic record and grain size records at Nir'Pa Co show that the lake level response to the ISM is more abrupt, suggesting a threshold for lake level changes. Weaker monsoon intensity at Nir'Pa Co corresponds with an El Niño-state in the Pacific and Indian Oceans as well as warmer temperatures on the plateau while stronger monsoon conditions reflect a La Niña-state and cooler temperatures on the plateau. Comparisons with paleoclimate records within the ISM extent and broader teleconnections shows that the period between 2.4 to 1.3 ka with weaker monsoon intensity was influenced by El Niño conditions in the Pacific.

2.7 Tables

Table 2.1: Average concentration of *n*-alkanes in Nir'Pa Co sediments

TIME PERIOD	NC23	NC25	NC27	NC29	NC31
249 TO -67 BP	$1.09x10^8$	$1.39 x10^8$	9.69E+07	$1.09 x10^8$	$1.28 x10^8$
675 TO 250 BP	$7.42 x10^7$	$9.52 x10^7$	$5.67 x10^7$	$5.33 x10^7$	$5.75 x10^7$
1000 TO 700 BP	$1.18 x10^8$	$1.58 x10^8$	$1.01 x10^8$	$1.02 x10^8$	$1.12 x10^8$
1250 TO 1000 BP	$1.16 x10^8$	$1.52 x10^8$	$1.02 x10^8$	$1.07 x10^8$	$1.15 x10^8$
2250 TO 1250 BP	$1.10 x10^8$	$1.39 x10^8$	$9.28 x10^7$	$9.51 x10^7$	$9.94 x10^7$
3400 TO 2250 BP	$1.07 x10^8$	$1.28 x10^8$	$8.83 x10^7$	$8.61 x10^7$	$8.52 x10^7$

2.8 Figures

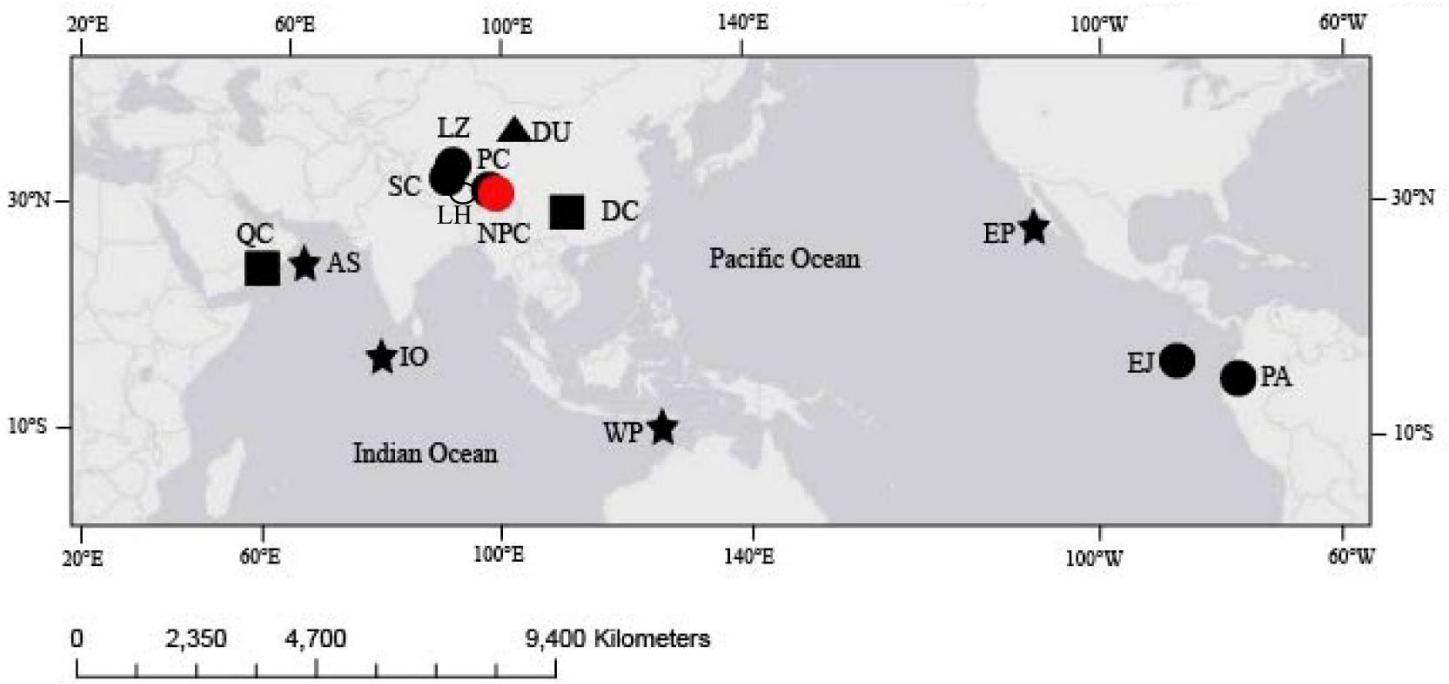

Figure 2.1. The location of Nir'Pa Co (NPC; red circle) in reference to other regional climate records. Lake sediment archives including El Junico (EJ), Lake Zigetang (LZ), Pallcacocha (PA), Paru Co (PC), and Selin Co (SC) are represented with circles. Cave records from Dongge Cave (DC) and Qunf Cave (QC) are represented with squares. The Dunde ice core (DU) is represented with a triangle. Marine sediment cores from the Arabian Sea (AS), Eastern Pacific (EP), and the Western Pacific (WP) are represented with stars. The Lhasa weather station (LH) is marked with an open circle.

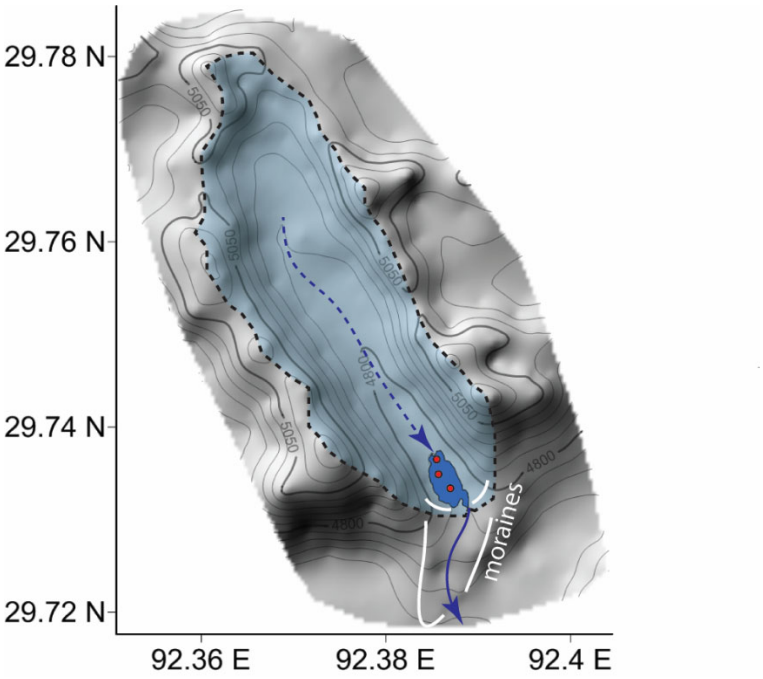

Figure 2.2. The Nir'Pa Co watershed and surrounding area with the lake at the end of a 5 km long glacially carved valley.

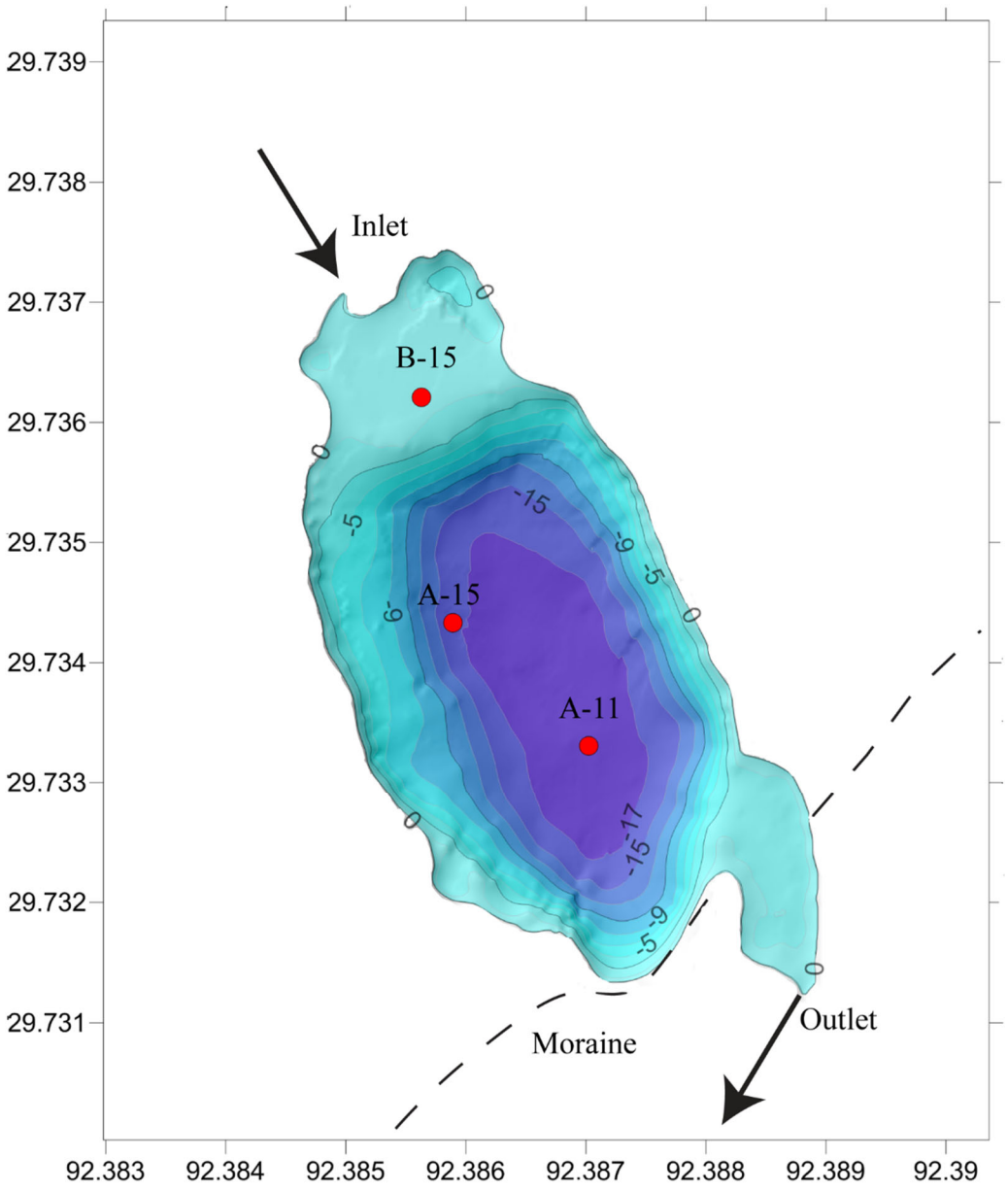

Figure 2.3. Bathymetric map of Nir'Pa Co with 2 m contour intervals. The respective core sites for A-11, A-15, and B-15 are designated with red circles. Location of the inlet and outlet to the lake are marked with the location of the moraine that terminates the watershed.

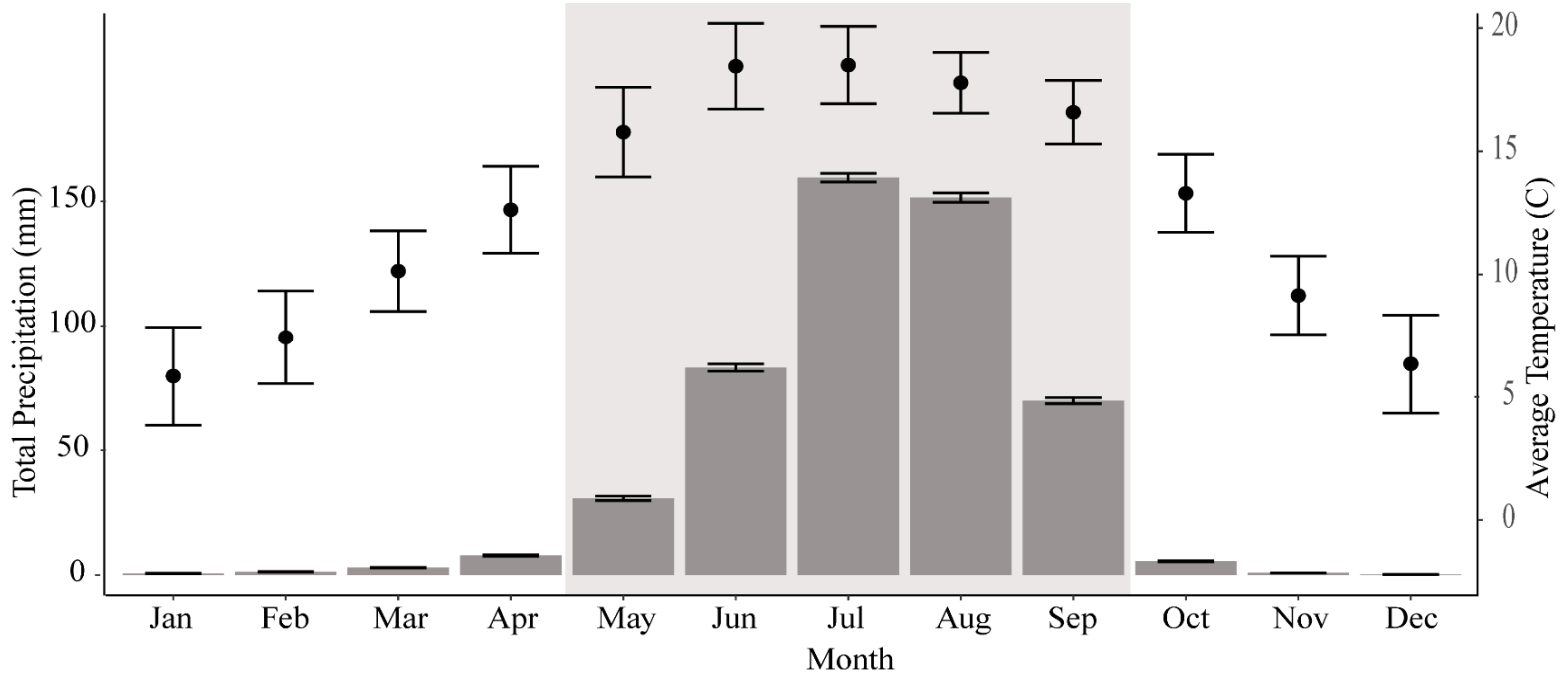

Figure 2.4. Monthly total precipitation (mm ± s.d.) and average temperature (°C ± s.d.) at the Lhasa weather station. The monsoon season (May-September) is marked with a shaded gray background.

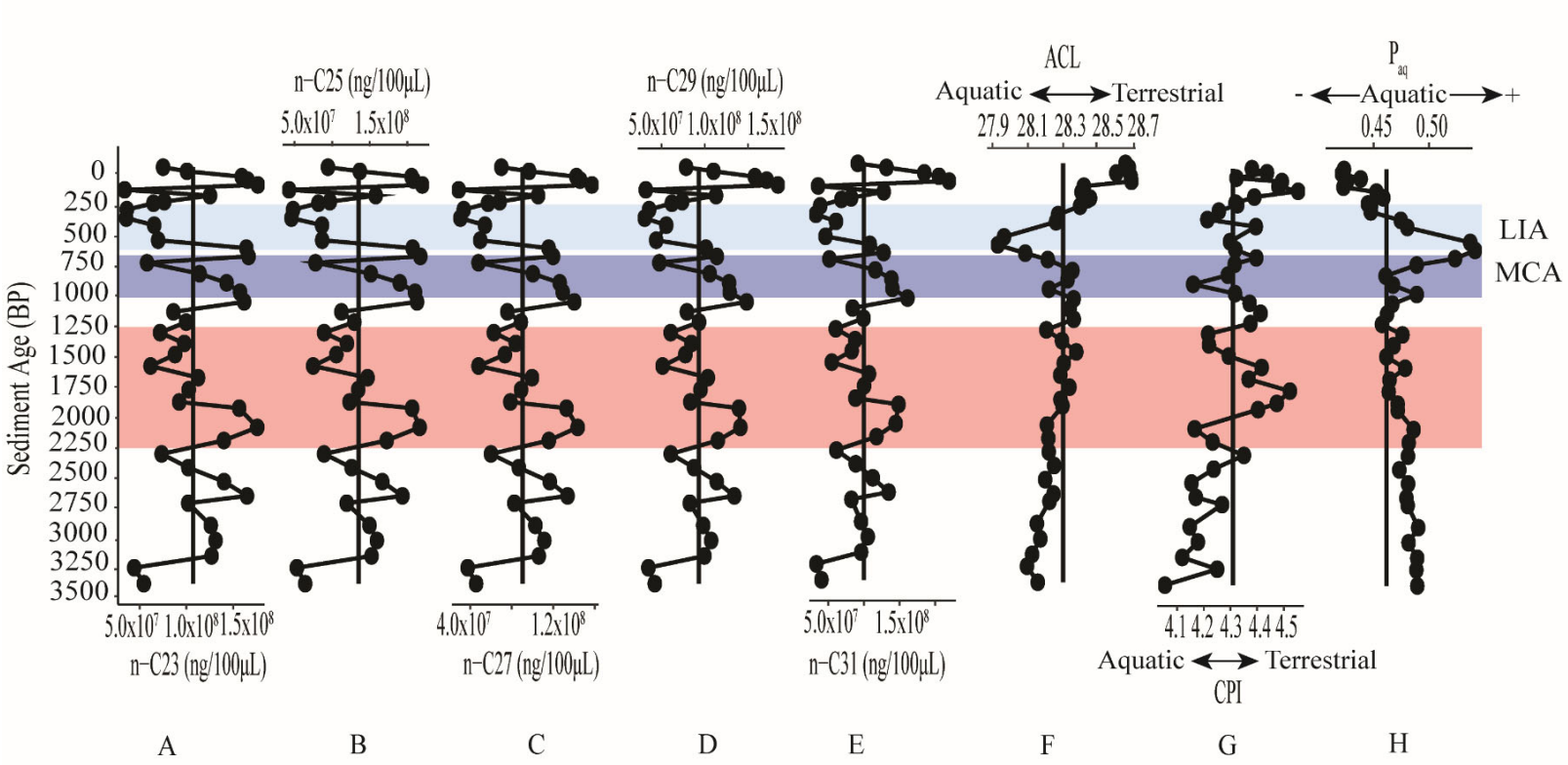

Figure 2.5. Total concentration of extracted long-chain C23 – C31 *n*-alkanes from sediment samples (ng/100 µL; A- E). Terrestrial lipid distribution as indicated with the Carbon Preference Index (CPI; F), Average Chain Length (ACL; G), and the aquatic vegetation index (P_{aq}, H). Vertical black lines indicate the average value. The LIA and MCA time periods are marked with light blue and dark blue backgrounds (indicating wetter conditions) while 2250-1250 BP is marked with red background (indicating drier conditions).

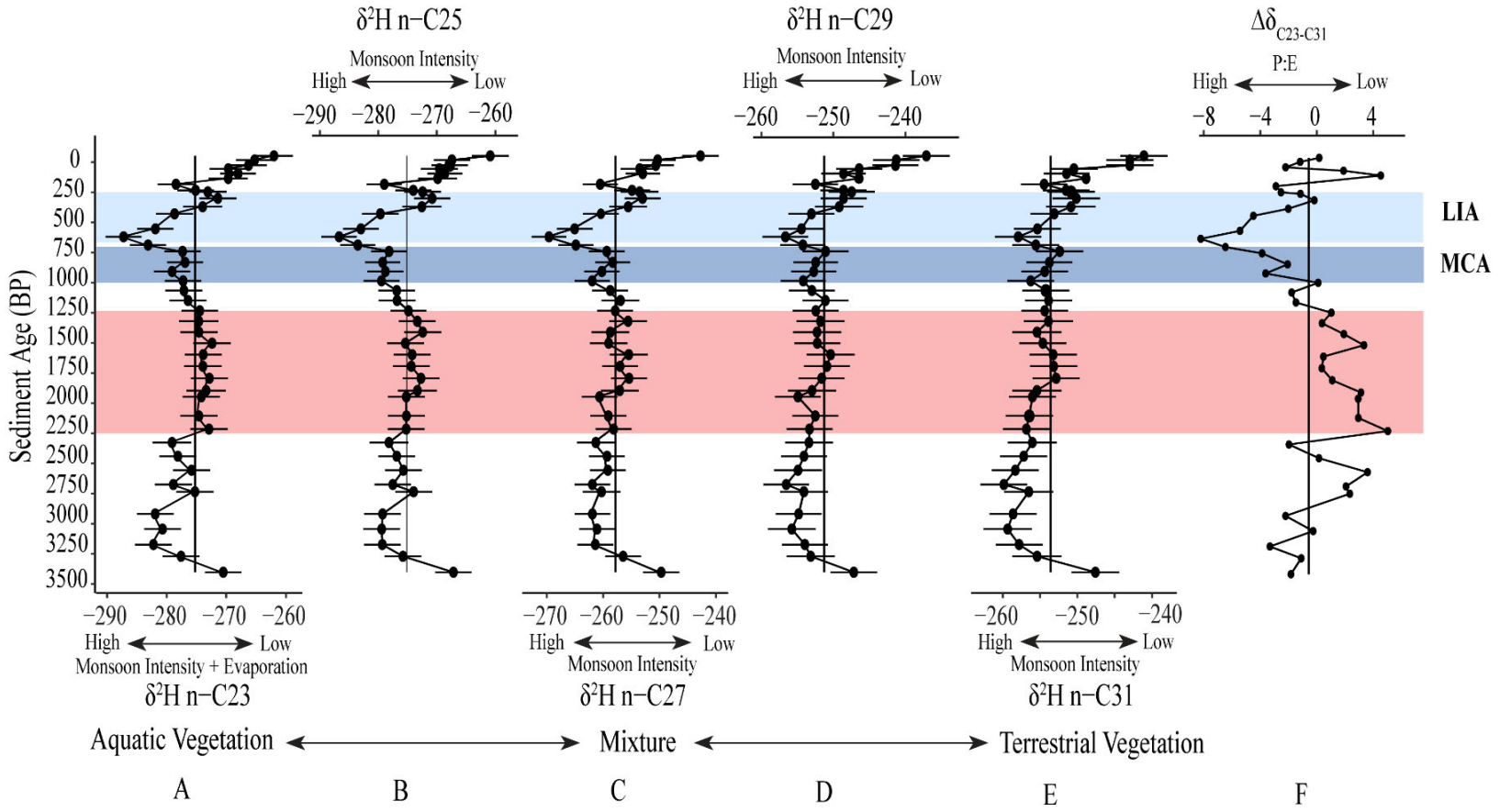

Figure 2.6. Leaf wax δ^2H (‰ VSMOW) ±1 σ s.e.m. for C23 (A), C25 (B), C27 (C), C29 (D), and C31 I *n*-alkanes. $\Delta\delta_{C23\text{-}C31}$ shows the variation between isotopic values between nC23 and nC31 (F). A more positive Δδ value indicates higher evaporation while a more negative Δδ indicates lower evaporation. Vertical black lines indicate average values. The LIA and MCA time periods are marked with light blue and dark blue backgrounds (indicating wetter conditions) while 2250-1250 BP is marked with red background (indicating drier conditions).

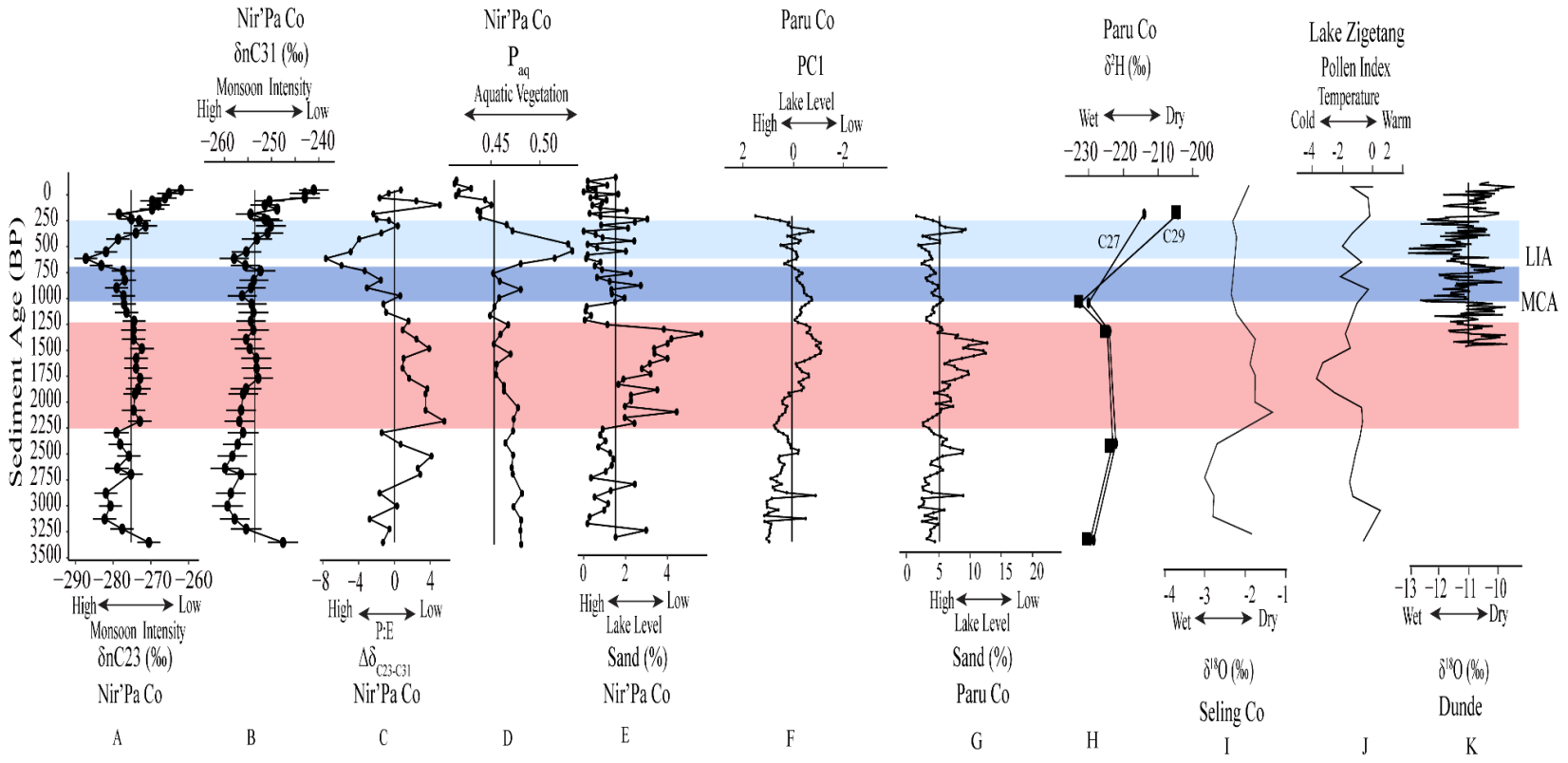

Figure 2.7. Nir'Pa Co δ^2H nC23 (‰; A), δ^2H nC31 (‰; B), $\Delta\delta_{C23\text{-}C31}$ (‰; C), P_{aq} (D), and sand grain size (%, E). Compared with local climate records from Paru Co sand (%; F), principal components (G), δ^2H for nC27 and nC29 (‰; H), Seling Co $\delta^{18}O$ (‰; I), Lake Zigetang pollen index (J), and Dunde ice core $\delta^{18}O$ (‰; K). Vertical black lines indicate the average value for each proxy. The LIA and MCA time periods are marked with light blue and dark blue backgrounds (indicating wetter conditions) while 2250-1250 BP is marked with red background (indicating drier conditions).

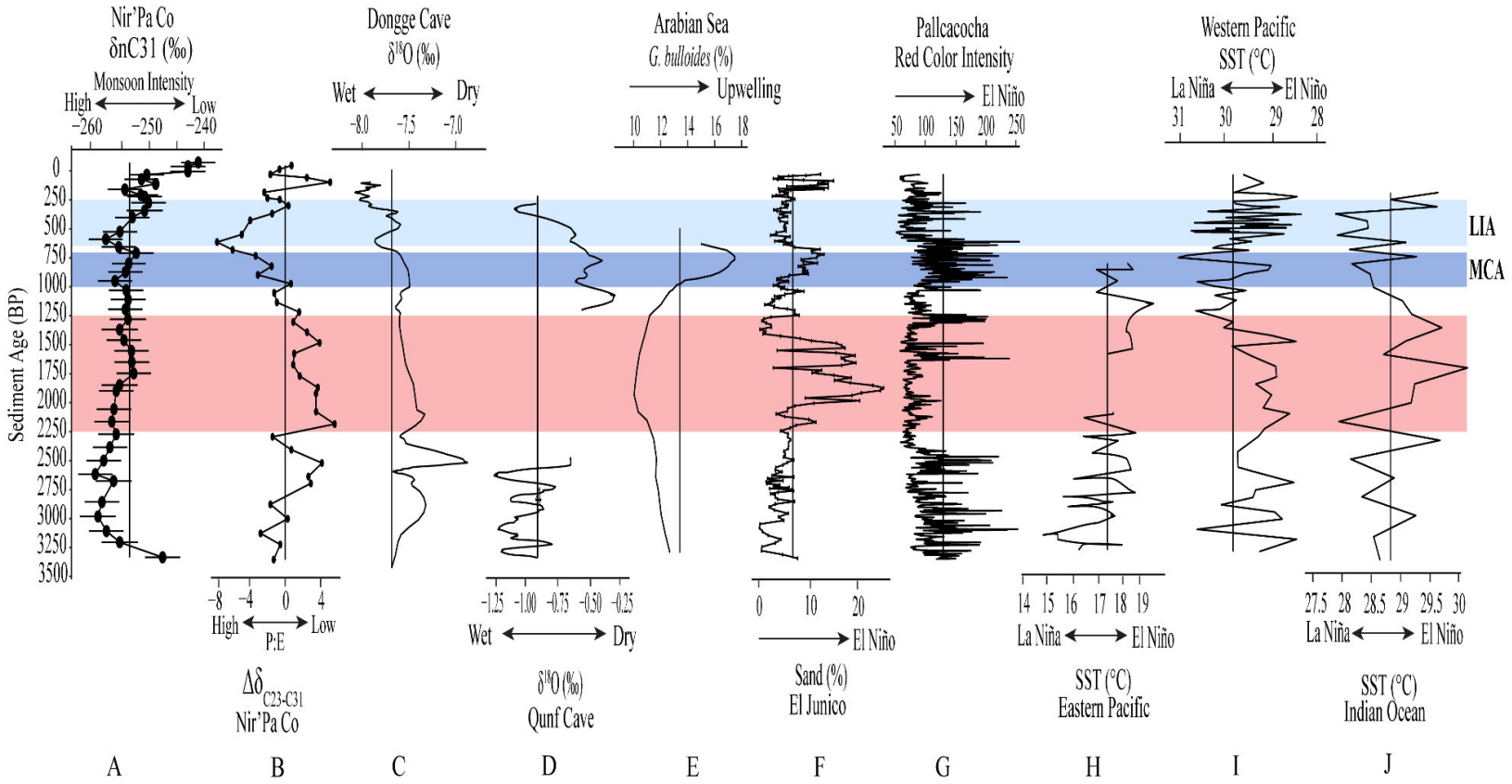

Figure 2.8. Comparison of Nir'Pa Co δ^2H nC31 (‰; A) and $\Delta\delta_{C23\text{-}C31}$ (B) data with regional monsoon records and global forcing. Regional monsoon records include Dongge Cave $\delta^{18}O$ (‰; C), Qunf Cave $\delta^{18}O$ (‰; D), and Arabian Sea marine core $\delta^{18}O$ (‰; E). Pacific records include El Junico sand grain size (%, F), Pallcacocha red sediment color intensity (G), Eastern (H) and Western Pacific (I) and Indian Ocean (J) SSTs (Sea Surface Temperatures °C). Vertical black lines indicate the average value for each proxy. The LIA and MCA time periods are marked with light blue and dark blue backgrounds (indicating wetter conditions) while 2250-1250 BP is marked with red background (indicating drier conditions).

2.9 References

Appleby, P. and Oldfield, F. 1978. The calculation of lead-210 dates assuming a constant rate of supply of unsupported 210Pb to the sediment. CATENA 5(1), 1-8.

Battarbee, R., Jones, V., Flower, R., Cameron, N., Bennion, H., Carbalho, L. and Juggins, S. (2001) Tracking environmental change using sediments. Smol, J., Birk, H. and Last, W. (eds), Kluwer Academic Publishers, Dordrecht.

Berkelhammer, M., Sinha, A., Stott, L., Cheng, H., Pausata, F. and Yoshimura, K. (2012) Climates, Landscapes, and Civilizations, pp. 75-87, Geophysical Monograms AGU, Washington D.C.

Bird, B., Lei, Y., Perello, M., Polissar, P., Yao, T., Finney, B., Bain, D., Pompeani, D. and Thompson, L. 2017. Late Holocene Indian summer monsoon variability revealed from a 3,300-year-long lake sediment record from Nir'pa Co, southeastern Tibet. The Holocene 27(4), 541-552.

Bird, B., Polissar, P., Lei, Y., Thompson, L., Yao, T., Finney, B., Bain, D., Pompeani, D. and Steinman, B. 2014. A Tibetan lake sediment record of Holocene Indian summer monsoon variability. Earth and Planetary Science Letters 399, 92-102.

Conroy, J.L., Overpeck, J.T., Cole, J.E., Shanahan, T.M. and Steinitz-Kannan, M. 2008. Holocene changes in eastern tropical Pacific climate inferred
from a Galápagos lake sediment record. Quaternary Science Reviews 27, 1166– 1180.

Diefendorf, A.F., Leslie, A.B. and Wing, S.L. 2015. Leaf wax composition and carbon isotopes vary among major conifer groups. Geochimica et Cosmochimica Acta 170(1), 145-156.

Dykoski, C., Edwards, R., Cheng, H., Yaun, D., Cai, Y., Zhang, M., Lin, Y., Qing, J., An, Z. and Revenaugh, J. 2005. A high-resolution, absolute-dated Holocene and deglacial Asian monsoon record from Dongge Cave, China. Earth and Planetary Science Letters 233, 71-86.

Ficken, K., Li, B., Swain, D. and Eglinton, G. 2000. An n-alkane proxy for the sedimentary input of submerged/floating freshwater aquatic macrophytes. Organic Geochemistry 31(7-8), 745-749.

Fleitmann, D., Burns, S., Mudelsee, M., Neff, U., Kramers, J., Mangini, A. and Matter, A. 2003. Holocene forcing of the Indian Monsoon recorded from a stalagmite from Southern Oman. Science 300, 1737-1739.

Fleitmann, D., Burns, S.J., Mangini, A., Mudelsee, M., Kramers, J., Villa, I., Neff, U., Al-Subbary, A.A., Buettner, A., Hippler, D. and Matter, A. 2007. Holocene ITCZ and Indian monsoon dynamics recorded in stalagmites from Oman and Yemen (Socotra). Quaternary Science Reviews 26, 170-188.

Gasse, F., Fontes, J.C., Campo, E.V. and Wei, K. 1996. Holocene environmental changes in Bangong Co basin (Western Tibet). Part 4: Discussion and conclusions. Palaeogeography, Palaeoclimatology, Palaeoecology 120, 79-92.

González-Rouco, F.J., Fernández-Donado, L., Raible, C.C., Barriopedro, D., Luterbacher, J., Jungclaus, J.H., Swingedouw, D., Servonnat, J., Zorita, E., Wagner, S. and Ammann, C.M. 2011. Medieval Climate Anomaly to Little Ice Age transition as simulated by current climate models. PAGES news 19(1), 7-8.

Gu, Z., Liu, J., Yuan, B., Liu, D., Liu, R., Liu, Y. and Zhang, G. 1993. Monsoon variation on the Tibetan Plateau since the past 12 000 years: geochemistry evidence from lake sediments in Selin Co. Chinese Science Bulletin 38, 61-64.

Guenther, F., Aichner, B., Siegwolf, R., Xu, B., Yao, T. and Gleixner, G. 2013. A synthesis of hydrogen isotope variability and its hydrological significance at the Qinghai-Tibetan Plateau. Quaternary International 313-314, 3-16.

Gupta, A., Anderson, D. and Overpeck, J. 2003. Abrupt changes in the Asian southwest monsoon during the Holocene and their links to the North Atlantic Ocean. Nature 421, 354-357.

Haug, G.H., Hughen, K.A., Sigman, D.M., Peterson, L.C. and Ro, U. 2001. Southward Migration of the Intertropical Convergence Zone Through the Holocene. Science 293, 1304-1308.

Herzschuh, U., Winter, K., Wunnemann, B. and Li, S. 2006. A general cooling trend on the central Tibetan Plateau throughout the Holocene recorded by the Lake Zigetang pollen spectra. Quaternary International 154-155, 113-121.

Li, B., Li, J. and Cui, Z. 1991. Quaternary glacial distribution map of Qinghai-Xizang (Tibet) Plateau 1:3,000,000. Shi, Y. (ed), Quaternary Glacier and Environment Research Center, Lanzhou University.

Mann, M., Zhang, Z., Rutherford, S., Bradley, R., Hughes, M., Shindell, D., Ammann, C., Faluvegi, G. and Ni, F. 2009. Global signatures and dynamical origins of the Little Ice Age and Medieval Climate Anomaly. Science 326, 1256-1260.

Marchitto, T.M., Muscheler, R., Ortiz, J.D., Carriquiry, J.D. and Geen, A.v. 2010. Dynamical Response of the Tropical Pacific Ocean to Solar Forcing During the Early Holocene. Science 330, 1378-1381.

Marzi, R., Torkelson, B. and Olson, R. 1993. A revised carbon preference index. Organic Geochemistry 20(8), 1303-1306.

Meyers, P.A. 2003. Applications of organic geochemistry to paleolimnological reconstructions: a summary of examples from the Laurentian Great Lakes. Organic Geochemistry 34(2), 261-289.

Miller, G.H., Geirsdóttir, Á., Zhong, Y., Larsen, D.J., Otto-Bliesner, B.L., Holland, M.M., Bailey, D.A., Refsnider, K.A., Lehman, S.J., Southon, J.R., Anderson, C., Björnsson, H. and Thordarson, T. 2012. Abrupt onset of the Little Ice Age triggered by volcanism and sustained by sea-ice/ocean feedbacks. Geophysical Research Letters 39(2), L02708.

Moy, C.M., Seltzer, G.O., Rodbell, D.T. and Anderson, D.M. 2002. Variability of El Nino/Southern Oscillation activity at millennial timescales during the Holocene epoch. Nature 420, 162-165.

Mügler, I., Sasche, D., Werner, M., Xu, B., Wu, G., Yao, T. and Gleixner, G. 2008. Effect of lake evaporation on δD values of lacustrine n-alkanes: A comparison of Nam Co (Tibetan Plateau) and Holzmaar (Germany). Organic Geochemistry 39, 711-729.

Olsson, I. (1986) Handbook of Holocene palaeoecology and paleohydrology Berglund, B. (ed), John Wiley & Sons, Chichester.

Polissar, P. and D'Andrea, W. 2014. Uncertainty in Paleohydrologic Reconstructions from Molecular dD values. Geochimica et Cosmochimica Acta 129, 146-156.

Polissar, P.J., Abbott, M.B., Wolfe, A.P., Bezada, M., Rull, V. and Bradley, R.S. 2006. Solar modulation of Little Ice Age climate in the tropical Andes. PNAS 103(24), 8937–8942.

Qui, J. 2008. China: The Third Pole Environment. Nature 454(7203), 393-396.

Seki, O., Meyers, P.A., Kawamura, K., Zheng, Y. and Zhou, W. 2009. Hydrogen isotopic ratios of plant wax n-alkanes in a peat bog deposited in northeast China during the last 16 kyr. Organic Geochemistry 40(6), 671-677.

Stott, L., Cannariato, K., Thunell, R., Haug, G.H., Koutavas, A. and Lund, S. 2004. Decline of surface temperature and salinity in the western tropical Pacific Ocean in the Holocene epoch. Nature 431, 56-59.

Stuiver, M. and Reimer, P.J. 1993. Extended 14C Data Base and Revised CALIB 3.0 14C Age Calibration Program. Radiocarbon 35(1), 215-230.

Thompson, L.G., Mosley-Thompson, E., Brecher, H., Davis, M., León, B., Les, D., Lin, P.-N., Mashiotta, T. and Mountain, K. 2006. Abrupt tropical climate change: Past and present. PNAS 103(28), 10536 –10543.

Tiwari, M., Ramesh, R., B.L.K.S., Jull, A.J.T. and Burr, G.S. 2006. Paleomonsoon precipitation deduced from a sediment core from the equatorial Indian Ocean. Geo-Marine Letters 26, 23-30.

Xia, Z.-H., Xu, B.-Q., Mügler, I., Wu, G.-J., Gleixner, G., Sachse, D. and Zhu, L.-P. 2008. Hydrogen isotope ratios of terrigenous n-alkanes in lacustrine surface sediment of the Tibetan Plateau record the precipitation signal. Geochemical Journal 42, 331-338.

3. HOLOCENE INDIAN SUMMER MONSOON INTENSITY OVER THE SOUTH-CENTRAL TIBETAN PLATEAU INFERRED FROM SEDIMENTOLOGY AND LEAF-WAX *n*-ALKANE HYDROGEN ISOTOPES

3.1 Introduction

The Indian summer monsoon (ISM) is the primary climatic system that delivers moisture to the Tibetan Plateau, accounting for more than 90% of annual precipitation for eastern and central Tibet (Tian et al., 2007). Assessing long-term and abrupt ISM variability on the Tibetan Plateau is critical because of this region's role as a water tower for much of South Asia; several of the largest rivers in South Asia have headwaters on the plateau that are reliant on stored monsoonal precipitation in the form of groundwater and glacial melt for baseflow. Model simulations suggest that these water resources are threatened by climate change (Kumar et al., 2006; Li et al., 2017; Sharmila et al., 2015), with projections of warmer air and sea surface temperatures, decreasing land-sea temperature gradients, a driving mechanism behind ocean-atmosphere circulation and the ISM. Understanding how these ocean-atmosphere circulation changes will impact the ISM is crucial, as the reliance on seasonal monsoon precipitation will increase as glaciers disappear from the landscape (Qui, 2008). Because instrumental records for the region are short (1930s to present) and spatially underrepresented at high elevations and remote regions of the Third Pole (Tian et al., 2007), paleoclimate records are essential for determining the long-term relationships between hydrologic variability and local and global climate drivers.

Given its importance, there has been considerable effort expended to reconstruct Holocene ISM variability in recent decades. The majority of research indicates that ISM precipitation reached a maximum during the early Holocene from 11.7 – 7 ka before a decline in intensity between 7.5 and 5 ka, with evidence of an earlier decline in local monsoon precipitation and intensity (*e.g.* lake levels and erosion indicators) before synoptic scale changes reflected by isotopic records in some records (Berkelhammer et al., 2012; Bird et al., 2014; Dykoski et al., 2005; Fleitmann et al., 2003; Gupta et al., 2003). The expression of the weakened monsoon varies both spatially and temporally, with evidence that the monsoon expanded in the early Holocene reaching as far as

northern Iran to the west (Djamali et al., 2010) and southeastern China to the east, contracting during the middle Holocene as a result of weakened monsoon winds and precipitation (Gupta et al., 2003; Magny and Haas, 2004). The middle Holocene weakening of the ISM was driven by declining boreal summer insolation in the Northern Hemisphere (NH), which peaked around 11 ka and began to gradual decline after 8 ka (Berger and Loutre, 1991; Fleitmann et al., 2003; Wu et al., 2018). Reduction in solar insolation resulted in a southerly shift in the Intertropical Convergence Zone (Fleitmann et al., 2003; Haug et al., 2001), weakened ISM winds near the Arabian Peninsula (Gupta et al., 2003), cooler temperatures in the NH (Marcott et al., 2013) and the Tibetan Plateau (Herzschuh et al., 2009; Herzschuh et al., 2006), and a shift to El Niño-like conditions in the Pacific (Conroy et al., 2008; Marchitto et al., 2010; Moy et al., 2002). High frequency paleoclimate records from the Tibetan Plateau indicate that superimposed on these millennial scale changes in ISM are more frequent shifts between wet and drought conditions during the early Holocene (Bird et al., 2014). This study seeks to identify how high-frequency Holocene ISM variability was expressed in the south-central Tibetan Plateau, near the westernmost extent of monsoon precipitation on the Plateau, and investigate how relative precipitation and lake level proxies respond to local and global climate drivers.

To this end, a high-resolution, multi-proxy lacustrine paleoclimate record from Cuobu, a small alpine lake located in the Gangdise Mountains on the southern Tibetan Plateau (Fig. 1). Local-scale hydroclimate at the lake and watershed level was investigated/reconstructed using sedimentology, sediment geochemistry including $\delta^{13}C$ and $\delta^{15}N$ isotopes and x-ray fluorescence (XRF), total organic matter and carbonate, and short-chain *n*-alkane hydrogen ($\delta^{2}H$) isotopes. Synoptic-scale ISM intensity was investigated using long-chain *n*-alkane $\delta^{2}H$. Isotopic difference between long-chain and short-chain *n*-alkane $\delta^{2}H$ were additionally used to estimate the ratio of local precipitation:evaporation (P:E) as an indicator of local effective moisture. The Cuobu record in conjunction with other sites on the Tibetan Plateau and from the broader ISM region is used to assess: 1) Holocene ISM variability near the westernmost extent of the ISM on the Tibetan Plateau, 2) distinguish the timing and differences between how local and synoptic hydroclimate proxies respond to changes in monsoon intensity, especially

during the middle Holocene, and 3) how high-frequency hydroclimate variability responds to local and global drivers of the ISM.

3.2 Study Area: Cuobu

Cuobu is a small (1.1 km^2) high elevation (4734 m a.s.l) alpine lake located on the southern Tibetan Plateau in the Gangdise Mountains (Fig. 3.1; 29.55813° N, 87.02519° E). The bathymetry of the lake is largely shallow with a deep northern basin that reaches a maximum water depth of 5.1 m. The lake's littoral zone is heavily vegetated with submerged and emergent macrophytes and algae. The watershed is sparsely vegetated with a few species of ferns, flowers, and mosses. The water chemistry of the lake was slightly basic (pH=8.54) with moderate conductivity (137 mS/m) and alkalinity (36 mEq/L).

The regional geology consists of Pleistocene andesite bedrock (Choubert et al., 1983) with fluvial and glacial features. The watershed for Cuobo (8.4 km^2) has been dominated by past glacial activity with the lake and its watershed resulting from the intersection of two valley glaciers (Fig. 3.2A). The watershed is flanked by steep mountain ranges to the north and southwest that reach maximum elevations of 5110 m a.s.l, while the eastern and southeastern edge of the watershed is flanked by a moraine (4750 m a.s.l), which separates the lake from a river channel, referred to here as the Cuobu River (Fig. 3.2B). The lake is situated at the eastern edge of the watershed within a wide and long (2.5 km by 3.3 km) valley and is dammed by a long terminal moraine (2.2 km).

Cuobu's main tributary is an ephemeral stream that enters the lake on its northwestern corner (Fig. 3.1). Two secondary tributaries include a small stream positioned on the western edge of the lake and an ephemeral stream on Cuobu's eastern shore. This ephemeral secondary tributary is an overflow point of Cuobu River to the east of Cuobu's watershed, which is situated approximately 20 m higher in elevation than modern lake level, separated by a medial moraine (Fig. 3.2C). The geomorphic features associated with the overflow tributary (*e.g.,* vegetation growing within the channel, limited incision) suggest that overflow events are infrequent under current climatic conditions, but may have been more frequent at times in the past when ISM precipitation

was greater and river height increased sufficiently to reactive the channel. The wider channel that surrounds the modern channel incision suggests that this river sustained greater waterflow than the current channel can support. Outflow from Cuobu occurs via an outlet on the southern edge of the lake, however, there is little surface geomorphic evidence for sustained surface flow from the outlet. Instead, it appears that today groundwater seepage reaches the surface approximately 200 m downslope from the outlet, at which point it forms a permanent surface stream that eventually flows into the Dogxung Zangbo (River), a tributary to the Yarlung Tsangpo River, which has carved a steep valley through the area.

Data from the Xigaze weather station, (located ~180 km south the lake at 3837 m a.s.l.; 29.25° N, 88.883° E) indicates that the regional climate is relatively dry, with an annual total of 367 mm of precipitation (1988-2018; Fig. 3.3), compared with the northeastern (*i.e.,* Mischke, 2008) and southeastern Tibetan Plateau (Bird et al., 2017; Bird et al., 2014). Approximately 99% of this annual precipitation occurs during the monsoon season (June-September: 363 mm), with peak precipitation in July and August. This is later in the season than eastern sites along the plateau, indicating that it takes longer for monsoon precipitation to reach the southcentral region as the monsoon system originates in the southeast of the plateau near the Nyainqêntanglha Mountains. Water isotopes indicate that precipitation is greater than evaporation (mean $\delta^{18}O$ = -16.6 ‰; mean $\delta^{2}H$ = -138.0 ‰). Mean temperatures are cool (mean annual temperature = 7.1°C, mean monthly temperatures = -2.5 – 15.4 °C), with ice cover during boreal winter months preventing evaporation during this time (Dec-Feb: mean temperature = -1.73°C, total precipitation: 0.2 mm).

3.3 Methods

3.3.1 Sample Collection

Sediment cores, surface sediments, water, and vegetation samples were retrieved from Cuobu and its watershed in June 2017 (Fig. 1). Two surface cores, A-17 (core length = 69 cm, water depth = 5.05 m) and B-17 (core length = 85 cm, water depth = 4.3 m), were retrieved using a modified piston corer. Three longer sediment cores were

collected using a modified Livingstone piston corer (Livingstone, 1955; Wright, 1967). Each 1-meter-long drive was overlapped by 30 to 50 cm to ensure complete stratigraphic recovery. The C-17 core consisted of 9 drives (water depth = 4.3 m; 728 cm total recovery). The D-17 core was collected at a water depth of 4.4 m and consisted of 5 drives for a total recovery of 371 cm. A third core collected nearby E-17 consisted of 7 drives for a total recovery of 357 cm (water depth = 4.6 m). A composite of the B-17 surface and D-17 Livingstone cores was made based on magnetic susceptibility with a total core length of 431 cm.

A transect of 14 surface sediment samples was collected across the northern side of the lake using an Ekman grab sampler to characterize the modern distribution of sediment characteristics, including all of the down-core sediment proxies, across the lake basin and their relationship with water depth and proximity to shore. Two soil samples were collected from southeast shore of the lake. Samples of aquatic and terrestrial vegetation within and surrounding the lake were additionally collected. A water sample was collected for isotopic analysis. Water chemistry, including temperature, pH, alkalinity, and conductivity was measured on site at 1-meter depth intervals using a Hydrolab MS5. Sediment, vegetation, and water samples were subsequently stored and analyzed at the Paleoclimatology and Sedimentology Laboratory at Indiana University-Purdue University Indianapolis (IUPUI).

3.3.2 Sediment Dating

Sediment ^{210}Pb, ^{214}Pb, and ^{137}Cs was measured by direct gamma counting of 21 dry, homogenized samples from the upper 41 cm of the B-15 surface core at the University of Pittsburgh. The ^{210}Pb age model was produced using the constant rate of supply (CRS) model (Appleby and Oldfield, 1978). Radiocarbon (^{14}C) dates of bulk sediment samples from the F-17 core (n=10) were measured with accelerator mass spectrometry at the Keck AMS Facility, University of California Irvine. Bulk sediment samples were dried and treated with 1 N HCl (KCCAMS, 2011; Olsson, 1986). An age model combining radiocarbon, ^{210}Pb, ^{214}Pb, and ^{137}Cs dates was established using the program Bacon (Blaauw and Christen, 2011). Dates used in this age model are reported in calendar years before present (0 ka; 0 ka = 1950 of the common era).

3.3.3 Initial Core Description

Surface and Livingstone cores were split, described, and imaged using a GeoTex Multi-Sensor Core Logger at IUPUI's (Indiana University-Purdue University, Indianapolis) Paleoclimatology and Sedimentology Laboratory. Volumetric samples (1 cm^3) were taken at 1 cm intervals for each core and drive respectively for bulk density and loss-on-ignition analysis. Wet samples were weighed, dried for 24 hours at 60 °C and reweighed to calculate dry bulk density (ρ_{dry}; g/cm^{-3}) and water content (%). Each sample was combusted 550 °C and 1000 °C for four hours and two hours, respectively, and weighed after each combustion to measure percent total organic matter (%TOM) and total carbonate (%TC; Heiri et al., 2001). Surface and Livingstone cores were subsampled at 1 cm and 0.5 cm resolutions respectively for further analysis.

Magnetic susceptibility is a measure of magnetic minerals in sediments, and is used to understand the deposition of lithics in lake sediments, with increased MS associated with higher influxes of terrestrial material to the lake during either wetter or drier conditions (Dearing, 1994; Thompson et al., 1975). Under wetter conditions the increase in MS is attributed to a greater volume of eroded terrestrial materials contributed to the lake; while drier conditions result in the concentration of terrestrial materials with lower lake levels winnowing these materials to the center of the lake. Conflicting scenarios for MS require an interpretation in conjunction with other proxies. MS was measured down-core at 0.5 cm intervals on the GeoTex Multi-Sensor Core Logger at IUPUI's Paleoclimatology and Sedimentology Laboratory.

3.3.4 Lithics & Grain Size

Distributions of sediment grain sizes were measured at 1 cm intervals across the B-17 and D-17 composite core. Grain size distributions of the surface sediments and soil samples were also measured. A portion of wet sediment (~1 g) was dried and weighed before soaking in 30% hydrogen peroxide (H_2O_2) for 24 hours. The sample was then treated with 5 aliquots of 20 mL of H_2O_2 at 70 °C to remove organic matter. Biogenic silica was removed by treating samples for 6 hours at 60 °C with 20 mL of 1 N sodium hydroxide (NaOH). Carbonates were removed from samples with greater than 3% TC as determined by LOI by treating samples with aliquots of 10 ml of hydrochloric acid (HCl)

for at least 1 hr or until there was no visible reaction. Samples were rinsed with DI water, freeze dried, and weighed to estimate %lithics. Sample preparation methods were modified from (Gray et al., 2010). Each sample was then treated with 2.5% sodium metaphosphate and sonicated. Each sample was run on a Malvern Mastersizer 2000 at IUPUI with final values the average of three measurements. Results were binned into 49 diameter size fractions between 0.2 and 2000 μm.

Grain size analysis is used to understand the influxes of sediments to the core site, but like MS, their interpretation needs to be considered within the context of other proxies. For instance, increases in grain size can indicate either lower lake levels, with the winnowing of coarse grains toward the deeper portions of the lake during low stands (Bird et al., 2017; Conroy et al., 2008; Dearing, 1997; Digerfeldt, 1986; Shuman et al., 2001; Shuman et al., 2009) or an increase in high-energy runoff and delivery of coarse terrestrial sediment to the lake during wet climatic conditions (*e.g.,* Conroy et al., 2008). In contrast, finer sediments can indicate either deeper lake levels during wetter climatic conditions (*i.e.,* increased distance between the core site and the sediment source) or a reduction in the energy of terrestrial runoff during drier conditions.

3.3.5 X-ray Florescence (XRF) Geochemistry

Scanning XRF geochemistry was measured at 0.5 cm resolution down the length of the B-17 surface core and D-17 Livingstone core drives. Measurements were made using an ITRAX XRF Core Scanner at the Large Lakes Observatory, University of Minnesota Duluth (Croudace et al., 2006) for select elements (Al – Ur) and are reported in counts per second (cps). A Cr source tube (30 kV, 55 mA) was used with a 15 second dwell time and 10 mm resolution. Peak optimization was made using Qspec 8.6.0 software.

3.3.6 Elemental Abundances & Isotopic Composition of Organic Carbon & Total Nitrogen

Measurements of total organic carbon (TOC), total nitrogen (TN), $\delta^{13}C$, and $\delta^{15}N$ were made at the Large Lakes Observatory, University of Minnesota Duluth. Sediment samples were measured at a 2 cm resolution for the composite B-17 and D-17 core.

Samples with less than 5% total carbonate as determined by LOI were homogenized and weighed (~4 mg) into tin capsules. Samples with greater than 5% total carbonate were homogenized and weighed (~12 mg) into silver capsules. The samples were injected with 50 µl DI water and placed in a desiccator with an open beaker of 12M HCl. Samples were acidified overnight and air-dried to remove HCl before being placed in tin capsules.

Measurements were made with a Thermo Finnigan Delta Plus XP isotope ratio mass spectrometer (IRMS) fitted with a Conflo III device and a Costech 4010 elemental combustion system at the Large Lakes Observatory, University of Minnesota Duluth. Samples were run against a series of standards including acetanilide, B-2153, B-2159, USGS41, and caffeine (standards from the National Institute of Standards and Technology). Values are reported in delta notation as the per mil (‰) deviation from Vienna Peedee Belemnite (VPDB) for $\delta^{13}C$ and air for $\delta^{15}N$.The coefficient of variation standards ranged between 1.4-3.8% for N and 0.5-2.5% for C while isotopic precision was 0.04-0.13‰ and 0.06-0.2‰ for $\delta^{13}C$ and $\delta^{15}N$.

The ratio of total organic carbon to total nitrogen (C:N) reflects shifts in organic matter sources in lacustrine systems, with values under 10 indicating aquatic derived organic matter and values above 15 indicating terrestrial organic matter (Meyers, 1999). The isotopic composition of organic carbon ($\delta^{13}C_{org}$) is affected by photosynthetic pathways, with C_3 land plants and algae being isotopically similar (range: - 30 to -25‰), depending on lake water CO_2, while C_4 plants are more enriched (range: -14 to -10‰; Meyers, 1999). The isotopic composition of total nitrogen ($\delta^{15}N$) is also affected by productivity source, but must be considered in conjunction with other productivity proxies due to its complex nature as it also impacted by other processes, such as nitrogen cycling within the water column (Meyers and Lallier-Vergès, 1999). Higher $\delta^{15}N$ is often correlated with terrestrial productivity and a higher C:N ratio (Thornton and McManus, 1994).

3.3.7 Lipid Extractions & δ^2H Isotopes

Thirty-four samples were collected from the composite core for long-chain *n*-alkane extraction and hydrogen isotopic measurements (δ^2H) at the Lamont-Doherty Earth Observatory, Columbia University. Lipids were extracted from homogenized

sediments with a 9:1 dichloromethane and methanol solvent on a Dionex Accelerated Solvent Extractor (ASE–350). The aliphatic fraction was isolated using hexane solvent across a silica gel column (70-230 mesh, 60A). Ketone and polar fractions were isolated subsequently using dichloromethane and methanol. The *n*-alkanes were purified with a second separation across a silver nitrate column (10% $AgNO_3$) with hexane solvent. N-alkane distribution and concentration was determined using an Agilent Technologies 7890A gas chromatography mass spectrometer (GCMS). Leaf wax δ^2H isotopic measurements were made on the extracted *n*-alkanes using a combined GCMS-IRMS (Thermo Scientific Trace GC Ultra GCMS and Delta V Plus IRMS; GC column: 30m, 0.25mm, 14.2psi, 60°C). A mixture of long-chain *n*-alkanes (Mix A7) and a reference sample were both used as standards. Values are reported in delta notation as the per mil (‰) deviation from VSMOW (Vienna Standard Mean Ocean Water). Sample isotopic values were corrected using MATLAB with uncertainties ranging between 3.2% and 4.2% (1 σ s.e.m.; (Polissar and D'Andrea, 2014).

Average chain length (ACL) quantifies whether short or long-chain *n*-alkanes are more abundant (Diefendorf et al., 2015; Mügler et al., 2008), while the carbon preference index (CPI) represents the ratio of odd to even carbon atoms in *n*-alkanes (Marzi et al., 1993). Higher values for both the ACL and CPI are indicative of more terrestrial organic matter in the lake, which suggests either increased productivity in the watershed and/or increased delivery of terrestrial organic matter to the lake.

$$\mathrm{ACL} = \frac{25[C25] + 27[C27] + 29[C29] + 31[C31] + 33[C33] + 35[C35] + 37[C37]}{[C25] + [C27] + [C29] + [C31] + [C33] + [C35] + [C37]}$$

$$CPI = \frac{([C23] + [C25] + [C27] + [C29] + [C31] + [C33] + [C35]) + ([C25] + [C27] + [C29] + [C31] + [C33] + [C35] + [C37])}{2\,X\,([\mathrm{C24}] + [\mathrm{C26}] + [\mathrm{C28}] + [\mathrm{C30}] + [\mathrm{C32}] + [\mathrm{C34}] + [\mathrm{C36}])}$$

In contrast to the ACL and CPI, the aquatic vegetation index (P_{aq}) quantifies the abundance of short-chain *n*-alkanes in the sediments, with higher values indicating increased aquatic vegetation productivity (Ficken et al., 2000; Seki et al., 2009).

$$Paq = \frac{[C23] + [C25]}{[C23] + [C25] + [C29] + [C31]}$$

3.3.8 Effective Moisture Estimation

Because the δ^2H of *n*-alkanes produced by aquatic vegetation (e.g., δ^2H_{C23}) reflect the δ^2H of lake water, it integrates isotopic variability related to both changes in ISM precipitation and lake volume changes as a result of evaporation. The later isotopic effects can be isolated by subtracting precipitation isotopic variability, captured by long-chain n-alkanes (δ^2H_{C31}), from aquatic isotopic variability (δ^2H_{C23}). The resulting so-called delta-delta index ($\Delta\delta^2H_{C23\text{-}C31}$) provides a semi-quantitative estimate of the ratio of precipitation to evaporation (P:E) where higher $\Delta\delta^2H_{C23\text{-}C31}$ values indicate a reduction in lake volume from greater evaporation relative to precipitation (i.e., lower effective moisture) whereas lower $\Delta\delta^2H_{C23\text{-}C31}$ values reflect an increase in effective moisture and lakes volumes as a result of reduced evaporation relative to precipitation (Aichner et al., 2010; Mügler et al., 2008; Seki et al., 2009).

3.4 Results

3.4.1 Core Description

The lithology of the composite core was characterized by massive units of light brown, fine grained sediments with small fragments of aquatic grasses throughout the core.

3.4.2 Age Model

Excess ^{210}Pb was highest in the top 2.5 cm (0.19-0.20 Bq/g) of the B-17 core and reached background levels at 22.5 cm (Table 3.1; Fig. 3.4). Only three samples had measurable ^{137}Cs at 2.5, 16.5, and 18.5 cm. Ten radiocarbon dates from bulk sediments were measured from the E-17 and D-17 core. Dates were calibrated using IntCal 13.0 (Reimer et al., 2013). The oldest radiocarbon date was 7910 ± 20 cal yr BP. Comparison between the ^{210}Pb and ^{14}C dates from the same depths at the top of the E-17 surface core

showed a carbon reservoir effect of 930 years, which was subtracted from all radiocarbon dates in the age model. The age model shows continuous deposition at the lake, with no hiatuses, and spans the past 8.34 ka (Fig. 3.5). Full age results for Cuobu are in Appendix 1, Table A 2.1.

3.4.3 Elemental Abundances & Isotopic Composition of Organic Carbon & Total Nitrogen

Total organic matter (%TOM) was lowest in the early Holocene from 8.3 – 5 ka, averaging 42.2% (Fig. 3.6A). %TOM gradually increased from 5 – 2 ka by 8.5%, then subsequently decreased from 2 ka to present (35.9%; Fig. 3.6A). Total carbonate (%TC) was low for most of the record with a mean of 5.6% (range: >0.01 – 41.2%), with elevated TC from 2.9 – 33.3% from 2.6 – 2.1 ka (Fig. 3.6B).

The ratio of total organic carbon to total nitrogen (C:N) averaged 9.3 across the Cuobu record (range: 6.1 – 12.2), with high C:N from 7.3 to 2.3 ka (range: 9.5-12.2) and lower C:N for the late Holocene (range: 6.1 – 9.2; Fig. 3.6E). At Cuobu, $\delta^{13}C_{org}$ was lowest at the beginning of the record, averaging -16.2 ‰, gradually increasing by 2.4 ‰ by 5 ka when $\delta^{13}C_{org}$ plateaued (Fig. 3.6C). $\delta^{13}C_{org}$ varied significantly over the last 3 ka, with an increase of 6.1 ‰ over the early Holocene from 0.9 to 0.5 ka. The trend for $\delta^{15}N$ follows a similar pattern as $\delta^{13}C_{org,}$ with lower $\delta^{15}N$ in the earliest part of the record, averaging 2.4 ‰ around 8.3 ka, gradually increasing by 0.6 ‰ until 5 ka (Fig. 3.6D). $\delta^{15}N$ values at Cuobu peak at 4.5 ‰ in the last 1 ka and remain elevated.

3.4.4 Lipid Biomarkers

Sedimentary *n*-alkanes are valuable biomarkers, providing a record of past vegetation and the isotopic composition of regional precipitation and lake water. Short-chain C23 *n*-alkanes are derived from aquatic vegetation (Ficken et al., 2000; Seki et al., 2009) and were the most abundant throughout the record, with concentrations ranging from 510 to 98,208 ng/g (mean: 26,691 ng/g), but decreased sharply after 2 ka (Fig. 3.7A). C25 and C27 *n*-alkanes are a mixture of aquatic and terrestrial vegetation and averaged 19,395 ng/g and 18,036 ng/g respectively (Fig. 3.7B and 3.7C). Long-chain C29 and C31 *n*-alkanes are synthesized by terrestrial vegetation (Mügler et al., 2008; Seki et

al., 2009). Both C29 (range: 749-28920 ng/g) and C31 (range: 1051-32,072 ng/g) were less abundant than short-chain *n*-alkanes in the record, with averages of 14,717 and 12,672 ng/g respectively (Fig. 3.7D and 3.7E), with C31 increasing over the past 2 ka.

ACL values ranged from 27.2 – 28.6 throughout the early and middle Holocene (8.3 to 2 ka, mean: 27.6), increasing sharply after 2 ka, with a range of 28.8 – 29.6 (mean: 29.1; Fig. 3.7F). The ACL suggests that aquatic vegetation remained high until 2 ka, when the plant community shifted to a terrestrial dominated vegetation community. CPI showed a similar pattern, with low values, ranging from 3.7 – 6.9, from 8.3 – 2 ka (mean: 4.4; Fig. 3.7G). After 2 ka, CPI increased, ranging from 6.1 – 8.3 (mean: 6.5), suggesting a shift from aquatic to terrestrial vegetation dominated contributions to the lake.

At Cuobu, P_{aq} was highest from 8.3 to 2 ka, averaging 0.68 (range: 0.57 – 0.76), and decreased by 0.32 over the last 2 ka (Fig. 3.8H). P_{aq} concurs with the ACL and CPI indices that aquatic vegetation remained high until 2 ka when terrestrial vegetation inputs increased.

3.4.5 Hydrogen Isotopes

Leaf wax *n*-alkane hydrogen (δ^2H) isotopes provide information about precipitation and lake water isotope signatures. Short-chain *n*-alkanes δ^2H (*i.e.,* C23) are produced by aquatic vegetation that incorporate hydrogen directly from lake water, which integrates variations in the isotopic composition of lake water (in part due to evaporation and lake volume changes) as well as variations in precipitation (Liu and Liu, 2016; Mügler et al., 2008; Seki et al., 2009). Short-chain C23 *n*-alkane δ^2H (δ^2H_{C23}) averaged -248.2 ‰ and ranged between -263.0 to -235.2 ‰ over the record (Fig. 3.8A). δ^2H_{C23} was low from 8.3 to 5 ka, averaging -253.1 ‰, before increasing by ~15 ‰ to -268 ‰ from 5 to 2.5 ka. From 2.5 ka to present, δ^2H_{C23} showed high isotopic variability, with a shift towards wetter conditions around 2 ka, with the largest decrease around 1 ka to an average of -260.2 ‰.

Terrestrial vegetation utilizes soil water during its photosynthetic processes, which is isotopically similar to precipitation and is incorporated in long-chain *n*-alkane δ^2H (Xia et al., 2008). With more than 90% of precipitation at Cuobu derived from the ISM, variations in long-chain *n*-alkane δ^2H (*i.e.,* C29, C31) are inferred to reflect changes

in the monsoon (*e.g.,* Bird et al., 2014). Long-chain *n*-alkanes δ^2H_{C29} and δ^2H_{C31} exhibited similar trends as the short-chain *n*-alkanes (Fig. 3.8D-E). δ^2H_{C29} was lower from 8.3 to 6 ka, averaging -253.1‰, before gradually increasing to a mean of -245.3 ‰ at 2.5 ka. After 2.5 ka, δ^2H_{C29} decreased, remaining low until 1 ka (-258.6 ‰), after which δ^2H_{C29} subsequently increased and remained high until the present (mean: -244.9 ‰). δ^2H_{C31} was low from 8.3 to 5 ka (mean: -261.1 ‰), but subsequently increased after 2 ka, with an isotopic range between -267.5 to -237.0 ‰.

Mid-chain length δ^2H_{C25} and δ^2H_{C27}, showed similar patterns to short-chain *n*-alkanes on millennial and centennial time scales, with lower values during the early Holocene (8.3 – 6 ka), with an isotopic range between -246.1 to -251.9 ‰ for δ^2H_{C25} and -247.2 to -250.7 ‰ for δ^2H_{C27} (mean: -250.0 ‰, mean $\delta^2H_{C27:}$ -249.1 ‰; Fig. 3.8B). δ^2H_{C25} increased by 9.9 ‰ between 6 to 2.5 ka (mean: -239.6 ‰); while δ^2H_{C27} increased by 9.6 ‰ (mean: -239.5 ‰).

3.4.6 Effective Moisture

The delta-delta index ($\delta^2H_{C23\text{-}C31}$) estimates the ratio of precipitation:evaporation (P:E) $\Delta\delta^2H_{C23\text{-}C31}$ in Cuobu was variable, but generally low during the early Holocene from 8.3 to 5 ka, averaging -6.7, suggesting precipitation exceeded evaporation (high P:E; Fig. 3.8F). Higher frequency variability indicates that superimposed on this trend of a wetter (high P:E) early Holocene, there were two periods of higher P:E interspersed with lower P:E conditions. At 5 ka, $\Delta\delta^2H_{C23\text{-}C31}$ increased and remained elevated until 1 ka, averaging -1.6. From 1 to 0.5 ka, $\Delta\delta^2H_{C23\text{-}C31}$ decreased again, averaging -6.1, and then increased from 0.5 ka to modern, averaging -12.4.

3.4.7 Sedimentology

Several sedimentological proxies are used to assess changes in the input of clastic materials eroded from the watershed into the lake. Bulk density is a measurement of the mass of sediment per a given volume and has an inverse relationship with organic matter and water content (Brady, 1984). In the Cuobu core, bulk density was highly variable, ranging 0.01 – 3.5 g x cm^{-3} throughout the record (mean: 0.14 g x cm^{-3}; Fig. 3.9A). Bulk

density was highest during the early Holocene from 8.3 to 6.5 ka, averaging 0.12 g x cm^{-3} and sharply declines around 6 ka and again from 4.5 to 3 ka.

Magnetic susceptibility (MS) ranged from -1.5 to 0 SI x 10^{-5} and averaged -0.78 SI x 10^{-5} for the record (Fig. 3.9B). MS was higher from 8.3 to 5 ka (mean: -0.62 SI x 10^{-5}) before decreasing from 5 ka to present (mean: -0.9 SI x 10^{-5}), with a sharp increase around 1 ka. High frequency variability of MS follows bulk density, indicating a stronger relationship between these proxies.

Both %clay and %silt was lower from 8.3 to 5 ka, with %clay ranging from 0.43 % to 20.8 % and %silt ranging from 5.7 % to 82.1% (mean: clay: 6.7 %; silt: 45.7 %; Fig. 3.9C and 3.9D). From 5 ka to present, %clay and %silt increased by 3.7 % and 12.6 % respectively (5 ka – present; mean %clay: 10.4 %; %silt: 59.8 %). Percent sand, showed the opposite trend of %clay and %silt, ranging 1.4 % to 93.6 % from 8.3 to 5 ka (mean: 47.6 %) and decreased from 5 ka to present by 17.5 % (mean: 29.7 %; Fig. 3.9E). A histogram of the grain size diameters shows that the Cuobu record had higher abundances of coarse sediments from 8.3 to 4.5 ka when the distribution abruptly shifts to favor finer sediments (Fig. 3.9F). Finer sediments were more abundant until 1 ka with short periods of coarser sediment influxes.

3.4.8 X-ray Fluorescence (XRF) Geochemistry

Of the forty-nine elements measured using XRF, I focus here on titanium (Ti), and zirconium (Zr). Ti and Zr are both conservative elements that are associated with lithic materials, with increased concentration of any of these elements being associated with greater terrestrial sediment inputs into the lake environment (Chassiot et al., 2018; Croudace et al., 2006; Cuven et al., 2010; Löwemark et al., 2011; Nesbitt and Markovics, 1997; Roberts et al., 2019). In the Cuobu record, Ti shows a pattern of higher concentrations during the early Holocene, ranging from 9348 – 18,577 cps (mean: 14,436 cps), than gradually decreased from 6 to 2.5 ka by 6270 (mean: 8165 cps; Fig. 3.9G). Ti concentrations increased again by 1929 in the late Holocene around 2.5 ka and remained high until present (mean: 10,121 cps). Zr showed a similar pattern as Ti, with higher concentrations in the early Holocene (8.3 – 6 ka) ranging from 430 to 1573 cps (mean: 927 cps; Fig. 3.9H). Average Zr gradually decreased by 353 from 6 to 3 ka when average

Zr increased again by 88.3 from 3 ka to present (mean: 661 cps). The full XRF dataset are in Appendix 2 Tables A 2.1 – 2.6.

3.4.9 Statistical Analysis

A Principal Components Analysis (PCA) was performed on select data from Cuobu including lithics, TOM and TC, n-alkane concentrations and their metrics (ACL, CPI, P_{aq}), $\Delta\delta^2H_{C23\text{-}C31}$, C:N ratios, and $\delta^{13}C$ and $\delta^{15}N$ isotopes. All data were normalized using a z-score with the mean subtracted from each value and divided by the standard deviation. The distribution of proxies as evidenced in a biplot of the PCA, shows the grouping of proxies and their relation to each other as they are correlated with the two principal components (Fig. 3.10). Principal Component 1 (PC1) accounts for 40.6% of the variability in the dataset, while Principal Component 2 (PC2) accounts for an additional 16.1% of the dataset variability. The PCA biplot shows that fine sediments (%clay and %silt), *n*-alkane concentrations (nC23 – nC29) and TC are all positively correlated with PC1 and PC2 (top right quadrant). P_{aq}, BD, and TOM are positively correlated with PC1 and negatively correlated with PC2 (bottom right quadrant). C:N, $\delta^{13}C$, $\delta^{15}N$, %lithics, ACL, CPI, δ^2H_{C23}, and Ti are all positively associated with PC1 and negatively associated with PC2 (top left quadrant). %sand, MS, Zr, mid-chain and long-chain *n*-alkane hydrogen isotopes (δ^2H_{C25} – δ^2H_{C25}) are all negatively associated with PC1 and PC2 (bottom left quadrant). A second PCA was conducted only on grain size proxies, %clay, %silt, and %sand, and the time series of PC1, which accounts for % of the dataset variability, closely follows the same trends as %sand.

3.5 Discussion

3.5.1 Inferred ISM Precipitation & Evaporation on the South-Central Tibetan Plateau

Leaf-wax *n*-alkane δ^2H show pronounced shifts in ISM strength and P:E balance at Cuobu during the last 8 ka. δ^2H isotopic composition is controlled by the amount of precipitation and the moisture source (Sachse, 2012), with lower δ^2H values inferred as greater precipitation. With terrestrial plants incorporating ISM precipitation during the growing season, I interpret δ^2H_{C31} as a signal of monsoon intensity over the region. At

Cuobu, low δ^2H_{C31} values suggest a strengthened ISM from 8.3 to ~5 ka, after which high δ^2H_{C31} indicates a weakened ISM from 5 to 1 ka. From 1 ka to the present, lower δ^2H_{C31} suggests a slight strengthening of the ISM. The interpretation of short-chain *n*-alkanes δ^2H_{C23} is more complex, with lake water incorporating the isotopic signals of evaporation and the ISM. Lake water isotopes (δ^2H_{C23}) at Cuobu showed similar long-term trends as δ^2H_{C31}, indicating that the isotopic composition of lake water largely tracked that of precipitation during the Holocene. Supporting wet local conditions between 8 and 5 ka, the $D\delta^2H_{C23\text{-}C31}$ record shows low values, indicating a positive P:E balance at Cuobu at the same time that the ISM was strengthened (low δ^2H_{C31}). While most of this period had higher effective moisture, there was a noted increase in the P:E balance between 6.2 to 6 ka, which corresponds to a drop in the C:N ratio, that indicates drought conditions locally. Following early Holocene pluvial conditions, $D\delta^2H_{C23\text{-}C31}$ shows a sharp increase between 5.5 and 4.5 ka, indicating a decrease in the local P:E balance that occurred when ISM intensity was also diminished (high δ^2H_{C31}). A decrease in the $\Delta\delta^2H_{C23\text{-}C31}$ record after 1 ka additionally supports wetter conditions locally from ~1 ka to the present that coincides with a suggested strengthening of the ISM during this time in the δ^2H_{C31} timeseries.

The interpretation of local hydroclimate is supported by the aquatic and terrestrial vegetation proxies. The $\delta^{13}C_{org}$ record suggests a high contribution of aquatic and/or C_3 land plants from 8.3 to 5 ka, after 5 ka there was a higher influx of C4 plant terrestrial vegetation productivity inputs to the lake, with terrestrial vegetation dominating over the last 1 ka. This corresponds to a shift from higher C:N ratio from 8.3 to 2 ka to lower C:N 2 ka to present, suggesting a shift from larger aquatic plants to planktonic aquatic productivity. The $\delta^{15}N$ record productivity interpretation, like the $\delta^{13}C_{org}$ record, indicates high aquatic productivity between 8.3 and 5 ka, with terrestrial vegetation inputs increasing throughout the middle and late Holocene with highest terrestrial productivity over the last 1 ka.

Wet conditions at Cuobu in the early Holocene correspond to high aquatic productivity from 8.3 to 5 ka indicated by high concentrations of short-chain *n*-alkanes (C23) and lower $\delta^{13}C$ and $\delta^{15}N$. Productivity shifted to terrestrial dominated vegetation inputs in Cuobu during the middle and late Holocene, with a mixed aquatic and terrestrial

vegetation signal indicated by $\delta^{13}C$ and $\delta^{15}N$ from 5 to 1 ka, while the *n*-alkanes concentrations shifted abruptly to higher long-chain concentrations between 2.5 and 2 ka. The decline in *n*-alkane derived aquatic productivity around 2.5 ka occurred much later than the shift to drier conditions indicated by δ^2H_{C31} and $\Delta\delta^2H_{C23\text{-}C31}$ or the mixed-vegetation signal suggested by the $\delta^{13}C$ and $\delta^{15}N$ isotope data. The difference in the timing between these vegetation proxies suggest that after ISM precipitation and effective moisture declined around 5 ka lake levels began to decline, but remained high enough to support a shift in vegetation communities from more aquatic planktonic species to a mixture of emergent and submerged macrophytes with terrestrial vegetation.

3.5.2 Monsoon-induced Cuobu River Overflow

Grain size variations are typically interpreted as reflecting either lake level change (Bird et al., 2017; Bird et al., 2014; Dearing, 1997; Digerfeldt, 1986; Shuman et al., 2001; Shuman et al., 2009) or the energy and amount of runoff entering a lake (Conroy et al., 2008). While, other lake-based paleoclimate studies from the Tibetan Plateau (TP) have interpreted grain size proxies, %sand in particular, as lake level indicators (Bird et al., 2017; Bird et al., 2014), this does not appear to be the case at Cuobu. If interpreted in terms of lake level, the Cuobu sand record would suggest low lake levels between 8.3 and 4.5 ka and after 1 ka and high lake levels from 4.5 to ~1 ka. This pattern of Holocene hydroclimate variability stands in stark contrast to the multitude of other ISM reconstructions from the TP that indicate a strengthened monsoon, in agreement with the δ^2H_{C31} record at Cuobu, and high lake levels during this time (Bird et al., 2017; Bird et al., 2014; Herzschuh et al., 2009; Zhu et al., 2008). Instead, I contend that the Cuobu sand records reflect changes in monsoon-derived runoff entering the lake whereby increased monsoonal runoff delivered greater quantities of sand and vice versa. This interpretation is consistent with lower δ^2H_{C31} and $\Delta\delta^2H_{C23\text{-}C31}$ between 8.3 and 4.5 ka, which respectively indicate intensified monsoonal precipitation and greater effective moisture at Cuobu when sand abundances were high. High frequency variability in %sand between 8.3 and 4.5 would indicate that runoff was highly variable during the early Holocene through the early half of the middle Holocene, with high runoff from 8.3 to 6.2 ka and 6 ka to 4.5 ka while runoff declined from 6.2 to 6 ka. Conversely, decreased sand

abundances between 4.5 and 1 ka occurred when δ^2H_{C31} and $\Delta\delta^2H_{C23\text{-}C31}$ increased, indicating a reduction in sand when monsoonal intensity weakened and effective moisture decreased. The Ti and Zr records further support interpreting sand abundances in terms of terrestrial eroded sediments and surface runoff to the lake. Higher titanium and zirconium concentrations from 8.3 to 5 ka corresponded with high %sand, with the influx of sand and terrestrial sediments co-occurring with wetter conditions at Cuobu as indicated by the $\Delta\delta^2H_{C23\text{-}C31}$ record.

Determining the mechanism responsible for Holocene sedimentology at Cuobu, with coarser sediments inferred as runoff, requires an understanding of the physical environment. The geomorphology of the site shows that Cuobu formed behind glacial moraines that both dammed the valley and separated the lake from the Cuobu River. One of the ephemeral tributaries to the lake is a dry stream channel that cuts across the moraine and forms a delta into the lake; connecting Cuobu with the Cuobu River. I suggest that the geomorphological setting of Cuobu is the primary driver of the grain size signal. Increased sand at Cuobu during a period of stronger monsoon intensity can be attributed to an influx of sediment from the Cuobu River. During the early Holocene ISM maximum, this stream could have been an important source of sediments to the lake and is closer to the core sites than the other tributaries, which supports coarser sediments influxes coming from this stream channel. Cuobu River is situated at a higher elevation than the lake, but at a lower base elevation than the moraine crest, requiring high river discharge to breach the moraine, contributing a flow of water and coarser sediments directly into the lake through the ephemeral stream channel. Modern observations of the site show that the overflow channel could have accommodated large water volumes and is perfectly situated at the lowest point of the moraine at the junction between the moraine and the mountain spur where the braided channel formed. In the early Holocene, increased ISM precipitation may have increased fluvial discharges and contributed to overland flooding. River height would need to be 5 m higher than modern water levels for overbank flooding to breach the moraine and connect the overflow tributary to the lake. When monsoon intensity declined during the middle Holocene, water levels fell at both Cuobu and Cuobu River disconnecting the flow of water and coarse sediments from river to the lake.

3.5.3 Synoptic vs. Local Hydroclimate at Cuobu

Cuobu shows a strong agreement between synoptic and local hydroclimate proxies, with millennial scale trends in ISM variability indicating pluvial (wet) conditions from 8.3 to 5 ka and 1 ka to present and drought conditions from 5 to 1 ka. Higher frequency variability during the early Holocene shows pluvials from 8.3 to 6.2 ka and again from 6 to 5 ka with drought conditions from 6.2 to 6 ka. Pluvials at Cuobu are indicated by high %sand, low $\Delta\delta^2H_{C31}$, high P:E balance (low $\Delta\delta^2H_{C23\text{-}C31}$), and increased aquatic productivity. Drought conditions are indicated by low %sand, high $\Delta\delta^2H_{C31}$, low P:E balance, and higher terrestrial vegetation inputs. PCA of the Cuobu synoptic and local hydroclimate proxies supports the association of fine sediments with TOM and *n*-alkane concentrations (C23 – C29) and coarse sediments are associated with mid-chain and long-chain *n*-alkane hydrogen isotopes ($\delta^2H_{C25} – \delta^2H_{C31}$). P:E balance ($\Delta\delta^2H_{C23\text{-}C31}$) is associated with short-chain *n*-alkane $\Delta\delta^2H_{C23}$, long-chain *n*-alkane concentrations (C31), $\delta^{13}C$, $\delta^{15}N$, ACL and CPI. A PCA of the grain size measurements was used to assess the time series of the sedimentology at Cuobu, with the PC1 time series strongly reflecting the %sand record (Fig. 3.11B). The strong relationship between synoptic and local hydroclimate proxies, with changes in large-scale monsoon drivers having an immediate impact on local monsoon expression, has also been observed in other hydroclimate records from the Tibetan Plateau (Bird et al., 2014).

To better understand spatiotemporal ISM variability on the Tibetan Plateau, I compare the Cuobu record with high-resolution paleoclimate records from Paru Co (Bird et al., 2014). A high elevation lake from the southeastern plateau, Paru Co (29.796°N, 92.352°E, elevation 4845 m a.s.l.; 520 km east of Cuobu) is a precipitation and lake level record for the last 11 ka in southeastern Tibet (Bird et al., 2014). Similar to Cuobu, long-chain *n*-alkane δ^2H_{C27} and δ^2H_{C29} indicate strengthened ISM precipitation at Paru Co until 5 ka when ISM intensity declined. Lake levels at Paru Co, as interpreted from %sand, and runoff intensity, interpreted from %lithics, also show similar trends with the Cuobu record. Specifically, runoff was high during the early and the late Holocene at Paru Co (8.3 – 7 and 1.5 – 0.5 ka), while lake levels remained high throughout the early and middle Holocene (8.3 – 5 ka). The centennial scale variability at Paru Co also shows agreement with Cuobu, with deeper lake levels and increased runoff at Paru Co

coinciding with higher %sand and greater effective moisture (low P:E) from 8.3 to 6.2 ka, after which lake levels and runoff at Paru Co decreased in conjunction with lower runoff and effective moisture at Cuobu. Runoff at Paru Co increased from 1.5 and 0.5 ka indicating an increase in monsoon intensity, which corresponds with higher effective moisture and increased %sand at Cuobu. A late Holocene increase in ISM intensity was also observed at another eastern TP lake, Nir'Pa Co, with increased %lithics and %sand over the last 1 ka indicating a stronger monsoon (Bird et al., 2017). These trends in local hydroclimate were driven, not only by synoptic ISM dynamics, but also local climate conditions including temperature.

3.5.4 Millennial & Orbital Scale Drivers of ISM Variability

Holocene ISM variability has been attributed to multiple drivers, including solar insolation, the migration of the ITCZ, and the ocean-atmosphere system. Northern Hemisphere (NH) solar insolation was highest during the early Holocene and began to decline around 8 ka (Berger and Loutre, 1991), which drove the southward migration of the ITCZ (Fleitmann et al., 2003; Haug et al., 2001) and cooler temperatures on the plateau (Herzschuh et al., 2009; Herzschuh et al., 2006). ITCZ record at Qunf Cave in Oman (17º10'N 54º18'N), shows that the ITCZ slowly migrated south from 8.3 ka until 5 ka (Fleitmann et al., 2003). The southward latitudinal displacement of the ITCZ stabilized from 5 to 3 ka, coinciding with the decline in effective moisture at Cuobu.

In addition to isolation-forced ITCZ variability, changes in the ocean-atmosphere system play a leading role in millennial and higher-frequency ISM variability. A strong sea surface temperature (SST) gradient in the equatorial Pacific (La Niña-like state: cool eastern and warm western equatorial Pacific) during the Holocene between 11 and 4 ka, for example, corresponded with enhanced ISM intensity, greater effective moisture, and high lake levels across much of the Tibetan Plateau (Conroy et al., 2008; Koutavas and Sachs, 2008; Marchitto et al., 2010; Moy et al., 2002). After 4 ka, the SST gradient reversed (El Niño-like state: warm eastern and cool western equatorial Pacific), which corresponded to reduced ISM intensity, lower effective moisture and lake levels across the Tibetan Plateau, and weaker ISM winds that reduced upwelling in the Arabian Sea (Gupta et al., 2003). The co-occurrence of pluvial conditions on the TP during La Niña-

like conditions is consistent with modern climatic relationships between the Tropical Pacific and ISM with weak annual monsoons linked to El Niño events and strong annual monsoons corresponding with La Niña events (Chowdary et al., 2016; Samanta et al., 2020; Surendran et al., 2015).

These orbital drivers of ISM variability are reflected in the millennial scale trends of synoptic and local hydroclimate at Cuobu. Wet conditions at Cuobu during the early Holocene ISM maximum were driven by high insolation and the northerly ITCZ, while the middle Holocene transition to dry conditions around 5 ka corresponds with drier conditions at other sites on the Tibetan Plateau and evidence of weakening ISM precipitation and winds throughout the region (Bird et al., 2014; Cai et al., 2012; Fleitmann et al., 2003; Fleitmann et al., 2007; Herzschuh et al., 2009). The timing of the middle Holocene transition at Cuobu shows that runoff (%sand) and P:E balance abruptly shifted in response to reduced solar insolation, the southward migration of the ITCZ, and the shift to El Niño-like conditions in the Pacific. Lake levels at Paru Co also decreased at this time, indicating that local hydroclimate on the southeastern TP was consistent at these sites that are over 500 km apart. While there is strong agreement with these orbital drivers on ISM expression at Cuobu on longer time scales, these drivers do not account for the higher-frequency variability seen in the Cuobu record, particularly during the early and late Holocene.

3.5.5 Drivers of Decadal & Centennial ISM Variability

Higher frequency variability at Cuobu is superimposed on the millennial trends of a wet early and late Holocene and a dry middle Holocene, which is driven by centennial and decadal scale variability in local climate and SSTs. Local hydroclimate is reflective of local and regional precipitation, temperature, and evaporation patterns. Temperature and effective moisture records from the Tibetan Plateau help explain how local climate can drive regional monsoon expression. One temperature record from the Tibetan Plateau at Lake Zigetang (90.9ºE 32.0ºN, 463 km northeast of Cuobu), shows that the early Holocene was a warm, humid environment as inferred by dominant temperate steppe vegetation (Herzschuh et al., 2006). After 5 ka, the eastern Tibetan Plateau transitioned to a drier, cooler environment; while there was a modest warming over the last 1 ka. This

warming over the last 1 ka corresponds to the decline in effective moisture seen at Cuobu, suggesting that higher evaporation reduced effective moisture even as monsoon intensity increased.

The Koucha Lake temperature and effective moisture pollen record (97.2 ºE 34.0ºN, 1,090 km northeast of Cuobu) also showed warmer, wetter conditions in the early Holocene until 7 ka, when effective moisture began to gradually decline (Herzschuh et al., 2009). Koucha Lake also supports a drier, arid hydroclimate in the eastern Tibetan Plateau during the middle and late Holocene (5 ka to modern), as evident in the Cuobu $\Delta\delta^2H_{C23\text{-}C31}$ record from 5 to 1 ka. A persistently drier, more evaporative middle and late Holocene is also evident in the ISM record at Tianmen Cave (90º4'E, 30º55'N; Fig. 3.12C) at the easternmost edge of the Tibetan Plateau (Cai et al., 2012). ISM intensity at Tianmen Cave gradually declined after ~ 7 ka with a hiatus in the record between 3.5 and 1 ka; indicating a drier climate in eastern Tibet from 7 to 1 ka. Calcite precipitation restarted temporarily around 1 ka, simultaneous with the higher effective moisture at Cuobu, increased runoff at Cuobu and Paru Co, and deeper lake levels exhibited at Nir'Pa Co (Bird et al., 2017).

Centennial monsoon variability at Cuobu during the early and late Holocene can be attributed to both local temperature records as well as SSTs. Early Holocene pluvials from 8.3 to 6.2 ka and 6 to 5 ka coincide with warmer temperatures and La Niña-state in the equatorial Pacific, while drought conditions from 6.2 to 6 ka correspond with colder temperatures on the TP and an El Niño-like state. Late Holocene increases in effective moisture and runoff at Cuobu from 1 ka to present are reflective of relatively warmer temperatures on the plateau with highly variable shifts between La Niña and El Niño-like states. Coherent patterns in centennial scale local hydroclimate between Tibetan Plateau records at Cuobu and Paru Co indicate that monsoon expression in the southeastern-southcentral Tibetan Plateau is strongly impacted by the land-sea thermal gradient. Warmer temperatures on the Tibetan Plateau and the Pacific Ocean are projected to continue and increase with climate change, threatening to suppress the land-sea thermal gradient that is a mechanical driver of the ISM (Kumar et al., 2006; Li et al., 2017; Sharmila et al., 2015). The Cuobu record shows that the land-sea gradient is an important driver of short-term scale variability in the ISM, with the suppression of this gradient

potentially driving a weaker monsoon expression and drier local hydroclimate conditions on the Tibetan Plateau in the future.

3.6 Conclusions

The multi-proxy Cuobu paleoclimate record indicates that the lake has experienced significant hydroclimate variations over the last 8.3 ka. Sedimentological indicators show that Cuobu had increased runoff in the early Holocene that abruptly decreased around 4.5 ka as indicated by a shift from coarser to finer dominated sediments. This runoff is attributed to increased discharge in the Cuobu River, which runs parallel to the lake, under a stronger ISM that breached the moraine that separates the river from the lake. The river contributed coarse sediments to the lake until monsoon intensity and water levels dropped around 4.5 ka, isolating the river from the lake and decreasing the discharge of coarse sediments and stream flow into the lake. Leaf-wax *n*-alkane isotopes support the interpretation of strong monsoon intensity in the early and late Holocene and weak monsoon intensity in the middle Holocene. $\Delta\delta^2H_{C23\text{-}C31}$, a proxy for effective moisture and the ratio of precipitation to evaporation, shows more effective moisture between 8.3 and 4.5 ka and 1 ka to present. Effective moisture was lower from 4.5 to 1 ka corresponding to a decline in ISM intensity observed in records across the Tibetan Plateau. The timing of the synoptic and local hydroclimate response to changes in the monsoon intensity are in-sync, suggesting a simultaneous response to large-scale orbital changes in the ISM. Both monsoon intensity and effective moisture increased after 1 ka, however, this increase was insufficient to reconnect the two water bodies. The timing of this decline in monsoon intensity corresponds to records across the Tibetan Plateau that show a decline in effective moisture around 5 ka and a shift to a cooler, drier hydroclimate that persisted until the monsoon intensity increased around 1 ka. The synchronous decline in ISM intensity around 5 ka in the southern central and eastern Tibetan Plateau occurs at the same time as the migration of the ITCZ in response to the reduction of solar insolation and warming conditions in the Pacific similar to an El Niño-like state.

3.7 Tables

Table 3.1: ^{210}Pb dates from Cuobu B-17 surface core

MEAN DEPTH (CM)	^{210}PB ACTIVITY	±	SUPPORTED 210PB OR 214PB ACTIVITY (BQ/G)	±	EXCESS ^{210}PB ACTIVITY	±	137CS ACTIVITY (BQ/G)	±	CAL. YR BP
2.50	**0.243**	**1.240**	**0.0544**	**0.045**	**0.18860**	**1.19490**	**0.0101**	**0.00517**	**-65**
4.50	**0.276**	**0.115**	**0.0739**	**0.056**	**0.20210**	**0.05900**	**N/A**	**N/A**	**-62**
6.50	**0.208**	**0.079**	**0.0444**	**0.019**	**0.16360**	**0.05940**	**N/A**	**N/A**	**-60**
8.50	**0.241**	**0.084**	**0.0601**	**0.028**	**0.18090**	**0.05660**	**N/A**	**N/A**	**-57**
10.50	**0.299**	**0.082**	**0.0374**	**0.017**	**0.26160**	**0.06510**	**N/A**	**N/A**	**-52**
12.50	**0.28**	**0.085**	**0.033**	**0.018**	**0.24700**	**0.06750**	**N/A**	**N/A**	**-40**
16.50	**0.249**	**0.067**	**0.0381**	**0.014**	**0.21090**	**0.05260**	**0.0201**	**0.019**	**-33**
18.50	**0.246**	**0.085**	**0.0359**	**0.033**	**0.21010**	**0.05260**	**0.0356**	**0.0321**	**-28**
20.00	**0.246**	**0.080**	**0.0304**	**0.027**	**0.21560**	**0.05280**	**N/A**	**N/A**	**136**
22.25	**0.185**	**0.094**	**0.0795**	**0.028**	**0.10550**	**0.06690**	**N/A**	**N/A**	**N/A**

Table 3.2: Radiocarbon dates from Cuobu B-17 and D-17 composite core

CORE	MEAN DEPTH (CM)	^{14}C YR	±	CAL YR	±
B17	**1.5**	**940**	**15**	**172.5**	**15**
B17	**5.5**	**910**	**15**	**156.5**	**15**
B17	**46**	**1740**	**15**	**730.5**	**15**
D17	**93**	**1915**	**15**	**935.5**	**15**
D17	**145**	**2460**	**20**	**1666.5**	**20**
D17	**200**	**3100**	**15**	**2378.5**	**15**
D17	**280**	**4415**	**15**	**4073.5**	**15**
D17	**313**	**5255**	**15**	**5066.5**	**15**
D17	**374**	**6210**	**20**	**7165.5**	**20**
D17	**414**	**7950**	**20**	**7910.5**	**20**

Figures 3.8

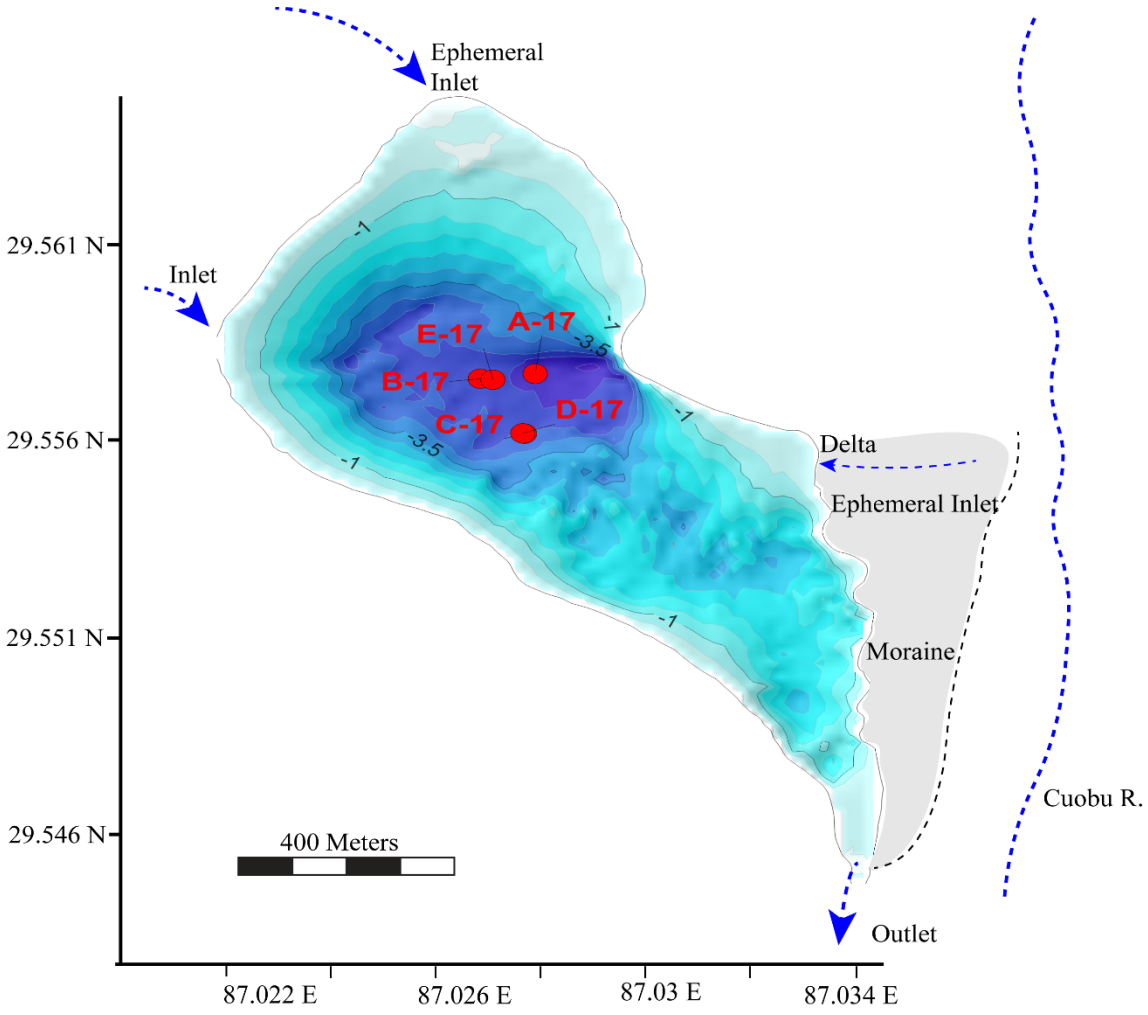

Figure 3.1. Bathymetric map of Cuobu with core sites marked (red colored dots with core names). Bathymetry mapped with 0.5 m contour intervals. Inlets and outlets to the lake are marked with blue dashed lines and arrows. Cuobu River is marked with a blue dashed line. Grey background and black dashed line designate the extent of a moraine between Cuobu and Cuobu River. A delta feature on the moraine is present where an ephemeral stream bed cuts across the moraine.

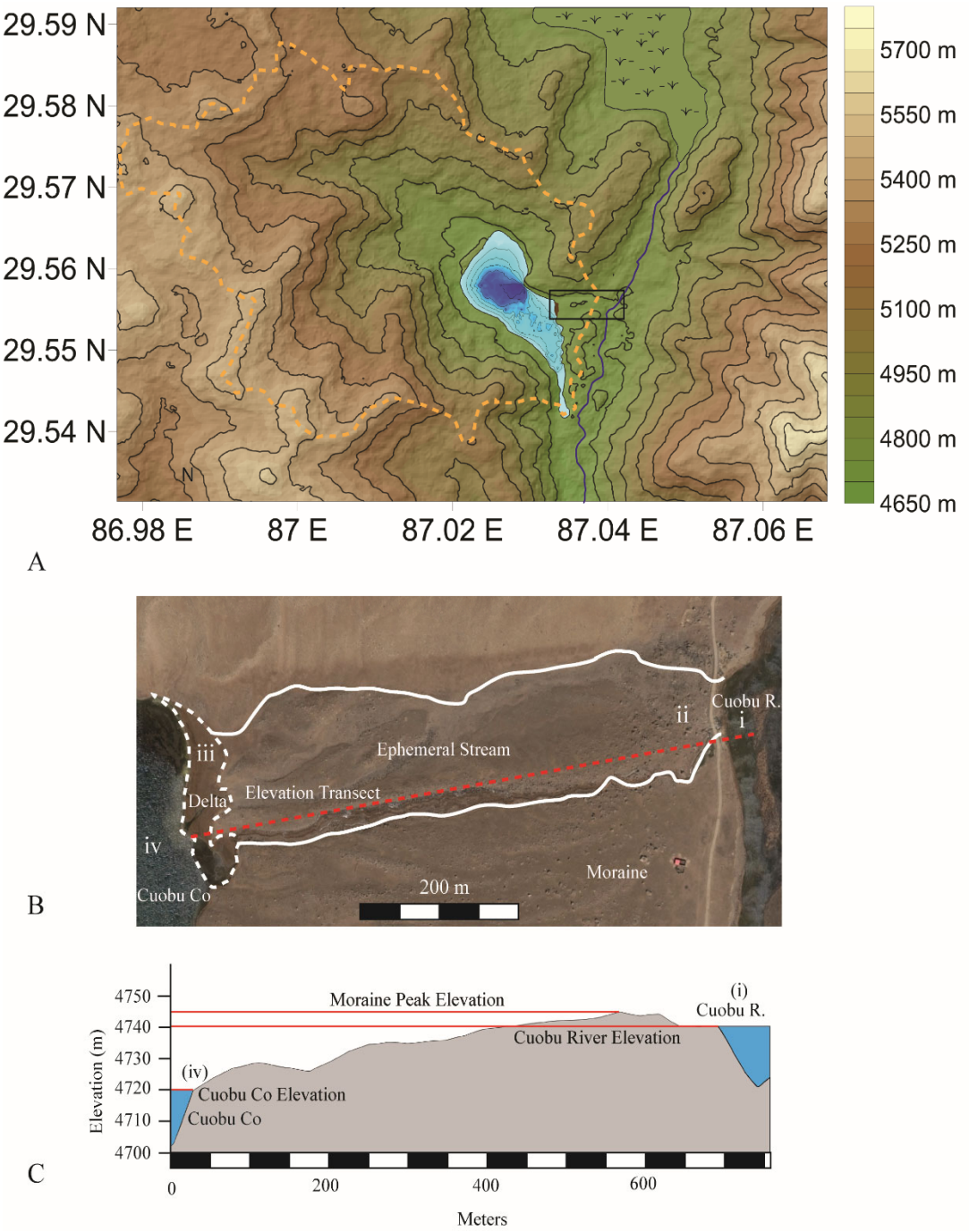

Figure 3.2. Topographic map of the area surrounding Cuobu, inset with the lake bathymetry (A). Cuobu watershed is designated with an orange dashed line. Topographic contours are at 50 m intervals while bathymetric contours are at 0.5 m intervals. An ephemeral stream (ii) and its delta (iii) that cut across the moraine are identified with a black box and shown in greater detail (B). The Cuobu River (i) is to the east of a moraine that forms the southeastern edge of Cuobu (iv). A transect (red dashed line) across the moraine is used to show the elevational profile (C) of the lake-moraine-river environment (B). The elevational profile is marked with red lines show the elevational difference between features.

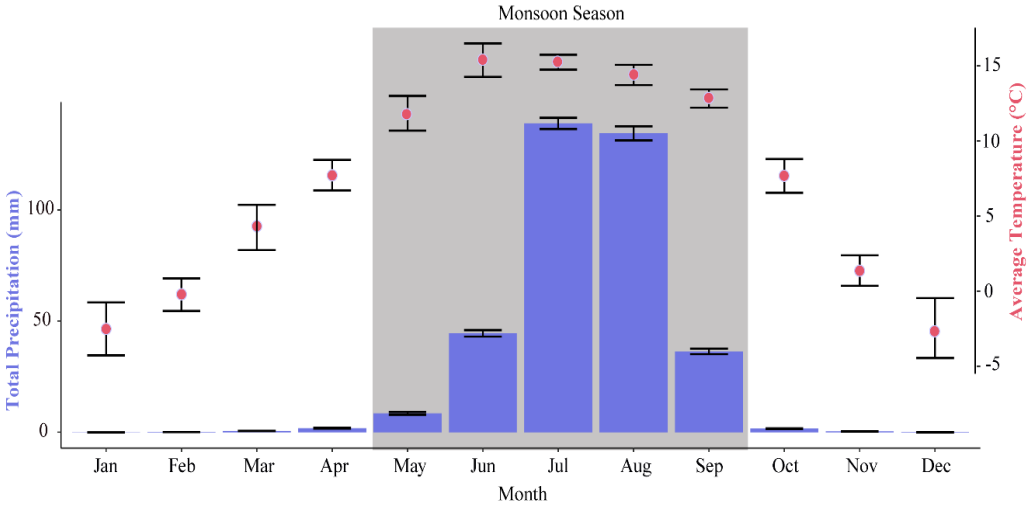

Figure 3.3. Average monthly temperature (°C ± s.d.) and total precipitation (mm ± s.d.) at Xigaze weather station from 1988-2018. Gray background indicates the annual monsoon season.

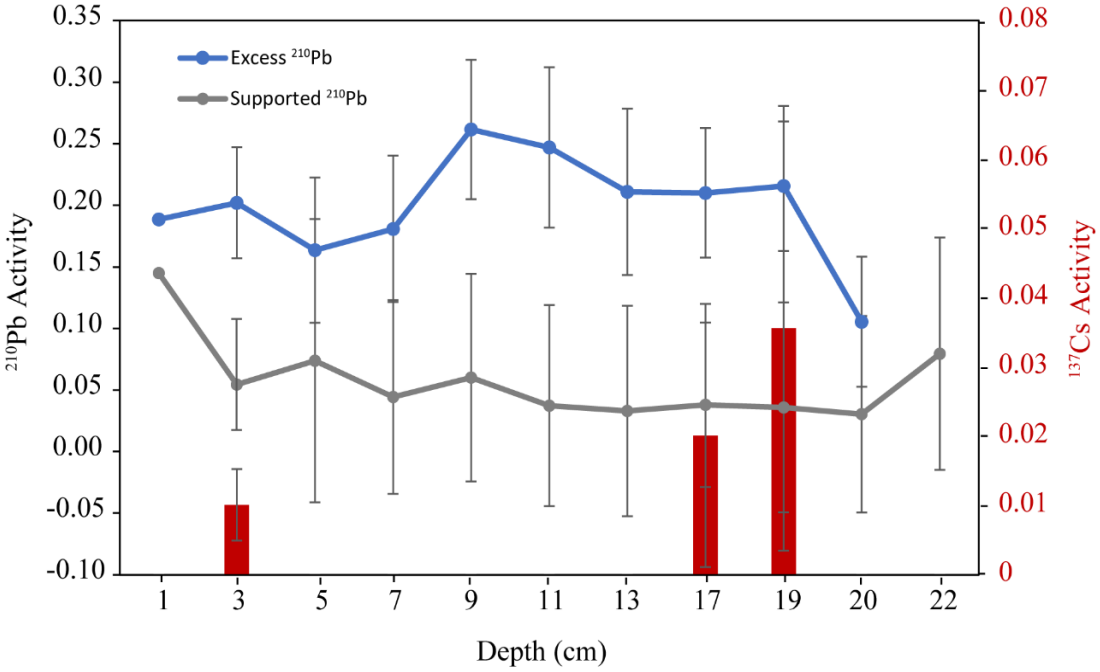

Figure 3.4. Excess and supported ^{210}Pb activity with ^{137}Cs activity in the top 22 cm of Cuobu sediment core.

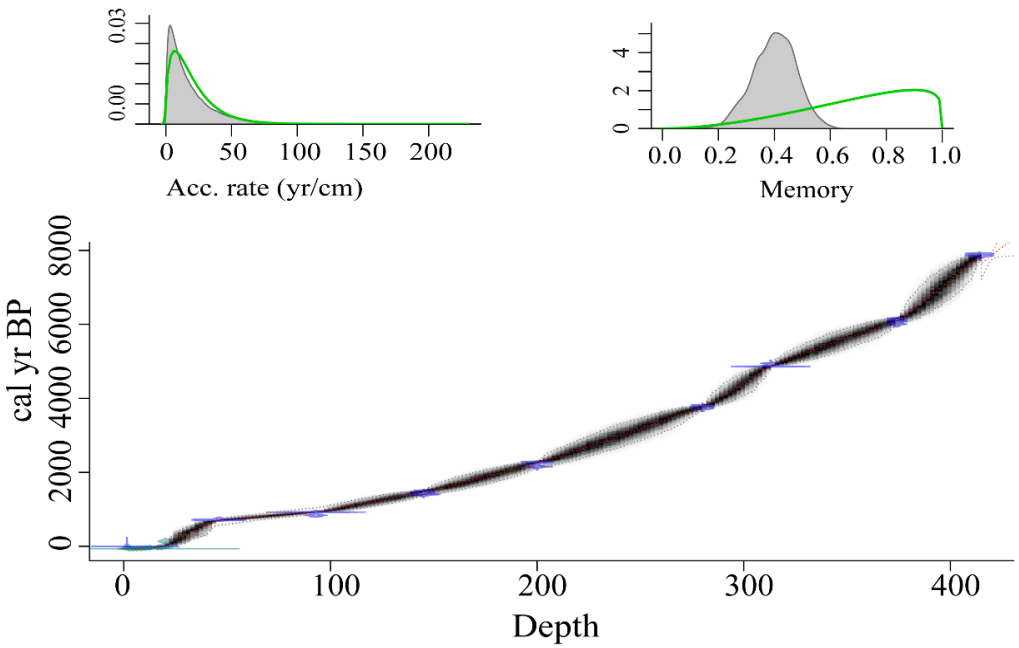

Figure 3.5. Age model for Cuobu produced by Bacon program using both ^{210}Pb and ^{14}C dates.

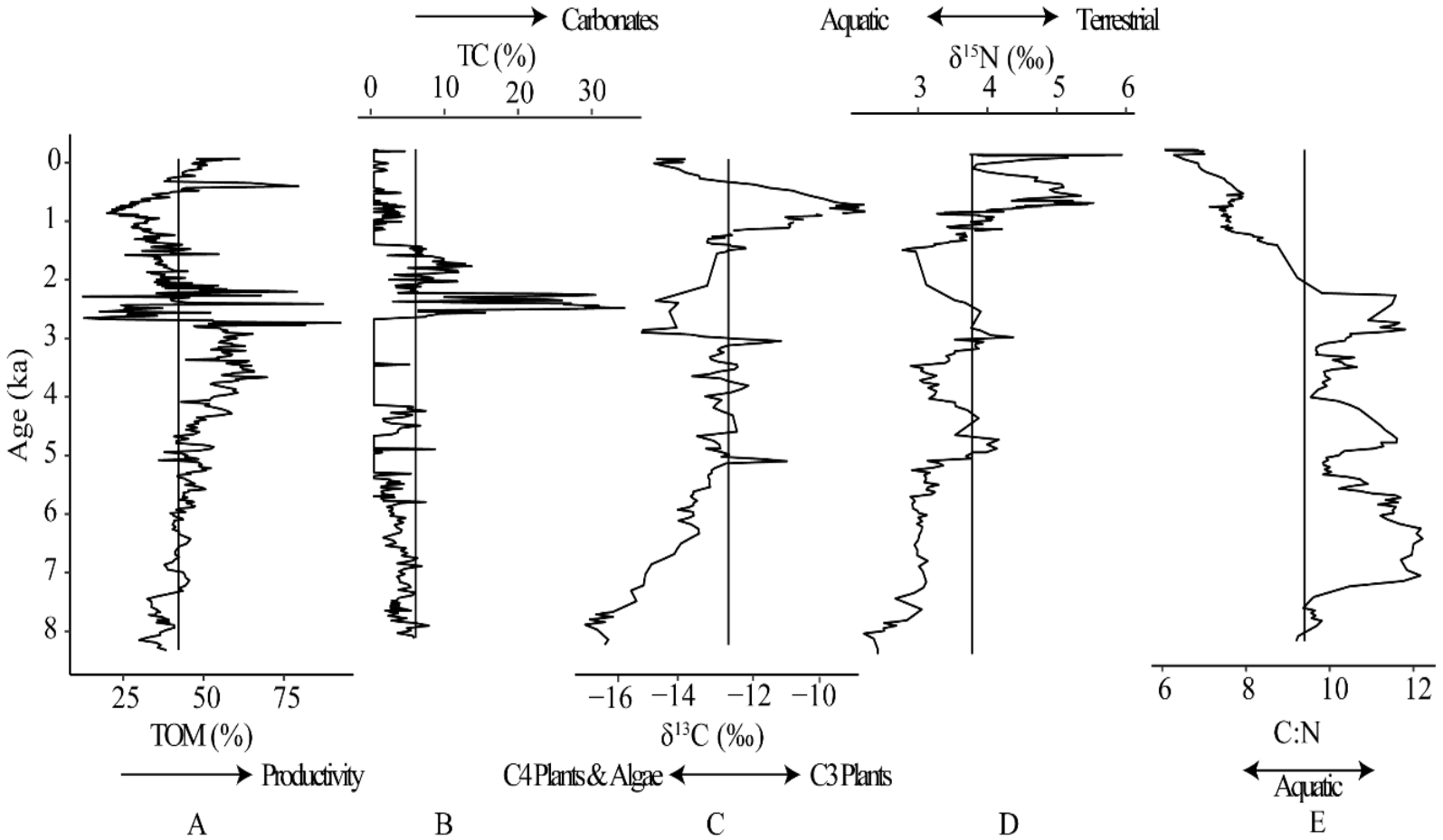

Figure 3.6. Cuobu B-17 and D-17 total organic matter (TOM %; A), total carbonates (TC %; B), $\delta^{13}C$ (‰; C), $\delta^{15}N$ (‰; D), and the ratio of C:N I. Black vertical line represents average values. The grey background indicates the period with highest C:N. Blue and red backgrounds indicate inferred wet and dry conditions at the lake.

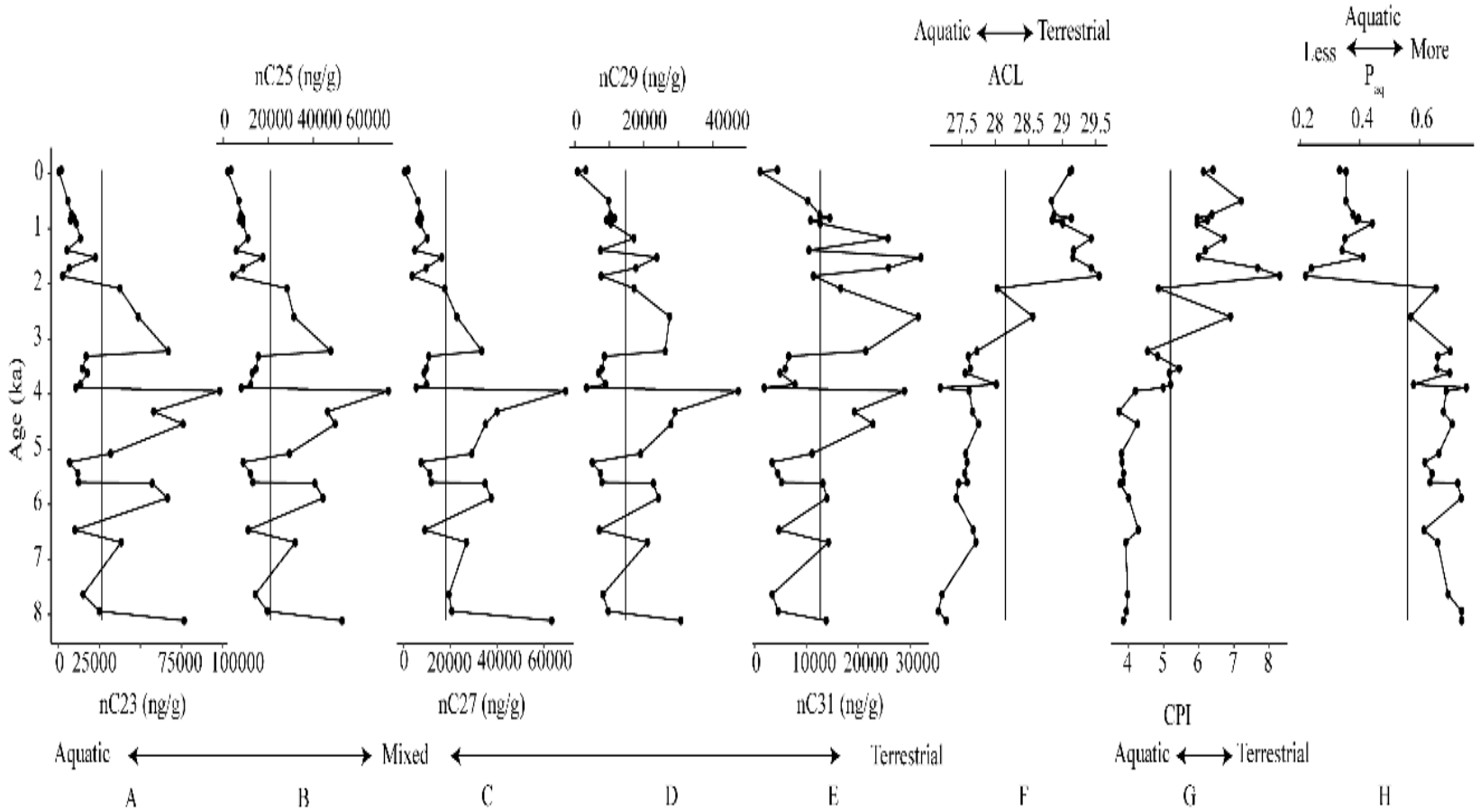

Figure 3.7. Concentration of leaf wax *n*-alkanes extracted from Cuobu B-17 and D-17 sediments (ng/g) for C23 (A), C25 (B), C27 (C), C29 (D), and C31 I. Indices to distinguish between terrestrial (long-chain) and aquatic (short-chain) *n*-alkanes include average chain length (ACL: F), carbon preference index (CPI: G), and aquatic vegetation index (P_{aq}: H). Black vertical line represents average values. Blue and red backgrounds indicate inferred wet and dry conditions at the lake.

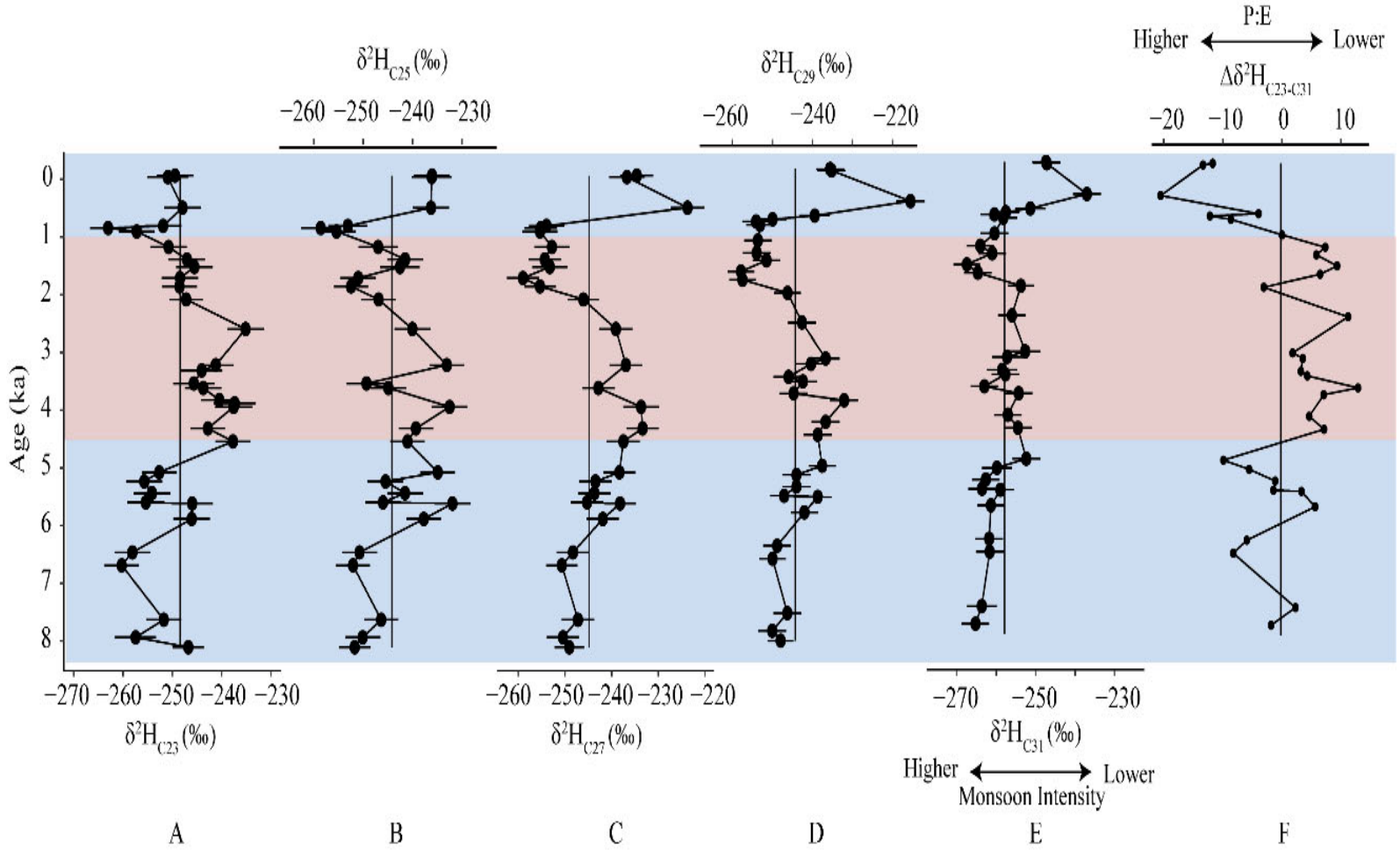

Figure 3.8. Coubo leaf wax *n*-alkane δ^2H (‰) for C23 (A), C25 (B), C27 (C), C29 (D), and C31 I. $\Delta\delta^2H_{C23\text{-}C31}$ is the balance of precipitation to evaporation (P:E; F). Black vertical line represents average values. Blue and red backgrounds indicate inferred wet and dry conditions respectively.

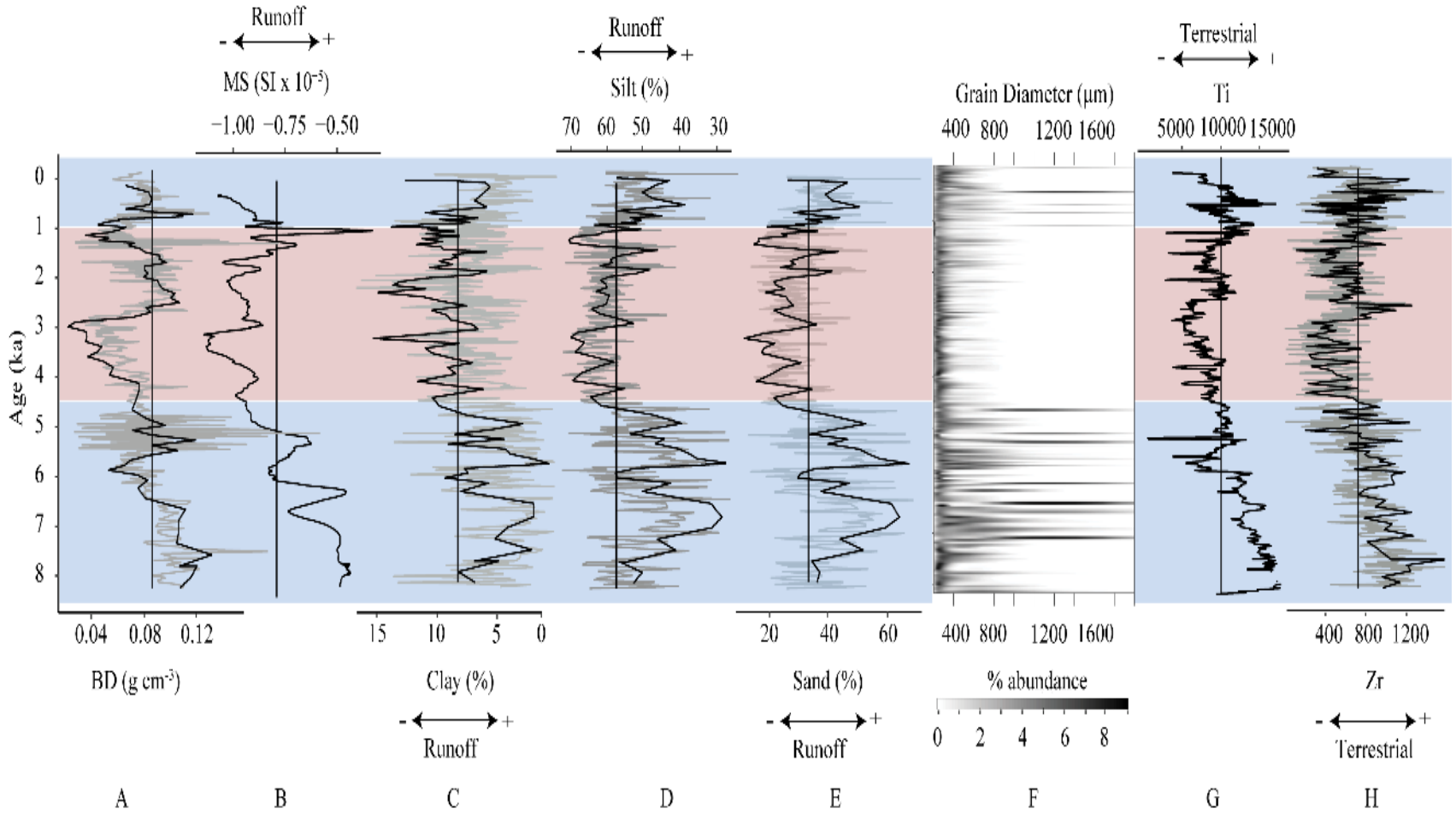

Figure 3.9. Cuobu 5 pt. moving average (MA) dry bulk density (BD g cm^{-3}: A), magnetic susceptibility (MS, SI 10 x $^{-5}$: B), 5 pt. MA percent clay I, 5 pt. MA percent silt (D), 5 pt. MA percent sand I, histogram of grain diameter size for each sample (F), Ti (G) and 5 pt. MA Zr (H). The full record is shaded behind each moving average. Black vertical line represents average values. Red and blue background indicate periods with dry and wet conditions respectively, based on grain size.

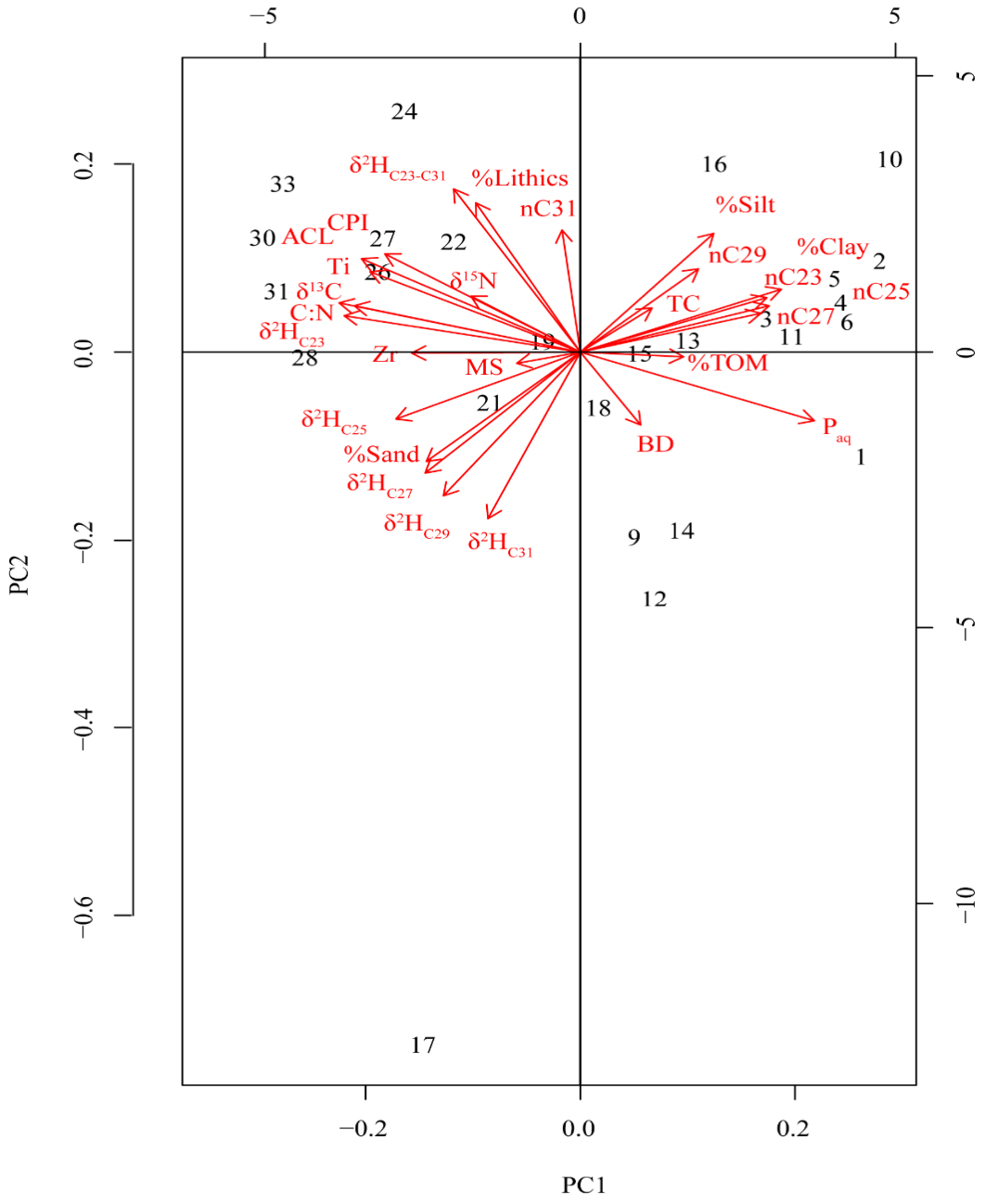

Figure 3.10. Principal Components Analysis (PCA) results from the Cuobu sediment record, indicating the contributions of each proxy in the overall variance of the dataset.

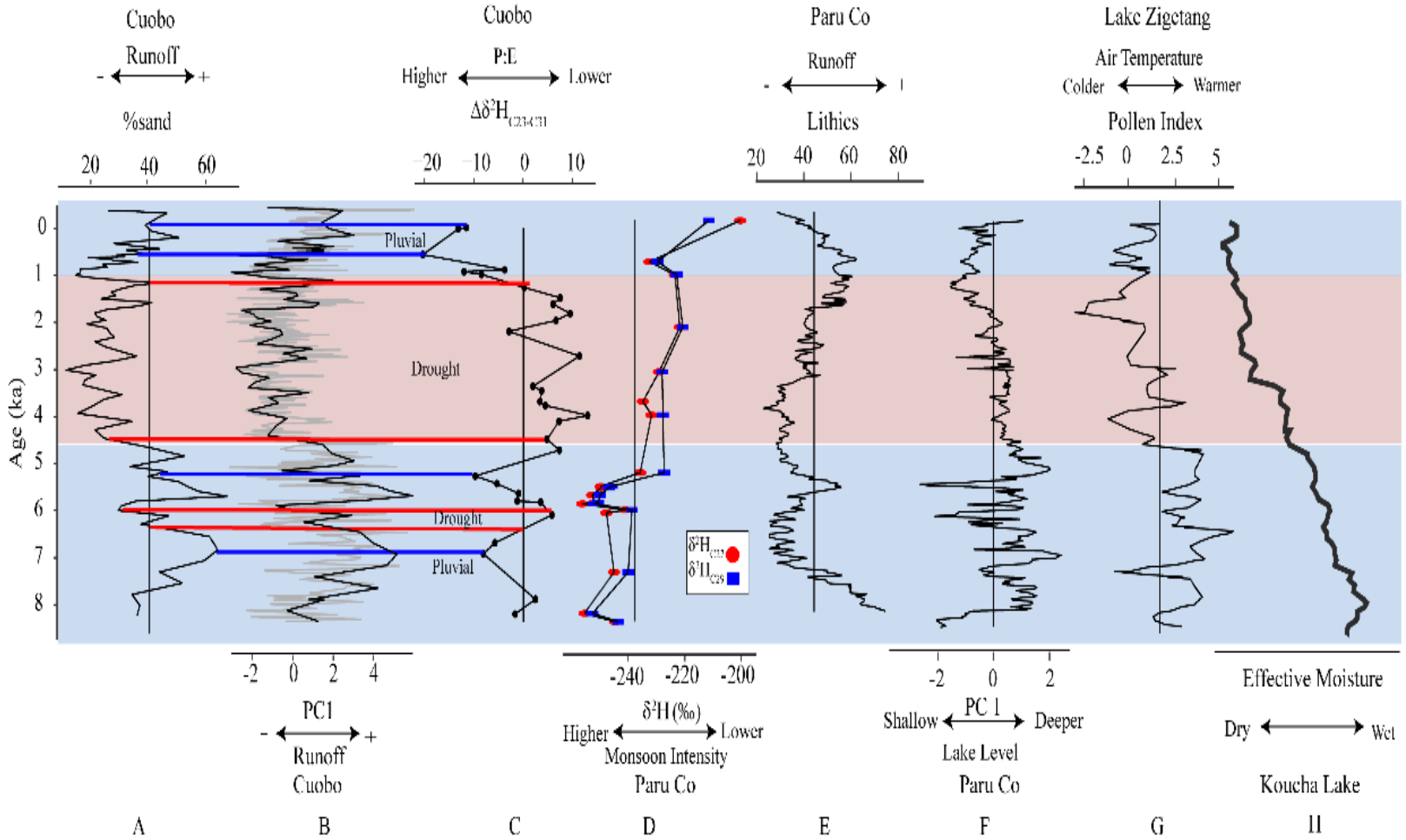

Figure 3.11. Cuobu 5 pt. moving average (MA) %sand (A), 5 pt. MA Principal Component 1 (PC1; B) and $\Delta\delta^2H_{C23\text{-}C31}$ (C) in comparison with Tibetan Plateau records from Paru Co *n*-alkane δ_2H_{C27} and δ_2H_{C29} (D) lithics I and primary component 1 (F), Lake Zigetang pollen index (G), and Koucha Lake effective moisture (H). The full record is shaded behind each moving average. Black vertical line represents average values. Blue and red backgrounds infer wet and dry conditions at Cuobu.

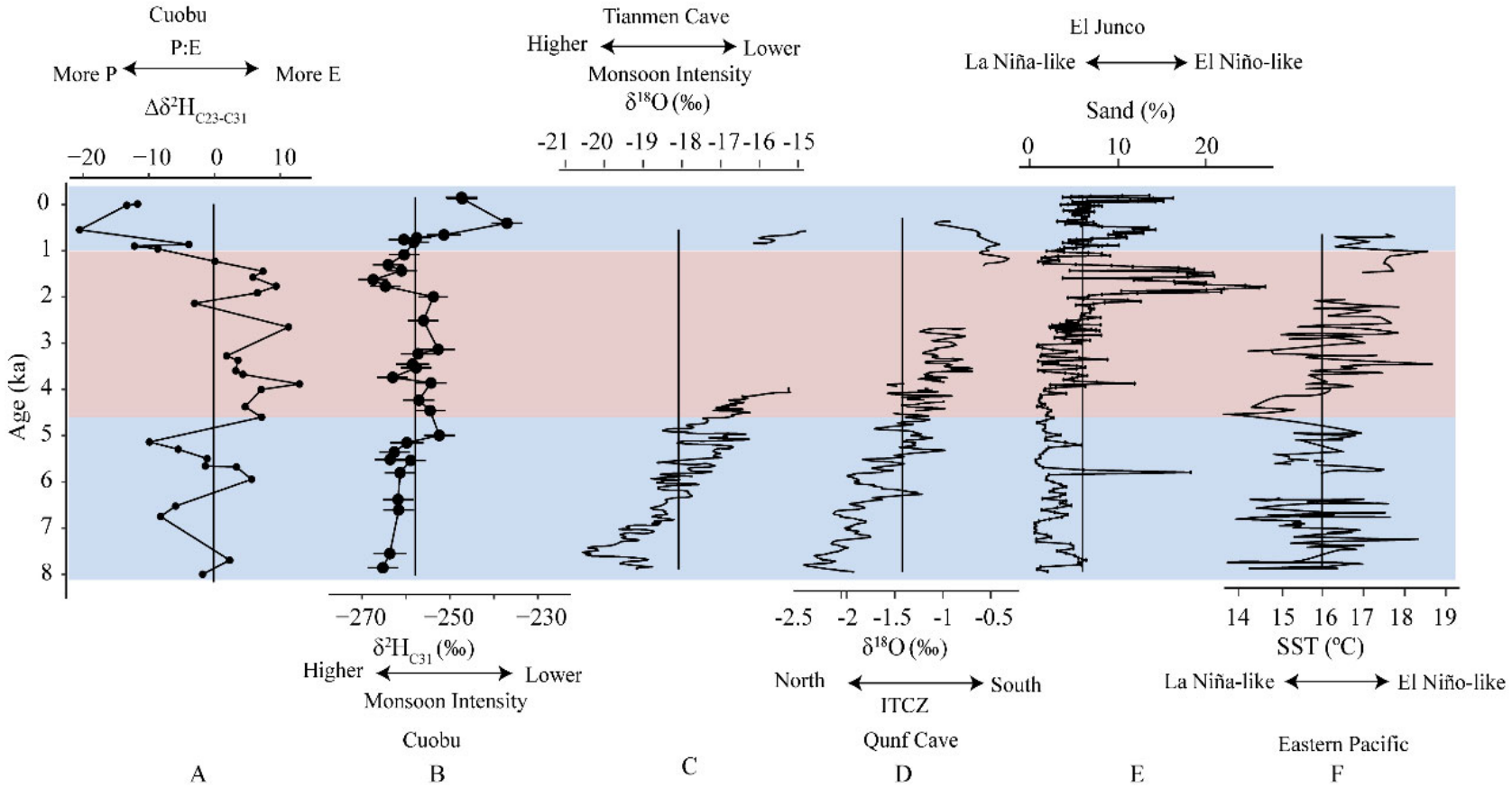

Figure 3.12. Cuobu $\Delta\delta^2H_{C23-C31}$ (A) and δ^2H_{C31} (B) records in conjunction with records from the ISM span and Pacific SSTs. Records are from Tianmen Cave (C), Qunf Cave (D), El Junco I, and Eastern Pacific SST (F). Black vertical line represents average values. Blue and red backgrounds infer wet and dry conditions at Cuobu.

3.9 References

Aichner, B., Herzchuh, U., Wilkes, H., Vieth, A. and Böhner, J. 2010. δD values of n-alkanes in Tibetan lake sediments and aquatic macrophytes – A surface sediment study and application to a 16-ka record from Lake Koucha. Organic Geochemistry 41, 779-790.

Appleby, P. and Oldfield, F. 1978. The calculation of lead-210 dates assuming a constant rate of supply of unsupported 210Pb to the sediment. CATENA 5(1), 1-8.

Berger, A. and Loutre, M. 1991. Insolation values for the climate of the last 10 million years. Quaternary Science Reviews 10, 297-317.

Berkelhammer, M., Sinha, A., Stott, L., Cheng, H., Pausata, F. and Yoshimura, K. (2012) Climates, Landscapes, and Civilizations, pp. 75-87, Geophysical Monograms AGU, Washington D.C.

Bird, B., Lei, Y., Perello, M., Polissar, P., Yao, T., Finney, B., Bain, D., Pompeani, D. and Thompson, L. 2017. Late Holocene Indian summer monsoon variability revealed from a 3,300-year-long lake sediment record from Nir'pa Co, southeastern Tibet. The Holocene 27(4), 541-552.

Bird, B., Polissar, P., Lei, Y., Thompson, L., Yao, T., Finney, B., Bain, D., Pompeani, D. and Steinman, B. 2014. A Tibetan lake sediment record of Holocene Indian summer monsoon variability. Earth and Planetary Science Letters 399, 92-102.

Blaauw, M. and Christen, J.A. 2011. Flexible paleoclimate age-depth models using an autoregressive gamma process. Bayesian Analysis 6(3), 457-474.

Brady, N. (1984), p. 750, Macmillan Publishing Co, New York.

Cai, Y., Zhang, H., Cheng, H., An, Z., Edwards, R., Wang, X., Tan, L., Liang, F., Wang, J. and Kelly, M. 2012. The Holocene Indian monsoon variability over the southern Tibetan Plateau and its teleconnections. Earth Planetary Science Letters 335-336, 135-144.

Chassiot, L., Miras, Y., Chapron, E., Develle, A.-L., Arnaud, F., Motelica-Heino, M. and Giovanni, C.D. 2018. A 7000-year environmental history and soil erosion record inferred from the deep sediments of Lake Pavin (Massif Central, France). Paleogeography, Paleoclimatology, and Palaeoecology 497, 218-233.

Choubert, G., Faure-Muret, A. and Chanteux, P. 1983. Atlas geologique du monde, Paris: UNESCO.

Chowdary, J.S., Harsha, H., Gnanaseelan, C., Srinivas, G., Parekh, A., Pillai, P. and Naidu, C. 2016. Indian summer monsoon rainfall variability in response to differences in the decay phase of El Niño. Climate Dynamics 48, 2707-2727.

Conroy, J.L., Overpeck, J.T., Cole, J.E., Shanahan, T.M. and Steinitz-Kannan, M. 2008. Holocene changes in eastern tropical Pacific climate inferred

from a Gala´pagos lake sediment record. Quaternary Science Reviews 27, 1166– 1180.

Croudace, I., Rindby, A. and Rothwell, R. 2006. ITRAX: description and evaluation of a new multi-function X-ray core scanner. Geological Society, London, Special Publications 267(1), 51-63.

Cuven, S.p., Francus, P. and Lamoureux, S.F. 2010. Estimation of grain size variability with micro X-ray fluorescence in laminated lacustrine sediments, Cape Bounty, Canadian High Arctic. Journal of Paleolimnology 44(3), 803-817.

Dearing, J. (1994) Environmental Magnetic Susceptibility, Chi Publishing, Kenilworth.

Dearing, J. 1997. Sedimentary indicators of lake-level changes in the humid temperate zone: a critical review. Journal of Paleolimnology 18, 1-14.

Diefendorf, A.F., Leslie, A.B. and Wing, S.L. 2015. Leaf wax composition and carbon isotopes vary among major conifer groups. Geochimica et Cosmochimica Acta 170(1), 145-156.

Digerfeldt, G. (1986) Handbook of Holocene Paleoecology and Paleohydrology, pp. 127-143, John Wiley & Sons, New York.

Djamali, M., Akhani, H., Andrieu-Ponel, V., Braconnot, P., Brewer, S., Beaulieu, J.d., Fleitmann, D., Fluery, J., Gasse, F., Guibal, F., Jackson, S., Lézine, A., Médail, F., Ponel, P., Roberts, N. and Stevens, L. 2010. Indian summer monsoon variations could have affected the early-Holocene woodland expansion in the Near East. The Holocene 20, 813-820.

Dykoski, C., Edwards, R., Cheng, H., Yaun, D., Cai, Y., Zhang, M., Lin, Y., Qing, J., An, Z. and Revenaugh, J. 2005. A high-resolution, absolute-dated Holocene and deglacial Asian monsoon record from Dongge Cave, China. Earth and Planetary Science Letters 233, 71-86.

Ficken, K., Li, B., Swain, D. and Eglinton, G. 2000. An n-alkane proxy for the sedimentary input of submerged/floating freshwater aquatic macrophytes. Organic Geochemistry 31(7-8), 745-749.

Fleitmann, D., Burns, S., Mudelsee, M., Neff, U., Kramers, J., Mangini, A. and Matter, A. 2003. Holocene forcing of the Indian Monsoon recorded from a stalagmite from Southern Oman. Science 300, 1737-1739.

Fleitmann, D., Burns, S.J., Mangini, A., Mudelsee, M., Kramers, J., Villa, I., Neff, U., Al-Subbary, A.A., Buettner, A., Hippler, D. and Matter, A. 2007. Holocene ITCZ and Indian monsoon dynamics recorded in stalagmites from Oman and Yemen (Socotra). Quaternary Science Reviews 26, 170-188.

Gray, A., Pasternack, G. and Watson, E. 2010. Hydrogen peroxide treatment effects on the particle size distribution of alluvial and marsh sediments. The Holocene 20(2), 293-301.

Gupta, A., Anderson, D. and Overpeck, J. 2003. Abrupt changes in the Asian southwest monsoon during the Holocene and their links to the North Atlantic Ocean. Nature 421, 354-357.

Haug, G.H., Hughen, K.A., Sigman, D.M., Peterson, L.C. and Ro, U. 2001. Southward Migration of the Intertropical Convergence Zone Through the Holocene. Science 293, 1304-1308.

Heiri, O., Lotter, A.F. and Lemcke, G. 2001. Loss on ignition as a method for estimating organic and carbonate content in sediments: reproducibility and comparability of results. Journal of Paleolimnology 25(1), 101-110.

Herzschuh, U., Kramer, A., Mischke, S. and Zhang, C. 2009. Quantitative climate and vegetation trends since the late glacial on the northeastern Tibetan Plateau deduced from Koucha Lake pollen spectra. Quaternary Research 71, 162-171.

Herzschuh, U., Winter, K., Wunnemann, B. and Li, S. 2006. A general cooling trend on the central Tibetan Plateau throughout the Holocene recorded by the Lake Zigetang pollen spectra. Quaternary International 154-155, 113-121.

KCCAMS, U. 2011. Acid/Base/Acid (ABA) sample pre-treatment, University of California Irvine, W.M. Keck Carbon Cycle Accelerator Mass Spectrometer Facility.

Koutavas, A. and Sachs, J. 2008. Northern timing of deglaciation in the eastern equatorial Pacific from alkenone paleothermometry. Paleooceanography 23(PA4205).

Kumar, K., Sahai, A., Kumar, K., Patwardhan, S., Mishra, P., Revadekar, J., Kamala, K. and Pant, G. 2006. High-resolution climate change scenarios for India for the 21st century. Current Science 90(3), 334-345.

Li, G., Xie, S.-P., He, C. and Chen, Z. 2017. Western Pacific emergent constraint lowers projected increase in Indian summer monsoon rainfall. Nature Climate Change 7, 708-712.

Liu, H. and Liu, W. 2016. N-Alkane distributions and concentrations in algae, submerged plants and terrestrial plants from the Qinghai-Tibetan Plateau. Organic Geochemistry 99, 10-22.

Livingstone, D. 1955. A Lightweight Piston Sampler for Lake Deposits. Ecology 36(1), 137-139.

Löwemark, L., Chen, H.-F., Yang, T.-N., Kylander, M., Yu, E.-F., Hsu, Y.-W., Lee, T.-Q., Song, S.-R. and Jarvis, S. 2011. Normalizing XRF-scanner data: A cautionary note on the interpretation of high-resolution records from organic-rich lakes. Journal of Asian Earth Sciences 40, 1250-1256.

Magny, M. and Haas, J.N. 2004. A major widespread climatic change around 5300 cal. Yr BP at the time of the Alpine Iceman. Journal of Quaternary Science 19.5, 423-430.

Marchitto, T.M., Muscheler, R., Ortiz, J.D., Carriquiry, J.D. and Geen, A.v. 2010. Dynamical Response of the Tropical Pacific Ocean to Solar Forcing During the Early Holocene. Science 330, 1378-1381.

Marcott, S.A., Shakun, J.D., Clark, P.U. and Mix, A.C. 2013. A Reconstruction of Regional and Global Temperature for the Past 11,300 Years. Science 339, 1198-1201.

Marzi, R., Torkelson, B. and Olson, R. 1993. A revised carbon preference index. Organic Geochemistry 20(8), 1303-1306.

Meyers, P.A. and Lallier-Vergès, E. 1999. Lacustrine sedimentary organic matter records of Late Quaternary paleoclimates. Journal of Paleolimnology 21, 345-372.

Moy, C.M., Seltzer, G.O., Rodbell, D.T. and Anderson, D.M. 2002. Variability of El Nino/Southern Oscillation activity at millennial timescales during the Holocene epoch. Nature 420, 162-165.

Mügler, I., Sasche, D., Werner, M., Xu, B., Wu, G., Yao, T. and Gleixner, G. 2008. Effect of lake evaporation on δD values of lacustrine n-alkanes: A comparison of Nam Co (Tibetan Plateau) and Holzmaar (Germany). Organic Geochemistry 39, 711-729.

Nesbitt, H. and Markovics, G. 1997. Weathering of grandioritic crust, long-term storage of elements in weathering profiles, and petrogenesis of siliciclastic sediments. Geochimica et Cosmochimica Acta 61(8), 1653-1670.

Olsson, I. (1986) Handbook of Holocene palaeoecology and paleohydrology Berglund, B. (ed), John Wiley & Sons, Chichester.

Polissar, P. and D'Andrea, W. 2014. Uncertainty in Paleohydrologic Reconstructions from Molecular dD values. Geochimica et Cosmochimica Acta 129, 146-156.

Qui, J. 2008. China: The Third Pole Environment. Nature 454(7203), 393-396.

Rashid, H., Flower, B., Poore, R. and Quinn, T. 2007. A ~25 ka Indian Ocean monsoon variability record from the Andaman Sea. Quaternary Science Reviews 26, 2586-2597.

Reimer, P.J., Bard, E., Bayliss, A., Beck, J.W., Blackwell, P.G., Ramsey, C.B., Buck, C.E., Cheng, H., Edwards, R.L., Friedrich, M., Grootes, P.M., Guilderson, T.P., Haflidason, H., Hajdas, I., Hatté, C., Heaton, T.J., Hoffmann, D.L., Hogg, A.G., Hughen, K.A., Kaiser, K.F., Kromer, B., Manning, S.W., Niu, M., Reimer, R.W., Richards, D.A., Scott, E.M., Southon, J.R., Staff, R.A., Turney, C.S.M. and Plicht, J.v.d. 2013. INTCAL13 AND MARINE13 RADIOCARBON AGE CALIBRATION CURVES 0–50,000 YEARS CAL BP. RADIOCARBON 55(4), 1869-1887.

Roberts, N., Allcock, S.L., Barnett, H., Mather, A., Eastwood, W.J., Jones, M., Primmer, N., Yiğitbaşıoğlu, H. and Vannière, B. 2019. Cause-and-effect in Mediterranean erosion: The role of humans and climate upon Holocene sediment flux into a central Anatolian lake catchment. Geomorphology 331, 36-48.

Samanta, D., Rajagopalan, B., Karnauskas, K.B., Zhang, L. and Goodkin, N.F. 2020. La Niña's Diminishing Fingerprint on the Central Indian Summer Monsoon. Geophysical Research Letters 47(2).

Seki, O., Meyers, P.A., Kawamura, K., Zheng, Y. and Zhou, W. 2009. Hydrogen isotopic ratios of plant wax n-alkanes in a peat bog deposited in northeast China during the last 16 kyr. Organic Geochemistry 40(6), 671-677.

Sharmila, S., Joseph, S., Sahai, A.K., Abhilash, S. and Chattopadhyay, R. 2015. Future projection of Indian summer monsoon variability under climate

change scenario: An assessment from CMIP5 climate models. Global and Planetary Change 124, 62-78.

Shuman, B., Bravo, J., Kaye, J., Lynch, J.A., Newby, P. and Webb, T. 2001. Late Quaternary Water-Level Variations and Vegetation History at Crooked Pond, Southeastern Massachusetts. Quaternary Research 53(3), 401-410.

Shuman, B., Henderson, A.K., Colman, S.M., Stone, J.R., Fritz, S.C., Stevens, L.R., Power, M.J. and Whitlocke, C. 2009. Holocene lake-level trends in the Rocky Mountains, U.S.A. Quaternary Science Reviews 28(19-20), 1861-1879.

Surendran, S., Gadgil, S., Francis, P. and Rajeevan, M. 2015. Prediction of Indian rainfall during the summer monsoon season on the basis of links with equatorial Pacific and Indian Ocean climate indices. Environmental Research Letters 10, 094004.

Thompson, R., Battarbee, R., O'Sullivan, P. and Oldfield, F. 1975. Magnetic susceptibility of lake sediments. Limnology and Oceanography 20(5), 687-698.

Thornton, S. and McManus, J. 1994. Application of organic carbon and nitrogen stable isotope and C/N ratios as source indicators of organic matter provenance in estuarine systems: Evidence from the Tay Estuary, Scotland. Estuarine, Coastal, and Shelf Science 38, 219-233.

Tian, L., Yao, T., MacClune, K., White, J., Schilla, A., Vaughn, B., Vachon, R. and Ichiyanagi, K. 2007. Stable isotopic variations in west China: A consideration of moisture sources. Journal of Geophysics Research 112, D10112.

Wright, H. 1967. A square-rod piston sampler for lake sediments. Journal of Sedimentary Petrology 37(3), 975-976.

Wu, D., Chen, X., Lv, F., Brenner, M., Curtis, J., Zhou, A., Chen, J., Abbott, M., Yu, J. and Chen, F. 2018. Decoupled early Holocene summer temperature and monsoon precipitation in southwest China. Quaternary Science Reviews 193, 54-67.

Xia, Z.-H., Xu, B.-Q., Mügler, I., Wu, G.-J., Gleixner, G., Sachse, D. and Zhu, L.-P. 2008. Hydrogen isotope ratios of terrigenous n-alkanes in lacustrine surface sediment of the Tibetan Plateau record the precipitation signal. Geochemical Journal 42, 331-338.

Zhu, L., Wu, Y., Wang, J., Lin, X., Ju, J., Xie, M., Li, M., Mäusbacher, R., Antje, S. and Daut, G. 2008. Environmental changes since 8.4 ka reflected in the lacustrine core sediments from Nam Co, central Tibetan Plateau. The Holocene 18, 831-839.

4. MULTI-PROXY EVIDENCE FOR AN EARLY HOLOCENE LOW LAKE STAND DURING A STRONG MONSOON: INVESTIGATING THE ELEVATION DEPENDENT EXPRESSION OF THE INDIAN SUMMER MONSOON ON THE TIBETAN PLATEAU

4.1 Introduction

Understanding hydroclimate variability in the Third Pole Environment, which encompasses the Tibetan Plateau and the surrounding region (Qui, 2008), is important for establishing how climate change impacts water availability for over a third of the world's population. The Indian Summer Monsoon (ISM) is the primary source of precipitation in the Third Pole region, with as much as 90% of annual precipitation falling during the boreal warm season between May and September (Tian et al., 2007). There is considerable evidence from paleoclimate archives that ISM intensity has varied throughout the Holocene and that there have been abrupt changes in its mean state from pluvials (wet phases) to droughts and vice versa. After an early Holocene maximum in precipitation from 11.7 to 7, ISM precipitation declined between 7 and 5 ka, with isotopic proxies indicating a gradual decline while sediment proxies indicating a more abrupt transition (Berkelhammer et al., 2012; Bird et al., 2017; Bird et al., 2014; Fleitmann et al., 2003; Fleitmann et al., 2007; Herzschuh et al., 2006). The middle Holocene transition to a weakened monsoon between 7 to 5 ka has been attributed to reduced solar insolation (Fleitmann et al., 2003) that resulted in a southward migration of the ITCZ (Haug et al., 2001) and increased El Niño-like conditions in the Pacific (Chen et al., 2016; Conroy et al., 2008; Emile-Geay and Tingley, 2016; Emile-Geay et al., 2016; Moy et al., 2002).

While many records agree that the ISM weakened during the middle Holocene (7 – 5 ka), questions remain about the elevation-dependent expression of this decline in monsoon intensity (Bird et al., 2014; Herzschuh et al., 2006). This is in part because there are few decadally-resolved records of ISM dynamics (Berkelhammer et al., 2012; Cai et al., 2012; Zhu et al., 2008) and even fewer decadal-resolved records found directly on the Tibetan Plateau, with most of these records in high-elevation regions (Bird et al., 2017; Bird et al., 2014). High-resolution records allow for the investigation of hydroclimate processes that occur on shorter time scales and capture variability missed by records

resolved on centennial and millennial time scales. Monsoon precipitation has also been shown to vary between synoptic and local hydroclimate proxies, with evidence to suggest that isotopic records (synoptic) show earlier decline than local, sedimentological proxies (Berkelhammer et al., 2012; Bird et al., 2017; Bird et al., 2014; Fleitmann et al., 2003; Herzschuh et al., 2009; Herzschuh et al., 2006), with evidence that the monsoon contracted during the middle Holocene transition with reduced precipitation and upwelling evident in the Arabian Sea and Arabian Peninsula (Fleitmann et al., 2003; Gupta et al., 2003). It is difficult to determine how this is reflected on the Tibetan Plateau since records are frequently from central and eastern Tibet, with limited records further east towards the Hengduan Mountains, a highly populated area of the Plateau. Low-resolution pollen and tree-ring records from the Hengduan Mountains are from high-elevation sites (Fan et al., 2008; Fan et al., 2009), and therefore may not necessarily reflect hydroclimate variability affecting lower elevation intermontane areas where populations are centered. Limited understanding of Holocene monsoon expression in these low-elevation, highly populated areas of the Tibetan Plateau reduces the accuracy of future monsoon rainfall projections under climate change.

Here I present a high-resolution, low elevation (2810 a.s.l.) sediment record from Galang Co (Fig. 4.1), an inter-montane valley lake in the Hengduan Mountains. The Galang Co record spans the last 12.3 ka and was developed to understand the expression of the ISM along elevational gradients across the eastern Tibetan Plateau. Local hydroclimate conditions throughout the Holocene was reconstructed using sedimentology, organic matter, X-ray fluorescence (XRF) geochemistry, and long- and short-chain leaf-wax *n*-alkane hydrogen isotopes. This record addresses: 1) hydroclimate variability at an under-represented area of the southeastern Tibetan Plateau, 2) how the expression of ISM precipitation differs between low and high elevation sites and across the eastern Tibetan Plateau, and 3) how the timing of the transition to a weak monsoon differs between synoptic and local ISM hydroclimate proxies.

4.2 Study Area: Galang Co

Galang Co is a small (0.1 km^2), low elevation lake (2810 a.s.l.) within the Hengduan Mountains of the southeastern Tibetan Plateau (Fig 4.2A, 29.90817° N,

95.60391° E). The lake is situated near the bottom of a deep valley at the confluence of the Parlung Zangpo and Quzong Zangpo rivers and surrounded by steep mountain terrain with nearby peaks rising to over 5900 m a.s.l. The lake's small watershed (4.2 km^2) consists of steep mountain slopes (4150-3750 m a.s.l.) to the northwest with a smaller hill (2900 a.s.l.) to the south of the watershed. Geomorphological observations of the lake's watershed made in the field and from satellite images show scarp features on the mountain along the north side of the lake and the heterogeneous mixture of rocks within the hill formation on the south edge of the lake that are suggestive of an ancient landslide. There are no geomorphic features that would suggest any additional landslides and there are no landforms indicating glaciation in the watershed (Fig. 4.2B). Historical marker observed in the area suggest that the watershed was the home of the Galang or Tubo Dynasty which existed from around 700 CE to the early 20th century. Today, a small village (est. population = 100) exists along the outlet of the lake, utilizing the Galang Co watershed for grazing and small-scale agriculture.

Field observations during coring indicate that Galang Co's bathymetry consists of a broad wetland and littoral zone that sharply transitions to a deep central basin with a maximum depth of 18 m. The inlet on the southwest corner of the lake is modified with an 8-foot stone structure, extending a few feet above the water level, powering prayer wheels at a stupa on the southwest edge of the lake. There is no impoundment present behind the structure, indicating that it does not impact lake levels. The littoral zone of the lake is densely vegetated with aquatic macrophytes, while the vegetation immediately surrounding the lake is comprised of thick groundcover vegetation, including ferns and mosses. The watershed of the lake transitions from wetland to a mixed deciduous-coniferous forest, which covers the rest of the watershed, including the surrounding slopes. This is consistent with the broader vegetation pattern of the region with montane-needle and broadleaf forests in the southeastern plateau below 3000 m elevation (Herzschuh et al., 2006). The northern shore of the lake transitions into a shallow wetland where water collects from the steep mountainside.

Modern regional climate data is derived from the Qamdo station (3307 m a.s.l.; 31.15° N, 97.167° E), which is ~220 km from Galang Co. Regional precipitation totals 367 mm and tracks the seasonal ISM cycle, with 89% of rainfall occurring between May

and September (330 mm; average summer temperature = 15.4°C; Fig. 4.3). Winters (December-February) are characterized by low precipitation (2.1 mm) and cold temperatures (-0.7 – 1.8°C), with winter ice cover on the lake from at least December through February.

4.3 Methods

4.3.1 Sample Collection

Sediment cores, water samples, surface sediments, and vegetation were collected at Galang Co in June 2015. The surface water chemistry of the lake was close to neutral (pH = 7.82) while conductivity and turbidity were low. Dissolved oxygen was 6.1 mg/L and the temperature was 17°C. Three surface sediment cores that captured the sediment-water interface were retrieved using a piston surface corer (Fig. 4.2). A 114 cm surface core, E-15, was acquired at a water depth of 17.3 m, while two shorter surface cores, A-15 (102 cm) and B-15 (115 cm), were collected at water depths of 17.5 m. The top 27 cm of E-15 were extruded at 1 cm intervals in the field while A-15 and B-15 were secured with Xorbitol® gel for transport and split at the Paleoclimatology and Sedimentology Laboratory at Indiana University-Purdue University Indianapolis (IUPUI). A longer sediment core, D-15, was retrieved from 17.7 meter water depth using a modified Livingstone piston corer (composite core length = 294 cm) (Livingstone, 1955; Wright, 1967). D-15 consisted of four-1 m drives that were overlapped by 30 cm in order to ensure complete sediment recovery. A replicate Livingstone core C-15 (composite core length = 266 cm; water depth=17.5 m) was also retrieved with a 30 cm overlap. Composite cores were made using a combination of field depths, images, and magnetic susceptibility to identify and correlate lithological units between drives.

Water samples were collected for isotopic analysis, while water chemistry, including temperature, pH, alkalinity, and conductivity, was measured in-situ using a Hydrolab MS5. Modern sediments from the surface-water interface were collected from the deep and shallow basins using an Ekman grab sampler. Two soil samples were also collected from the surrounding watershed. Samples of aquatic and terrestrial vegetation communities within and surrounding the lake were additionally collected. All samples

were stored at 4°C before analysis at the Paleoclimatology and Sedimentology Laboratory at IUPUI.

4.3.2 Geochronology

Sediments were dated using a combination of ^{210}Pb, ^{214}Pb, ^{137}Cs, and ^{14}C radiometric techniques. The ^{210}Pb, ^{214}Pb, and ^{137}Cs activities were measured by direct gamma counting on 13 samples from the upper 35 cm of the E-15 surface core at the University of Pittsburgh (Appleby and Oldfield, 1978). Radiocarbon (^{14}C) dates of charcoal samples from the D-15 core (n = 9) were determined using accelerator mass spectrometry (AMS) at the Keck AMS Facility, University of California Irvine. Charcoal samples were isolated by wet sieving at 63 μm before undergoing acid-base-acid (1 N HCl and 1 N NaOH) pretreatment based on UCI protocols (KCCAMS, 2011; Olsson, 1986). Radiocarbon dates were calibrated using the IntCAL 13 dataset (Reimer et al., 2013) and an age model was produced using the Bacon software program (Blaauw and Christen, 2011). All dates for the Galang Co E-17 and D-17 composite core are reported in calendar years before present (0 ka; 0 ka = 1950 CE).

4.3.3 Initial Core Description

All cores were split, imaged, and described before sub-sampling. High resolution images of the cores were made at IUPUI using a GeoTek Multi-Sensor Core Logger. Volumetric samples (1 cm^3) were collected from the work half of all cores at 1 cm intervals, weighed, and dried at 60 °C for 24 hours before being reweighed to determine dry bulk density (ρ_{dry}; g/cm^{-3}) and water content (%water). The sediment was then combusted at 550 °C for four hours, weighed, combusted again at 1000 °C for two hours, and weighed again in order to calculate total organic matter (%TOM) and total carbonate (%TC) from weight loss (Boyle, 2001; Heiri et al., 2001). The surface cores were then sliced into sections at a 1 cm resolution while Livingstone cores were sliced into 0.5 cm section for further analysis.

4.3.4 Grain Size

Approximately ~1 g of wet sediment was taken from cores E-15 and D-15 cores at 1 cm intervals, and from homogenized samples of the surface sediments and soil samples for grain size analysis. The samples were dried at 60 °C for 24 hours before weighing. Organic matter was removed by soaking the samples in 30 % hydrogen peroxide (H_2O_2) for 24 hours at room temperature before treating them with up to 5-20 ml aliquots of 30 % H_2O_2 at 70°C (Gray et al., 2010). Biogenic silica was then removed from the samples by soaking them in 20 mL of 1 N NaOH for six hours at 60 °C. The samples were subsequently centrifuged and rinsed with DI H_2O to remove any trace NaOH before freeze drying and reweighing to calculate lithics (%). Because carbonates were not present, the samples were not treated with HCl. Samples were lastly stored in 2.5% sodium metaphosphate and sonicated before grain size analysis, which was conducted using a Malvern Mastersizer 2000 at IUPUI. Grain size results were reported in a range of 49 particle diameter size bins between 0.2 and 2000 μm with an average of three replicates per sample.

4.3.5 XRF Geochemistry

Sedimentary geochemistry for elements ranging between aluminum (Al) to uranium (U) (atomic numbers 13 – 92) were measured using scanning x-ray florescence (XRF) at 0.5 cm resolution. XRF analysis was conducted at the Large Lakes Observatory, University of Minnesota Duluth using an ITRAX XRF Core Scanner (Croudace et al. 2006). Cores were scanned using a Cr source tube (30 kV; 55 mA) with a 15 second dwell time and a 10 mm measurement resolution. Raw data was processed using Qspec 8.6.0 software. All measurements are reported as counts per second (cps).

4.3.6 Carbon and Nitrogen Isotopes

Samples from the composite E-15 and D-15 core were collected at 2 cm intervals (n=148), dried, homogenized, and weighed into tin capsules (~4 mg) before C and N isotopic analysis at the Large Lakes Observatory, University of Minnesota Duluth. Measurements of total organic carbon (TOC), total nitrogen (TN), organic $\delta^{13}C$, and $\delta^{15}N$ were made using a Thermo Finnigan Delta Plus XP Isotope Ratio Mass Spectrometer

(IRMS) combined with a Costech 4010 elemental combustion system. Measurements are reported as per mil (‰) with $\delta^{13}C$ relative to the Vienna Peedee Belemnite (VPDB) and $\delta^{15}N$ relative to atmospheric nitrogen. A series of standards were used including acetanilide, caffeine, B-2153, B-2159, and USGS41 (National Institute of Standards and Technology) with coefficient of variation for C and N ranging between 0.5-1.1 %. Isotopic precision for standards was 0.03-0.26 ‰ for N measurements and 0.05-0.18 ‰ for C.

The carbon isotopic composition of organic matter ($\delta^{13}C_{org}$) is often used in conjunction with C:N to distinguish between C3 and C4 plant groups due to isotopic fractionation differences between their photosynthesis pathways (Meyers and Lallier-Vergès, 1999). It is difficult to differentiate the $\delta^{13}C_{org}$ signature between algal and C3 plants when lake and atmospheric CO_2 are at equilibrium (both typically range between -30 to -25 ‰), but C4 plants have more positive isotopic values with a range between -14 and -10 ‰. Interpreting $\delta^{15}N$ is complex because it is affected by organic matter source and available nitrogen in the water column and must be considered in conjunction with other productivity proxies, such as C:N and $\delta^{13}C_{org}$ (Meyers and Lallier-Vergès, 1999; Talbot, 2002). C3 land plants typically have an average $\delta^{15}N$ of 1 ‰ while phytoplankton have an average $\delta^{15}N$ of 8 ‰. Because total organic matter can be derived from both terrestrial and aquatic sources, the ratio of elemental organic carbon to total nitrogen (C:N) provides useful information about changes in the sources of organic matter to lacustrine systems. C:N values under 10 indicate aquatic sourced organic matter, typically algae, while values greater than 15 are indicative of C3 and C4 land plants (Meyers and Lallier-Vergès, 1999).

4.3.7 Lipid Biomarker Extraction & δ^2H Analysis

Lipids were extracted from a sub-set of thirty-five samples from the composite sediment core at the Lamont-Doherty Earth Observatory, Columbia University. Lipids were extracted from freeze-dried and homogenized sediments with dichloromethane and methanol solvent (9:1) using a Dionex Accelerated Solvent Extractor – 350. The total lipids extract was separated into aliphatic, ketone, and polar fractions through subsequent elutions using hexane, dichloromethane, and methanol solvent across a silica gel column

(70-230 mesh, 60A). The aliphatic fraction then underwent separation across a silver nitrate column (10 % $AgNO_3$) with hexane elution for *n*-alkanes and ethyl acetate elution for *n*-alkenes. The concentration of *n*-alkanes for each sample was determined using an Agilent Technologies 7890A gas chromatography mass spectrometer (GCMS).

The contribution of aquatic vs. terrestrial vegetation to the sediments was assessed using three indices. The average chain length (ACL) index quantifies the distribution of short vs. long chain *n*-alkanes with lower values (< 25) indicating aquatic vegetation and higher values (> 25) indicating terrestrial vegetation (Diefendorf et al., 2015; Mügler et al., 2008). The carbon preference index (CPI) represents the ratio of odd to even carbon atoms in leaf-wax *n*-alkanes with relative lows and highs indicating aquatic and terrestrial vegetation, respectively. The relative abundances of aquatic vs. terrestrial vegetation deposited in the lake was also assessed with the P_{aq} index, where higher values indicate greater abundance of aquatic plants (Ficken et al., 2000; Seki et al., 2009).

$$\mathrm{ACL} = \frac{25[C25] + 27[C27] + 29[C29] + 31[C31] + 33[C33] + 35[C35] + 37[C37]}{[C25] + [C27] + [C29] + [C31] + [C33] + [C35] + [C37]}$$

$$CPI = \frac{([C23] + [C25] + [C27] + [C29] + [C31] + [C33] + [C35]) + ([C25] + [C27] + [C29] + [C31] + [C33] + [C35] + [C37])}{2\,X\,([\mathrm{C24}] + [\mathrm{C26}] + [\mathrm{C28}] + [\mathrm{C30}] + [\mathrm{C32}] + [\mathrm{C34}] + [\mathrm{C36}])}$$

$$Paq = \frac{[C23] + [C25]}{[C23] + [C25] + [C29] + [C31]}$$

Twenty long-chain *n*-alkane extract samples then underwent hydrogen isotopic analysis (δ^2H). δ^2H measurements of the *n*-alkanes were made using a combined Thermo Scientific Trace GC Ultra GCMS and Delta V Plus IRMS (GC column: 30m, 0.25mm, 14.2psi, 60 °C). Samples were run with an isotopic standard (Mix A7) and a lab standard to assess drift. Raw isotopic values underwent drift correction using MATLAB. Isotopic variability ranged between 3.5-4.5 % for samples (Polissar and D'Andrea, 2014). Measurements are reported in delta notation as per mil (‰) with measurements relative to the VSMOW (Vienna Standard Mean Ocean Water). The average chain length (ACL),

carbon preference index (CPI), and aquatic vegetation index (P_{aq}) were calculated to assess changes in the distribution of *n*-alkanes and assess whether they were sourced by aquatic or terrestrial vegetation (Diefendorf et al., 2015; Ficken et al., 2000; Marzi et al., 1993).

Hydrogen isotopic measurements of the short-chain n-alkane nC23 reflects the isotopic composition of the lake water in which aquatic plants grow. The isotopic composition of lake water in turn incorporates changes in the isotopic composition of inflows (primarily precipitation) and subsequent modification from evaporation (Mügler et al., 2008). The isotopic measurements of longer chain n-alkanes (e.g., nC29 and nC31) incorporate the isotopic signature of soil water, which closely tracks the isotopic composition of precipitation.

4.4 Results

4.4.1 Core Description

A 294-cm-long composite core was constructed using the E-15 surface and D-15 Livingstone cores. The composite core was differentiated into two distinct halves based on visual stratigraphy (Fig. 4.4). The bottom 144 cm of the core from 294 to 150 cm consisted of a light brown peat material with bands of white coarse sand and gravel between 283-280 cm and 270-265 cm and a tan sand layer from 220-215 cm. The top 150 cm of the core consisted of massive units of dark to light brown muds with interspersed fragments of organic matter, including charcoal and grasses. There were two distinct white clay bands between 125-120 cm and 145-142 cm.

4.4.2 Age Model

Excess ^{210}Pb activity was highest at the top of the E-15 core, peaking at 10 cm, before decaying to background levels at 32 cm (Table 4.1; Fig. 4.5). An age model was developed for the top 31.25 ± 0.25 cm based on the constant rate of supply (Appleby and Oldfield, 1978). Three samples had ^{137}Cs activity at 14.75, 16.25, and 23.75 ± 0.25 cm depth, which were dated to -38 ± 3.4, -34 ± 3.8, and -3 ± 5.6 BP. The oldest ^{210}Pb date was at 31cm depth and dated as 67.3 ± 13 BP. Eight radiocarbon dates (Table 4.2) were

obtained from charcoal fragments and calibrated using the IntCal 13 dataset (Reimer et al., 2013) using the program Bacon (Blaauw and Christen, 2011). The oldest ^{14}C date for D-15 at 271-269 cm was calibrated to 11.27 ka. Dates below this depth were extrapolated by extending the age model in Bacon. The ^{210}Pb and ^{14}C dates were used to assess the age-depth relationship and an age model was established using the Bacon program spanning the last 12.3 ka (Fig. 4.6). The full age model dataset is in Appendix 3, Table A 3.1.

4.4.3 Organic Matter Chemistry

Total organic matter was highest during the early Holocene (11.7 – 6.2 ka) averaging 44.5% until 6.2 ka (Fig. 4.7A). Total organic matter subsequently decreased throughout the end of the middle (5 – 3 ka; average: 33 %) and late Holocene (3 ka to present; average 27.4 %). Total carbonate was low throughout the record (3.0 %) with a few isolated high carbonate intervals (17.7-34 %) from 11 – 10.9 ka (Fig. 4.7B).

The ratio of elemental organic carbon to total nitrogen (C:N) ranged between 8.6 and 28.1 with an average of 11.5 in the record (Fig. 4.7C). C:N was elevated during the early Holocene from 11.7 to 9.3 ka (average: 14.87) and slowly decreased from 9.3 to 6 ka (average: 12.13), suggesting a greater contribution of organic matter from terrestrial plants to the lake. After 6.0 ka, C:N was consistently lower for the rest of the record (average: 10.13).

Organic matter $\delta^{13}C_{org}$ at Galang Co varied significantly during the Holocene with $\delta^{13}C$ values averaging -27.2 ‰ and ranging between -32.41 ‰ to -12.4 ‰ (Fig. 4.7D). The most positive values of $\delta^{13}C_{org}$ occurred during the early Holocene between 11.9 – 11 ka (average: -21.59 ‰). After 11 ka, $\delta^{13}C_{org}$ varied between -29 and -25 ‰ before decreasing to an average -30.2 ‰ over the last 1 ka.

Galang Co sedimentary $\delta^{15}N$ averaged 0.99 ‰ and ranged between -1.25 ‰ and 2.37 ‰ throughout the record (Fig. 4.7E). $\delta^{15}N$ ranged between -1 and 0.5 ‰ between 11.3 – 6.2 ka. After 6.2 ka, $\delta^{15}N$ increased by 1.7 ‰ and varied between 0.6 to 2.4 ‰ (average: 1.8 ‰), remaining elevated until 1 ka, at which point $\delta^{15}N$ decreased to 0.9 ‰.

4.4.4 Sedimentology & Magnetic Susceptibility

Dry bulk density was variable throughout the record, averaging 0.2 g cm^{-3}, with lower values during the early Holocene (11.7 – 9.1 ka; Fig. 4.8A). MS was low, averaging 1.3 SI x 10^{-5} SI, until 6.2 ka before increasing to an average of 12.16 SI x 10^{-5} SI over the last 6 ka (Fig. 4.8B). Percent lithics varied during the Holocene (average: 51.9 %; range: 0.7-98 %) with low lithics between 11.7 – 11 ka and 7.5 – 6.5 ka corresponding to high organic matter (Fig. 4.8C). Lithics were higher from 6.5 ka to present (average: 60.1 %; range: 1.1-98 %) corresponding with finer sediments.

Clay content was low from 11.7 to 6 ka (average: 4.33 %; range: <0.1-18.5 %) before increasing and remaining high over the last 6 ka (average: 6.73 %; range: 0.2-35.3 %; Fig. 4.8D). Silt (average: 51.7 %; range: <0.1-86.1 %) and sand (average: 42.8 %; range: <0.1-100 %) abundances showed an inverse relationship throughout the Holocene (Fig. 4.8E and 4.8F). Silt content was lowest in the early Holocene from 11.7 to 6 ka, averaging 45%, before increasing around 6 ka to an average of 58.4 % when there was a noticeable change towards finer sediments in the core lithology. Percent sand was highest from 11.7 to 6 ka during the early Holocene averaging 50.6 % and declined after 6 ka by 15.7 %. Grain size diameters shows an abundance of coarser sediments from 11.7 until around 6 ka, when grain size distribution shifted to finer sediments for the rest of the Holocene (Fig. 4.8G).

4.4.5 XRF Geochemistry

Of the forty-seven elements measured on the composite core using XRF, I focus on iron, manganese, titanium, and zirconium for hydroclimatic interpretations. Titanium (Ti) and Zirconium (Zr) are conservative elements typically associated with clastic detritus, where higher Ti is interpreted as representing more terrestrial sediments being deposited into the lake, and vice versa (Croudace et al., 2006). Measurements of Ti (range: 701-113,073 cps) were lower in the early Holocene, averaging 13,226 cps from 11.7 to 6 ka (Fig. 4.9A). Ti concentrations increased after 6 ka, averaging 17,940 cps, indicating an increase in terrestrial sediments being deposited into the lake. Zr (range: 0-

3413 cps) follows a similar pattern with Ti, with lower Zr from 11.7 to 6 ka, averaging 959 cps (Fig. 4.9C). Zr increased after 6 ka, averaging 1485 cps.

Iron (Fe) is also linked with clastic material, but this relationship is additionally influenced by the lake's redox potential, with Fe staying in solution under anoxic conditions because it is redox sensitive (Cuven et al., 2010; Nesbitt and Markovics, 1997). Fe content showed a significant transition from low measurements, average 68,188 cps, between 11.7 and 6 ka and subsequent higher values in the rest of the record after 6 ka, averaging 159,015 cps (Fig. 4.9B). Redox potential of the lake was inferred by the ratio of manganese (Mn) to Fe (Naeher et al., 2013). The Mn: Fe ratio was higher between 11.7 and 6 ka, averaging 0.052, than declined after 6 ka to an average of 0.025 (Fig. 4.9D). The full XRF dataset is in Appendix 4, Tables A 4.1 – 4.6.

4.4.6 δ^2H Lipid Biomarkers

Long-chain *n*-alkanes (e.g., nC29 and nC31) are typically produced by terrestrial vascular plants while short chain *n*-alkanes (e.g., nC23) are generally produced by emergent and submerged aquatic macrophytes (Ficken et al., 2000; Seki et al., 2009). Mid-chain *n*-alkanes (e.g., nC25) can reflect a mixture of aquatic and terrestrial vegetation sources (Mügler et al., 2008; Seki et al., 2009). Overall the concentration of *n*-alkanes varied with the highest concentrations in the mid-chain *n*-alkanes nC25 (average: 6094 ng/g) and nC27 (average: 5913 ng/g), and with lower concentrations in short-chain and long-chain *n*-alkanes: nC23 (average: 3847 ng/g), nC29 (average: 4869 ng/g), and nC31 (average: 2528 ng/g; Fig 4.10). The concentration of leaf-wax *n*-alkanes in general were low for most of the Holocene before an increase in the concentrations of nC23-nC29 around 1.7 ka and subsequent decline (Fig. 4.10A-D). The concentration of nC31 was high between 11.7-8 ka before decreasing and remaining low throughout the remainder of the Holocene (Fig. 4.10E).

The ACL at Galang Co averaged 27.7 throughout the Holocene with values between 26.9 and 28.6, indicating that aquatic vegetation dominated the record (Fig. 4.10F). The CPI was highly variable over the record, ranging from 1.9 to 9 (average: 5.5), with higher CPI during the first half of the record from 12 to 5 ka, suggesting a higher abundance of terrestrial vegetation (Fig. 4.10G). P_{aq} was high for most of the record,

varying between 0.28 and 0.69 and averaging 0.5 indicating a high contribution of aquatic vegetation to the lake (Fig. 4.10H).

The concentration of sedimentary *n*-alkanes was generally low throughout the Galang Co core, limiting δ^2H measurements to twenty of the thirty-five samples selected. Δ^2H isotopic measurements on short-chain and long-chain *n*-alkanes ranged from -243.1 ‰ to -156.3 ‰ (Fig. 4.11). δ^2H_{C23} was higher from 10.7 – 7.7 ka, averaging -192.2 ‰, then decreased by 18 ‰ during the middle Holocene (6 – 2.5 ka) to 174.2 ‰ (Fig. 4.11A). After 2.5 ka, δ^2H_{C23} increased by 43.3 ‰ to an average of -167.4 ‰. Both δ^2H_{C25} and δ^2H_{C27} averaged -215.8 and -218.8 ‰ during the early Holocene (10.7 – 7.7 ka), increased during the middle Holocene (6 – 2.5 ka) by 21.1 ‰ and 12.6 ‰ for averages of -194.7 ‰ and -206.2 ‰ respectively and subsequently decreased from 2.5 ka to present (Fig. 4.11B and 4.11C). Both long-chain *n*-alkanes δ^2H_{C29} and δ^2H_{C31} were lower during the early Holocene from 10.7 – 7.7 ka, averaging -230.1 and -223.8 ‰ (Fig. 4.11D and 4.11E). δ^2H_{C29} decreased by -13.1 ‰ at 5.6 ka then subsequently increased and remained higher throughout the middle and late Holocene, averaging -222.7 ‰ from 5.3 ka to present. Δ^2H_{C31} record is limited after 7 ka with few data points, increasing to an average of -217.1 ‰ from 2.7 ka to present.

4.5 Discussion

4.5.1 Holocene Hydroclimate & Lake Level Variability at Galang Co

The co-occurrence of peat, high C:N, low $\delta^{15}N$, high $\delta^{13}C_{org}$, and coarse grain sizes at Galang Co between 11.7 and 6.2 ka strongly suggests that water levels were at a minimum during the early and middle Holocene. High organic matter inputs to the lake between 11.7 to 6.2 ka, which coincides with low $\delta^{15}N$, high C:N, and high $\delta^{13}C_{org}$, all suggest high influxes of terrestrial vegetation (C3 and C4 plants) to the lake. Shallow lake conditions are additionally supported by high Mn:Fe ratios from 11.7 to 6.2 ka, which indicate oxygen-rich conditions during this time, with shallow waters being more oxygen-rich than deeper waters. The onset of deeper lake conditions between 7 and 6 ka is suggested by rapid changes in sedimentology, including a transition to finer sediments and greater aquatic productivity as indicated by higher $\delta^{15}N$ and C:N values below 10.

Anoxic conditions as evident with lower Mn:Fe from 6.2 ka to present, indicate deeper lake conditions at Galang Co were established in the middle Holocene and have persisted through the present day.

The short-chain *n*-alkane δ^2H_{C23} results support the Galang Co lake level interpretations based on sedimentological and geochemical data. Specifically, high (low) δ^2H values of nC23 correspond to lower (deeper) lake levels. δ^2H_{C23} was high during the early Holocene from 11 to 7.7 ka, indicating increased evaporation when lake levels were low as indicated by peat-rich, coarse sediments. δ^2H_{C23} decreased in the middle Holocene (6 – 2 ka) as the lake transitioned to a deeper steady-state as indicated by the predominance of fine-grained sediments and high aquatic productivity. Based on this relationship, I interpret δ^2H_{C23} as a signal of effective moisture at Galang Co. Stronger ISM intensity, inferred by long-chain *n*-alkane δ^2H_{C29} and $\delta^2H_{C31,}$ persisted in the early Holocene (11 – 6 ka) when effective moisture was lowest, likely as a result of high evaporation. Both evaporation and monsoon intensity decreased in the middle Holocene around 6 ka resulting in greater effective moisture that persisted until the late Holocene when effective moisture declined around 1.5 ka. This relationship between monsoon precipitation, effective moisture, and lake levels at Galang Co stands in contrast to many of the existing records from the Tibetan Plateau, but as is discussed below, is not incompatible with the well-established Holocene trend of the ISM.

The Galang Co local hydroclimate record stands in sharp contrast to many of the ISM and lake level reconstructions from other sites on the Tibetan Plateau, which indicate greater effective moisture and deeper lake levels during the early Holocene (11 – 7 ka) when the ISM was strengthened, followed by a decline in effective moisture in the middle Holocene (7 – 3 ka) as the ISM weakened. This trend is evident at Paru Co (29.8°N, 92.4°E, 4845 m a.s.l.), a shallow high altitude lake approximately 300 km west of Galang Co, where high effective moisture and deeper lake levels are evident in the early Holocene (Bird et al., 2014). High %lithics and %sand, inferred as runoff and lake level signals respectively, indicate that effective moisture remained high until at least 7 ka when runoff declined while lake levels didn't fall until 5 ka (Fig. 4.12G-H).

An effective moisture and temperature record at Koucha Lake in eastern Tibet (34.0°N, 97.2°E, 4540 m a.s.l.), located 400 km northeast of Galang Co, shows a

maximum in effective moisture in the early Holocene (11.7 – 6 ka) simultaneous with warmer temperatures indicated by a steppe dominated plant community (Herzschuh et al., 2009). The warmer, wetter Tibetan Plateau during the early Holocene is also evident in the Lake Zigetang pollen record (90.9ºE 32.0ºN), where warmer temperatures persisted until 5 ka, when the climate transitioned to cooler and drier conditions (Herzschuh et al., 2006). High effective moisture derived from the pollen record coincided with lower carbonate $\delta^{18}O$ in the sediments from Koucha Lake between 11.7 – 7 ka, indicating lower lake levels (Mischke et al., 2008). Colder temperatures and drier conditions became dominant after 6 ka, evidenced by a transition to a high-alpine meadow vegetation community, and coincides with deeper lake levels inferred from higher $\delta^{18}O$. The contradiction between high effective moisture in the watershed and lower lake levels at Koucha Lake indicates is suggested to be an indication that high evaporation impacted lake levels even as the local hydroclimate was warmer and wetter.

The sharp contrast between Galang Co and other monsoon records is also evident when compared with records across the broader ISM extent. The timing of the transition to a deeper lake at Galang Co around 6.2 ka coincides with declining monsoon intensity at Dongge, Mawmluh, and Qunf Caves (Fig. 4.13C-E). Mawmluh Cave in northeastern India (25.3°N, 91.9°E, 1290 m a.s.l.), supports a strong monsoon in the early Holocene, with depleted $\delta^{18}O$ between 8 to 6 ka (Berkelhammer et al., 2012). Monsoon intensity subsequently declined after 6 ka with a hiatus in the record after 3.5 ka, interpreted as a significant reduction in effective moisture. Another $\delta^{18}O$ record from Dongge Cave (25.3°N, 108.1°E, 680 m a.s.l.), located in southeastern China, also shows a strengthened monsoon from 11-5 ka (Dykoski et al., 2005). The Dongge Cave is at the farthest east extent of the ISM and follows the same precipitation patterns as other ISM records, with a stronger monsoon during the early Holocene with a noted decline towards weaker monsoon conditions after 5 ka. These cave records indicate that monsoon intensity and effective moisture was greatest in the early Holocene and declined between 6 and 5 ka when solar insolation declined and the ITCZ shifted southward (Fleitmann et al., 2003).

4.5.2 Hydroclimate Drivers of Galang Co Effective Moisture

I hypothesize that low effective moisture in the Galang Co record is attributed to local hydroclimate conditions. Whatever mechanism is responsible for the hydroclimate response at Galang Co, a reversal of this condition must have occurred around the mid-Holocene decline in the monsoon resulting in a deeper lake. The timing of the transition from a shallow to a deep lake at Galang Co occurs at the same time as monsoon intensity declines in other records, supporting the conclusion that hydroclimate is the driver of effective moisture and lake levels at Galang rather than other hydrological factors. Strong monsoon conditions in the early Holocene (11.7 to 7 ka) at ISM sites were driven by broader climate mechanisms, including higher solar insolation, the position of the ITCZ, and a La Niña-state in the Pacific (Berkelhammer et al., 2012; Bird et al., 2014; Emile-Geay and Tingley, 2016; Emile-Geay et al., 2016; Fleitmann et al., 2003).

However, I propose that the more likely mechanism is evaporation driven by temperatures and ice cover. The early Holocene was warmer as observed in the Koucha Lake and Lake Zigetang pollen records which could have resulted in reduced ice cover on the lake. Ice plays an important role in reducing evaporation from a lake surface during the winter season, with modern studies of Tibetan Plateau lakes indicating that ice cover results in lower evaporation and greater lake levels (Lazhu et al., 2016; Lei et al., n.d.). Evaporation on Plateau lakes is highest during the fall and winter due to the large temperature differences between the lake water and air (Lei et al., n.d.), providing further evidence that a decline in ice cover on Galang could be responsible for the anti-phase effective moisture pattern observed in the early and middle Holocene. An ice free Galang Co would have allowed for year-round evaporation driving a reduction in effective moisture and decreasing lake levels. Evaporation rates in the early Holocene would have been higher due to warmer temperatures and could account for low lake levels if Galang Co had little or no ice cover during the year. When temperatures cooled on the Plateau during the middle Holocene between 6 and 5 ka, winter ice cover would have been reestablished and could reduce the evaporation season on the lake by up to six months, resulting in higher effective moisture and lake levels. Another possible driver of the effective moisture trends at Galang Co is a rainout or orographic effect with high convection in the early Holocene resulting in rainout along southern slopes in the

Himalayas and southern Tibet. When monsoon intensity and, subsequently, convection declined, moisture remained in the atmosphere longer, reaching low altitude inter-montane valleys in the eastern plateau. The inter-montane valley where Galang is situated is flanked by high elevation mountains in three-directions, to the east, west and south, which could prevent moisture from reaching the site during high convection and may be responsible for the contradictory moisture record at this site. Further research is needed to determine which mechanism is responsible and requires the development of additional records from this region, including low-elevation sites, to see if this phenomenon is unique to Galang Co.

4.5.3 Elevation-Dependent Expression of Monsoon Precipitation

As I hypothesized, Galang Co is an effective moisture record of the southeastern Tibetan Plateau, which shows that the early Holocene (11.7 – 7 ka) was extremely evaporative (low P:E balance). Evaporation began to decline between 7 and 6 ka, after which effective moisture increased (higher P:E balance). The middle Holocene transition in lake conditions at Galang Co from 7 to 6 ka coincides with shift towards a global weaker monsoon and cooler Northern Hemisphere temperatures. Solar insolation, a driver of the decline in monsoon intensity, declined after reaching an early Holocene maximum, and steadily decreased through the middle and late Holocene (Berger and Loutre, 1991). Lower solar insolation is a driving force of the southerly shift of the ITCZ, weaker monsoon winds, and more El Niño-like conditions in the Pacific. An ITCZ record at Qunf Cave in southern Oman (17.2°N, 54.3°E, 650 m a.s.l.), also supports stronger monsoon intensity from 10 – 6 ka with depleted $\delta^{18}O$ during this period indicating a more northerly ITCZ position (Fleitmann et al., 2003). After 6 ka, the ITCZ moved further south as evidenced by increasing $\delta^{18}O$ at Qunf Cave, where a hiatus in the record from 2.7 to 1.3 ka coincides with reduced ISM winds in the Arabian Sea (Gupta et al., 2003). Pacific sea surface temperatures (SSTs) from the eastern Pacific near the Baja Peninsula (Marchitto et al., 2010), Laguna Pallcacocha (Moy et al., 2002), and the sand record at El Junco (Conroy et al., 2008) indicate a La Niña-like state in the Pacific between 11.7 – 6 ka before a transition to more frequent El Niño-like conditions from 6 ka to present. The timing of the state-change in these ISM drivers, support our hypothesis that the transition

to a wetter local hydroclimate at Galang Co is the result of a climatic change rather than local hydrological change.

As a low-elevation site on the Tibetan Plateau, Galang Co exhibits a strong local hydroclimate response to the decline in ISM precipitation, however, the lake level interpretation shows an anti-phase response to other high elevation records. A lack of low-elevation paleoclimate records from the region has limited our understanding of monsoon expression in low-elevation areas of the Tibetan Plateau, increasing the importance of the interpretation of the Galang Co record. I have hypothesized that this anti-phase lake level relationship is the result of high evaporation in the early Holocene driven by warmer temperatures and reduced ice coverage. Lower lake levels, despite higher precipitation, in the early Holocene suggests that local hydroclimate at low-elevation sites is driven by evaporation.

The anti-phase trend of high precipitation and low lake levels, was also observed at Koucha Lake, where the pollen record indicated high effective moisture and warmer temperatures, while the carbonate sediment record shows low lake levels (Herzschuh et al., 2009; Mischke et al., 2008). Both Galang Co and Koucha Lake were evaporation-controlled lakes, exhibiting lower lake levels despite higher monsoon precipitation in the warmer, early Holocene. Lakes are more susceptible to evaporation, as the lake experiences year-round evaporation, while the vegetation community is largely dormant during the driest parts of the year. As the monsoon coincides with the growing season, plant communities are reflective of trends in the ISM, with pollen and long-chain *n*-alkane proxies being minimally affected by evaporation. The seasonality of the pollen record at Koucha Lake and the long-chain *n*-alkane record (δ^2H_{C29} and δ^2H_{C31}) at Galang Co is the most likely explanation for indicators of high early Holocene ISM precipitation in the respective watersheds, while lower lake levels persisted. Projections of warmer temperatures on the Tibetan Plateau with climate change indicate that southeastern Tibetan Plateau will become drier, as evaporation increases, ice cover decreases, and other moisture sources, such as glacial melt, decrease (Yao et al., 2007; Yao et al., 2012). Lakes, like Galang Co, may be more strongly impacted by these changes, with greater evaporation occurring during the fall and winter months, that would be exacerbated by reduction in ice cover. The Galang Co Holocene ISM interpretation suggests that as air

temperatures continue to warm on the Tibetan Plateau, evaporation rates will play a larger role in determining water availability.

4.6 Conclusions

Galang Co demonstrates a unique contradiction to other ISM paleoclimate records from the Tibetan Plateau, with a shallow lake during the ISM maximum from 11.7 to 6.2 ka and a deeper lake after monsoon intensity declined after 6.2 ka. Rising lake levels at Galang Co from 7 – 6.2 ka coincide with the gradual weakening of the mid-Holocene monsoon at other sites, evidenced by falling lake levels at Paru Co and higher $\delta^{18}O$ at Dongge, Mawmluh, and Qunf Caves. The concurrent timing of the change in lake levels at Galang Co with declining ISM intensity at other sites from the Tibetan Plateau suggest that shifts in effective moisture at Galang Co was driven by broader climate forcing. This inverse relationship between ISM precipitation and effective moisture indicate that Galang Co was an extremely evaporative environment during the early Holocene and that evaporation declined after 6.2 ka. I suggest that ice cover drove this change, with warmer temperatures in the early Holocene resulting in limited ice cover on Galang Co and year-round evaporation. During the middle Holocene, temperatures on the Tibetan Plateau declined, increasing ice coverage on the lake and reducing evaporation. A lack of low-elevation sites on the Tibetan Plateau limits our ability to confirm whether the lake level responses at Galang Co to synoptic ISM intensity is consistent with other sites or is driven by local conditions. New records are needed both at low-elevation sites and in the easternmost extent of the ISM on the Tibetan Plateau to determine the mechanisms responsible for Galang Co's low lake stand during a strong monsoon. The Galang Co record suggests that low-elevation lakes in the southeastern Tibetan Plateau are vulnerable to high evaporation when temperatures increase that can drive lower lake levels despite increased precipitation, indicating that climate change can have a significant impact on water availability in this highly populated region.

4.7 Tables

Table 4.1: ^{210}Pb and ^{137}Cs results from Galang Co E-15 Core.

DEPTH (CM)	^{210}PB ACTIVITY	±	SUPPORTED 210PB OR 214PB ACTIVITY (BQ/G)	±	EXCESS ^{210}PB ACTIVITY	±	137CS ACTIVITY (BQ/G)	±	CAL. YR BP
2.75	0.336	0.113	0.0923	0.0375	0.2437	0.0755	NA	NA	-58.1392
5.75	0.55	0.145	0.171	0.0508	0.379	0.0942	NA	NA	-52.8343
10.25	1.04	0.289	0.287	0.105	0.753	0.184	NA	NA	-45.3396
14.75	0.759	0.197	0.185	0.0599	0.574	0.1371	0.0221	0.0178	-37.8562
16.25	0.536	0.15	0.15	0.0591	0.386	0.0909	0.0154	0.0148	-34.2936
17.75	0.26	0.0915	0.0839	0.0371	0.1761	0.0544	NA	NA	-27.2629
19.25	0.544	0.177	0.197	0.0832	0.347	0.0938	NA	NA	-17.1551
23.75	0.253	0.0638	0.103	0.0275	0.15	0.0363	0.00815	0.00679	-3.37822
25.25	0.304	0.0841	0.154	0.0404	0.15	0.0437	NA	NA	33.14854
26.5	0.255	0.0655	0.132	0.029	0.123	0.0365	NA	NA	56.26261
31.25	0.218	0.0917	0.116	0.0687	0.102	0.023	NA	NA	67.37271
32.75	0.146	0.0706	0.12	0.0507	0.026	0.0199	NA	NA	NA
34.25	0.21	0.0783	0.146	0.0475	0.064	0.0308	NA	NA	NA

Table 4.2: ^{14}C dates from Galang Co D-15 Core.

CORE	MEAN DEPTH (CM)	^{14}C YR	±	CAL YR	±
D15	83	3085	30	3295	30
D15	140	6100	130	5030	130
D15	147	5100	60	5830	60
D15	162	6110	190	6600	190
D15	178	6360	80	7440	80
D15	201	6610	20	7504	20
D15	221	6980	20	7902	20
D15	270	9975	25	11273	25

4.8 Figures

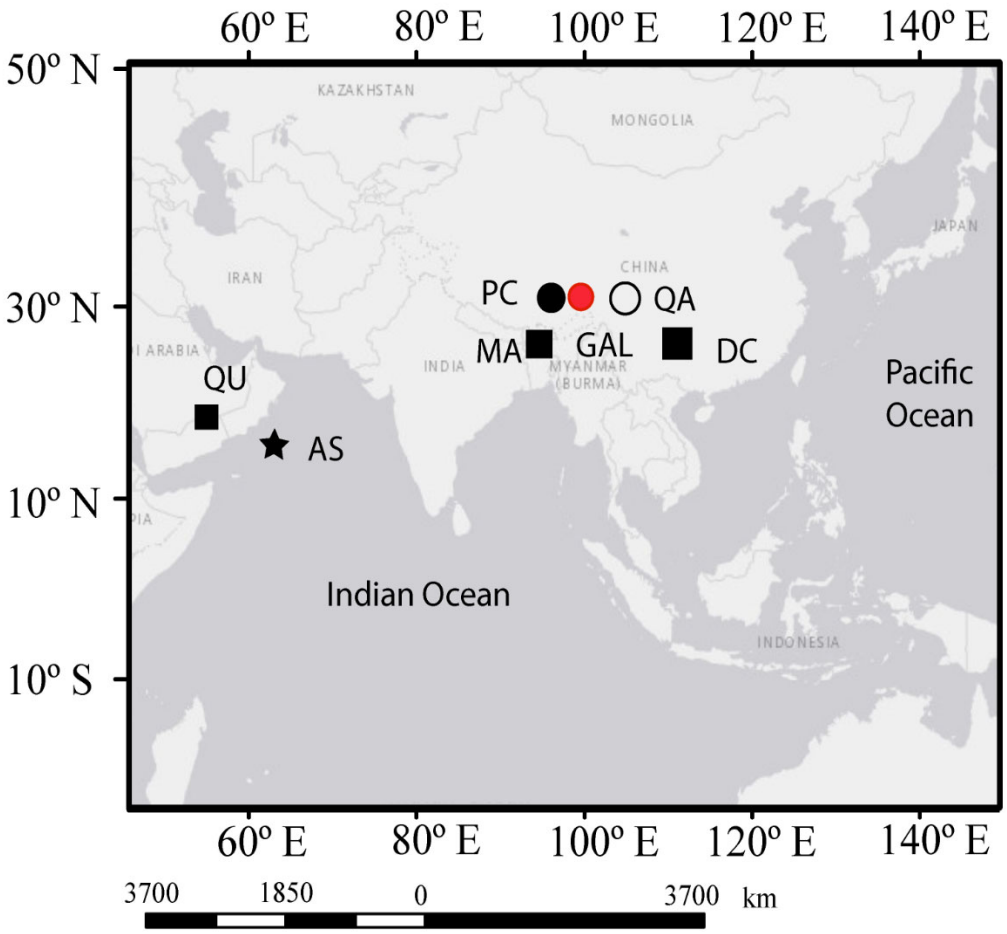

Figure 4.1. Paleoclimate archives from the greater ISM region including Galang Co (GAL; red), Paru Co (PC), Mawmluh Cave (MA); Dongge Cave (DC), Qunf Cave (QC), Arabian Sea (AS), Eastern Pacific (EP), and El Junco (EJ). Lake and marine sediments are marked with circles and stars respectively. Cave records are marked with squares. The Qamdo weather station (QA) is marked with an open circle.

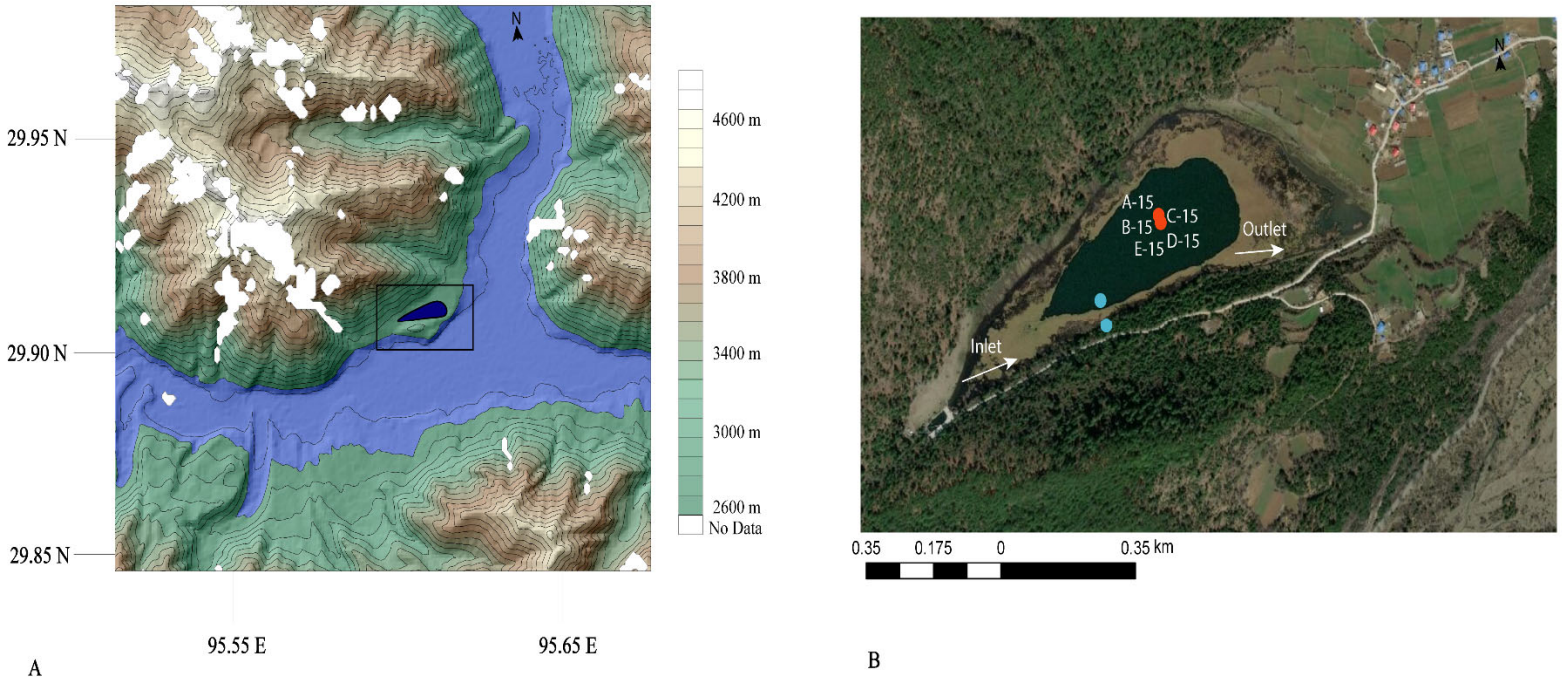

Figure 4.2. Galang Co (blue outline) and its watershed relative to the Parlang Zangbo River and surrounding region (A). Galang Co and its surrounding shoreline with the modified inlet on the southwest corner of the lake and the outlet on the southeast (B). On the lake, locations of core sites are marked with red circles while the surface sediments and soil samples are marked with blue circles.

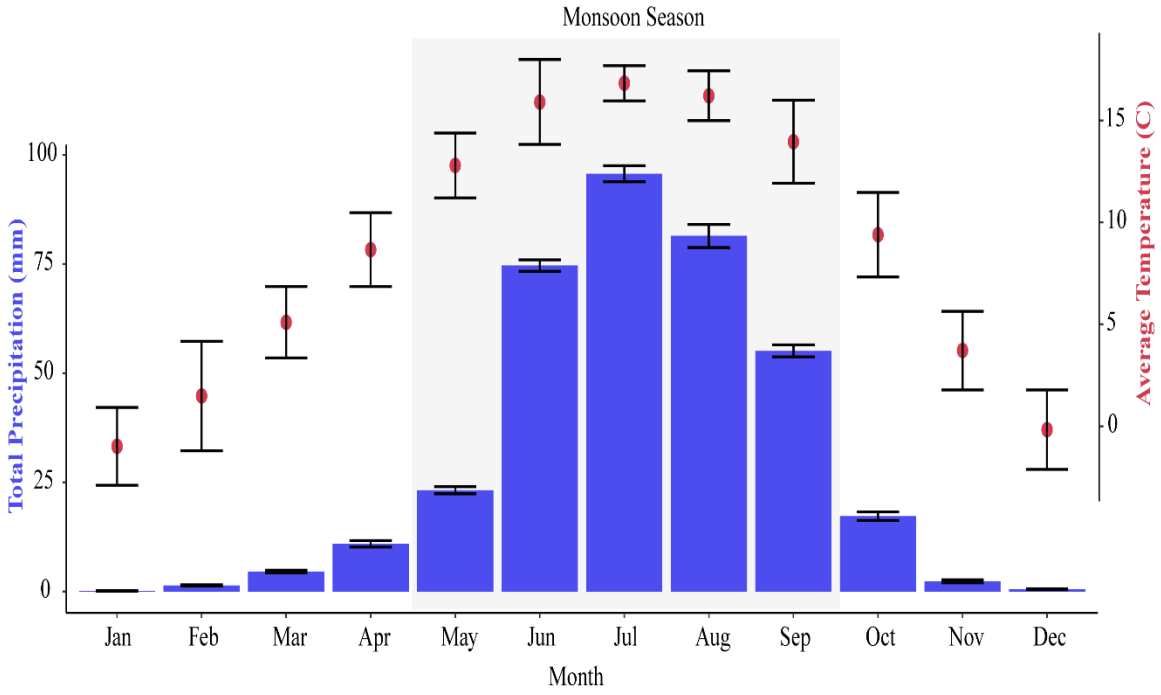

Figure 4.3. Thirty-year average of monthly total precipitation (mm ± s.d.) and average temperature (°C ± s.d.) at Qamdo weather station.

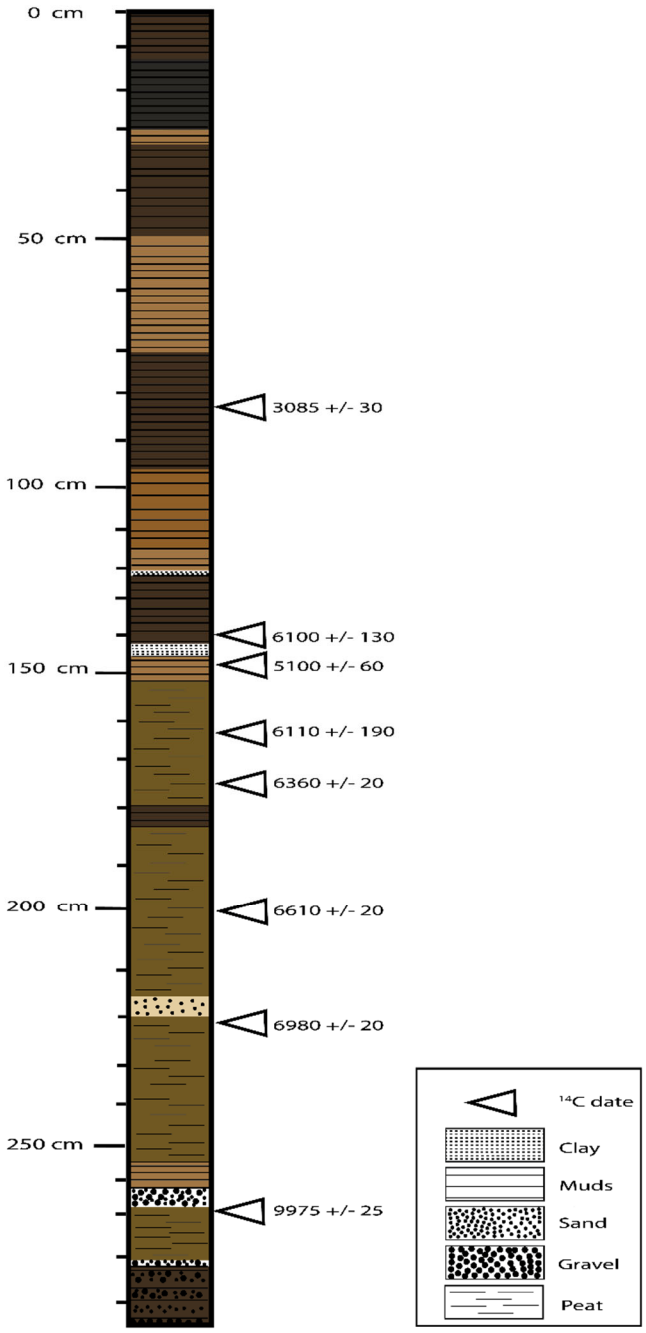

Figure 4.4. Stratigraphy of the composite Galang Co E-17 surface and D-17 Livingstone core. Core lithological units have been colored and marked to include clay (dashed lines), mud (silt and clay; horizontal lines), sand (small dots), gravel (large dots), and peat (solid grey). The location of radiocarbon dated material are designated with triangles.

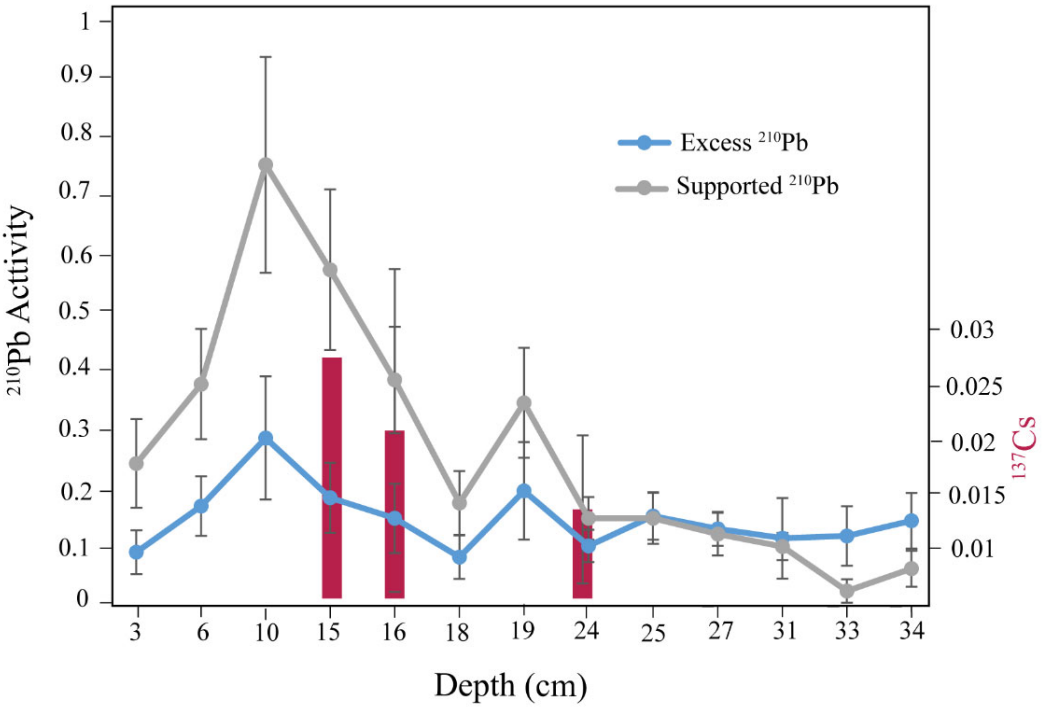

Figure 4.5. Supported (grey) and excess (blue) ^{210}Pb activity (± 1 s.e.m,) and ^{137}Cs activity (gray bar) from the top 35 cm of the E-17 surface core.

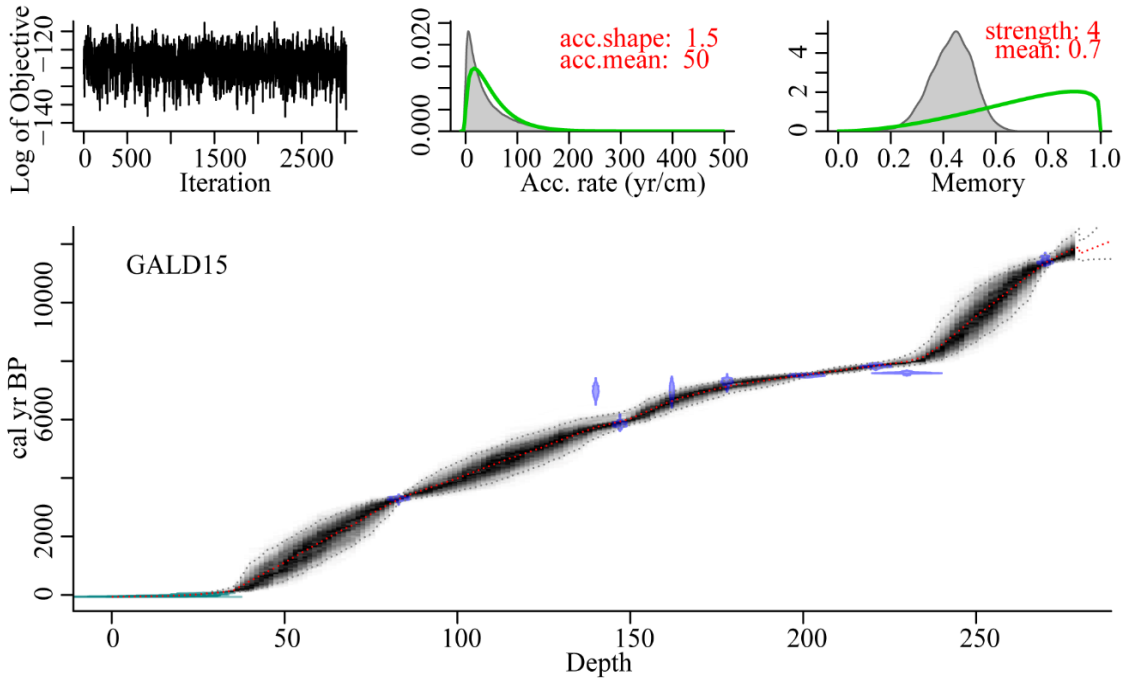

Figure 4.6. Age model for Galang Co composite E-17 and D-17 core over the past 12.3 ka using both 210Pb and 14C dates.

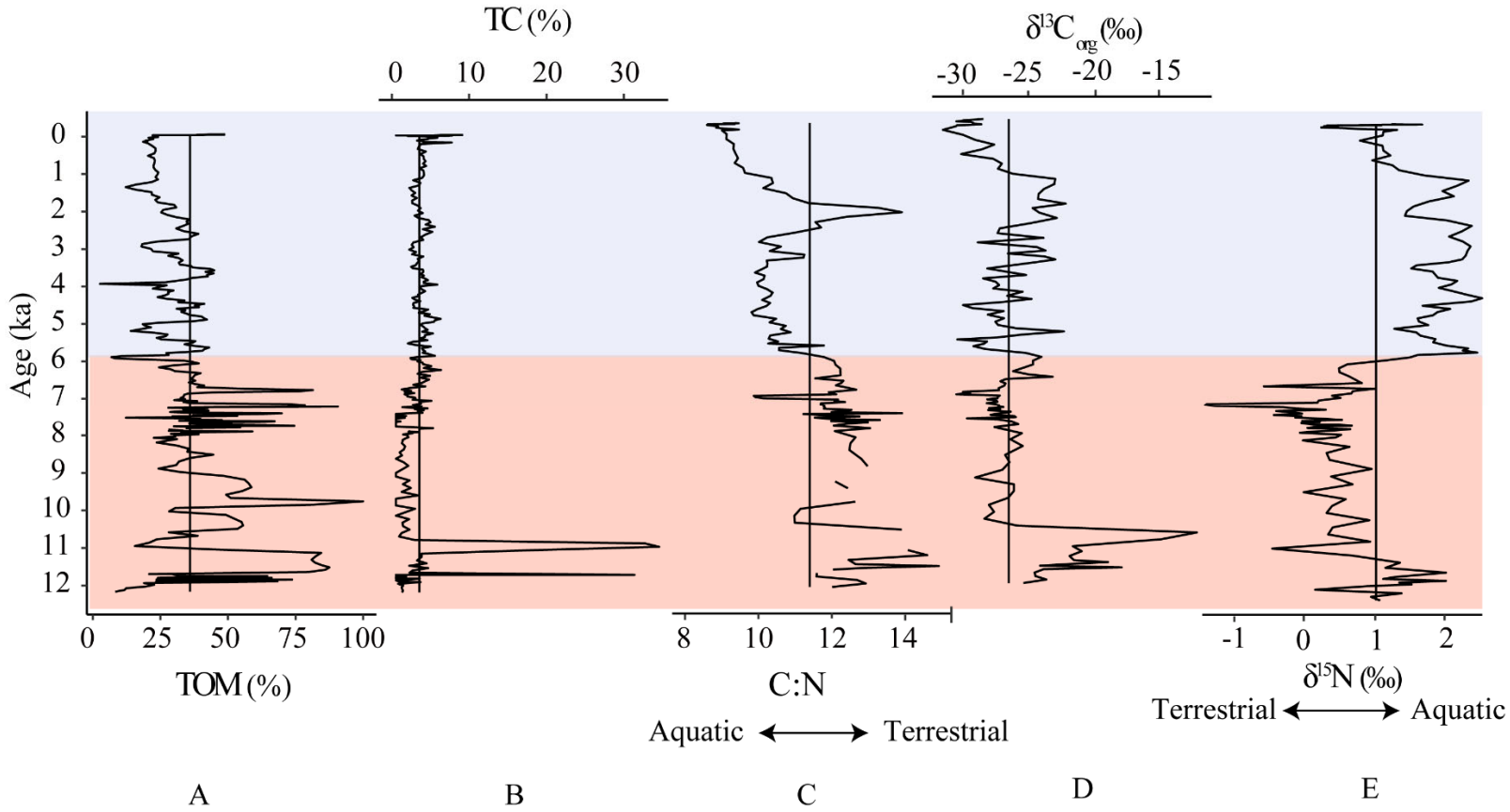

Figure 4.7. Sedimentology and geochemistry of Galang Co E-17 and D-17 composite core including total organic matter (TOM %; A) and total carbonates (TC %; B) as derived from loss-on-ignition and the ratio of elemental carbon to nitrogen (C: N; C), organic matter $\delta^{13}C$ (VPDB ‰; D), and sediment $\delta^{15}N$ (air ‰;E). Black vertical lines denote average values over the record. Red and blue backgrounds indicate shallow and deeper lake conditions respectively.

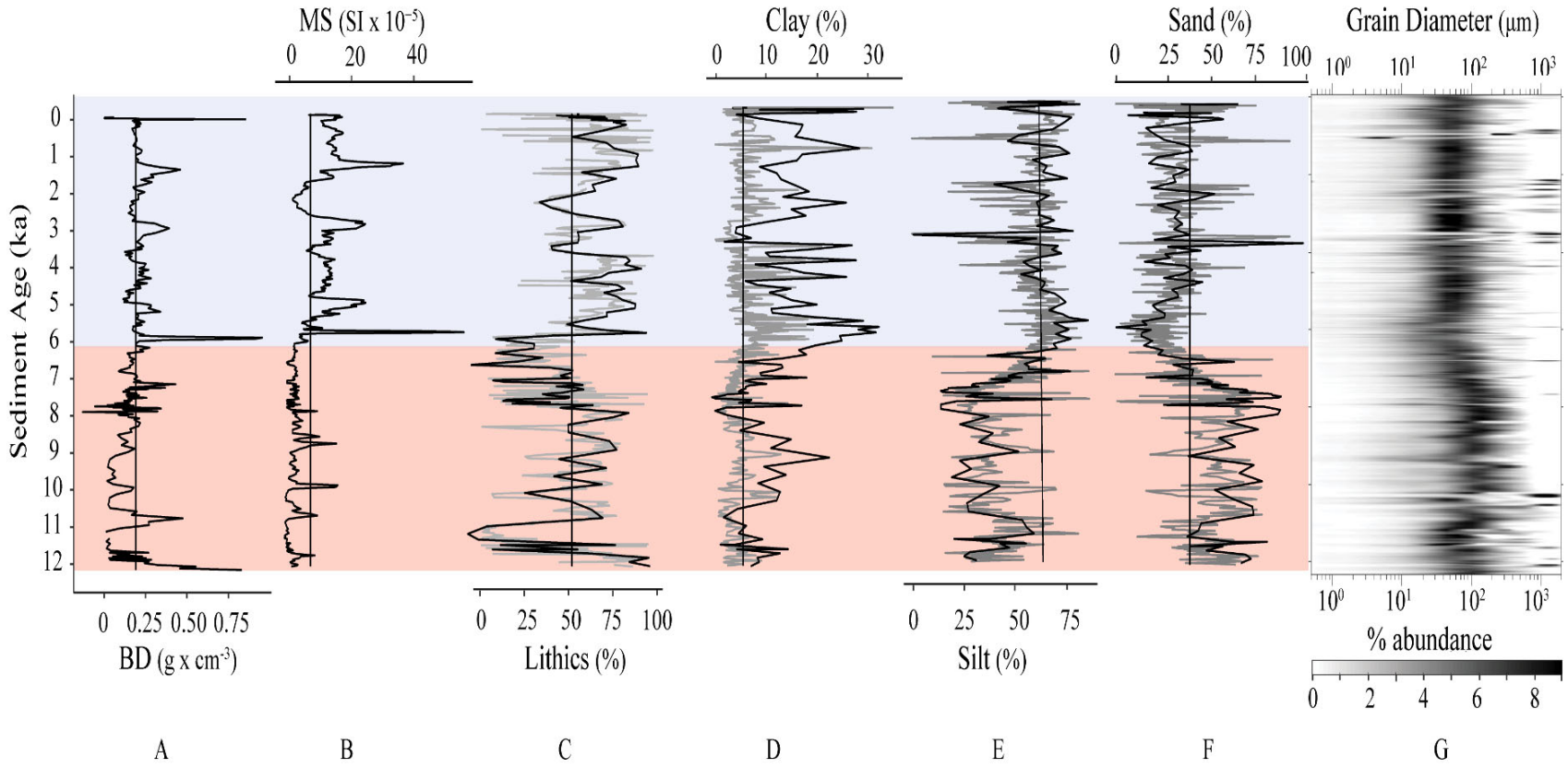

Figure 4.8. Physical sedimentology of Galang Co E-17 and D-17 composite core including dry bulk density (BD g x cm^{-3}; A), wet sediment magnetic susceptibility (MS SI x 10^{-5}), 5 point moving average (MA) percent total lithics I, percent clay 5 pt. MA (D), percent silt 5 pt. MA I, percent sand 5 pt. MA (F), and a histogram of grain size diameters (G). Black vertical lines denote average values over the record. Red and blue backgrounds indicate shallow and deeper lake conditions respectively.

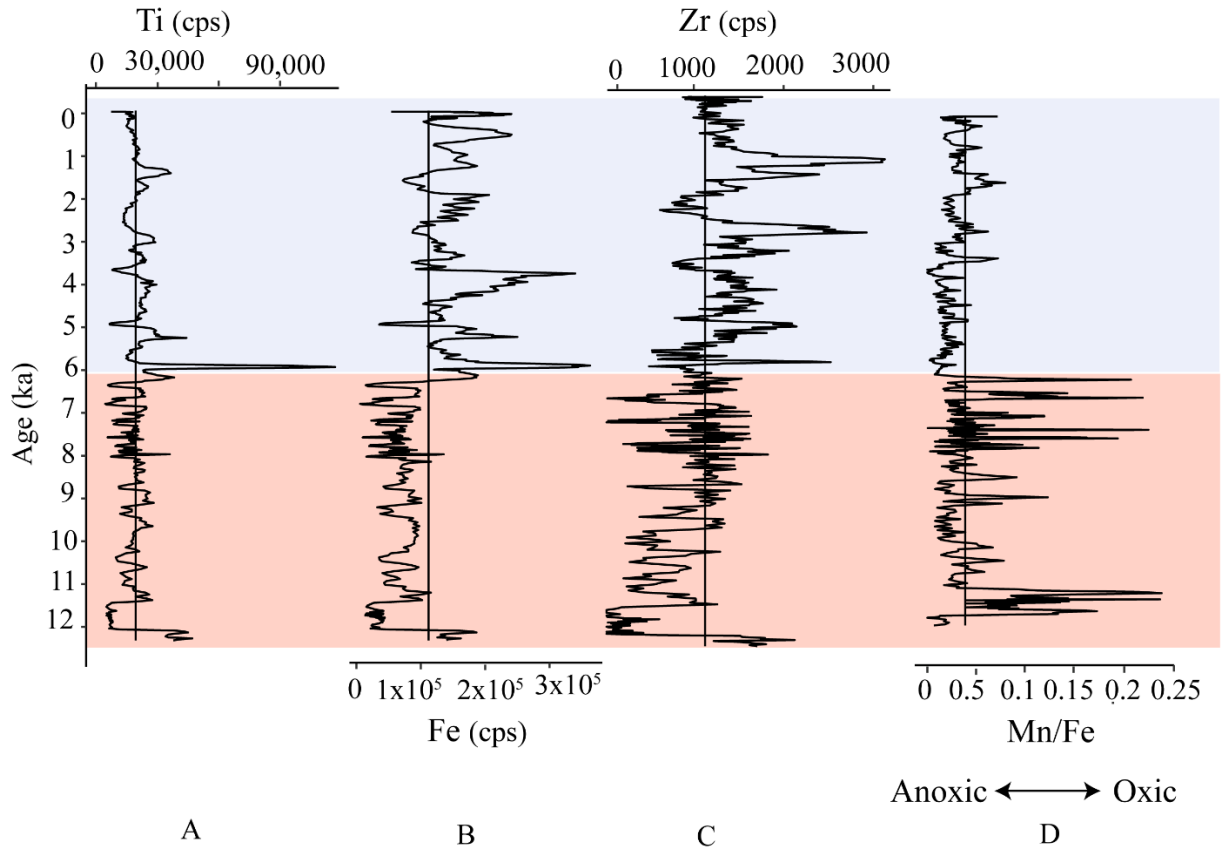

Figure 4.9. Select elemental XRF results from Galang Co E-17 and D-17 composite core including Ti (A), Fe (B), and Zr (C) and the ratios of Mn: Fe (F). All measurements are in counts per second (cps). Black vertical lines represent average values over the record. Red and blue backgrounds indicate shallow and deeper lake conditions respectively.

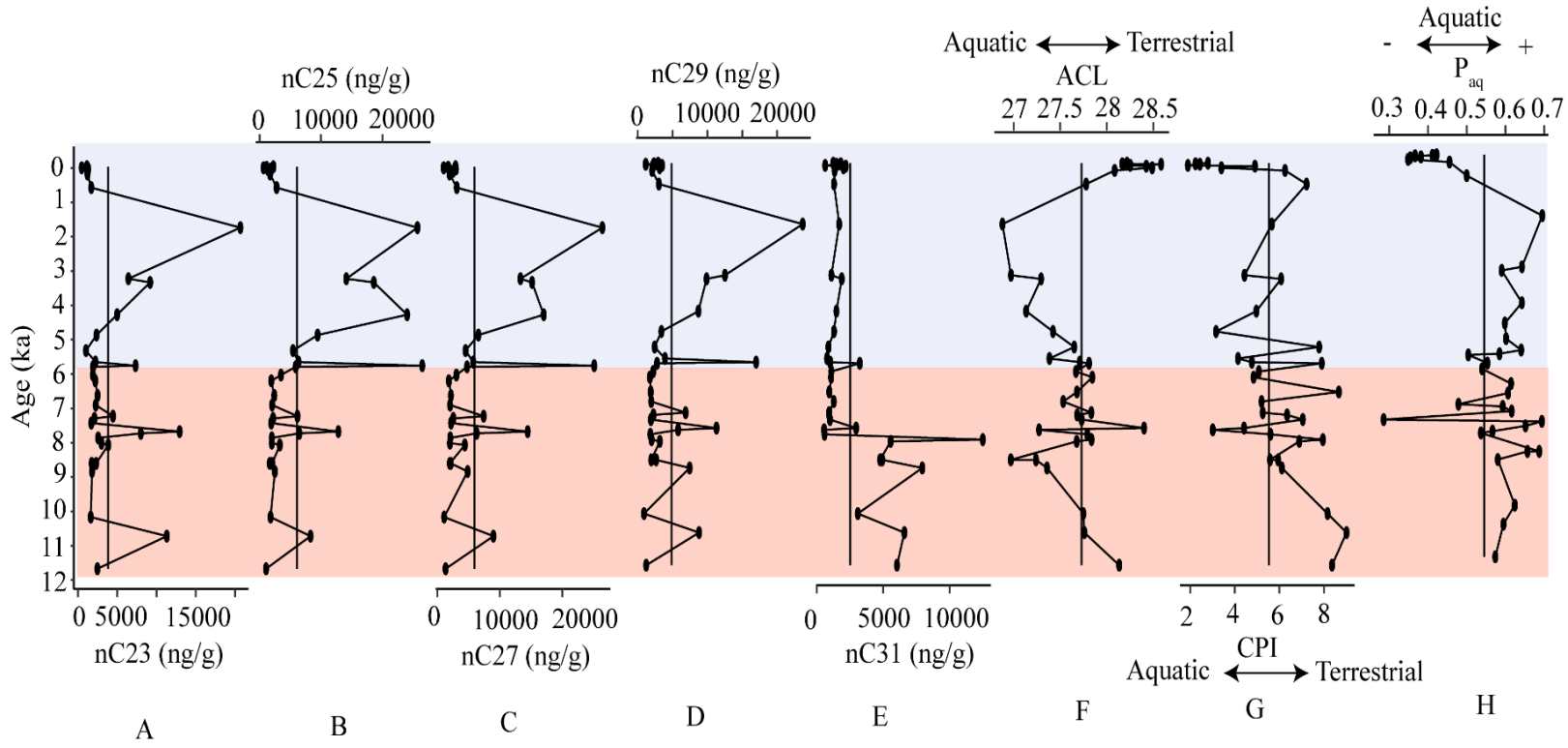

Figure 4.10. The concentration of Galang sediment *n*-alkanes (ng/g) for nC23 (A), nC25 (B), nC27 (C), nC29 (D), and nC31 I carbon chain lengths. The average chain length (ACL; F), carbon preference index (CPI; G), and aquatic vegetation index (P_{aq}; H) of sediment *n*-alkanes. Black vertical lines denote average values over the record. Red and blue backgrounds indicate shallow and deeper lake conditions respectively.

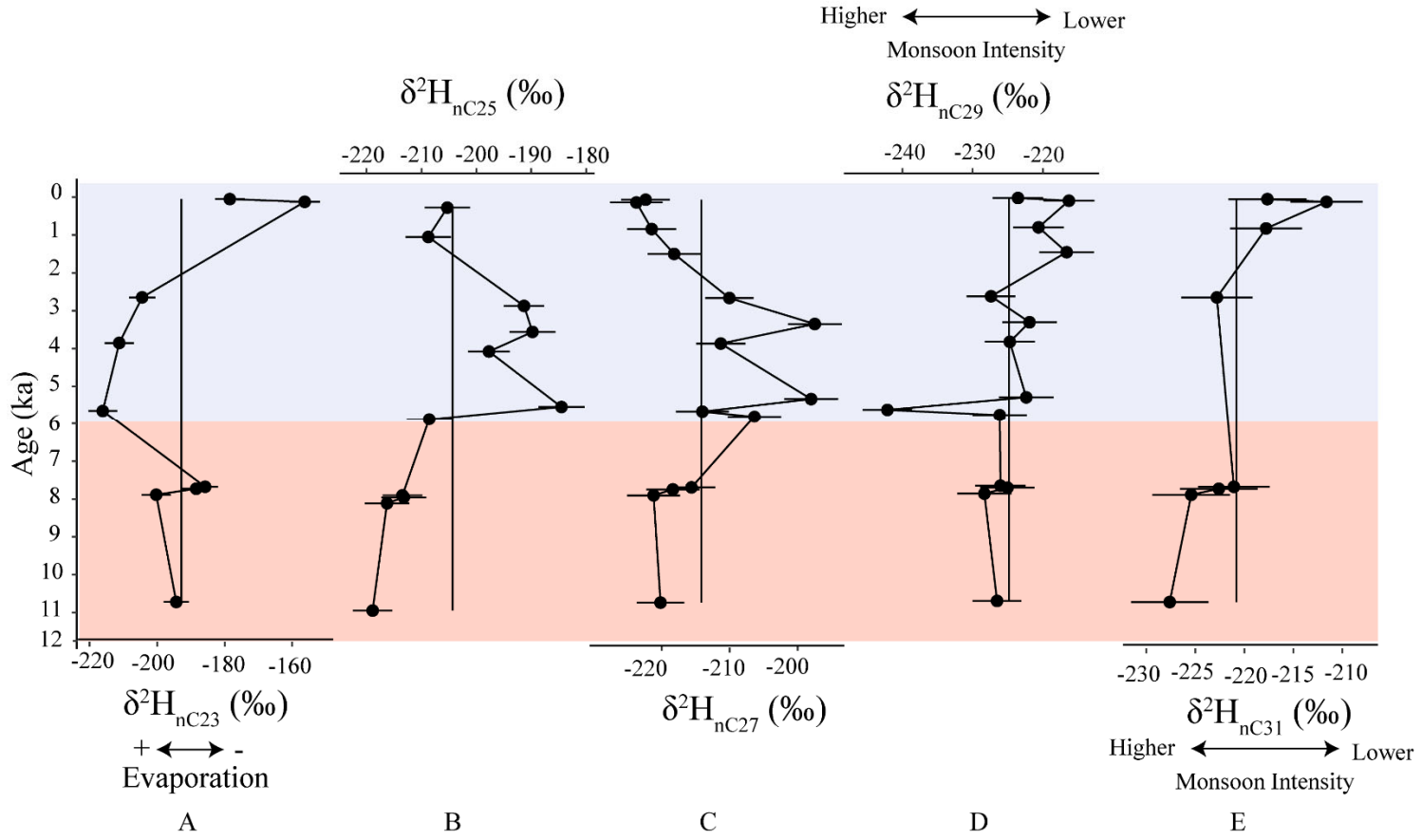

Figure 4.11. Galang E-17 and D-17 composite core sediment δ^2H (‰) for nC23 (A), nC25 (B), nC27 (C), nC29 (D), and nC31 I carbon chain lengths. Black vertical lines denote average values over the record. Red and blue backgrounds indicate shallow and deeper lake conditions respectively.

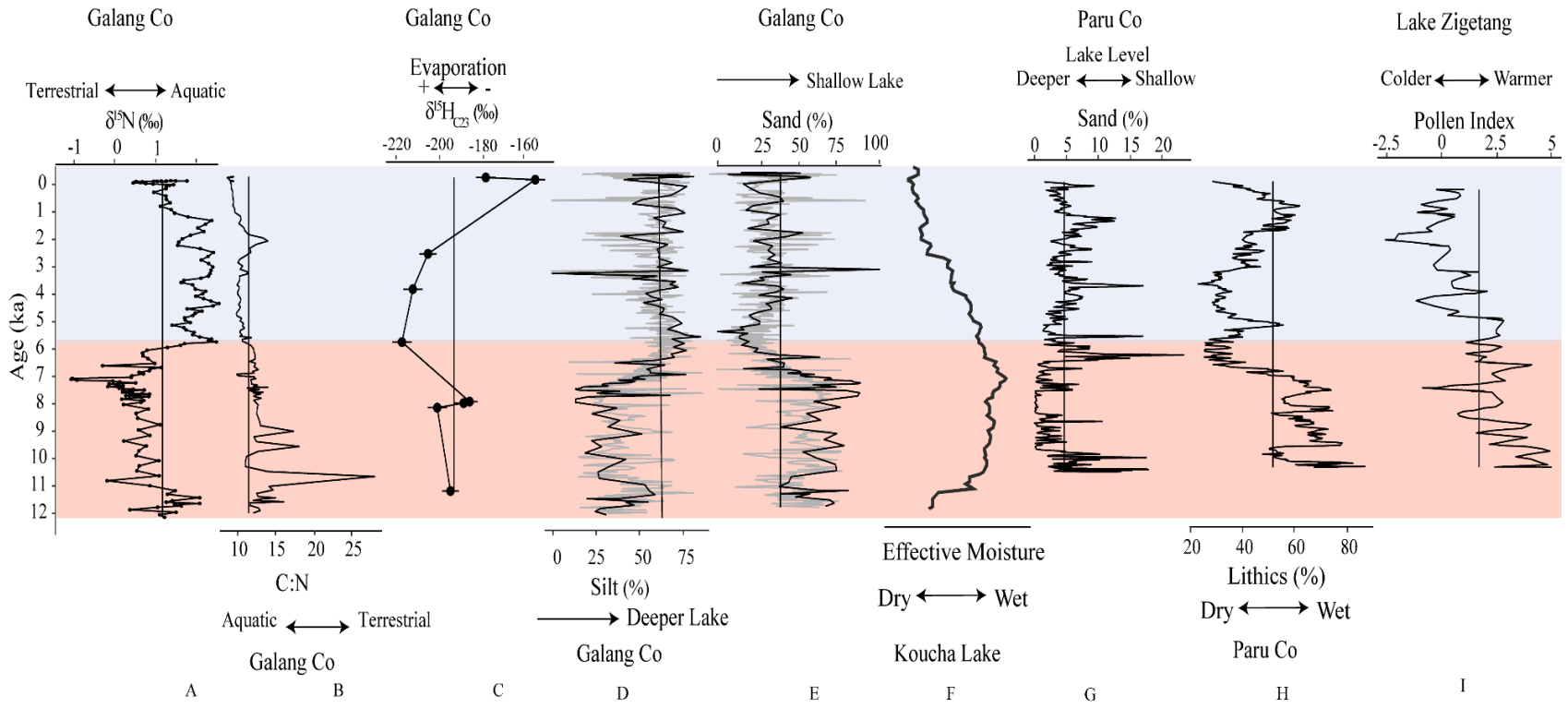

Figure 4.12. Galang Co δ15N (‰; A), ratio of C to N (B), δ^2H_{C23} (C), percent silt 5 pt. MA (D), percent sand 5 pt. MA (E) in conjunction with the reconstruction of effective moisture from Koucha Lake (F), the sand and lithics records from Paru Co (%; G-H), and temperature reconstruction from Lake Zigetang. Grey background indicates period of low lake level in Galang Co (12.5-6 ka). Average values over the record are designated as vertical lines. Red and blue backgrounds indicate shallow and deeper lake conditions respectively.

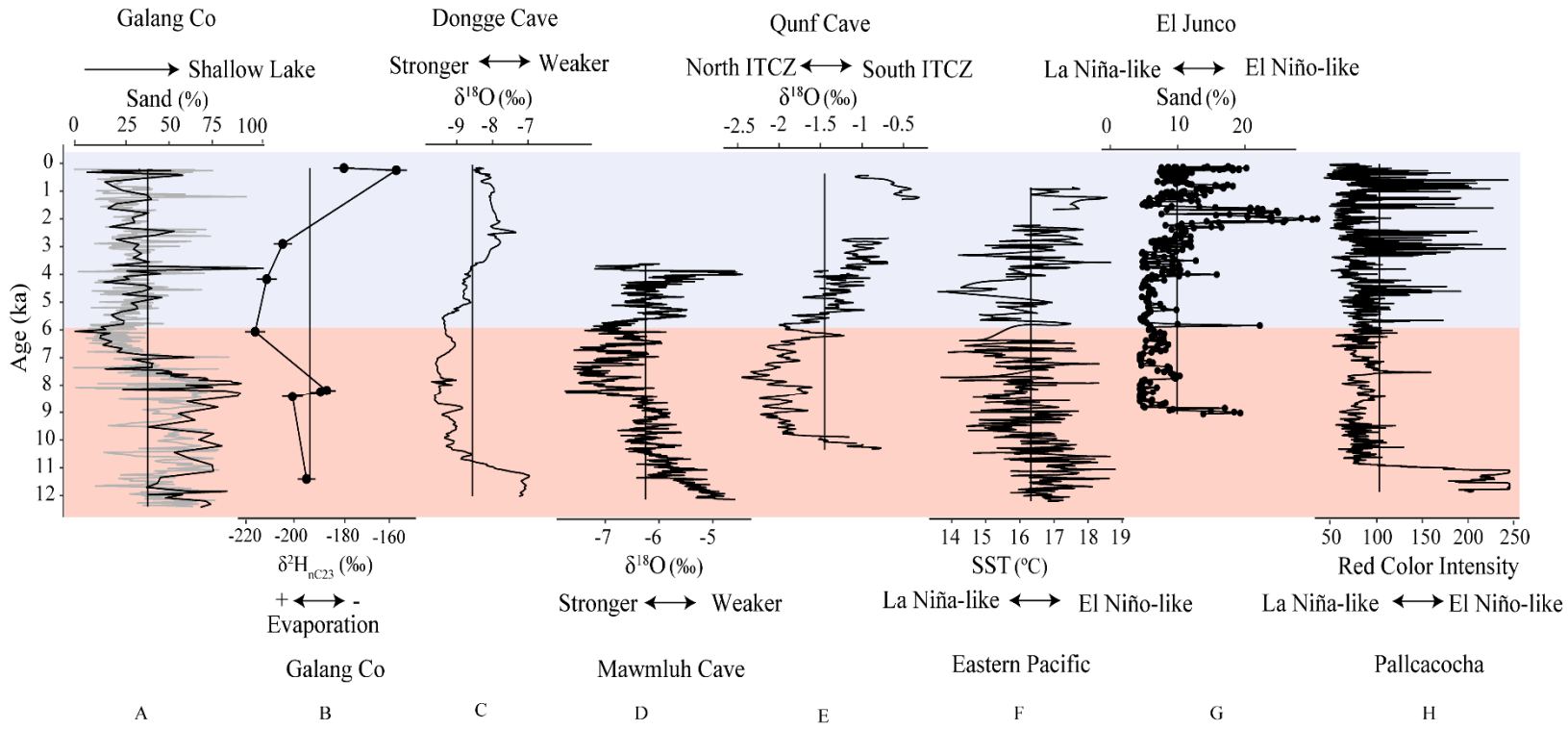

Figure 4.13. Galang Co sand 5 pt. MA (%; A) and δ^2H_{C23} (‰; B) compared with records from the broader ISM extent, the East Asian Monsoon, and the El Niño-Southern Oscillation. Records include Dongge Cave $\delta^{18}O$ (‰; C), Mawmluh Cave $\delta^{18}O$ (‰; D), Qunf Cave $\delta^{18}O$ (‰; E), Eastern Pacific SSTs (°C; F), El Junco sand (%: G), and Pallcacocha (red color intensity). Grey background represents low lake level stand (12.5-6 ka) at Galang Co. Vertical lines denotes average values over each record. Red and blue backgrounds indicate shallow and deeper lake conditions respectively.

4.9 References

Appleby, P. and Oldfield, F. 1978. The calculation of lead-210 dates assuming a constant rate of supply of unsupported 210Pb to the sediment. CATENA 5(1), 1-8.

Berger, A. and Loutre, M. 1991. Insolation values for the climate of the last 10 million years. Quaternary Science Reviews 10, 297-317.

Berkelhammer, M., Sinha, A., Stott, L., Cheng, H., Pausata, F. and Yoshimura, K. (2012) Climates, Landscapes, and Civilizations, pp. 75-87, Geophysical Monograms AGU, Washington D.C.

Bird, B., Lei, Y., Perello, M., Polissar, P., Yao, T., Finney, B., Bain, D., Pompeani, D. and Thompson, L. 2017. Late Holocene Indian summer monsoon variability revealed from a 3,300-year-long lake sediment record from Nir'pa Co, southeastern Tibet. The Holocene 27(4), 541-552.

Bird, B., Polissar, P., Lei, Y., Thompson, L., Yao, T., Finney, B., Bain, D., Pompeani, D. and Steinman, B. 2014. A Tibetan lake sediment record of Holocene Indian summer monsoon variability. Earth and Planetary Science Letters 399, 92-102.

Blaauw, M. and Christen, J.A. 2011. Flexible paleoclimate age-depth models using an autoregressive gamma process. Bayesian Analysis 6(3), 457-474.

Boyle, J. (2001) Tracking Environmental Change Using Lake Sediments. Last, W. and Smol, J. (eds), pp. 83-141, Kluwer Academic Publishers, Dordrecht.

Cai, Y., Zhang, H., Cheng, H., An, Z., Edwards, R., Wang, X., Tan, L., Liang, F., Wang, J. and Kelly, M. 2012. The Holocene Indian monsoon variability over the southern Tibetan Plateau and its teleconnections. Earth Planetary Science Letters 335-336, 135-144.

Chen, S., Hoffmann, S.S., Lund, D.C., Cobb, K.M., Emile-Geay, J. and Adkins, J.F. 2016. A high-resolution speleothem record of western equatorial Pacific rainfall: Implications for Holocene ENSO evolution. Earth and Planetary Science Letters 442, 61-71.

Conroy, J.L., Overpeck, J.T., Cole, J.E., Shanahan, T.M. and Steinitz-Kannan, M. 2008. Holocene changes in eastern tropical Pacific climate inferred from a Galápagos lake sediment record. Quaternary Science Reviews 27, 1166– 1180.

Croudace, I., Rindby, A. and Rothwell, R. 2006. ITRAX: description and evaluation of a new multi-function X-ray core scanner. Geological Society, London, Special Publications 267(1), 51-63.

Cuven, S.p., Francus, P. and Lamoureux, S.F. 2010. Estimation of grain size variability with micro X-ray fluorescence in laminated lacustrine sediments, Cape Bounty, Canadian High Arctic. Journal of Paleolimnology 44(3), 803-817.

Diefendorf, A.F., Leslie, A.B. and Wing, S.L. 2015. Leaf wax composition and carbon isotopes vary among major conifer groups. Geochimica et Cosmochimica Acta 170(1), 145-156.

Dykoski, C., Edwards, R., Cheng, H., Yaun, D., Cai, Y., Zhang, M., Lin, Y., Qing, J., An, Z. and Revenaugh, J. 2005. A high-resolution, absolute-dated Holocene and deglacial Asian monsoon record from Dongge Cave, China. Earth and Planetary Science Letters 233, 71-86.

Emile-Geay, J. and Tingley, M. 2016. Inferring climate variability from nonlinear proxies: application to palaeo-ENSO studies. Climate of the Past 12, 31-50.

Emile-Geay, J., Cane, M., Seager, R., Kaplan, A. and Almasi, P. 2016. El Niño as a mediator of the solar influence on climate. Paleoceanography and Paleoclimatology 22(3), PA3210.

Fan, Z.-X., Brauning, A. and Cao, K.-F. 2008. Tree-ring based drought reconstruction in the central Hengduan Mountains region (China) since A.D. 1655. International Journal of Climatology 28, 1879–1887.

Fan, Z.-X., Bräuning, A., Yangc, B. and Cao, K.-F. 2009. Tree ring density-based summer temperature reconstruction for the central Hengduan Mountains in southern China. Global and Planetary Change 65(1-2), 1-11.

Ficken, K., Li, B., Swain, D. and Eglinton, G. 2000. An n-alkane proxy for the sedimentary input of submerged/floating freshwater aquatic macrophytes. Organic Geochemistry 31(7-8), 745-749.

Fleitmann, D., Burns, S., Mudelsee, M., Neff, U., Kramers, J., Mangini, A. and Matter, A. 2003. Holocene forcing of the Indian Monsoon recorded from a stalagmite from Southern Oman. Science 300, 1737-1739.

Fleitmann, D., Burns, S.J., Mangini, A., Mudelsee, M., Kramers, J., Villa, I., Neff, U., Al-Subbary, A.A., Buettner, A., Hippler, D. and Matter, A. 2007. Holocene ITCZ and Indian monsoon dynamics recorded in stalagmites from Oman and Yemen (Socotra). Quaternary Science Reviews 26, 170-188.

Gray, A., Pasternack, G. and Watson, E. 2010. Hydrogen peroxide treatment effects on the particle size distribution of alluvial and marsh sediments. The Holocene 20(2), 293-301.

Gupta, A., Anderson, D. and Overpeck, J. 2003. Abrupt changes in the Asian southwest monsoon during the Holocene and their links to the North Atlantic Ocean. Nature 421, 354-357.

Haug, G.H., Hughen, K.A., Sigman, D.M., Peterson, L.C. and Ro, U. 2001. Southward Migration of the Intertropical Convergence Zone Through the Holocene. Science 293, 1304-1308.

Heiri, O., Lotter, A.F. and Lemcke, G. 2001. Loss on ignition as a method for estimating organic and carbonate content in sediments: reproducibility and comparability of results. Journal of Paleolimnology 25(1), 101-110.

Herzschuh, U., Kramer, A., Mischke, S. and Zhang, C. 2009. Quantitative climate and vegetation trends since the late glacial on the northeastern Tibetan Plateau deduced from Koucha Lake pollen spectra. Quaternary Research 71, 162-171.

Herzschuh, U., Winter, K., Wunnemann, B. and Li, S. 2006. A general cooling trend on the central Tibetan Plateau throughout the Holocene recorded by the Lake Zigetang pollen spectra. Quaternary International 154-155, 113-121.

KCCAMS, U. 2011. Acid/Base/Acid (ABA) sample pre-treatment, University of California Irvine, W.M. Keck Carbon Cycle Accelerator Mass Spectrometer Facility.

Lazhu, Yang, K., Wang, J., Lei, Y., Chen, Y., Zhu, L., Ding, B. and Qin, J. 2016. Quantifying evaporation and its decadal change for Lake Nam Co, central Tibetan Plateau. Journal of Geophysical Research: Atmospheres 121, 7578-7591.

Lei, Y., Yao, T., Yang, K., La, Z., Ma, Y. and Bird, B.W. n.d. Thermal regime, energy budget and lake evaporation at a deep alpine lake (Paiku Co) in the central Himalayas. In preparation.

Livingstone, D. 1955. A Lightweight Piston Sampler for Lake Deposits. Ecology 36(1), 137-139.

Marchitto, T.M., Muscheler, R., Ortiz, J.D., Carriquiry, J.D. and Geen, A.v. 2010. Dynamical Response of the Tropical Pacific Ocean to Solar Forcing During the Early Holocene. Science 330, 1378-1381.

Marzi, R., Torkelson, B. and Olson, R. 1993. A revised carbon preference index. Organic Geochemistry 20(8), 1303-1306.

Meyers, P.A. and Lallier-Vergès, E. 1999. Lacustrine sedimentary organic matter records of Late Quaternary paleoclimates. Journal of Paleolimnology 21, 345-372.

Mischke, S., Kramer, M., Zhang, C., Shang, H., Herzschuh, U. and Erzinger, J. 2008. Reduced early Holocene moisture availability in the Bayan Har Mountains, northeastern Tibetan Plateau, inferred from a multi-proxy lake record. Palaeogeography, Palaeoclimatology, Palaeoecology 267, 59-67.

Moy, C.M., Seltzer, G.O., Rodbell, D.T. and Anderson, D.M. 2002. Variability of El Nino/Southern Oscillation activity at millennial timescales during the Holocene epoch. Nature 420, 162-165.

Mügler, I., Sasche, D., Werner, M., Xu, B., Wu, G., Yao, T. and Gleixner, G. 2008. Effect of lake evaporation on δD values of lacustrine n-alkanes: A comparison of Nam Co (Tibetan Plateau) and Holzmaar (Germany). Organic Geochemistry 39, 711-729.

Naeher, S., Gilli, A., North, R.P., Hamann, Y. and Schubert, C.J. 2013. Tracing bottom water oxygenation with sedimentary Mn/Fe ratios in Lake Zurich, Switzerland. Chemical Geology 352, 125-133.

Nesbitt, H. and Markovics, G. 1997. Weathering of grandioritic crust, long-term storage of elements in weathering profiles, and petrogenesis of siliciclastic sediments. Geochimica et Cosmochimica Acta 61(8), 1653-1670.

Olsson, I. (1986) Handbook of Holocene palaeoecology and paleohydrology Berglund, B. (ed), John Wiley & Sons, Chichester.

Polissar, P. and D'Andrea, W. 2014. Uncertainty in Paleohydrologic Reconstructions from Molecular dD values. Geochimica et Cosmochimica Acta 129, 146-156.

Qui, J. 2008. China: The Third Pole Environment. Nature 454(7203), 393-396.

Reimer, P.J., Bard, E., Bayliss, A., Beck, J.W., Blackwell, P.G., Ramsey, C.B., Buck, C.E., Cheng, H., Edwards, R.L., Friedrich, M., Grootes, P.M., Guilderson, T.P., Haflidason, H., Hajdas, I., Hatté, C., Heaton, T.J., Hoffmann, D.L., Hogg, A.G., Hughen, K.A., Kaiser, K.F., Kromer, B., Manning, S.W., Niu, M., Reimer, R.W., Richards, D.A., Scott, E.M., Southon, J.R., Staff, R.A., Turney, C.S.M. and Plicht, J.v.d. 2013. INTCAL13 AND MARINE13 RADIOCARBON AGE CALIBRATION CURVES 0–50,000 YEARS CAL BP. RADIOCARBON 55(4), 1869-1887.

Seki, O., Meyers, P.A., Kawamura, K., Zheng, Y. and Zhou, W. 2009. Hydrogen isotopic ratios of plant wax n-alkanes in a peat bog deposited in northeast China during the last 16 kyr. Organic Geochemistry 40(6), 671-677.

Talbot, M.R. (2002) Tracking Environmental Change Using Lake Sediments. Volume 2: Physical and Geochemical Methods. Last, W.M. and Smol, J.P. (eds), pp. 401-439, Kluwer Academic Publishers, New York.

Tian, L., Yao, T., MacClune, K., White, J., Schilla, A., Vaughn, B., Vachon, R. and Ichiyanagi, K. 2007. Stable isotopic variations in west China: A consideration of moisture sources. Journal of Geophysics Research 112, D10112.

Wright, H. 1967. A square-rod piston sampler for lake sediments. Journal of Sedimentary Petrology 37(3), 975-976.

Yao, T., Pu, J., Lu, A., Wang, Y. and Yu, W. 2007. Recent glacial retreat and its impact on the hydrological processes on the Tibetan Plateau, China, and surrounding regions. Arctic, Antarctic, and Alpine Research 39(4), 642-650.

Yao, T., Thompson, L., Yang, W., Yu, W., Gao, Y., Guo, X., Yang, X., Duan, K., Zhao, H., Xu, B., Pu, J., Lu, A., Xiang, Y., Kattel, D. and Joswiak, D. 2012. Different glacial status with atmospheric circulations in Tibetan Plateau and surroundings. Nature Climate Change 2, 663-667.

Zhu, L., Wu, Y., Wang, J., Lin, X., Ju, J., Xie, M., Li, M., Mäusbacher, R., Antje, S. and Daut, G. 2008. Environmental changes since 8.4 ka reflected in the lacustrine core sediments from Nam Co, central Tibetan Plateau. The Holocene 18, 831-839.

5. CONCLUSIONS

This dissertation provides three high-resolution paleoclimate records of Holocene (11.7 ka to present) Indian summer monsoon (ISM) expression in Tibet. Sediments from three small lakes, Nir'Pa Co, Cuobu, and Galang Co, situated along an east-west transect on the southeastern Tibetan Plateau address knowledge gaps of the spatial and temporal patterns of monsoon precipitation and local hydroclimate conditions in connection with broader regional and global climate drivers. Nir'Pa Co is a late Holocene, leaf wax *n*-alkane hydrogen isotopes (δ^2H) hydroclimate record (chapter 2), Cuobu is a 8.3 ka record of effective moisture, runoff, and leaf wax *n*-alkane δ^2H hydroclimate (chapter 3), and Galang Co is a lower-elevation effective moisture and lake level record for the entire Holocene (chapter 4). Each record uses a combination of sedimentological (*i.e.,* grain size, total organic matter), geochemical (*i.e.,* XRF), and isotopic proxies (*i.e.,* leaf-wax *n*-alkanes hydrogen (δ^2H), organic carbon ($\delta^{13}C$), and nitrogen ($\delta^{15}N$)) to characterize local and synoptic hydroclimate conditions on centennial and millennial time scales.

Synoptic hydroclimate, inferred by long-chain *n*-alkane δ^2H, is a measure of regional ISM precipitation signals and, as demonstrated in this dissertation, may not be reflective of local hydroclimate conditions. In contrast, local hydroclimate conditions including effective moisture, lake levels and runoff, inferred from short-chain *n*-alkane δ^2H, $\Delta\delta^2H_{C23\text{-}C31}$, grain size, XRF, carbon and nitrogen isotopes, explain how the lake and its watershed responded to altered monsoon precipitation patterns. The use of leaf-wax *n*-alkane δ^2H was crucial to this work, as this proxy captures growing season precipitation and evaporation signals that occur simultaneous with the monsoon season. Long-chain *n*-alkanes captured precipitation isotopic signatures through terrestrial vegetation, while aquatic vegetation-derived short-chain *n*-alkanes reflected the precipitation and evaporation signals captured by lake water. This multi-proxy, high temporal resolution approach addressed questions about the relationship between local and synoptic hydroclimate indicators of changes in monsoon intensity with respect to 1) regional and global climate drivers and events and 2) local hydrological and elevation conditions.

All three paleoclimate records are consistent with the well-documented pattern of an ISM-maximum in the early Holocene that transitioned to a weaker monsoon in the

middle Holocene with weaker conditions continuing to the present, however, each record shows that local hydroclimate and monsoon expression is more complex on shorter time scales and can be greatly impacted by site specific geomorphology and hydrology. Both the Galang and Cuobu records show that the early Holocene, when the ISM is recognized at its strongest, there were distinct periods of dry conditions locally. Cuobu indicated that intense precipitation in the early Holocene resulted in greater hydrological connectivity, due to higher lake and river water levels. Meanwhile, an anti-phase relationship observed at Galang, between ISM precipitation and lake levels in the early Holocene, indicates that it is possible to have low lake levels, even with heavy precipitation, if evaporation rates reach an unknown threshold. The Nir'Pa Co late Holocene leaf-wax δ^2H record demonstrates that even as monsoon intensity was at its weakest during the Holocene, there were distinct periods of drought and pluvial (wet) conditions. These changes in late Holocene monsoon intensity do not appear to be connected with globally-recognized climate events, the Medieval Climate Anomaly (MCA) and the Little Ice Age (LIA). Instead, these changes may be attributed to other broader scale climate drivers, such as sea surface temperatures and land surface gradients.

The connection between synoptic and local hydroclimate indicators varied between records, dependent on the mechanisms responsible for local hydroclimate variability and the sensitivity of the lake system to precipitation changes. The Nir'Pa Co δ^2H and grain size records suggested that synoptic long-chain *n*-alkane δ^2HC31 showed earlier evidence of monsoon weakening than grain size-inferred lake levels. Just as in the other records, when local hydroclimate responded to the monsoon weakening, that response was abrupt, indicating some threshold when monsoon precipitation declines before lake level responds. Abrupt changes in local hydroclimate are also highly visible in the Cuobu and Galang grain size records, but for both of these lakes, the timing of variability in runoff and lake levels, respectively, is concurrent with synoptic shifts in ISM expression.

While this dissertation has addressed several questions about the expression of the Holocene ISM on the Tibetan Plateau, particularly in relation to synoptic and local hydroclimate, it has also shown where further research is needed. The Galang Co record showed an anti-phase effective moisture and ISM precipitation relationship, however,

limited records in the region and, particularly, in low-elevation sites prevents further analysis on determining whether ice cover changes in the early and middle Holocene drove this relationship. The grain size record at Cuobu interpreted as a river runoff signal, suggests that rivers on the Tibetan Plateau may have peaked during the early Holocene, altering hydrological connections. To determine whether these proposed mechanisms are correct and answer other questions about the ISM, additional high-resolution paleoclimate records from the Tibetan Plateau and the broader ISM region need to be developed, with an emphasis on greater spatial and elevation representation. Paleoclimate records remain a crucial tool for improving our understanding of this complex and vital monsoon system and how it will respond to changes in climate drivers.

6. APPENDICES

Appendix 1: Cuobu age model produced by Bacon® with composite depths vs. mean age.

Table A 1.1 Depth and Mean Age (BP) for Cuobu composite core.

Depth (cm)	Mean Age (BP)	Depth (cm)	Mean Age (BP)
1	-66.5	33	390
2	-65.4	34	418
3	-64.4	35	446
4	-63.3	36	467.2
5	-62.3	37	488.4
6	-59.9	38	509.5
7	-57.6	39	530.9
8	-55.3	40	551.9
9	-53	41	580.2
10	-50.6	42	608.4
11	-46.6	43	636.7
12	-42.6	44	665.1
13	-38.7	45	693.4
14	-34.8	46	699.6
15	-30.9	47	705.8
16	-20.4	48	711.9
17	-10.1	49	717.9
18	0.3	50	723.7
19	10.6	51	728.5
20	20.9	52	733.3
21	55	53	738
22	88.8	54	742.7
23	122.4	55	747.4
24	155.8	56	752
25	189.5	57	756.8
26	212.9	58	761.4
27	236.3	59	766.2
28	259.7	60	770.8
29	282.9	61	776
30	306.4	62	781.1
31	334	63	786.2
32	362	64	791.3

Depth (cm)	Mean Age (BP)
65	796.2
66	801.1
67	806.1
68	811
69	815.9
70	820.8
71	825.6
72	830.5
73	835.2
74	840
75	844.8
76	849.4
77	854
78	858.7
79	863.3
80	868.1
81	873
82	877.9
83	882.9
84	888
85	893.1
86	898.1
87	903
88	908.1
89	913
90	917.9
91	923.7
92	929.6
93	935.5
94	941.5
95	947.5
96	957.6
97	967.6
98	977.6
99	987.8
100	997.6
101	1007.4
102	1017
103	1026.8

Depth (cm)	Mean Age (BP)
104	1036.3
105	1045.9
106	1055.5
107	1065.4
108	1075.1
109	1085
110	1094.8
111	1105.5
112	1116.1
113	1126.7
114	1137.4
115	1148.1
116	1158.6
117	1168.9
118	1179.4
119	1189.9
120	1200.2
121	1210.9
122	1221.5
123	1232.2
124	1242.7
125	1253.3
126	1263.6
127	1273.9
128	1284.1
129	1294.5
130	1304.8
131	1314.5
132	1324.3
133	1334.2
134	1344
135	1353.9
136	1364.1
137	1374.3
138	1384.6
139	1395
140	1405.4
141	1415.6
142	1425.6

Depth (cm)	Mean Age (BP)
143	1435.8
144	1446.1
145	1456.1
146	1470.6
147	1485.2
148	1499.5
149	1513.6
150	1527.5
151	1541.8
152	1556.3
153	1570.6
154	1584.9
155	1599.2
156	1612.5
157	1625.7
158	1639
159	1652.1
160	1665.3
161	1678.9
162	1692.2
163	1705.7
164	1719.3
165	1732.6
166	1747.1
167	1761.9
168	1776.9
169	1791.7
170	1806.6
171	1821
172	1835.4
173	1849.7
174	1863.5
175	1877.4
176	1890.5
177	1903.8
178	1917.2
179	1930.8
180	1944.3
181	1959.6

Depth (cm)	Mean Age (BP)
182	1975.1
183	1990.7
184	2006.4
185	2022
186	2035.4
187	2048.9
188	2062.6
189	2076.4
190	2089.9
191	2104.8
192	2119.7
193	2134.7
194	2149.5
195	2164.4
196	2179.1
197	2193.8
198	2208.8
199	2223.8
200	2238.7
201	2257.4
202	2275.9
203	2294.2
204	2312.5
205	2330.6
206	2349.1
207	2367.4
208	2385.4
209	2403.2
210	2421.2
211	2439.9
212	2458.7
213	2477.3
214	2496
215	2514.8
216	2532.8
217	2550.9
218	2568.9
219	2586.9
220	2604.9

Depth (cm)	Mean Age (BP)
221	2625.3
222	2645.6
223	2666.1
224	2686.5
225	2706.9
226	2725.1
227	2743.4
228	2761.6
229	2780.1
230	2798.3
231	2818.2
232	2838.1
233	2858.2
234	2878.1
235	2897.7
236	2916
237	2934.1
238	2952.5
239	2970.7
240	2988.8
241	3007.5
242	3026
243	3044.5
244	3062.9
245	3081.5
246	3101.4
247	3121
248	3140.9
249	3160.6
250	3180.6
251	3200.2
252	3220.2
253	3240
254	3260
255	3279.7
256	3299.3
257	3318.9
258	3338.4
259	3358

Depth (cm)	Mean Age (BP)
260	3377.5
261	3397.1
262	3417.1
263	3436.7
264	3456.5
265	3476.1
266	3496.9
267	3517.6
268	3538.5
269	3559.5
270	3580.2
271	3598.5
272	3617.2
273	3635.9
274	3655.5
275	3674.8
276	3692.8
277	3710.8
278	3728.6
279	3746.8
280	3765.2
281	3794.8
282	3825
283	3854.6
284	3883.6
285	3912.7
286	3944.4
287	3975.8
288	4007.8
289	4039.1
290	4069.6
291	4101.9
292	4134.4
293	4166.7
294	4199.3
295	4231.8
296	4266.2
297	4300.7
298	4335.3

Depth (cm)	Mean Age (BP)
299	4369.8
300	4404.4
301	4439.1
302	4473.9
303	4508.7
304	4543.3
305	4578.1
306	4616.3
307	4655.8
308	4694.9
309	4734.3
310	4773.6
311	4804.5
312	4836.9
313	4869.4
314	4901.7
315	4933.6
316	4953.8
317	4973.8
318	4993
319	5012.2
320	5031.1
321	5050.3
322	5069.3
323	5088.4
324	5107.2
325	5125.9
326	5146.1
327	5166.4
328	5187.1
329	5207.4
330	5227.4
331	5246.9
332	5266.5
333	5286
334	5305.4
335	5324.9
336	5345.9
337	5366.8

Depth (cm)	Mean Age (BP)
338	5387.6
339	5408.6
340	5429
341	5449
342	5469
343	5489.2
344	5509.3
345	5529.1
346	5548.8
347	5568.8
348	5588.8
349	5608.8
350	5628.6
351	5647.9
352	5667.5
353	5687.1
354	5706.7
355	5726.3
356	5745.3
357	5764.4
358	5783.3
359	5802.2
360	5820.9
361	5839.6
362	5858.3
363	5876.9
364	5895.6
365	5914.6
366	5934.2
367	5954.3
368	5974.8
369	5995.2
370	6015.8
371	6036.6
372	6057.7
373	6079.7
374	6101.2
375	6122.6
376	6161.6

Depth (cm)	Mean Age (BP)
377	6200.4
378	6239.6
379	6278.5
380	6317.6
381	6360
382	6402.4
383	6444.6
384	6486.4
385	6527.9
386	6574.2
387	6620.4
388	6666.8
389	6712.6
390	6758.6
391	6800.7
392	6843
393	6885.6
394	6928.2
395	6970.7
396	7016.8
397	7062.7
398	7108.8
399	7155.2
400	7201.7
401	7245.7
402	7290.9
403	7335.7
404	7380.7

Depth (cm)	Mean Age (BP)
405	7425.5
406	7471
407	7517.3
408	7563.6
409	7609.8
410	7656.1
411	7698.9
412	7741.8
413	7784.9
414	7828.4
415	7656.1
416	7698.9
417	7741.8
418	7784.9
419	7828.4
420	7873
421	7916.5
422	7959.4
423	8002.3
424	8045.3
425	8087.6
426	8130.8
427	8173.2
428	8216.1
429	8258.4
430	8301.2
431	8344.1

Appendix 2: Cuobu XRF Geochemistry

Table A 2.1 Cuobu XRF Geochemistry Al - Ca

Depth (cm)	Al	Ar	As	Au	Ba	Bi	Br	Ca
27	67	23916	241	407	3086	640	12	23465
27.5	184	19929	234	487	225	253	0	7172
28	255	11320	802	641	713	1138	0	15346
28.5	217	10670	1076	864	624	1120	73	16093
29	179	12182	1067	470	522	643	0	16735
29.5	184	11470	1088	550	638	878	0	14702
30	218	10086	1116	913	636	1052	0	15285
30.5	205	10114	797	404	754	831	216	14020
31	216	9359	786	531	585	726	0	14472
31.5	241	8966	1406	1034	379	1034	144	14269
32	236	9077	1251	1076	523	678	216	15286
32.5	172	9136	1194	680	593	814	89	14995
33	210	8523	1022	1006	481	922	553	13822
33.5	201	8128	1157	1013	437	562	69	14154
34	205	7616	770	879	557	658	0	14928
34.5	260	8469	984	812	648	769	0	13774
35	182	9066	1136	823	484	914	0	14744
35.5	117	10111	913	597	738	444	0	14281
36	201	10441	1332	723	459	995	0	14929
36.5	155	9919	873	740	630	949	0	15586
37	295	9627	1161	820	934	981	0	16928
37.5	217	10000	1024	697	627	916	0	18828
38	214	9510	1032	664	575	1073	0	19795
38.5	249	9774	1068	725	552	1027	0	16806
39	222	10689	1522	657	475	649	0	16690
39.5	195	10949	1397	906	666	980	0	16648
40	237	9638	964	898	694	721	0	15123
40.5	164	10486	1117	792	529	807	199	17003
41	207	11087	1171	915	661	809	137	16294
41.5	244	11099	1169	467	827	783	0	16150
42	240	10775	1288	554	487	933	0	15653
42.5	222	11165	1084	543	492	478	53	15616
43	223	11045	1313	741	720	722	0	15479
43.5	175	9871	1121	617	581	960	0	14837
44	190	8766	1151	984	733	738	0	14956
44.5	194	10019	1133	517	485	1033	17	14756
45	165	10439	1145	900	669	848	0	14665

Depth (cm)	Al	Ar	As	Au	Ba	Bi	Br	Ca
45.5	238	10224	1118	850	811	803	103	14342
46	285	10214	1375	805	366	823	29	14704
46.5	270	9642	941	573	518	618	284	15200
47	183	8608	1387	927	384	765	0	14587
47.5	228	7898	1094	1057	739	705	0	13967
48	227	7931	1433	707	651	908	0	13743
48.5	136	7932	1331	677	656	841	0	15461
49	180	8583	1098	890	816	678	0	15914
49.5	202	9558	1216	831	710	1026	0	15361
50	181	9164	1126	588	601	920	47	15887
50.5	220	9365	1625	812	721	860	121	16949
51	224	10792	927	674	620	789	0	16148
51.5	195	10064	1203	816	577	834	0	15190
52	207	8133	969	911	645	759	0	14485
52.5	263	7827	1650	1031	561	1205	0	15219
53	154	8608	1271	719	746	636	0	14573
53.5	236	9138	1378	1191	545	879	0	15532
54	222	7984	993	692	628	628	0	13445
54.5	226	7483	1061	589	554	922	0	14395
55	272	9729	1079	849	867	936	0	16660
55.5	170	8106	1519	1168	585	834	0	15731
56	220	8555	1316	1032	457	735	379	15563
56.5	229	8971	1208	794	458	940	0	15955
57	174	9380	1147	627	719	324	0	15920
57.5	206	8750	993	601	893	386	0	14885
58	149	8656	1089	945	560	807	0	14701
58.5	150	9212	1396	911	687	966	0	15227
59	215	7571	1136	851	412	815	223	15511
59.5	229	8189	1074	998	674	865	0	15604
60	223	7649	1363	704	396	696	0	16301
60.5	221	8431	1511	873	558	809	0	15442
61	181	7733	1447	681	553	881	0	14033
61.5	226	8194	1130	577	744	947	0	15164
62	217	10083	1464	871	630	1039	203	15167
62.5	146	9066	1372	812	429	897	0	14878
63	236	7592	1184	834	630	729	0	14251
63.5	172	8758	952	777	583	714	0	15423
64	182	10162	1032	979	796	744	215	14875
64.5	176	9958	1207	1036	629	903	0	15609

Depth (cm)	Al	Ar	As	Au	Ba	Bi	Br	Ca
65	193	10555	1105	755	431	858	8	16048
65.5	176	11129	1288	729	668	904	151	16336
66	223	12432	904	641	838	548	0	15537
66.5	206	12108	837	717	705	594	0	15679
67	199	9618	1285	581	498	833	219	16687
67.5	195	8060	1261	782	688	1072	0	16699
68	249	8054	1258	900	1137	1043	11	16834
68.5	213	7965	890	817	816	817	0	16135
69	193	8741	1453	719	746	836	0	17261
69.5	186	9240	1314	626	721	899	0	15413
70	206	9405	1475	1021	682	852	0	15492
70.5	229	8371	1354	933	863	713	0	14378
71	232	7805	1148	926	303	880	0	15388
71.5	248	8636	1301	840	674	715	0	16240
72	200	8950	1442	724	878	569	75	18031
72.5	277	8098	1108	840	962	1090	0	17034
73	210	8343	1511	945	837	896	0	16856
73.5	276	8279	1185	764	838	969	0	18833
74	291	11996	822	926	643	519	0	15483
74.5	131	17977	422	377	273	351	0	8577
75	114	17419	944	698	384	311	0	9480
75.5	133	15359	1064	539	522	500	41	10838
76	238	10183	780	569	590	557	0	13938
76.5	243	8571	855	834	291	851	0	14853
77	220	8352	1148	906	610	924	0	15410
77.5	208	8517	1377	923	743	707	318	16121
78	247	8166	1209	737	835	892	705	15624
78.5	182	7548	1224	729	676	526	0	16049
79	240	8357	1039	685	975	585	130	17270
79.5	271	8128	1194	656	459	690	0	16590
80	279	7647	1166	714	682	1030	21	17469
80.5	187	7906	816	1027	726	945	0	15789
81	217	10016	849	1013	837	546	0	15225
81.5	218	10524	952	794	674	739	0	15518
82	235	9687	1490	701	510	577	0	15698
82.5	237	10242	1188	546	1134	882	0	15960
83	225	12435	965	669	762	671	40	17195
83.5	150	13613	732	204	560	161	0	9712
84	123	12966	1239	598	456	397	69	9714

Depth (cm)	Al	Ar	As	Au	Ba	Bi	Br	Ca
84.5	116	12654	933	584	633	395	0	10241
85	104	12433	1101	380	257	145	0	10558
85.5	89	12070	1373	478	484	324	0	10933
86	92	11583	776	341	644	537	313	11499
86.5	146	11235	801	478	631	548	431	11625
87	137	11612	740	285	519	287	0	12356
87.5	79	11610	504	641	565	97	198	12080
88	106	11680	618	475	469	419	143	12377
88.5	160	11551	921	381	566	683	0	11804
89	135	11539	641	303	767	261	0	11792
89.5	98	12028	731	454	309	417	0	10904
90	126	12219	651	463	430	185	729	10615
90.5	101	12180	512	417	287	351	366	10433
91	140	11954	438	162	377	251	0	11144
91.5	102	10899	599	444	387	622	0	12122
92	125	9782	827	301	166	265	0	13398
92.5	166	9369	739	405	299	443	0	13905
93	133	10130	966	441	295	506	0	13444
93.5	126	9711	985	679	398	311	44	13489
94	70	9851	995	319	287	270	0	13656
94.5	83	9700	1199	505	320	560	0	13383
95	110	9484	1064	373	616	417	0	13706
95.5	121	8756	1396	413	611	454	154	13816
96	121	9754	888	287	584	488	0	13867
96.5	124	11307	894	577	411	356	0	12105
97	102	9170	1312	689	536	400	175	13957
97.5	167	8928	1653	686	445	645	0	14050
98	142	8464	1430	622	567	704	323	14006
98.5	74	7614	1889	517	714	647	0	14379
99	138	5860	1235	514	570	347	195	14642
99.5	53	4908	1654	691	458	512	219	14207
100	120	7220	1413	542	398	447	137	13721
100.5	90	7717	1794	664	591	549	0	13041
101	136	7730	1809	538	357	380	10	13616
101.5	120	5844	1877	432	565	471	0	14326
102	154	4243	2345	638	620	287	0	14003
102.5	137	4911	1908	642	427	742	12	14988
103	132	4900	1979	672	282	573	0	14260
103.5	76	4656	2170	513	737	622	0	13864

Depth (cm)	Al	Ar	As	Au	Ba	Bi	Br	Ca
104	107	5100	2074	663	645	383	0	17124
104.5	151	4562	2381	774	539	556	0	13988
105	173	4117	2423	594	604	564	0	13775
105.5	170	4213	2451	811	554	527	71	14240
106	225	4310	2386	726	555	579	166	14401
106.5	71	4477	2657	935	573	592	58	14730
107	140	4946	2380	1127	374	420	164	14901
107.5	113	5219	2123	906	394	678	0	15041
108	133	4728	2579	819	507	558	0	15222
108.5	107	4365	2791	818	460	482	0	14791
109	180	4612	2622	782	517	575	117	15107
109.5	201	4981	2587	673	848	837	0	15477
110	121	4608	2458	764	438	404	0	15203
110.5	154	4355	2587	759	327	576	33	14561
111	118	3392	2633	921	425	337	183	13627
111.5	165	3574	2732	801	537	564	38	14412
112	151	3345	2435	827	395	350	0	14028
112.5	136	3444	2681	720	421	514	0	14702
113	167	3468	2042	851	317	545	57	14218
113.5	153	3721	2296	513	772	700	446	14884
114	178	4503	2532	593	697	421	0	15537
114.5	83	5109	2756	638	743	419	0	15952
115	111	5144	2511	814	959	445	0	15484
115.5	137	5076	2523	927	576	490	0	15108
116	135	4932	2516	562	552	455	0	15079
116.5	178	4241	2571	929	788	737	0	14875
117	183	3839	2671	769	255	671	0	14705
117.5	165	5534	2188	853	628	496	0	14494
118	116	8627	1421	431	228	324	0	12006
118.5	114	9014	1473	463	511	318	0	12647
119	108	8398	1620	570	848	587	94	12956
119.5	171	5225	2078	539	308	601	211	14833
120	101	4361	2724	827	722	441	0	15764
120.5	140	3772	2570	741	793	466	0	15673
121	143	3724	2622	961	474	727	0	15068
121.5	181	3705	2229	676	690	451	0	15956
122	161	4090	1856	770	653	398	0	16359
122.5	97	4264	1855	870	544	518	58	16017
123	126	4101	1602	516	719	708	0	15870

Depth (cm)	Al	Ar	As	Au	Ba	Bi	Br	Ca
123.5	150	4914	1744	581	561	655	27	16008
124	156	4091	1802	872	714	514	0	15050
124.5	187	3809	1854	806	729	922	18	15060
125	91	3937	1654	615	511	881	0	15794
125.5	196	4189	1649	586	600	536	0	15580
126	102	4503	1403	840	844	443	0	16419
126.5	87	5159	1644	574	426	641	0	16309
127	174	4495	1383	563	318	552	0	14467
127.5	154	4487	1603	625	489	569	0	15842
128	124	4840	1490	546	316	680	0	15619
128.5	168	5027	1541	904	496	640	0	15460
129	161	4861	1656	802	764	510	0	16082
129.5	158	4776	1765	692	562	647	0	15622
130	159	4215	1753	858	480	854	0	15446
130.5	125	4131	1997	718	477	686	0	14654
131	101	4654	1701	784	704	552	0	15476
131.5	184	5190	1698	858	515	611	0	16267
132	182	4801	1458	637	663	584	0	16169
132.5	136	5146	1458	847	869	944	0	16044
133	187	5093	1886	935	473	442	0	15937
133.5	89	5287	1690	664	517	467	0	15935
134	153	5122	1748	829	612	695	0	16117
134.5	124	5350	1927	920	351	605	0	16405
135	151	5553	1701	776	629	797	0	16151
135.5	167	5552	1910	521	988	569	204	16560
136	167	5250	1812	917	745	705	0	16239
136.5	155	5158	1986	770	451	574	0	16316
137	144	5062	2117	665	576	488	0	15655
137.5	161	5659	2042	509	706	443	0	16297
138	94	14090	432	456	327	53	0	9241
138.5	145	15023	152	244	200	46	0	7069
139	45	15954	354	261	144	240	0	6524
139.5	176	6972	1707	506	670	463	99	13594
140	164	6047	2350	762	625	368	0	15711
140.5	186	5830	1717	624	776	683	0	15948
141	135	6110	2022	912	176	622	0	15585
141.5	142	5704	2128	818	280	595	70	15766
142	129	6320	1728	577	613	541	0	15999
142.5	168	5914	1849	756	489	531	133	15697

Depth (cm)	Al	Ar	As	Au	Ba	Bi	Br	Ca
143	97	5441	1904	526	723	572	0	15456
143.5	167	5556	2151	727	637	204	0	15957
144	168	5682	2157	448	513	679	0	15185
144.5	145	5916	1777	760	880	599	100	15823
145	150	5833	2023	886	487	806	0	16019
145.5	165	6010	2076	529	443	508	0	15702
146	147	5995	2172	739	443	427	73	16045
146.5	111	6299	2260	952	577	689	0	15863
147	199	6585	1996	619	795	574	95	16175
147.5	130	6496	1624	495	809	414	0	15899
148	176	6577	2256	1038	763	594	0	16176
148.5	125	7257	1776	543	736	543	0	16391
149	114	6778	1340	636	498	627	0	15765
149.5	80	7423	1063	564	727	587	0	15838
150	104	8697	1253	584	432	509	103	13526
150.5	102	7734	1095	736	317	356	0	10171
151	109	10320	648	341	321	473	181	10768
151.5	139	6040	1130	503	64	425	0	10839
152	162	6082	1910	657	598	815	0	15691
152.5	207	7870	2314	571	930	697	0	15929
153	141	7965	2540	741	721	350	0	16152
153.5	138	9914	502	1017	115	599	0	15688
154	101	9667	1200	1075	115	153	0	15381
154.5	174	9900	1027	957	80	94	0	15137
155	116	10101	1335	941	122	0	0	14616
155.5	141	10105	1336	831	124	70	37	14874
156	168	9801	847	781	112	233	0	14986
156.5	150	10554	1059	844	144	0	0	14651
157	107	11056	1292	727	91	164	0	13778
157.5	150	10806	1457	822	159	0	62	13777
158	117	10361	1617	1177	195	139	0	13828
158.5	179	9828	1939	1017	132	53	121	13735
159	79	9528	1921	1145	235	0	18	14243
159.5	130	9610	1514	1017	126	78	0	14239
160	86	9277	1343	1098	169	0	0	14897
160.5	176	8979	1289	925	84	79	0	14284
161	116	9029	957	980	135	173	0	14865
161.5	150	9201	1119	1016	83	220	0	14594
162	124	9378	758	977	252	454	140	15131

Depth (cm)	Al	Ar	As	Au	Ba	Bi	Br	Ca
162.5	190	9255	1411	945	163	16	0	14819
163	101	9168	1382	1143	112	420	307	14905
163.5	164	8871	1323	820	171	256	0	14715
164	115	8457	1023	1168	110	362	465	14579
164.5	127	8534	1245	832	142	93	0	15110
165	73	8465	940	1238	153	108	458	15088
165.5	123	8194	919	947	120	457	132	15084
166	128	8523	1359	1135	138	232	356	15186
166.5	100	8190	1800	819	132	237	0	14589
167	141	8332	1386	836	79	0	0	14631
167.5	145	8681	1064	830	162	93	0	14259
168	129	11345	899	912	6	26	0	9385
168.5	107	11283	771	950	103	0	0	6599
169	58	10643	519	752	71	216	0	7747
169.5	124	9657	895	794	78	87	0	11287
170	146	6744	1008	973	211	248	180	14552
170.5	86	8417	1276	781	137	0	74	14571
171	118	9046	1025	895	63	317	0	14581
171.5	178	8972	1467	1109	76	108	40	13575
172	70	9424	1343	1005	182	263	147	13529
172.5	68	9014	1970	1001	137	0	0	14058
173	143	9172	1813	995	159	0	0	14054
173.5	134	9314	1118	845	130	320	0	13710
174	167	9255	1449	613	167	11	42	14572
174.5	153	9010	1777	882	73	0	0	14481
175	172	9083	1448	1119	59	60	0	14575
175.5	135	9009	1246	848	114	116	0	15157
176	185	9219	1306	1270	80	0	75	14948
176.5	201	9020	1365	862	142	293	69	15107
177	128	9136	662	893	209	437	245	15004
177.5	177	8813	1003	972	145	131	26	14169
178	135	8999	997	716	122	168	0	15238
178.5	121	9578	1097	1088	186	100	0	14263
179	113	9072	1220	1009	192	12	64	14479
179.5	172	9822	1150	826	72	0	39	14080
180	128	9439	674	1212	121	162	0	14128
180.5	107	9268	659	695	119	537	0	14592
181	144	8920	922	1186	166	264	0	14879
181.5	107	8961	1229	1017	170	45	94	14806

Depth (cm)	Al	Ar	As	Au	Ba	Bi	Br	Ca
182	95	9277	1097	1020	126	162	183	14598
182.5	95	9085	1344	979	173	0	127	14767
183	94	9155	1453	926	56	0	0	14286
183.5	103	9206	1163	1090	123	162	0	14626
184	111	9182	1341	1173	208	0	0	14787
184.5	86	9095	1150	1015	195	162	0	15024
185	161	9128	1782	1401	199	0	0	14745
185.5	79	9600	1241	1146	156	100	0	14537
186	150	9748	1221	1037	95	78	0	14424
186.5	123	10301	920	637	188	205	0	13186
187	146	8847	1433	886	234	0	0	13945
187.5	175	8850	1606	1004	113	0	0	14409
188	121	8905	1693	920	228	33	0	14723
188.5	131	8769	1576	926	154	379	213	14431
189	169	8880	1372	711	195	305	109	14118
189.5	194	9445	1275	879	81	192	0	13969
190	89	9148	1586	1108	209	102	0	14759
190.5	92	8180	1457	662	102	0	0	14422
191	226	6662	1553	751	52	76	0	14667
191.5	131	8153	1186	1171	161	130	0	15606
192	129	7950	868	1079	209	282	0	15356
192.5	138	7746	1302	1185	158	564	144	15432
193	144	7756	1860	1162	163	145	0	15089
193.5	136	8010	2342	1081	156	133	0	15461
194	144	7970	2651	928	171	266	0	14291
194.5	137	8285	3376	1085	71	76	18	14341
195	151	8756	2914	723	156	131	0	14790
195.5	112	8804	2557	984	248	221	0	15083
196	114	8069	1809	1219	107	28	0	16245
196.5	197	8439	1549	1006	184	217	152	16088
197	159	8030	1201	885	152	140	0	16123
197.5	155	8542	986	1094	220	638	0	16573
198	195	8364	833	818	208	455	0	16638
198.5	151	8454	1115	774	107	165	0	16681
199	179	8356	1417	1061	136	336	0	16613
199.5	241	8535	1897	701	113	0	0	16710
200	99	8637	1644	904	146	189	0	16421
200.5	158	8664	1225	830	73	245	0	16273
201	161	8356	1968	904	143	210	64	15899

Depth (cm)	Al	Ar	As	Au	Ba	Bi	Br	Ca
201.5	125	9051	1766	1007	188	180	0	15380
202	145	8647	1990	1164	239	0	0	15672
202.5	101	10953	1455	693	113	0	65	13329
203	125	13756	1149	591	123	0	0	8377
203.5	85	14742	946	563	127	0	0	7520
204	116	14383	679	392	63	0	122	7986
204.5	135	6917	1342	894	79	0	0	13678
205	155	8410	1357	1062	172	400	0	16284
205.5	123	7945	1641	810	198	177	0	16691
206	111	8151	1817	874	244	29	0	16549
206.5	135	8270	1739	932	182	287	0	15772
207	199	8699	1190	951	171	297	0	16759
207.5	143	8488	1162	994	201	262	93	16969
208	164	8598	2288	859	196	0	13	15874
208.5	136	8724	1755	918	233	184	0	16073
209	72	8588	1867	1026	195	0	0	16216
209.5	181	9036	1188	1025	118	171	0	16732
210	126	8968	1511	1023	191	0	0	16926
210.5	119	8336	1045	1088	120	160	82	17144
211	126	8304	1276	900	228	278	0	16802
211.5	104	8534	1032	879	139	0	36	17255
212	123	8412	892	888	98	392	0	17288
212.5	108	8421	1213	931	168	290	9	16868
213	137	8414	611	967	217	381	607	17414
213.5	109	8825	902	947	104	273	0	17013
214	132	9956	1160	816	211	38	200	15465
214.5	137	9129	1152	878	179	214	0	15950
215	95	6365	1194	900	164	100	0	17553
215.5	142	8019	1335	792	128	33	0	17379
216	136	7924	1320	767	135	215	0	17825
216.5	141	8711	1709	937	132	80	76	17892
217	163	8738	2123	972	194	0	0	17341
217.5	180	8534	2392	865	138	0	0	17614
218	185	8815	1953	1018	130	0	0	17506
218.5	143	8742	1274	811	115	331	0	17453
219	95	9203	1174	707	135	161	0	17418
219.5	148	9831	678	1033	50	271	320	17194
220	198	10367	1393	1151	188	221	167	17164
220.5	165	9360	1200	987	75	314	0	16901

Depth (cm)	Al	Ar	As	Au	Ba	Bi	Br	Ca
221	148	9872	1706	1073	206	0	0	17212
221.5	182	9739	836	855	139	296	15	17510
222	140	9520	1051	1035	69	25	0	17237
222.5	162	9512	999	1232	199	292	0	17830
223	178	9254	832	907	156	381	252	17678
223.5	92	9437	875	1034	122	200	0	17898
224	121	13311	981	606	189	0	0	13101
224.5	88	8154	1583	773	305	0	0	16129
225	157	9317	751	806	142	388	246	17695
225.5	130	8915	1016	1159	213	0	0	18188
226	126	9188	725	1112	155	129	0	18533
226.5	177	8816	818	1111	142	146	0	16618
227	90	8043	909	1228	155	108	29	17926
227.5	169	8453	746	718	73	90	0	18136
228	129	8355	1146	870	195	0	202	17775
228.5	105	8632	849	850	177	103	0	17928
229	199	8540	802	1023	128	105	0	18264
229.5	93	8527	434	1053	179	158	42	17288
230	128	8842	821	1171	180	210	0	17854
230.5	136	7944	886	1016	150	109	0	17892
231	131	7477	539	1163	76	583	0	18133
231.5	84	1605	1062	853	0	766	0	9340
232	122	1723	709	450	0	536	233	9718
232.5	145	2114	1233	763	12	713	157	9806
233	125	3007	540	872	0	634	0	9590
233.5	123	2731	550	529	0	447	198	7554
234	207	1770	826	928	73	752	0	10310
234.5	151	1779	1011	825	107	724	93	9801
235	143	1645	909	644	0	737	122	9846
235.5	139	1338	1306	794	0	514	11	9396
236	117	1344	1383	943	94	486	110	9585
236.5	132	1123	1398	1088	0	797	0	9412
237	138	1396	1438	980	0	582	141	10309
237.5	132	1486	1565	889	0	792	13	10226
238	115	1178	1468	749	102	696	327	9655
238.5	153	847	1398	1225	0	704	141	8523
239	169	893	1723	730	0	535	247	8539
239.5	100	2320	1243	717	0	663	0	9896
240	129	3238	780	581	33	325	22	9425

Depth (cm)	Al	Ar	As	Au	Ba	Bi	Br	Ca
240.5	136	2885	1358	604	0	791	0	10001
241	107	1552	1305	734	11	407	0	8667
241.5	133	1272	1754	916	0	940	228	9355
242	127	1081	1605	855	0	654	0	8889
242.5	142	944	1728	709	0	674	0	8790
243	150	693	1400	974	0	795	206	7420
243.5	137	2048	1142	1064	0	295	0	6847
244	158	3193	983	777	23	539	74	5995
244.5	138	3581	869	501	0	449	241	6472
245	127	3697	810	590	0	86	0	6013
245.5	122	2058	1395	845	119	712	27	8682
246	125	1500	1256	521	46	439	0	9298
246.5	93	1400	1182	988	0	431	0	8958
247	135	1544	1175	963	0	664	0	9433
247.5	136	1460	1380	782	0	660	94	9373
248	171	1285	1357	994	0	634	0	8416
248.5	97	1071	1177	645	0	679	328	8212
249	112	1162	1458	872	0	779	63	8501
249.5	97	1404	1348	1035	103	753	21	9222
250	77	1240	1471	977	82	732	82	8380
250.5	131	1162	1429	729	0	578	0	8446
251	142	1023	1928	964	5	875	221	7830
251.5	142	778	1817	1116	0	749	0	7013
252	167	779	1602	712	0	637	0	7310
252.5	180	971	1779	928	10	624	206	7743
253	148	1097	1692	1039	123	759	0	8096
253.5	52	851	1913	1033	0	432	0	7262
254	153	984	1694	1071	0	615	0	7692
254.5	114	1212	1606	852	0	870	0	8202
255	140	1373	1889	1151	136	708	0	8381
255.5	98	1238	1690	714	35	697	0	8395
256	163	1209	2128	985	0	497	0	8423
256.5	169	1065	1866	1216	0	717	0	8462
257	110	1213	1760	720	0	585	0	8778
257.5	92	1318	2090	948	0	658	154	8429
258	138	989	1717	983	94	665	0	8081
258.5	125	974	1768	898	33	750	0	8081
259	114	1081	1721	712	12	640	0	7714
259.5	129	960	1412	1313	0	808	0	8234

Depth (cm)	Al	Ar	As	Au	Ba	Bi	Br	Ca
260	152	1142	1605	794	0	540	0	9300
260.5	163	2060	1658	1028	73	652	0	10588
261	174	3286	1803	780	0	844	0	12909
261.5	158	3369	1688	793	0	686	0	13955
262	141	3210	1402	865	0	719	0	13798
262.5	137	3689	2162	821	270	549	101	14250
263	91	4434	1996	733	0	487	0	14708
263.5	138	4709	2182	894	0	782	304	14620
264	174	5145	1747	987	117	756	0	14762
264.5	130	4833	1656	755	145	553	0	14809
265	101	5215	1722	768	20	853	0	15115
265.5	103	4787	2269	1071	21	790	0	14036
266	165	3456	2053	751	7	617	0	13721
266.5	115	4149	2021	638	155	674	0	14839
267	118	6530	1727	659	169	721	0	13862
267.5	95	6722	1644	519	121	593	0	13807
268	103	7149	1225	619	163	564	0	12147
268.5	119	4404	2160	906	93	639	0	13059
269	119	2742	1935	905	172	829	0	13061
269.5	132	3334	2507	846	0	857	0	14506
270	193	3231	2032	781	74	709	118	13136
270.5	167	3122	1918	1068	191	864	245	14395
271	124	3439	2338	771	72	680	0	14140
271.5	141	4589	1945	729	75	594	0	14504
272	180	3429	1782	1011	157	755	207	13976
272.5	130	4033	2304	813	177	970	0	15331
273	129	3274	1697	950	10	843	290	14884
273.5	158	3630	1693	732	129	731	0	15874
274	146	5083	2047	911	0	764	0	17548
274.5	107	4644	1799	894	157	567	0	18650
275	159	4352	2118	980	186	585	0	18784
275.5	208	4879	1711	755	130	757	367	18201
276	173	5943	1705	596	198	586	0	16911
276.5	132	4840	1641	656	205	780	125	17706
277	208	4907	1517	1034	132	932	0	16760
277.5	181	5029	1873	798	272	713	0	17857
278	147	5781	2307	632	126	793	0	18030
278.5	126	6088	2088	932	194	639	0	17359
279	164	6256	1685	651	267	683	0	17798

Depth (cm)	Al	Ar	As	Au	Ba	Bi	Br	Ca
279.5	156	6437	1925	510	75	835	0	17428
280	76	5595	1646	757	0	684	0	17106
280.5	139	5756	1518	633	0	575	0	16917
281	153	5771	1863	723	56	838	0	18190
281.5	186	6316	1946	535	318	700	166	18339
282	156	5475	2326	973	0	1070	91	17435
282.5	165	5681	2233	818	150	691	0	17336
283	154	6204	1941	737	246	592	242	17841
283.5	176	6054	1781	649	24	801	0	17439
284	149	5688	1643	805	269	616	0	17701
284.5	158	6022	1548	784	12	639	0	17319
285	90	5894	1952	482	412	631	0	16702
285.5	121	6555	2119	752	167	491	0	16369
286	182	5829	1777	698	148	510	0	16042
286.5	117	10687	1119	463	63	471	298	10446
287	94	12095	837	566	16	322	882	8456
287.5	65	11819	706	434	102	351	0	8023
288	116	5591	1470	616	0	514	0	11533
288.5	145	6712	1730	680	73	692	218	16565
289	167	7104	1753	806	166	723	0	16641
289.5	129	7438	1472	753	296	442	0	15873
290	109	7779	1711	354	0	563	0	15723
290.5	128	7956	1503	751	216	434	0	15912
291	45	7985	1224	396	135	497	0	15434
291.5	111	8080	1127	462	0	593	0	16530
292	185	8369	1336	573	247	620	0	15445
292.5	172	8520	1506	888	150	656	176	15383
293	138	8201	1388	446	108	399	0	15967
293.5	143	8509	1194	712	18	642	36	15802
294	132	8659	1473	520	131	583	0	14545
294.5	111	8518	1212	406	15	491	0	15967
295	126	9165	1194	495	76	692	231	15891
295.5	140	9782	1107	396	184	392	0	15416
296	115	6564	1232	597	150	423	0	11020
296.5	137	10482	695	476	0	308	92	9771
297	103	11600	257	308	0	425	0	8601
297.5	89	9398	327	511	32	257	0	9482
298	150	7550	1298	438	0	506	88	15042
298.5	184	7997	1322	452	0	384	0	14629

Depth (cm)	Al	Ar	As	Au	Ba	Bi	Br	Ca
299	123	9166	1248	531	5	263	0	15285
299.5	138	9238	1323	847	0	391	0	15590
300	129	9075	1742	513	117	336	0	15266
300.5	144	9391	1706	796	101	581	0	15577
301	122	9821	1136	497	160	716	0	14105
301.5	182	10010	1603	680	127	500	188	14539
302	160	10146	1583	863	52	724	53	14734
302.5	144	10468	1248	549	159	567	0	14039
303	124	8527	1275	653	0	680	0	12078
303.5	129	10588	1095	386	0	517	0	13802
304	72	10638	1139	516	87	510	0	13785
304.5	98	10872	926	469	71	487	0	13881
305	114	11233	1017	495	0	574	0	13200
305.5	157	11058	1054	770	143	671	234	13489
306	136	11704	948	641	158	775	15	12767
306.5	187	11739	985	801	0	437	0	12862
307	157	11983	715	586	0	414	116	12716
307.5	123	3778	1072	725	322	844	0	14761
308	122	4174	1168	901	93	889	0	15186
308.5	159	4264	1077	944	307	1067	0	15316
309	208	4280	1008	994	243	424	0	15040
309.5	144	4132	1117	1154	114	811	0	15407
310	101	4230	1136	899	357	615	0	15522
310.5	99	4738	1236	1076	415	812	0	15695
311	221	5454	1389	911	492	444	86	16377
311.5	141	5633	1105	803	114	625	0	14653
312	95	5332	883	956	238	998	0	15086
312.5	105	4480	1078	800	411	659	0	14408
313	177	3822	1066	1005	0	1125	110	14300
313.5	131	4316	921	1128	396	903	207	14886
314	104	4272	991	621	291	963	0	14728
314.5	126	5258	861	1009	246	931	12	15370
315	110	4806	1490	884	183	597	0	15445
315.5	186	4852	1355	1012	379	503	233	16259
316	125	5054	1261	946	184	613	31	15452
316.5	165	4886	833	668	174	856	220	16176
317	170	4770	895	890	462	639	0	15431
317.5	100	4205	1286	843	101	771	0	15525
318	97	4707	1278	1122	192	724	0	15888

Depth (cm)	Al	Ar	As	Au	Ba	Bi	Br	Ca
318.5	79	5594	1606	659	0	574	0	15977
319	125	4981	967	1048	190	581	0	15529
319.5	142	5256	1083	741	469	456	0	15274
320	133	5170	1465	885	493	541	257	16011
320.5	131	5229	1195	970	566	830	0	15396
321	164	5053	961	782	734	309	246	15080
321.5	103	4568	1003	894	721	779	24	14809
322	69	5302	1240	1102	367	694	0	15636
322.5	152	5898	1525	1011	777	873	0	15347
323	139	5850	988	767	362	870	0	16112
323.5	98	5999	720	756	434	676	0	15589
324	136	6042	800	920	564	640	0	15856
324.5	111	6006	1368	791	572	616	98	15805
325	84	6665	1359	650	451	263	0	16133
325.5	137	8108	809	666	233	603	0	16160
326	137	8370	896	727	495	702	53	16579
326.5	126	8497	592	635	489	678	0	15316
327	76	8101	902	684	322	582	0	15938
327.5	140	7493	973	795	277	670	0	15837
328	142	7286	1146	788	499	740	0	16331
328.5	137	6583	1231	674	467	625	0	15802
329	114	6729	809	720	606	390	228	15382
329.5	143	5997	1308	739	426	469	0	14867
330	179	5580	1200	950	628	546	0	15104
330.5	164	5704	1664	984	574	875	0	15752
331	124	5810	1612	832	378	859	284	17200
331.5	132	6690	1127	698	750	528	0	17279
332	176	7358	1903	812	459	677	0	17128
332.5	94	8874	1404	637	431	641	124	16975
333	138	9581	1217	435	119	546	0	16045
333.5	130	8202	1759	944	436	647	0	16973
334	166	7358	1480	855	587	842	0	16767
334.5	110	7864	1506	735	595	363	264	17194
335	150	8033	1162	822	731	843	0	17947
335.5	93	15936	759	341	216	0	0	4799
336	0	16915	105	195	14	181	0	2849
336.5	27	17415	45	112	7	58	0	3273
337	115	7494	984	596	338	500	131	11993
337.5	118	5195	1348	690	517	513	38	17389

Depth (cm)	Al	Ar	As	Au	Ba	Bi	Br	Ca
338	137	9325	1601	641	495	670	0	17395
338.5	134	10022	1034	546	51	550	0	16056
339	136	9762	1667	640	834	515	0	16295
339.5	140	10396	1136	778	762	355	0	15478
340	121	10317	1215	551	405	386	0	14629
340.5	134	9242	1287	661	424	466	0	16604
341	185	9403	450	719	111	654	20	16646
341.5	166	9717	961	697	557	330	0	16748
342	116	10239	1448	678	504	581	0	15540
342.5	98	10366	527	783	321	585	34	14853
343	98	10030	890	379	467	408	87	14908
343.5	140	10102	994	794	231	556	0	15119
344	108	10720	810	641	522	541	0	14801
344.5	129	10621	1154	464	186	492	0	15841
345	103	10600	709	675	283	480	13	15313
345.5	112	10472	1085	595	493	304	0	15102
346	121	10861	671	626	449	601	0	14929
346.5	84	11232	413	434	289	307	0	14171
347	92	10913	798	377	389	612	0	15328
347.5	181	11118	830	615	485	390	0	14243
348	172	11473	799	722	517	439	0	13988
348.5	125	11604	670	623	471	584	86	14272
349	145	11351	798	688	297	621	188	14439
349.5	129	11815	737	500	102	282	0	13657
350	107	11287	687	484	449	252	0	13174
350.5	152	11332	1335	595	668	203	0	13500
351	81	12401	717	698	66	481	0	12755
351.5	156	11857	1024	564	106	570	242	12765
352	138	11596	843	518	567	490	0	13290
352.5	171	11731	812	583	238	207	0	13272
353	152	14550	500	481	314	205	0	7938
353.5	63	14444	605	366	190	64	0	6786
354	62	13162	551	361	83	223	86	7336
354.5	49	13104	648	357	117	307	0	8825
355	117	6419	1137	716	78	375	0	14416
355.5	128	6953	1191	502	268	414	0	16985
356	131	12492	676	456	384	638	0	13109
356.5	154	12173	807	737	38	524	0	12592
357	81	12646	1003	499	485	306	0	12160

Depth (cm)	Al	Ar	As	Au	Ba	Bi	Br	Ca
357.5	162	12796	795	404	599	308	0	11483
358	126	12780	1014	552	338	392	31	12151
358.5	157	13513	451	426	517	261	0	10805
359	96	14175	919	459	433	367	0	8873
359.5	121	13941	686	429	274	167	0	9097
360	127	14206	543	522	468	335	0	8103
360.5	113	14371	96	497	566	208	146	8765
361	132	13667	395	508	425	225	0	9216
361.5	100	13267	836	386	610	367	0	10104
362	111	13163	687	505	525	567	19	10307
362.5	115	12968	839	502	654	376	0	10326
363	144	12478	732	470	271	554	0	11248
363.5	103	12905	0	620	467	458	0	10917
364	139	12802	219	676	460	569	322	11809
364.5	83	12659	602	459	358	445	0	12094
365	68	11945	634	533	688	504	0	13112
365.5	104	12405	733	622	560	449	0	12426
366	103	12153	640	595	172	327	0	12405
366.5	116	12044	601	693	363	453	0	12826
367	179	14018	853	506	288	482	0	10138
367.5	71	14083	267	351	482	152	191	10094
368	123	13169	448	564	826	290	0	11102
368.5	111	8220	1027	606	961	420	0	17532
369	90	8529	1340	690	806	382	248	18857
369.5	128	8813	1386	887	961	805	0	18199
370	133	8602	1365	862	1001	472	0	18369
370.5	207	8800	1396	578	1034	480	49	18960
371	118	8898	1345	644	509	501	20	18590
371.5	177	8758	1281	840	858	879	129	19391
372	119	9081	1167	735	694	455	0	18704
372.5	187	8705	1161	672	603	549	0	17957
373	156	8424	1049	358	482	445	74	18403
373.5	126	7945	880	954	545	674	117	18872
374	145	8004	1153	691	796	362	0	18352
374.5	138	9499	786	583	804	464	0	17122
375	163	8755	1009	548	794	423	0	16901
375.5	156	8947	988	759	623	307	0	17220
376	109	7488	1010	774	647	657	68	18782
376.5	97	7094	1005	760	783	622	0	18993

Depth (cm)	Al	Ar	As	Au	Ba	Bi	Br	Ca
377	156	7560	873	599	1193	636	0	19172
377.5	122	7418	1151	535	934	557	0	19664
378	122	7112	923	630	767	675	0	19484
378.5	110	7223	817	498	936	323	273	18615
379	206	6972	927	766	629	294	0	18955
379.5	122	6911	1117	877	922	642	20	18888
380	132	6465	539	540	838	423	80	18457
380.5	166	6215	1015	863	501	668	0	18242
381	130	8576	1074	586	672	286	0	19025
381.5	102	7774	702	518	411	437	0	15543
382	155	6386	821	600	367	189	0	18342
382.5	67	6490	1119	510	855	381	0	18649
383	117	6833	1127	775	997	233	0	19374
383.5	199	6981	1255	775	1199	679	153	19659
384	146	7433	1323	743	742	558	0	19512
384.5	113	7341	1023	480	887	516	0	21234
385	100	7302	1038	703	593	792	0	19687
385.5	97	7373	904	481	646	576	0	19929
386	142	7521	971	645	711	443	0	20015
386.5	181	7587	1137	670	809	851	0	19565
387	117	7206	998	813	1149	515	0	20391
387.5	152	7459	912	478	1257	601	0	21341
388	145	8432	1100	581	1402	476	0	21499
388.5	168	8962	1310	724	1189	532	0	21062
389	171	8850	1519	521	861	463	0	21021
389.5	96	10387	1558	707	1018	412	0	20839
390	117	9964	1028	695	404	558	0	19594
390.5	183	9380	1007	751	770	481	0	19957
391	103	9103	770	569	525	571	0	19603
391.5	74	8970	955	405	718	562	0	19746
392	110	8885	858	477	718	729	0	19533
392.5	128	8805	1385	472	611	489	0	19328
393	151	9330	1523	557	700	805	78	18518
393.5	147	8973	1501	613	612	283	0	18017
394	124	8682	1233	618	461	598	0	18960
394.5	188	8799	605	619	558	487	0	19797
395	134	8895	771	539	616	426	0	19249
395.5	112	9509	599	651	541	597	0	19182
396	101	8906	702	297	506	465	72	17635

Depth (cm)	Al	Ar	As	Au	Ba	Bi	Br	Ca
396.5	127	8616	914	601	583	558	0	19375
397	134	8992	798	424	763	642	0	19380
397.5	138	8745	727	467	431	1064	156	19789
398	113	8892	683	450	467	377	0	19872
398.5	186	8609	1107	583	578	399	0	20420
399	125	8822	860	533	842	695	0	20532
399.5	145	9133	389	695	1095	243	0	20943
400	135	8966	861	433	879	601	165	21236
400.5	148	8969	925	702	569	571	0	21180
401	97	8988	1461	660	897	686	0	21097
401.5	125	8965	931	650	1043	426	0	20699
402	94	8717	956	685	1005	523	0	20980
402.5	119	8729	697	456	735	599	0	21194
403	68	8643	899	469	842	582	0	21350
403.5	175	8504	983	415	759	748	0	21405
404	129	8813	1874	977	931	874	209	21400
404.5	148	8782	1450	730	514	685	0	21679
405	128	8992	2232	466	933	459	0	23127
405.5	134	9431	1591	471	1372	588	0	21014
406	83	8192	1254	319	976	450	0	21932
406.5	142	7977	2018	614	1171	784	0	22135
407	93	7888	1505	501	920	362	0	22857
407.5	131	7488	1513	776	955	597	23	23483
408	152	8270	1466	649	1038	363	0	23233
408.5	105	8316	1388	402	723	407	0	23320
409	127	8442	1818	777	983	471	33	23668
409.5	136	9062	1512	674	591	629	0	23730
410	131	8144	1384	612	937	736	202	23140
410.5	193	7963	1075	573	980	561	0	23291
411	132	8050	1289	581	729	482	9	23479
411.5	146	8476	1144	737	815	535	0	22755
412	119	7714	941	569	1071	660	137	23242
412.5	178	7948	1052	591	660	532	0	23790
413	149	7854	1098	579	714	551	0	22996
413.5	155	7502	969	546	476	453	0	23201
414	107	8385	881	466	792	283	0	22811
414.5	202	9514	687	481	667	316	0	19332
415	128	10163	616	434	515	453	0	18537
415.5	97	9422	624	286	876	227	0	20343

Depth (cm)	Al	Ar	As	Au	Ba	Bi	Br	Ca
416	151	8616	992	618	259	339	161	23833
416.5	160	8081	945	675	1009	752	67	24253
417	169	7678	1245	853	575	635	0	23979
417.5	152	7614	1112	491	1014	610	320	23958
418	169	7548	1375	729	766	731	0	23959
418.5	165	7579	1230	663	939	519	0	24915
419	143	7518	980	515	1099	432	0	25308
419.5	110	7612	1023	574	872	487	0	24536
420	123	7598	999	359	570	283	175	25518
420.5	164	7652	864	393	882	301	0	25369
421	132	7417	1132	614	990	572	0	25618
421.5	132	7714	1247	716	1066	279	140	25713
422	135	7351	1010	525	987	475	0	26144
422.5	163	7550	849	658	394	409	0	26268
423	136	7512	1221	727	982	441	0	24811
423.5	132	6991	871	591	461	481	0	25012
424	148	7024	1535	616	1133	602	0	24577
424.5	166	7070	1251	498	1234	521	0	25248
425	154	7477	1097	464	806	527	0	24529
425.5	183	7312	1131	769	1227	851	117	25120
426	82	7558	775	523	1250	405	121	25564
426.5	153	7361	985	632	1191	646	0	24810
427	125	7060	1044	563	940	507	0	25383
427.5	135	6611	1438	604	1168	483	0	25100
428	165	6438	1162	689	1264	593	0	24001
428.5	185	7149	975	495	829	533	0	23972
429	158	8925	703	438	380	299	433	19689
429.5	116	9842	631	461	529	260	397	19859
430	112	11037	1047	392	594	334	507	16566
430.5	128	8027	959	534	842	357	214	18779
431	102	4119	1320	780	432	425	223	12602

Table A 2.2 Cuobu XRF Geochemistry Cl – Hf

Depth (cm)	Cl	Co	Cu	Eu	Fe	Ga	Ge	Hf
27	264	0	460	3102	15005	69	70	0
27.5	32	0	906	2236	15269	582	356	50
28	0	0	1760	7862	29854	1069	524	443
28.5	24	0	1470	8418	32194	875	505	676
29	53	0	1306	8677	33019	864	823	546
29.5	0	0	1142	7438	32852	437	837	697
30	21	15	1591	7597	33778	1002	962	436
30.5	0	55	1134	7845	32239	717	668	462
31	0	0	1223	8376	32909	897	720	602
31.5	19	0	1319	8114	34689	753	984	747
32	53	0	1212	7898	36548	477	556	505
32.5	23	0	1467	8234	39882	388	734	345
33	0	0	1227	8189	34826	955	712	372
33.5	12	0	1110	6677	34304	939	994	612
34	8	0	1238	7874	35733	815	407	365
34.5	0	0	1209	7071	34209	1111	674	538
35	0	0	1359	8254	37105	1032	421	492
35.5	0	0	1237	8029	33922	657	678	551
36	43	0	1158	8412	35055	807	716	714
36.5	0	0	1021	8135	37304	600	522	482
37	53	0	1488	8727	41717	897	746	493
37.5	339	0	1111	8105	36553	1063	612	603
38	391	25	1161	7496	38401	1273	792	429
38.5	54	0	1241	8185	42793	974	591	434
39	59	0	1290	7576	44572	607	841	350
39.5	25	0	1390	8900	42717	796	712	693
40	0	0	1160	8276	39579	796	598	425
40.5	81	114	1171	8089	43857	624	491	638
41	73	0	1149	8583	45592	806	639	504
41.5	62	0	1117	8283	44324	1165	753	431
42	16	0	1184	8999	43258	1046	347	641
42.5	37	0	1370	8854	42416	942	779	405
43	60	0	1135	8346	40095	859	588	570
43.5	74	0	1259	7474	42569	1307	774	439
44	61	0	1105	7123	43468	1090	517	251
44.5	68	0	1308	7537	42083	1011	740	297
45	92	0	1269	7143	41606	784	365	358
45.5	23	0	1217	7043	39118	441	716	233
46	40	0	1098	6940	43595	899	733	482

Depth (cm)	Cl	Co	Cu	Eu	Fe	Ga	Ge	Hf
46.5	124	0	1297	6593	41994	940	790	253
47	99	0	1240	6510	42435	928	837	351
47.5	50	0	1062	6735	42319	989	627	229
48	58	0	901	7059	42154	961	546	294
48.5	56	0	952	7648	40418	755	830	425
49	48	0	1089	7807	39781	654	717	379
49.5	0	0	1343	7566	39712	989	626	500
50	37	0	1075	7743	46278	526	557	307
50.5	55	0	1187	8120	44844	1292	754	421
51	71	0	985	7775	42344	523	786	641
51.5	85	0	979	7533	40810	846	361	312
52	115	0	1133	7018	42522	848	812	264
52.5	33	0	1417	7491	47005	1190	599	307
53	21	0	937	7712	47490	909	348	307
53.5	23	0	1120	8141	49313	397	682	230
54	0	0	1097	6672	38861	741	828	238
54.5	51	0	1279	6908	41024	1010	661	444
55	119	69	1362	7727	44345	1147	396	501
55.5	73	0	1264	7107	43639	975	630	493
56	21	0	1104	7473	46349	960	778	282
56.5	39	30	1099	7440	47560	1260	685	316
57	0	0	1047	7800	44598	815	954	271
57.5	22	0	1095	7352	38635	820	887	407
58	31	0	1133	6475	41576	1294	635	416
58.5	39	0	993	7331	43595	549	978	338
59	19	0	1025	7042	46162	119	1002	322
59.5	41	0	1308	7636	42839	912	758	277
60	28	0	1137	7451	44990	505	707	311
60.5	100	0	1022	7643	45246	736	771	336
61	0	76	1102	6991	39467	776	650	81
61.5	21	0	879	7185	41730	685	765	356
62	34	0	1276	8248	45346	739	598	360
62.5	0	0	844	7322	43910	880	663	412
63	14	0	1019	7077	41186	1153	441	213
63.5	0	0	741	7713	44211	298	621	275
64	6	95	1365	6707	41338	585	961	356
64.5	36	0	1076	7633	43178	647	647	455
65	20	0	1127	7292	45588	790	721	336
65.5	33	0	1079	7936	45048	1111	500	331

Depth (cm)	Cl	Co	Cu	Eu	Fe	Ga	Ge	Hf
66	53	43	1086	7260	44695	660	689	429
66.5	62	0	1199	7355	42619	572	403	181
67	35	0	1362	7682	47033	940	490	242
67.5	31	0	919	7826	52762	922	615	428
68	0	0	1314	8218	51267	1356	731	315
68.5	48	0	934	7825	49259	829	720	339
69	69	0	953	7926	51364	995	866	468
69.5	0	0	1164	6756	46286	744	666	318
70	0	0	1052	7766	50120	962	666	351
70.5	8	0	1190	6658	43536	1034	218	323
71	26	0	1236	7933	47218	868	464	205
71.5	48	0	1394	8565	53955	1393	804	303
72	25	0	1198	9209	54555	508	1077	478
72.5	27	0	1080	7363	51591	1248	522	284
73	27	0	1154	8096	50558	1095	776	485
73.5	5	0	1089	8273	56196	858	1096	390
74	110	0	828	5433	47664	862	624	220
74.5	79	0	455	2216	23216	455	546	0
75	55	11	587	2230	26760	568	428	38
75.5	68	45	797	4622	31504	616	668	362
76	55	65	998	6044	42478	513	533	253
76.5	0	25	1024	6832	44388	1026	406	445
77	0	0	1327	7749	46279	1330	659	329
77.5	54	0	1157	6584	45821	783	565	408
78	0	0	1049	7153	48675	924	1206	258
78.5	18	0	953	7584	50834	1017	488	288
79	0	0	977	8165	51461	923	1358	271
79.5	7	0	1068	7375	50317	725	558	373
80	0	0	1117	7615	50190	939	915	332
80.5	0	0	1019	7466	50297	698	791	413
81	0	0	1064	7030	47948	718	521	346
81.5	38	0	956	6849	44154	743	726	374
82	17	0	1276	7515	46487	829	776	344
82.5	0	64	1106	7016	47094	1015	738	443
83	5	0	877	6853	45895	686	973	440
83.5	22	0	532	3969	63993	707	205	225
84	46	0	680	4187	100466	546	436	125
84.5	20	0	408	4265	96589	689	234	306
85	32	0	423	4199	68025	572	355	265

Depth (cm)	Cl	Co	Cu	Eu	Fe	Ga	Ge	Hf
85.5	31	0	698	4462	86294	676	440	211
86	0	36	762	4137	75061	336	343	241
86.5	54	0	799	4821	75238	722	665	178
87	19	0	541	4553	43971	605	434	275
87.5	23	81	586	3792	39379	376	448	277
88	40	60	669	3909	40623	562	474	235
88.5	22	0	669	4086	41333	546	539	257
89	33	0	667	4018	43565	540	266	276
89.5	0	0	736	2847	32203	567	359	149
90	54	0	519	3141	35488	534	330	212
90.5	36	0	508	2341	27122	536	438	96
91	18	0	323	3221	30982	373	416	181
91.5	4	0	478	4212	30319	208	342	318
92	20	0	977	4288	36065	542	592	195
92.5	28	0	761	5085	41263	316	395	285
93	11	0	925	4939	37096	565	291	337
93.5	29	0	797	4775	51565	703	339	226
94	37	0	575	5215	64719	570	545	321
94.5	0	59	653	6204	95813	739	410	318
95	14	0	702	5689	75232	397	517	219
95.5	8	0	408	6462	71989	297	466	284
96	0	5	877	5711	64198	857	328	304
96.5	0	0	860	4258	43123	609	570	265
97	0	0	692	6124	105413	559	652	282
97.5	0	4	596	6495	116970	305	598	272
98	0	17	671	7085	139521	942	496	337
98.5	0	14	864	7345	128364	717	358	302
99	0	0	506	6568	88964	625	530	292
99.5	0	0	672	6281	92635	1003	680	273
100	33	0	572	5909	87918	553	465	126
100.5	0	0	647	5490	104487	792	617	352
101	38	229	463	6228	125838	533	422	340
101.5	0	0	410	8392	140424	755	385	113
102	0	29	413	8134	170900	585	673	127
102.5	0	0	730	7924	142904	956	495	224
103	0	0	555	7323	151630	743	301	279
103.5	0	0	612	8294	159718	555	656	181
104	0	0	621	7722	158784	525	308	238
104.5	0	0	574	7920	171076	708	411	166

Depth (cm)	Cl	Co	Cu	Eu	Fe	Ga	Ge	Hf
105	0	75	495	8724	206332	747	500	145
105.5	4	150	513	8214	215602	683	313	167
106	0	64	524	7725	187062	629	491	273
106.5	0	0	479	8721	211796	593	481	145
107	0	0	478	9046	202772	465	452	333
107.5	0	70	770	8121	155814	777	415	215
108	0	71	539	8043	204564	844	641	218
108.5	5	47	543	9093	214388	1049	299	173
109	0	0	488	7603	157846	681	458	387
109.5	0	0	620	8077	151522	662	763	434
110	0	15	606	7452	152947	776	272	172
110.5	0	0	582	7872	184217	1034	424	154
111	0	0	439	8464	188051	806	536	187
111.5	25	0	278	8147	177391	832	632	194
112	0	117	398	7390	170190	628	758	181
112.5	0	37	477	7910	169429	783	246	40
113	15	32	603	6978	167382	675	693	89
113.5	0	0	556	7618	143019	785	548	164
114	0	29	416	8838	180063	955	564	182
114.5	0	295	455	7821	197630	643	623	238
115	0	172	429	8186	217695	716	527	267
115.5	0	75	382	8431	222688	813	227	154
116	19	142	323	8150	182315	547	605	235
116.5	0	0	493	8912	196937	997	356	100
117	24	86	448	8275	206658	477	426	251
117.5	0	0	510	7339	154909	1244	578	238
118	41	196	584	4347	131560	420	431	27
118.5	34	314	475	4643	144862	414	372	117
119	17	235	448	5997	130677	560	204	136
119.5	18	0	368	7946	145572	764	444	361
120	12	0	517	7466	166012	903	475	200
120.5	0	0	487	8062	166846	834	580	79
121	0	23	647	6936	154208	879	467	195
121.5	0	0	590	7187	131754	824	572	24
122	0	86	369	7397	129569	651	641	185
122.5	20	0	616	7337	117589	837	587	203
123	12	0	529	6839	93042	711	407	324
123.5	0	65	750	6370	97764	583	664	222
124	0	11	467	6483	118454	264	558	167

Depth (cm)	Cl	Co	Cu	Eu	Fe	Ga	Ge	Hf
124.5	0	0	452	7541	130545	958	768	248
125	0	0	768	6907	111863	947	552	362
125.5	0	0	483	7397	134608	800	648	104
126	22	83	597	7043	119125	301	636	286
126.5	0	123	743	6344	100765	967	430	293
127	0	0	519	6693	106512	525	474	323
127.5	0	81	594	6049	91120	459	397	268
128	0	0	553	6721	82837	588	830	325
128.5	23	0	486	7031	103326	615	486	260
129	0	0	574	7068	121047	703	531	309
129.5	0	0	499	7682	143106	280	645	266
130	0	0	717	7449	147065	892	495	296
130.5	0	0	709	7676	138463	668	493	228
131	0	0	683	7053	119645	443	242	314
131.5	6	0	399	7870	120773	796	698	292
132	0	0	473	7369	102542	501	356	352
132.5	0	0	452	7387	112502	668	532	401
133	0	0	552	7252	139277	662	605	331
133.5	0	0	608	7810	135618	677	874	161
134	0	91	627	6824	114117	807	521	386
134.5	0	226	603	7789	149225	891	359	307
135	9	269	633	7331	150639	883	564	261
135.5	8	25	726	8134	163650	747	553	223
136	0	0	353	8007	146273	866	712	471
136.5	0	264	567	7679	198362	810	316	274
137	0	129	430	8744	208662	739	688	232
137.5	0	78	598	8402	197253	796	650	202
138	61	0	415	1318	52924	286	419	0
138.5	71	0	347	1194	29305	155	105	0
139	38	28	218	1196	27882	181	105	95
139.5	16	0	636	6032	104646	849	758	264
140	20	195	514	7283	169296	758	466	317
140.5	0	0	477	8485	149100	487	459	212
141	0	307	553	7412	180972	759	364	294
141.5	20	87	470	8097	179365	523	610	227
142	0	128	507	7833	147587	412	219	182
142.5	20	194	463	7411	177648	828	308	178
143	0	0	586	7658	164974	1054	825	220
143.5	0	298	513	7789	183768	890	444	181

Depth (cm)	Cl	Co	Cu	Eu	Fe	Ga	Ge	Hf
144	0	102	670	7684	147587	809	552	246
144.5	0	27	363	7887	140513	554	522	322
145	0	199	621	7348	135170	910	448	321
145.5	0	155	678	7846	143967	693	581	238
146	0	29	535	7997	164116	646	591	154
146.5	0	0	614	8342	157515	653	457	405
147	0	212	389	8527	151396	814	527	298
147.5	0	283	461	7954	173604	560	21	153
148	10	324	640	7980	160789	991	396	492
148.5	0	0	705	7860	129621	895	574	360
149	0	100	718	6714	117721	892	183	283
149.5	0	0	832	6348	83964	528	495	352
150	0	0	615	5341	67822	616	539	317
150.5	16	0	443	2958	57718	23	360	0
151	17	0	521	3374	31762	444	423	118
151.5	0	0	497	4326	54116	494	639	227
152	0	169	758	7551	122423	762	477	426
152.5	0	220	511	8359	149478	688	247	459
153	0	231	552	8739	168867	742	429	334
153.5	0	276	842	865	59252	530	429	465
154	7	483	757	244	68533	807	526	554
154.5	26	143	930	944	39293	451	406	438
155	71	368	690	1991	68439	565	607	555
155.5	8	145	857	1016	57081	852	390	370
156	45	144	993	1280	35325	675	389	451
156.5	21	217	885	934	51078	377	681	347
157	6	396	729	1178	83212	674	581	331
157.5	46	712	805	855	124782	193	527	385
158	16	620	967	39	121769	754	352	471
158.5	0	389	818	1234	95697	927	581	328
159	0	625	896	688	117740	955	353	438
159.5	0	758	624	908	107942	611	455	528
160	0	408	800	1361	92656	590	240	447
160.5	26	296	893	1044	75237	653	760	528
161	0	268	1072	1504	66907	321	344	362
161.5	0	354	1012	897	45624	654	381	437
162	11	112	866	1746	34472	452	690	476
162.5	18	69	896	599	47439	657	611	444
163	10	287	1103	1656	88486	489	339	426

Depth (cm)	Cl	Co	Cu	Eu	Fe	Ga	Ge	Hf
163.5	0	422	619	1279	86490	401	867	599
164	30	332	702	1064	81739	335	703	331
164.5	8	132	768	1508	70114	576	604	321
165	0	9	758	636	41456	501	536	367
165.5	32	409	956	1836	48581	322	753	499
166	0	269	752	1922	65944	640	666	357
166.5	16	362	756	2027	84255	332	601	364
167	0	137	745	1894	56334	596	362	298
167.5	0	379	909	1096	50719	702	449	363
168	78	356	471	0	43221	261	217	188
168.5	46	255	531	0	44951	596	353	100
169	47	354	601	0	41699	309	240	154
169.5	89	387	614	158	63176	700	347	318
170	0	386	960	613	97548	677	421	297
170.5	0	510	794	875	91447	553	657	504
171	27	356	804	1387	90882	677	593	439
171.5	0	567	687	322	96105	387	446	455
172	0	738	883	519	120790	764	564	454
172.5	0	690	586	394	141496	715	438	583
173	11	752	735	723	157392	594	530	281
173.5	0	606	808	432	132817	399	351	359
174	0	678	677	1093	140265	828	518	451
174.5	0	676	552	0	118973	301	601	408
175	0	459	620	1265	92677	736	610	287
175.5	19	667	826	964	92268	400	404	490
176	0	644	890	1029	89089	723	552	512
176.5	29	432	768	527	94218	749	575	466
177	12	582	936	313	87608	550	689	491
177.5	0	316	917	867	91937	535	569	423
178	0	448	778	565	87453	544	335	433
178.5	0	396	768	955	68497	507	220	390
179	34	474	1047	758	73376	336	484	296
179.5	0	330	829	494	73016	373	618	277
180	12	465	874	0	70175	605	290	453
180.5	0	512	782	247	68979	414	334	519
181	0	436	1174	594	55897	934	699	576
181.5	13	230	934	1995	61428	485	763	307
182	6	436	763	290	66017	394	530	513
182.5	0	335	843	1229	60264	634	456	363

Depth (cm)	Cl	Co	Cu	Eu	Fe	Ga	Ge	Hf
183	0	428	936	331	66041	800	542	484
183.5	0	608	943	660	79478	579	696	354
184	0	282	730	1037	80854	172	370	264
184.5	0	664	494	0	99288	332	299	413
185	44	572	830	807	88162	725	639	476
185.5	0	350	891	810	81092	624	273	505
186	0	341	792	410	70607	344	306	412
186.5	0	209	826	0	58004	366	356	230
187	0	521	907	230	90082	440	421	199
187.5	0	694	798	688	114834	760	540	239
188	24	875	572	1681	139990	552	383	455
188.5	11	802	827	627	128717	618	872	399
189	10	499	626	870	94170	435	610	268
189.5	0	587	725	209	79804	838	364	467
190	0	552	967	723	80228	510	297	415
190.5	10	450	769	1264	69535	755	480	388
191	52	542	555	1103	86191	537	619	313
191.5	10	190	1100	0	50127	522	529	426
192	39	183	838	535	54332	747	375	481
192.5	0	480	913	709	66826	574	834	388
193	4	350	866	443	88022	585	475	463
193.5	33	643	857	17	123616	853	618	377
194	0	724	752	621	145012	1012	617	157
194.5	10	1030	664	0	206331	816	734	283
195	0	1065	805	920	172721	741	556	211
195.5	0	650	763	647	117285	231	257	375
196	0	163	969	1500	38853	241	593	363
196.5	0	93	897	1622	37774	570	822	306
197	0	52	680	1206	34745	562	507	360
197.5	0	227	807	863	33423	734	493	496
198	0	216	1169	1209	34488	584	443	452
198.5	0	0	689	823	36243	537	589	391
199	4	408	988	1600	34627	661	594	520
199.5	38	297	918	372	44018	871	736	477
200	0	311	790	56	68454	616	727	500
200.5	0	399	1093	1174	54899	943	502	507
201	0	770	686	799	109272	407	795	410
201.5	0	596	680	1412	97337	757	516	526
202	0	502	652	354	90513	548	413	526

Depth (cm)	Cl	Co	Cu	Eu	Fe	Ga	Ge	Hf
202.5	19	503	929	0	72716	654	667	311
203	41	500	579	0	48620	380	400	113
203.5	52	368	516	0	43667	301	367	97
204	0	140	463	0	23625	198	445	131
204.5	0	415	662	802	68319	713	437	205
205	42	273	981	1344	80361	653	797	482
205.5	22	496	875	1212	80030	587	573	481
206	0	314	677	1178	82562	591	726	510
206.5	0	873	698	27	115841	559	844	351
207	39	640	663	674	77407	171	475	486
207.5	14	248	747	1363	62809	659	664	564
208	0	427	838	617	90981	441	927	326
208.5	37	925	698	598	117504	387	638	510
209	0	821	799	0	101806	713	433	450
209.5	0	289	863	1115	66642	785	817	660
210	23	367	838	1110	49701	791	662	607
210.5	30	563	1022	0	55534	377	538	427
211	13	770	879	346	108285	784	382	589
211.5	0	573	813	696	65447	554	873	478
212	0	345	577	1628	59154	377	565	486
212.5	42	596	855	408	95139	849	735	522
213	49	640	732	390	94903	440	486	465
213.5	14	300	592	695	98887	1090	505	554
214	39	637	801	1019	92415	939	465	664
214.5	62	680	638	455	110969	858	831	681
215	46	604	905	1315	115799	651	833	370
215.5	54	585	675	369	100689	965	430	344
216	34	971	760	1890	151818	573	415	508
216.5	7	1258	752	37	179937	612	757	549
217	30	981	603	1006	183169	670	590	387
217.5	29	1418	832	0	174126	257	616	438
218	29	801	462	232	129287	512	319	709
218.5	7	961	946	479	130251	667	646	612
219	0	478	709	195	84803	706	664	422
219.5	23	325	590	828	84169	669	601	454
220	18	518	975	197	69871	757	610	574
220.5	33	404	603	0	61172	376	384	601
221	28	237	759	619	66711	880	483	499
221.5	47	266	778	665	71017	513	499	510

Depth (cm)	Cl	Co	Cu	Eu	Fe	Ga	Ge	Hf
222	14	466	953	0	59871	669	634	411
222.5	15	516	767	0	76761	456	527	330
223	14	377	824	0	75526	494	823	481
223.5	30	415	724	1102	65301	463	486	524
224	12	336	590	0	40256	556	244	325
224.5	0	355	679	0	57230	722	821	403
225	8	256	846	264	68884	520	591	432
225.5	12	349	1135	133	40913	427	652	507
226	0	148	1058	763	37044	634	330	331
226.5	30	56	1009	1190	30756	986	535	478
227	4	151	896	0	39488	653	834	526
227.5	61	94	733	151	47632	647	784	531
228	14	543	918	115	45143	808	566	325
228.5	24	148	1014	1022	37295	711	838	427
229	21	80	897	500	37523	698	510	405
229.5	0	372	879	0	50190	617	360	453
230	0	455	830	0	51242	354	507	502
230.5	0	304	945	906	42107	614	290	365
231	0	387	953	433	41448	829	370	424
231.5	0	0	654	4912	34146	540	737	316
232	0	0	607	4543	29552	584	832	211
232.5	0	0	861	5604	30582	653	597	249
233	0	0	692	3847	26949	435	472	236
233.5	0	0	691	3183	24107	569	597	89
234	0	0	753	4800	35864	743	771	335
234.5	0	0	752	5297	37324	821	449	272
235	0	0	705	5438	40140	751	764	256
235.5	0	0	1044	5279	41724	970	693	214
236	7	0	718	5613	40340	625	658	257
236.5	0	0	845	5323	40855	716	602	117
237	0	0	667	5730	43023	539	923	318
237.5	7	0	824	5718	41271	553	669	189
238	34	0	638	5353	42003	704	867	75
238.5	0	0	600	4909	49671	619	353	90
239	0	0	989	4547	37866	908	655	223
239.5	0	0	792	5255	40055	772	532	244
240	0	0	814	4441	44420	351	120	175
240.5	0	0	518	6472	55783	757	355	406
241	0	0	673	4898	42220	562	849	95

Depth (cm)	Cl	Co	Cu	Eu	Fe	Ga	Ge	Hf
241.5	0	0	729	5634	57027	917	810	264
242	5	0	468	5573	49416	502	622	181
242.5	0	0	629	4681	38651	770	712	106
243	0	0	609	4201	39219	709	836	212
243.5	0	0	654	2781	32517	829	732	208
244	28	0	395	2824	26598	552	602	144
244.5	13	0	531	2910	26312	351	679	139
245	0	0	505	3231	27480	494	435	172
245.5	0	0	668	4109	31739	554	688	203
246	0	0	674	5255	38023	616	792	85
246.5	0	0	419	5000	34881	296	765	262
247	0	0	696	5462	33741	532	863	232
247.5	0	0	682	4944	35899	597	828	172
248	0	0	822	5046	40574	386	270	251
248.5	0	0	436	4907	45537	627	651	90
249	0	0	787	5270	40920	797	705	254
249.5	0	0	742	5961	43464	554	678	328
250	0	0	753	5003	48296	790	620	237
250.5	0	0	576	5164	47514	506	810	112
251	0	0	633	5240	44193	609	817	99
251.5	0	0	720	3963	39065	471	589	0
252	0	0	465	3892	34079	840	567	74
252.5	0	0	814	4577	29790	758	907	170
253	0	0	805	4877	40654	733	583	145
253.5	5	0	875	4914	47522	807	660	0
254	0	0	605	5599	56969	478	699	90
254.5	0	0	724	5839	58214	777	775	59
255	0	0	812	5388	55410	831	719	228
255.5	0	0	604	4983	47348	627	821	146
256	0	0	621	5194	45143	887	734	201
256.5	0	0	791	5359	44817	576	606	167
257	0	0	207	4821	52054	687	368	266
257.5	0	0	1000	4882	43925	453	632	210
258	17	0	719	4366	32974	864	810	43
258.5	0	0	683	4957	42024	765	757	99
259	0	0	731	5209	35926	960	806	78
259.5	14	0	765	3830	27686	799	759	278
260	31	0	722	4584	30434	569	507	250
260.5	0	0	791	4901	32868	452	599	234

Depth (cm)	Cl	Co	Cu	Eu	Fe	Ga	Ge	Hf
261	0	0	774	5408	33256	742	766	393
261.5	17	0	803	4944	33852	843	775	328
262	0	0	705	5065	35312	376	560	182
262.5	18	0	776	7072	90971	642	355	173
263	0	0	783	7496	121178	540	592	383
263.5	0	0	830	6546	83777	893	829	238
264	8	0	949	6371	44803	616	576	469
264.5	0	0	951	5177	30250	779	504	341
265	0	0	1103	4968	30020	607	632	376
265.5	0	0	787	6601	72916	522	660	388
266	5	0	665	5377	42463	589	668	311
266.5	27	0	720	4845	27674	472	479	261
267	0	0	717	5144	33941	621	324	527
267.5	22	0	823	5575	46077	441	559	250
268	27	0	766	4733	42344	867	288	259
268.5	20	0	590	4966	35542	459	959	382
269	21	0	710	4784	45838	484	513	146
269.5	0	0	624	4795	48303	520	527	422
270	0	0	790	5394	51466	682	777	158
270.5	0	0	688	5804	47727	353	629	168
271	0	0	729	6192	56812	728	884	409
271.5	0	0	707	6647	52859	449	665	231
272	19	0	896	5980	56970	686	547	68
272.5	0	0	989	6740	79527	601	725	258
273	0	0	926	6131	61813	300	591	203
273.5	0	0	849	6660	65716	953	566	134
274	0	0	1025	6573	65135	898	945	369
274.5	0	0	956	5889	40788	234	417	280
275	0	0	922	5642	34491	576	543	364
275.5	27	0	1143	5722	37628	793	1006	391
276	48	0	872	5450	36674	852	856	442
276.5	0	0	811	5699	39296	740	1034	304
277	35	0	946	5344	38161	690	636	267
277.5	0	0	896	6242	46404	506	638	335
278	24	0	723	6119	47998	803	398	310
278.5	0	0	941	5643	46523	943	590	326
279	0	0	1008	5550	41138	385	437	343
279.5	16	0	1004	5791	34757	1033	899	522
280	0	0	949	5726	40685	483	628	390

Depth (cm)	Cl	Co	Cu	Eu	Fe	Ga	Ge	Hf
280.5	0	0	855	5595	42718	898	954	334
281	0	0	948	5779	37506	821	523	327
281.5	0	0	883	6819	40822	351	423	295
282	0	0	948	5745	46160	1050	594	491
282.5	0	0	654	6414	62710	518	495	365
283	0	0	960	6333	65785	760	600	434
283.5	0	0	994	6434	52831	905	735	439
284	6	0	1011	6058	47486	786	549	315
284.5	0	0	971	5994	52343	333	571	372
285	0	0	697	6154	66682	435	529	341
285.5	11	0	729	6434	93446	1010	983	507
286	0	151	697	6361	110754	380	298	329
286.5	0	0	595	2854	63684	684	171	79
287	8	0	495	1702	33943	635	361	93
287.5	0	0	549	2656	29247	453	488	129
288	0	0	551	5341	69134	235	453	243
288.5	0	15	794	6853	93674	1151	668	238
289	5	0	864	5891	56210	366	625	460
289.5	0	0	708	6512	61931	607	578	285
290	0	0	1024	6029	54512	430	626	271
290.5	0	0	1248	6181	39474	641	615	323
291	0	0	913	5470	32129	561	365	293
291.5	0	0	735	6916	50994	157	491	368
292	0	0	863	6815	50754	729	652	426
292.5	0	0	1134	6351	72976	727	834	430
293	0	0	708	7317	96578	720	558	162
293.5	0	0	610	7962	108311	824	438	374
294	0	0	781	7034	89732	714	557	448
294.5	0	0	825	5849	57961	641	647	345
295	28	0	1152	6899	61734	859	474	384
295.5	23	0	675	7327	88520	504	559	348
296	0	0	738	4028	70954	428	503	29
296.5	9	0	492	2533	31642	370	308	0
297	16	0	528	1938	22876	394	286	0
297.5	20	0	414	2425	18548	87	370	187
298	32	0	776	5194	30422	615	872	396
298.5	0	0	799	4679	31096	244	653	470
299	0	0	805	6933	94298	813	826	224
299.5	0	0	1062	6404	54671	415	505	321

Depth (cm)	Cl	Co	Cu	Eu	Fe	Ga	Ge	Hf
300	5	0	788	6867	82294	466	932	396
300.5	0	0	968	6595	92621	650	514	262
301	0	0	700	5900	59736	466	483	266
301.5	27	0	836	6734	83609	622	597	440
302	0	0	913	7007	107915	538	285	309
302.5	23	0	751	4593	40325	400	263	341
303	0	0	532	4611	67743	403	761	234
303.5	47	0	788	6299	93182	507	324	247
304	15	0	767	5509	56509	728	451	467
304.5	0	0	841	4914	41700	487	662	311
305	0	0	826	4866	32953	777	249	157
305.5	0	0	882	4557	37092	595	570	339
306	4	0	889	3800	27229	556	338	311
306.5	17	0	764	4461	35504	698	506	396
307	44	0	882	4394	34494	520	447	132
307.5	0	454	741	3399	82389	679	372	127
308	57	146	546	2749	43208	383	564	134
308.5	0	282	675	2684	56344	693	892	232
309	0	338	530	2940	72223	595	695	271
309.5	0	728	696	2786	102313	728	299	174
310	17	507	618	2901	92562	717	534	72
310.5	38	272	699	2992	67172	447	524	209
311	24	533	802	3046	82800	474	603	215
311.5	0	321	869	3283	78959	550	700	126
312	33	548	825	3470	82597	649	772	344
312.5	0	596	732	2895	76461	724	729	200
313	59	586	512	3096	98528	882	713	340
313.5	41	509	859	4352	122706	612	560	257
314	20	984	770	3110	126133	1046	376	392
314.5	47	582	690	3586	108941	741	256	267
315	51	532	721	3641	89246	537	615	179
315.5	0	628	814	3982	126385	577	973	377
316	0	872	617	3907	135200	696	602	150
316.5	6	923	601	2997	117179	641	510	226
317	0	698	819	4138	138289	553	384	0
317.5	0	551	769	3668	136309	814	516	173
318	9	814	517	3857	135598	615	528	231
318.5	0	600	778	3919	117777	707	952	237
319	0	1204	640	2972	145870	487	561	143

Depth (cm)	Cl	Co	Cu	Eu	Fe	Ga	Ge	Hf
319.5	9	1014	851	3754	175145	727	751	126
320	0	1125	479	4017	195217	479	549	64
320.5	39	1151	691	3713	169449	851	735	220
321	27	1029	505	4333	185228	222	687	50
321.5	17	1477	652	3412	200886	677	500	227
322	0	1547	517	4295	219200	891	686	332
322.5	0	1681	583	3062	195669	656	604	224
323	4	1235	555	3995	177188	340	478	171
323.5	0	1066	689	3995	179443	586	636	132
324	0	1334	479	2770	161474	570	329	113
324.5	0	1382	670	3151	170534	970	518	210
325	33	1279	688	3064	165851	829	487	293
325.5	0	481	747	2993	83590	438	459	186
326	18	430	933	3493	86003	730	671	251
326.5	67	462	728	3397	79692	300	474	302
327	27	210	893	2990	51499	662	542	175
327.5	0	269	814	2720	37963	555	359	261
328	19	90	777	2678	37059	455	485	266
328.5	47	695	665	3052	97680	345	644	225
329	9	658	552	3614	115856	293	702	97
329.5	6	1096	507	2881	134148	481	451	203
330	64	1179	637	2962	152170	750	403	175
330.5	8	776	769	2622	98046	738	576	247
331	0	455	788	2583	62388	865	603	235
331.5	0	491	521	2487	57715	908	758	375
332	29	826	1015	3232	98314	911	432	243
332.5	0	843	833	3684	105774	796	358	205
333	29	482	599	2633	50149	883	650	383
333.5	0	790	854	3123	109993	502	583	279
334	0	574	556	3305	88581	975	477	389
334.5	33	669	713	3313	109830	518	549	161
335	0	561	719	2744	71577	703	604	287
335.5	76	215	298	0	10017	267	176	60
336	95	158	219	0	1914	175	191	13
336.5	51	140	258	0	1805	24	82	26
337	34	122	433	1743	43077	393	175	103
337.5	0	808	787	2734	108022	709	500	243
338	0	912	792	2697	103673	907	404	254
338.5	17	703	576	2862	107101	599	464	156

Depth (cm)	Cl	Co	Cu	Eu	Fe	Ga	Ge	Hf
339	13	805	760	3411	125144	762	314	267
339.5	58	1275	470	2956	168788	459	375	261
340	52	1697	468	3066	194745	345	306	114
340.5	75	1357	581	2797	147006	670	553	258
341	41	628	692	3087	99922	599	455	179
341.5	17	663	721	2972	97237	359	704	136
342	0	936	618	3096	114895	522	553	251
342.5	26	728	660	2579	105042	660	421	191
343	33	981	536	3148	153885	680	453	163
343.5	58	1015	702	3058	118510	913	326	253
344	42	1095	468	3384	156546	892	289	120
344.5	40	775	773	2891	105649	860	685	198
345	85	931	596	2976	120880	438	279	103
345.5	27	837	776	2526	94387	682	602	167
346	47	475	765	2503	64512	718	577	308
346.5	49	449	767	2032	54939	625	292	135
347	47	455	591	2446	72508	287	0	166
347.5	38	802	549	3138	114053	526	408	138
348	41	715	693	2195	83269	667	502	282
348.5	24	428	785	1788	39498	668	486	243
349	32	326	1048	1874	46129	590	607	187
349.5	47	525	651	2037	66535	269	424	182
350	45	1416	610	2235	180115	695	700	220
350.5	85	1120	642	2437	138011	502	480	412
351	79	897	705	1856	93180	655	389	236
351.5	0	822	846	1982	101314	927	704	155
352	63	756	686	2643	106178	649	412	324
352.5	52	760	556	2984	108913	556	252	306
353	9	412	704	553	38041	178	273	164
353.5	48	365	398	502	44166	440	183	175
354	42	534	329	369	50283	494	313	128
354.5	0	309	372	1696	48484	289	181	129
355	15	524	661	2279	86025	502	410	169
355.5	0	443	794	2806	90661	453	509	114
356	62	658	535	2159	70079	458	544	331
356.5	37	1242	713	2722	153433	706	413	173
357	35	877	735	1576	92718	560	319	157
357.5	15	576	460	1945	96941	508	344	293
358	72	631	537	2331	90986	505	316	98

Depth (cm)	Cl	Co	Cu	Eu	Fe	Ga	Ge	Hf
358.5	80	776	705	1214	77850	374	134	110
359	52	454	705	821	55784	560	360	134
359.5	63	883	699	850	83474	594	261	178
360	66	934	570	548	89588	586	380	192
360.5	51	360	737	466	24933	608	564	202
361	58	772	436	1073	69922	289	387	176
361.5	113	1063	711	869	110156	390	411	283
362	51	703	508	1633	83661	593	418	124
362.5	34	1147	514	1837	119902	619	472	215
363	35	735	543	1785	79292	497	519	197
363.5	70	462	662	1658	48907	491	161	258
364	0	390	550	1319	35172	786	655	281
364.5	49	366	769	1680	32195	870	600	117
365	55	530	488	1796	64830	640	405	362
365.5	126	620	510	1983	84797	495	506	242
366	40	661	668	1958	84442	643	378	151
366.5	96	779	731	1864	75319	595	267	186
367	51	709	505	993	55395	476	293	217
367.5	4	366	656	1115	43591	569	340	187
368	55	362	695	1571	30567	289	555	288
368.5	51	606	664	5119	181121	558	461	95
369	0	246	644	3900	128192	627	368	291
369.5	0	307	820	3940	113934	607	218	288
370	71	521	718	5136	201789	286	122	70
370.5	52	198	785	4754	113143	498	821	354
371	0	366	915	3977	133752	450	280	248
371.5	81	246	1056	3620	92894	661	613	305
372	36	92	613	4997	174012	531	411	200
372.5	0	679	844	3998	161738	1101	520	168
373	29	218	753	3937	102590	301	893	224
373.5	10	227	1009	3799	87925	380	440	224
374	49	507	878	3722	128346	401	609	265
374.5	50	123	839	4422	106758	553	511	281
375	68	627	598	3533	168057	491	544	184
375.5	69	569	793	4153	141937	467	280	110
376	0	404	816	3948	126943	329	651	197
376.5	24	283	810	3750	112853	652	332	153
377	43	118	874	3476	68326	396	773	122
377.5	43	211	690	2730	60372	658	286	367

Depth (cm)	Cl	Co	Cu	Eu	Fe	Ga	Ge	Hf
378	22	40	812	3258	46942	874	503	276
378.5	0	0	814	3470	61371	440	770	294
379	0	0	654	3640	48878	725	657	317
379.5	44	0	955	3247	43647	464	491	429
380	49	0	712	2978	39886	259	412	215
380.5	24	0	708	3362	42237	299	659	336
381	82	0	795	3255	38128	637	646	265
381.5	35	0	809	2551	31408	567	379	205
382	43	0	764	2969	46784	512	446	186
382.5	0	0	987	3845	66278	833	826	138
383	18	0	939	3666	52304	483	656	264
383.5	80	0	845	3034	51986	482	402	283
384	0	6	756	3306	46974	521	477	313
384.5	41	36	1074	3137	49590	720	491	238
385	0	41	961	3038	51639	653	315	347
385.5	0	0	784	3658	56038	517	390	221
386	45	0	1042	3906	73900	633	726	322
386.5	74	175	956	3286	75900	1054	175	245
387	38	24	925	2632	50562	576	472	345
387.5	75	51	804	3808	51593	456	591	185
388	0	164	967	3232	51845	521	197	180
388.5	54	0	853	3906	52265	368	617	261
389	6	0	1022	3752	51582	901	497	125
389.5	48	0	798	3122	52873	397	218	400
390	62	0	858	3207	45760	563	381	175
390.5	0	34	1096	2860	47241	876	375	327
391	21	52	949	2996	49103	625	436	140
391.5	67	0	940	3391	48766	575	621	354
392	19	0	1073	3182	51485	727	499	242
392.5	9	0	949	3405	48383	352	602	265
393	14	0	790	3484	47544	703	294	102
393.5	46	44	764	2654	49292	344	447	189
394	0	0	795	2465	42710	352	483	251
394.5	58	58	1074	2374	43029	653	700	256
395	21	0	929	2557	43329	401	613	146
395.5	25	0	704	2678	45475	796	435	238
396	29	0	745	2686	46218	309	408	280
396.5	30	0	835	2743	44966	499	364	272
397	0	0	947	2728	47258	477	257	103

Depth (cm)	Cl	Co	Cu	Eu	Fe	Ga	Ge	Hf
397.5	39	165	600	2667	51303	736	575	280
398	29	52	923	3051	52986	578	577	298
398.5	25	120	680	2876	63868	490	630	277
399	18	45	941	2775	67627	717	217	227
399.5	26	23	774	2752	51733	247	716	155
400	19	181	741	2788	55747	545	417	194
400.5	58	57	610	3147	57491	273	82	184
401	10	61	784	3278	75010	1004	549	311
401.5	62	40	898	3021	77624	562	653	284
402	22	0	1025	3182	57405	497	482	289
402.5	0	0	929	3261	51764	495	404	77
403	76	183	943	2333	49648	496	498	243
403.5	41	90	762	2964	50370	522	496	363
404	24	290	911	2934	63978	573	617	248
404.5	11	12	874	3162	69373	555	178	14
405	61	293	900	2840	88423	644	539	197
405.5	77	65	406	3073	56931	752	436	237
406	37	160	999	2489	48597	737	701	58
406.5	63	0	1164	3480	60662	840	495	221
407	28	163	741	3351	60524	466	475	319
407.5	0	135	755	3203	59275	757	492	136
408	14	33	1039	3430	54492	922	438	294
408.5	15	0	792	3130	55145	540	560	141
409	7	73	916	2847	55235	471	269	181
409.5	42	0	940	3519	56937	513	408	309
410	67	34	785	3034	56691	611	725	406
410.5	0	0	796	3357	55491	461	572	180
411	16	82	791	3379	60014	460	405	289
411.5	53	148	952	3066	59495	462	325	286
412	0	209	905	2665	57698	711	466	234
412.5	46	58	915	3187	59364	539	586	198
413	60	244	599	3000	63108	609	449	206
413.5	48	171	798	3042	60531	404	439	50
414	46	38	701	2473	60771	623	387	193
414.5	0	118	713	1890	51638	606	366	319
415	32	223	691	1598	45803	488	591	158
415.5	32	40	722	2432	45961	400	443	43
416	51	82	725	3615	59060	815	671	277
416.5	66	32	830	3414	59444	868	464	187

Depth (cm)	Cl	Co	Cu	Eu	Fe	Ga	Ge	Hf
417	40	75	947	2445	57628	499	793	321
417.5	0	25	744	3266	63119	505	538	53
418	38	155	979	2590	63832	624	566	237
418.5	0	75	842	3249	58160	517	454	262
419	20	54	859	3128	58484	625	654	242
419.5	39	18	853	3151	59183	586	564	312
420	74	83	881	3230	62185	690	699	319
420.5	47	15	1114	2855	60380	861	287	185
421	35	0	875	3593	61248	548	668	112
421.5	8	0	826	2991	63707	400	563	280
422	42	0	871	3608	58636	704	723	205
422.5	50	0	1005	3864	62110	678	389	331
423	80	231	807	2778	58859	775	602	358
423.5	72	117	761	2918	60370	490	840	273
424	34	286	905	2945	63284	986	736	245
424.5	82	278	779	2448	61919	468	608	223
425	52	98	637	2763	61921	656	604	345
425.5	30	124	886	2858	59599	534	715	325
426	41	188	965	2865	56240	711	760	316
426.5	34	0	811	2881	55820	687	359	200
427	60	53	958	2868	58555	851	523	206
427.5	14	111	797	2775	61344	914	932	293
428	63	162	1095	2697	62327	625	460	125
428.5	31	96	848	3177	61934	862	446	199
429	59	218	681	1867	50011	806	752	222
429.5	35	378	758	1724	50808	557	352	167
430	38	189	435	1822	55004	469	412	224
430.5	22	170	517	1745	60812	438	429	151
431	8	0	568	1299	45807	417	278	0

Table A 2.3 Cuobu XRF Geochemistry Hg – Mo

Depth (cm)	Hg	I	Ir	K	La	Mg	Mn	Mo
27	120	45	484	141	830	45	1496	
27.5	224	20	222	2208	940	42	328	
28	243	86	153	4936	2015	42	0	
28.5	471	32	358	5707	2031	0	0	
29	396	80	532	5653	1906	86	0	
29.5	534	86	534	5090	1838	83	0	
30	613	154	288	5745	2017	80	0	
30.5	37	38	277	5095	1889	26	0	
31	683	115	566	5282	1960	49	0	
31.5	697	50	484	5009	1786	44	0	
32	329	132	566	5184	1897	89	0	
32.5	500	97	855	5198	2061	0	0	
33	115	6	322	4892	1892	66	0	
33.5	266	52	360	4864	1793	0	0	
34	690	88	291	5010	1861	35	0	
34.5	455	17	130	4503	1915	170	0	
35	567	54	230	5795	1955	47	0	
35.5	359	25	525	5300	1944	91	0	
36	501	0	228	5824	1796	72	0	
36.5	534	49	319	6360	1770	0	0	
37	564	51	508	8368	1941	69	0	
37.5	555	15	133	6330	1843	19	0	
38	297	65	0	6643	1840	91	0	
38.5	345	72	204	7564	1984	24	0	
39	377	10	529	8331	1863	69	0	
39.5	531	42	594	7677	2040	0	0	
40	440	69	393	7128	1937	60	0	
40.5	502	19	402	7897	1987	0	0	
41	177	50	547	8442	1927	94	0	
41.5	517	22	70	7386	2018	16	0	
42	575	0	343	7893	1967	99	0	
42.5	402	13	291	7579	1960	23	0	
43	266	77	195	7308	1903	61	0	
43.5	439	0	0	8158	1854	112	0	
44	749	82	448	8629	1762	82	0	
44.5	343	0	123	7813	1919	12	0	
45	540	0	538	7155	1655	25	0	
45.5	402	22	566	6973	1666	0	0	

Depth (cm)	Hg	I	Ir	K	La	Mg	Mn	Mo
46	584	86	318	8623	1741	121	0	
46.5	154	44	151	7991	1659	5	0	
47	637	70	543	8083	1505	22	0	
47.5	544	0	116	7952	1753	50	0	
48	628	0	219	6972	1663	43	0	
48.5	285	0	256	7822	1758	41	0	
49	486	0	510	8218	1909	0	0	
49.5	561	48	213	7786	1861	0	0	
50	128	75	260	8652	1861	54	0	
50.5	392	0	177	10499	1886	115	0	
51	493	79	748	9486	1895	51	0	
51.5	693	0	393	8723	1633	41	0	
52	216	35	156	7998	1677	72	0	
52.5	431	59	240	8513	1697	44	0	
53	615	20	33	7893	1908	62	0	
53.5	445	0	529	9218	1756	69	0	
54	279	19	218	6536	1772	81	0	
54.5	664	36	419	7223	1675	62	0	
55	607	60	353	10235	1838	72	0	
55.5	740	93	583	10031	1786	114	0	
56	258	79	114	8905	1848	19	0	
56.5	654	9	0	9251	1817	9	0	
57	310	12	351	9650	1865	98	0	
57.5	448	25	514	8683	1724	60	0	
58	354	0	0	8039	1713	46	787	
58.5	475	74	463	8625	1795	17	0	
59	358	19	590	9968	1629	0	0	
59.5	798	73	400	9385	1729	79	0	
60	784	49	697	10464	1803	13	0	
60.5	576	0	331	9150	1835	125	0	
61	582	0	226	7541	1728	54	0	
61.5	478	43	280	8460	1761	96	0	
62	385	0	455	9820	1864	36	0	
62.5	548	0	198	8733	1726	43	0	
63	726	41	82	8276	1755	38	0	
63.5	352	130	392	9628	1960	107	0	
64	194	73	618	8540	1874	28	0	
64.5	576	0	371	9484	1765	8	0	
65	321	0	267	9977	1820	27	0	

Depth (cm)	Hg	I	Ir	K	La	Mg	Mn	Mo
65.5	222	0	67	10890	1870	95	0	
66	458	0	520	10209	1775	0	0	
66.5	251	16	547	10375	1660	136	0	
67	228	18	404	10808	1749	17	0	
67.5	474	0	112	11862	1739	0	0	
68	688	36	106	11544	1887	14	0	
68.5	422	14	396	10431	1843	10	0	
69	237	43	151	11309	1835	19	0	
69.5	410	0	182	10181	1743	20	53	
70	650	0	420	9769	1886	46	0	
70.5	659	0	0	8899	1819	70	0	
71	584	0	394	10031	1598	96	0	
71.5	385	104	23	10978	1839	67	0	
72	192	36	551	13430	1931	8	0	
72.5	575	0	361	12707	1891	56	0	
73	728	6	338	11444	1782	43	0	
73.5	248	0	464	14569	1904	86	0	
74	554	0	439	11316	1586	0	0	
74.5	97	12	36	4226	835	0	0	
75	347	9	212	5227	912	0	892	
75.5	136	0	179	6749	1164	16	0	
76	430	0	469	9392	1571	84	0	
76.5	405	33	188	9687	1625	43	0	
77	445	22	0	10239	1745	69	0	
77.5	514	90	647	10446	1824	52	111	
78	181	61	300	10861	1721	0	0	
78.5	782	0	381	10951	1655	35	0	
79	167	0	537	13252	1962	42	0	
79.5	585	22	252	11968	1775	39	0	
80	398	24	334	12572	1888	27	0	
80.5	410	0	234	11061	1840	73	0	
81	943	52	558	10097	1831	77	0	
81.5	375	40	522	10319	1772	0	0	
82	440	55	449	10744	1771	69	0	
82.5	495	0	508	10421	1987	0	0	
83	118	0	408	12391	1718	0	0	
83.5	312	40	109	4479	830	27	0	
84	215	49	437	4233	830	0	0	
84.5	195	28	216	5429	957	54	0	

Depth (cm)	Hg	I	Ir	K	La	Mg	Mn	Mo
85	159	0	289	5249	848	21	0	
85.5	405	40	289	5422	826	64	0	
86	274	31	432	5848	947	12	0	
86.5	6	63	238	5593	940	38	0	
87	173	30	390	6202	1007	54	0	
87.5	52	44	502	6789	1036	0	0	
88	177	47	421	7157	1011	0	0	
88.5	172	0	39	6121	1003	23	0	
89	302	21	452	6087	985	99	0	
89.5	244	0	324	5083	848	0	0	
90	209	0	198	4580	863	20	0	
90.5	9	0	17	4848	730	27	0	
91	215	65	52	4928	931	25	0	
91.5	280	64	311	5502	942	20	0	
92	209	6	334	7055	1150	53	709	
92.5	234	61	589	8496	1350	34	0	
93	196	20	192	6820	1088	34	0	
93.5	252	7	269	6872	1139	22	0	
94	154	34	186	6433	1119	6	0	
94.5	377	49	380	7174	1179	14	0	
95	124	0	226	6531	1312	0	0	
95.5	224	88	359	6660	1215	38	0	
96	265	0	234	5691	1118	10	0	
96.5	300	39	317	4844	1048	0	0	
97	107	48	175	8235	1204	12	0	
97.5	442	7	514	7570	1351	33	0	
98	320	75	226	6629	1248	33	0	
98.5	593	0	227	7830	1188	12	0	
99	260	82	297	7483	1312	51	0	
99.5	169	29	197	6151	1134	0	0	
100	224	74	295	7523	1149	0	0	
100.5	590	58	142	6964	989	9	0	
101	389	36	294	6066	1091	52	0	
101.5	505	28	8	7208	1282	22	0	
102	642	61	477	6549	1189	61	0	
102.5	260	52	8	5912	1257	0	0	
103	753	11	363	4893	1231	46	0	
103.5	493	0	497	5673	1307	21	0	
104	589	74	490	5313	1308	24	0	

Depth (cm)	Hg	I	Ir	K	La	Mg	Mn	Mo
104.5	616	0	240	6283	1148	62	0	
105	539	26	78	6230	1163	9	0	
105.5	720	44	407	5473	1112	89	0	
106	775	111	280	6563	1177	30	0	
106.5	608	57	719	6983	1322	65	0	
107	746	0	732	6043	1400	61	0	
107.5	813	82	334	5614	1254	69	0	
108	601	22	159	6361	1285	37	0	
108.5	763	78	52	6347	1233	36	0	
109	451	68	237	6696	1435	6	0	
109.5	527	35	317	8324	1264	46	0	
110	626	87	262	6797	1422	42	0	
110.5	751	0	262	6697	1317	90	0	
111	610	67	222	6021	1108	0	0	
111.5	639	124	338	6728	1085	28	0	
112	574	29	311	8056	1089	44	0	
112.5	615	62	0	8702	1152	85	0	
113	384	31	243	8001	1054	0	0	
113.5	138	71	85	7371	1190	73	0	
114	496	0	208	7593	1414	0	0	
114.5	618	53	341	7457	1248	5	0	
115	718	96	64	7897	1213	0	0	
115.5	1049	0	237	6778	1161	50	0	
116	397	10	341	6004	1332	36	0	
116.5	849	51	116	7196	1343	55	0	
117	915	36	614	7008	1178	5	0	
117.5	738	86	95	6658	1263	22	0	
118	454	0	385	6347	804	5	0	
118.5	427	48	394	6034	990	19	0	
119	521	0	124	7091	1072	29	0	
119.5	511	0	221	7668	1232	0	0	
120	625	0	257	9059	1358	0	0	
120.5	500	33	216	9089	1106	27	0	
121	619	103	281	9951	1244	29	0	
121.5	388	27	107	9468	1178	5	0	
122	451	30	235	9595	1372	28	0	
122.5	357	94	237	10198	1321	0	0	
123	587	45	21	8336	1341	27	0	
123.5	266	94	370	9115	1405	23	0	

Depth (cm)	Hg	I	Ir	K	La	Mg	Mn	Mo
124	680	49	503	7875	1257	37	0	
124.5	524	25	287	8296	1353	24	0	
125	649	54	84	8539	1375	57	0	
125.5	630	115	146	8982	1311	33	0	
126	502	80	543	8390	1367	77	0	
126.5	535	33	139	8242	1415	0	0	
127	371	51	129	6917	1213	27	0	
127.5	567	125	529	7941	1380	0	0	
128	301	124	271	6994	1358	45	0	
128.5	568	53	430	7315	1257	0	0	
129	762	0	497	7482	1292	0	0	
129.5	637	89	630	7189	1324	72	0	
130	598	106	141	7172	1234	49	0	
130.5	567	125	264	6620	1110	85	0	
131	619	0	376	7483	1220	40	0	
131.5	356	51	63	8022	1347	65	0	
132	656	82	429	8856	1329	88	0	
132.5	480	92	231	7999	1311	22	0	
133	662	48	479	8242	1285	24	0	
133.5	255	83	198	8462	1394	0	0	
134	620	40	168	8216	1394	0	0	
134.5	687	56	67	8671	1316	57	0	
135	424	77	81	9275	1368	10	0	
135.5	454	74	375	9587	1432	14	0	
136	365	112	147	7730	1429	42	0	
136.5	702	71	6	7962	1399	18	0	
137	544	24	120	8462	1371	51	0	
137.5	590	93	280	8533	1381	0	0	
138	0	61	435	4066	648	0	721	
138.5	114	0	208	3070	516	0	370	
139	8	0	74	1838	484	0	269	
139.5	265	0	94	6092	1263	10	0	
140	675	101	514	8001	1425	41	0	
140.5	665	30	417	9267	1241	71	0	
141	836	113	410	8617	1346	69	0	
141.5	553	81	485	8639	1324	30	0	
142	492	0	316	8049	1377	32	0	
142.5	510	62	98	7709	1463	0	0	
143	369	46	34	9198	1342	22	0	

Depth (cm)	Hg	I	Ir	K	La	Mg	Mn	Mo
143.5	674	21	184	7656	1423	0	0	
144	563	94	248	7689	1286	51	0	
144.5	244	110	266	7235	1362	54	0	
145	712	136	108	8149	1360	59	0	
145.5	581	31	199	7382	1311	21	0	
146	510	30	288	7917	1378	60	0	
146.5	573	82	512	7603	1321	39	0	
147	410	72	169	7039	1424	98	0	
147.5	606	66	362	7038	1381	15	0	
148	792	45	271	6806	1350	67	0	
148.5	594	101	276	6494	1411	12	0	
149	578	76	155	7357	1361	9	0	
149.5	411	57	423	6467	1350	0	0	
150	0	121	54	5565	1025	0	0	
150.5	480	0	481	3832	769	0	407	
151	55	38	138	3959	814	23	0	
151.5	273	71	239	3256	750	0	0	
152	628	15	158	6523	1242	36	0	
152.5	809	35	352	6833	1391	16	0	
153	548	81	488	6489	1488	0	0	
153.5	737	54	2686	8272	258	33	5521	444
154	682	142	2643	7807	631	0	5022	793
154.5	555	0	2714	6705	372	20	5578	470
155	477	151	2692	6961	185	0	5742	425
155.5	830	45	2736	6087	107	54	4425	459
156	647	66	2809	6998	339	57	4754	483
156.5	464	124	2771	6835	257	34	5786	355
157	690	74	2381	5953	106	0	3928	948
157.5	680	115	2341	6227	302	0	3369	751
158	1176	236	2353	5814	347	0	3008	555
158.5	710	118	2738	4827	243	0	3900	744
159	740	82	2767	4787	242	0	5239	867
159.5	745	162	2551	4980	287	77	5637	715
160	625	24	2754	4889	318	0	3323	504
160.5	893	98	2627	4544	216	12	3472	625
161	793	7	2780	5492	264	0	5033	543
161.5	905	144	2679	5946	291	0	5074	649
162	807	117	2811	6040	374	48	6523	453
162.5	705	169	2876	5310	214	77	3442	438

Depth (cm)	Hg	I	Ir	K	La	Mg	Mn	Mo
163	931	159	2788	5602	188	0	5445	400
163.5	521	175	2698	5327	446	0	3776	1059
164	671	81	3018	5311	0	30	4376	1130
164.5	740	92	2605	5836	141	0	4647	269
165	791	141	2666	5763	270	0	5471	506
165.5	733	181	2867	5595	114	39	6682	731
166	695	60	2741	5641	289	15	4550	519
166.5	647	126	2850	4496	137	11	5450	814
167	582	0	2825	5303	217	82	6209	649
167.5	564	174	2834	5739	410	35	5653	332
168	574	22	1748	3241	90	0	4100	279
168.5	544	55	1476	1715	42	0	3772	38
169	599	0	1614	1609	167	27	3264	507
169.5	594	69	1852	2511	175	0	3772	345
170	734	182	2745	4877	448	51	5559	209
170.5	670	70	2862	5750	339	0	5052	716
171	647	109	2912	4997	492	0	4474	735
171.5	1053	172	2559	4351	182	0	5594	907
172	748	55	2574	4490	101	0	4308	470
172.5	642	104	2714	4830	0	16	3578	708
173	826	180	2499	5461	283	33	3617	1428
173.5	678	109	2622	4842	391	67	4152	388
174	532	0	2536	5758	285	0	4630	961
174.5	710	156	2572	4902	476	52	4049	738
175	669	46	2789	5482	240	40	3923	294
175.5	560	73	2990	6084	362	47	4680	539
176	971	21	2805	5908	216	41	6052	496
176.5	918	0	2682	6068	414	63	4680	946
177	695	102	2627	5352	558	15	5123	814
177.5	681	102	2710	5574	614	41	5508	666
178	657	0	2591	6043	609	37	4590	445
178.5	651	132	2796	5084	301	0	5095	548
179	772	65	2832	5410	575	0	5305	669
179.5	423	169	2686	4723	270	100	5506	602
180	852	168	2681	5495	69	21	4324	209
180.5	625	38	2862	5373	229	0	4804	100
181	770	86	2784	5662	389	77	6005	406
181.5	716	213	3113	5250	318	20	6202	316
182	583	151	3019	5126	374	40	4920	350

Depth (cm)	Hg	I	Ir	K	La	Mg	Mn	Mo
182.5	883	214	2848	5816	325	32	6194	684
183	932	176	2658	5663	320	0	5619	797
183.5	650	130	2818	5245	156	0	5018	492
184	777	0	2865	5063	6	0	4720	354
184.5	586	60	2634	5330	104	0	5058	881
185	1017	32	2772	5704	92	82	5820	725
185.5	758	188	2614	5262	251	0	4581	674
186	834	72	2869	5233	243	12	5912	593
186.5	738	154	2360	5471	376	0	4504	760
187	789	40	2593	5491	387	12	4418	663
187.5	507	140	2628	5337	214	53	4503	662
188	851	113	2627	5152	298	48	5539	541
188.5	837	0	2629	4854	265	18	4901	410
189	696	94	2773	4799	278	62	3877	568
189.5	733	79	2558	4702	242	50	5958	1003
190	994	34	2727	5969	247	27	4958	653
190.5	804	153	2687	4775	362	0	6023	241
191	668	168	2612	6193	351	71	7281	284
191.5	816	171	2757	7931	135	86	5051	487
192	824	89	2770	8150	105	15	5515	741
192.5	806	161	2876	8054	348	63	7025	632
193	838	132	2637	6331	269	59	4506	419
193.5	915	0	2775	5866	411	5	3721	567
194	543	73	2486	4936	308	78	5675	834
194.5	1083	149	2585	6248	0	31	2336	570
195	654	44	2817	6762	236	22	4442	368
195.5	911	78	2717	8053	92	0	5406	631
196	543	39	3008	8441	0	12	6907	594
196.5	598	147	2832	8787	160	91	5550	594
197	759	188	2863	9378	354	17	6809	565
197.5	751	136	3015	9449	408	28	5290	587
198	677	73	2955	9589	425	52	6334	634
198.5	417	165	2973	9724	232	23	5794	888
199	724	0	2991	8665	366	70	7081	881
199.5	623	0	2773	9353	464	52	5184	602
200	692	15	2775	8920	423	0	5637	605
200.5	549	5	2875	9214	209	0	6843	438
201	690	0	2820	7774	398	39	6821	1141
201.5	728	23	2650	6536	73	5	6618	910

Depth (cm)	Hg	I	Ir	K	La	Mg	Mn	Mo
202	779	158	2909	7614	302	0	4463	820
202.5	369	86	2278	5620	300	0	4819	675
203	478	0	1459	2459	153	0	3697	652
203.5	346	27	1395	1927	328	52	3108	589
204	296	24	1265	2756	80	22	2880	469
204.5	575	0	2541	5290	434	28	5112	858
205	599	100	2899	8168	170	29	5732	743
205.5	601	176	2840	7896	291	0	4984	788
206	766	136	2845	7461	612	15	5794	899
206.5	798	105	2780	6270	490	44	6817	984
207	736	228	2960	7998	395	75	6633	512
207.5	686	99	2833	7783	448	0	5930	406
208	622	27	2763	6469	49	0	6015	978
208.5	677	34	2821	6457	369	9	5527	599
209	768	64	2872	8267	283	30	5322	1058
209.5	741	0	2741	7784	387	81	5099	437
210	469	0	3042	8563	339	38	5966	1090
210.5	542	57	2802	7790	430	57	5357	312
211	763	33	2583	6863	112	50	5454	860
211.5	651	229	2820	8136	484	42	5831	222
212	508	0	3040	7855	171	50	6896	741
212.5	762	129	2803	7496	307	40	5530	643
213	824	198	2675	8724	363	6	5618	493
213.5	799	166	2440	6055	515	48	5299	722
214	593	122	2504	5250	456	14	4545	603
214.5	731	102	2489	5219	133	5	5723	586
215	777	42	2756	8102	247	0	4326	936
215.5	771	131	2695	8482	542	23	5954	850
216	674	0	2459	8702	610	10	6642	477
216.5	537	155	2786	9150	484	35	4262	343
217	741	57	2611	9419	672	0	4746	622
217.5	561	163	2626	8217	932	46	5918	348
218	419	72	2873	7022	551	28	4976	785
218.5	700	97	2756	5609	269	41	5695	887
219	545	298	2684	7597	274	0	5958	364
219.5	701	24	2643	7380	321	0	5701	888
220	848	197	2563	6583	424	0	5721	423
220.5	650	177	2795	6866	392	24	5351	725
221	708	215	2642	6469	676	48	5657	835

Depth (cm)	Hg	I	Ir	K	La	Mg	Mn	Mo
221.5	790	125	2639	7299	411	9	3939	455
222	528	0	2842	7278	576	58	5392	650
222.5	858	142	2621	8034	790	75	3682	545
223	755	48	2656	8358	969	58	5607	722
223.5	731	0	2598	7176	870	5	6457	267
224	606	0	1891	4369	640	0	2966	475
224.5	697	193	2681	3660	513	84	5991	662
225	658	202	2875	5193	627	32	5588	696
225.5	483	50	2772	4511	198	43	6244	896
226	547	69	2656	4745	299	38	5646	633
226.5	757	59	2740	3794	295	19	4866	829
227	803	104	2837	3526	317	33	5200	614
227.5	577	73	2917	4162	704	16	5412	605
228	700	103	2612	4314	485	96	6570	532
228.5	500	64	2744	3901	251	32	6272	519
229	725	118	2667	4011	450	0	5511	455
229.5	613	132	2513	3879	218	55	6684	715
230	719	184	2873	4010	510	65	6563	664
230.5	907	57	2632	3339	498	67	6701	636
231	820	197	2795	3914	862	58	6639	656
231.5	577	82	491	1915	633	5	0	
232	177	75	261	2376	775	8	0	
232.5	656	68	423	2389	759	29	0	
233	364	108	376	2287	777	15	0	
233.5	171	66	350	2343	568	64	0	
234	580	131	268	2619	829	58	0	
234.5	456	102	288	2628	806	86	0	
235	451	84	0	2212	687	56	0	
235.5	415	106	129	2637	716	66	0	
236	582	127	284	2587	692	51	0	
236.5	644	135	373	3265	711	96	0	
237	528	103	394	3435	793	0	0	
237.5	422	98	370	3653	832	22	0	
238	423	100	232	3647	775	12	0	
238.5	575	81	447	3345	605	25	0	
239	502	71	237	2711	622	39	0	
239.5	449	127	243	2861	697	18	0	
240	352	86	418	2420	696	66	0	
240.5	460	89	42	1922	795	47	0	

Depth (cm)	Hg	I	Ir	K	La	Mg	Mn	Mo
241	407	26	177	1723	628	50	0	
241.5	527	108	169	2473	631	85	0	
242	393	59	367	2594	678	19	0	
242.5	638	77	85	2554	699	63	0	
243	458	4	304	2048	623	43	0	
243.5	645	59	441	2012	517	74	295	
244	533	117	418	1514	378	75	0	
244.5	142	45	156	1498	384	39	0	
245	343	16	271	1246	448	0	0	
245.5	530	51	526	1887	615	33	0	
246	402	107	387	1840	648	0	0	
246.5	385	82	572	2041	699	38	0	
247	408	100	312	1865	768	33	0	
247.5	396	108	371	2276	718	26	0	
248	1018	114	589	1812	589	43	0	
248.5	273	88	86	1963	581	80	0	
249	509	84	161	1937	726	13	0	
249.5	501	124	480	2033	749	43	0	
250	492	132	135	1979	568	11	0	
250.5	461	63	274	1814	665	87	0	
251	463	83	91	1892	626	86	0	
251.5	671	56	504	1629	583	87	0	
252	819	162	41	1796	563	61	598	
252.5	299	76	351	1730	644	51	0	
253	701	119	242	2166	642	0	0	
253.5	490	154	269	2045	563	73	0	
254	593	133	403	1922	570	37	0	
254.5	575	147	293	1737	706	42	0	
255	426	66	240	2073	785	80	0	
255.5	381	105	460	2553	632	16	0	
256	585	83	106	2574	632	0	0	
256.5	570	166	597	2441	551	48	0	
257	614	78	313	2714	743	0	0	
257.5	353	80	575	2521	695	49	0	
258	425	44	24	2370	548	104	0	
258.5	547	0	266	2254	711	102	0	
259	428	124	82	2032	708	73	0	
259.5	744	125	341	3058	704	14	0	
260	747	112	433	2810	752	55	0	

Depth (cm)	Hg	I	Ir	K	La	Mg	Mn	Mo
260.5	577	120	447	3293	743	35	0	
261	698	108	295	3777	882	65	0	
261.5	464	126	391	5188	913	19	0	
262	381	22	432	4667	841	34	7	
262.5	547	89	299	4188	1059	28	0	
263	620	35	513	4777	1080	97	0	
263.5	305	117	312	5804	1042	0	117	
264	810	126	462	4615	946	37	0	
264.5	676	120	240	4402	1162	27	0	
265	488	0	460	4611	890	41	0	
265.5	640	128	504	4054	921	61	0	
266	400	153	316	3970	942	67	0	
266.5	671	81	506	3970	993	24	0	
267	846	61	453	3868	1007	31	0	
267.5	380	105	383	3585	845	7	0	
268	632	34	53	2672	782	65	0	
268.5	348	111	511	3249	917	13	0	
269	655	45	442	3729	897	30	0	
269.5	697	66	276	4982	909	24	0	
270	242	138	399	3027	984	57	0	
270.5	455	58	759	4221	1002	58	0	
271	506	82	263	3738	937	0	0	
271.5	686	139	663	3641	1015	56	0	
272	416	174	304	4120	963	28	0	
272.5	815	108	402	4418	1159	0	0	
273	461	64	732	4665	908	35	0	
273.5	735	105	156	5198	990	70	0	
274	667	82	286	5380	1121	18	0	
274.5	448	74	510	3048	1057	26	0	
275	705	99	596	4197	1049	94	0	
275.5	264	51	425	4896	1160	21	0	
276	350	129	322	4498	1373	87	0	
276.5	253	53	344	4470	1147	43	0	
277	318	88	376	4635	1087	50	0	
277.5	665	106	417	4845	1077	79	0	
278	687	54	364	4283	1156	49	0	
278.5	392	87	199	3900	1093	0	0	
279	584	125	536	4292	1035	10	0	
279.5	142	106	208	4958	1003	43	0	

Depth (cm)	Hg	I	Ir	K	La	Mg	Mn	Mo
280	702	160	445	5061	1131	10	0	
280.5	148	142	252	5154	1033	73	0	
281	507	108	292	4133	1093	74	0	
281.5	609	119	420	6089	1237	11	0	
282	416	0	47	5990	1056	9	0	
282.5	577	34	429	6787	1109	23	0	
283	315	72	410	6255	1297	41	0	
283.5	476	88	338	5962	1159	21	0	
284	392	56	306	6344	1147	54	0	
284.5	607	112	587	6544	1021	0	0	
285	486	153	492	6340	1126	23	0	
285.5	482	159	352	4958	1251	22	0	
286	857	132	623	5804	1132	14	0	
286.5	106	0	124	3069	691	24	153	
287	289	7	0	2016	460	0	487	
287.5	320	0	186	2223	401	45	0	
288	349	49	464	2773	770	37	0	
288.5	43	57	86	5837	1166	10	0	
289	495	152	737	5875	1142	47	0	
289.5	451	43	453	5004	1086	26	0	
290	251	54	481	4673	1015	0	0	
290.5	476	147	457	4654	1042	0	0	
291	356	118	454	5298	1021	0	0	
291.5	248	141	455	4916	1253	68	0	
292	257	152	307	4641	1138	14	0	
292.5	565	100	543	4734	1026	61	0	
293	419	109	384	5768	1081	15	0	
293.5	432	39	243	5347	1010	32	0	
294	367	88	149	4795	1182	37	0	
294.5	412	96	598	5652	998	17	0	
295	323	138	148	5861	1080	48	0	
295.5	389	52	487	5586	1114	0	0	
296	322	62	473	4451	656	26	0	
296.5	134	0	205	3124	540	0	0	
297	249	38	202	3131	536	0	87	
297.5	0	64	346	3503	660	114	0	
298	272	72	380	5076	893	52	0	
298.5	124	6	637	4517	1015	45	0	
299	512	122	405	5709	1324	34	0	

Depth (cm)	Hg	I	Ir	K	La	Mg	Mn	Mo
299.5	612	99	587	5646	1133	72	0	
300	140	133	468	5781	1088	54	0	
300.5	407	24	262	5993	1084	51	0	
301	421	67	442	5250	1009	0	0	
301.5	159	91	598	5361	1038	14	0	
302	523	51	571	5885	1090	0	0	
302.5	547	99	442	6145	828	34	0	
303	290	75	294	4165	891	9	0	
303.5	535	136	494	4989	1079	0	0	
304	375	114	480	5275	953	0	0	
304.5	48	37	553	5127	843	37	0	
305	321	54	309	4538	874	69	0	
305.5	152	78	357	5205	729	21	0	
306	337	52	519	5805	879	27	0	
306.5	383	104	484	5727	964	52	0	
307	104	93	111	5360	893	24	0	
307.5	691	131	355	6318	1106	0	3096	1148
308	699	104	454	7170	1187	59	2904	731
308.5	754	199	464	7324	1095	17	3844	965
309	649	169	601	6955	1088	43	4048	478
309.5	982	155	564	7098	1124	51	4333	547
310	549	133	187	7176	1153	17	3110	926
310.5	793	127	630	7285	1142	99	3863	818
311	633	133	594	8002	1319	19	2993	1017
311.5	217	95	456	6647	1167	42	2476	952
312	574	188	386	7315	1256	8	2496	1076
312.5	841	81	488	6602	1158	52	3827	793
313	752	133	246	6277	1179	21	2638	937
313.5	573	160	426	6690	1228	6	2938	1039
314	710	129	118	6371	1206	15	3385	732
314.5	634	71	489	6533	1273	43	3051	389
315	659	133	451	6838	1193	23	3721	820
315.5	531	197	712	7616	1361	87	1533	879
316	573	164	564	7598	1208	70	1936	692
316.5	487	173	381	7907	1247	49	3272	908
317	684	145	486	7456	1190	41	2195	966
317.5	853	123	458	7977	1271	23	3157	1423
318	783	180	649	7998	1235	24	1344	931
318.5	353	146	567	7510	1244	0	2226	1195

Depth (cm)	Hg	I	Ir	K	La	Mg	Mn	Mo
319	828	182	448	7476	1243	0	2799	950
319.5	901	118	460	8014	1184	18	2731	1015
320	562	141	537	7650	1277	23	1029	1186
320.5	805	244	395	7839	1189	44	1945	976
321	412	28	668	7023	1078	0	1209	732
321.5	850	70	465	6853	1214	39	3231	476
322	1019	166	298	7289	1487	0	1316	648
322.5	949	173	477	6567	1199	49	2815	493
323	731	234	631	6870	1179	32	1037	403
323.5	547	222	456	6957	1236	53	1411	979
324	776	147	450	7957	1321	62	2086	537
324.5	572	191	559	7562	1413	101	3643	386
325	333	207	405	7952	1494	0	2796	811
325.5	427	155	617	7769	1271	16	2060	364
326	535	148	690	8215	1380	64	2985	636
326.5	532	195	559	7257	1235	55	2454	832
327	335	115	583	7110	1280	52	1855	756
327.5	600	183	606	6905	1175	45	3202	713
328	683	153	314	7445	1332	21	3180	1123
328.5	366	200	627	7413	1204	0	2764	577
329	123	227	630	6735	1224	0	1711	244
329.5	569	168	534	6874	1286	16	2773	996
330	651	140	370	6355	1258	13	3414	718
330.5	666	200	621	7991	1269	66	3051	1025
331	392	230	502	8828	1230	24	4448	855
331.5	365	220	342	8740	1343	0	4839	855
332	747	167	521	8446	1320	40	3262	1210
332.5	264	231	167	8371	1305	0	998	1338
333	607	144	139	7410	1294	0	1938	1040
333.5	658	172	634	8216	1358	11	2626	493
334	563	169	441	8392	1151	0	2778	997
334.5	502	171	630	7935	1239	53	3116	1041
335	323	234	530	9405	1347	18	2833	553
335.5	0	88	263	1769	293	0	1730	90
336	0	94	105	0	191	0	561	55
336.5	0	48	209	0	192	0	801	0
337	337	114	508	5906	752	0	1456	533
337.5	478	138	607	10061	1136	46	3827	910
338	700	163	398	10057	1293	0	2257	951

Depth (cm)	Hg	I	Ir	K	La	Mg	Mn	Mo
338.5	658	149	368	8510	1238	7	1162	994
339	661	155	381	9270	1120	0	1510	580
339.5	392	101	598	9024	1330	51	1214	940
340	333	196	560	7761	1186	68	1775	1183
340.5	338	139	214	8501	1054	13	3406	836
341	412	189	495	9349	1219	44	2264	1092
341.5	397	70	752	9081	1345	45	1904	1022
342	489	103	587	7663	1036	26	994	1230
342.5	382	147	381	8042	1084	35	1848	855
343	390	218	336	8112	1218	22	1795	713
343.5	505	195	135	7667	1166	0	861	1109
344	509	210	278	7574	1107	0	296	1178
344.5	412	156	216	7711	1180	63	989	885
345	381	153	671	7346	1148	43	1928	1085
345.5	191	159	412	7598	1277	42	1169	1098
346	440	185	520	7745	1098	16	836	767
346.5	323	132	481	7594	1247	25	3048	732
347	663	94	609	7153	1080	0	1729	792
347.5	326	162	367	7021	1069	26	1185	1251
348	266	114	367	7095	1044	31	1804	769
348.5	273	170	461	7073	1113	0	2761	467
349	5	106	395	7590	1019	47	2031	745
349.5	364	132	549	7148	1063	0	1667	699
350	204	172	289	6238	1076	0	2103	772
350.5	511	156	519	6469	1200	0	1946	867
351	254	139	302	6291	973	21	1858	1040
351.5	115	89	379	6390	1032	28	1657	947
352	354	74	380	6539	1190	12	1288	954
352.5	411	145	546	6109	1129	0	7	719
353	8	87	642	3711	516	34	1750	538
353.5	6	52	206	2374	549	0	1670	488
354	64	93	130	2136	550	0	1319	500
354.5	122	99	115	3852	693	0	705	245
355	577	212	527	6501	874	7	3018	783
355.5	548	176	461	7910	1246	71	3179	936
356	364	141	550	6341	1130	19	1792	392
356.5	367	158	456	6236	889	71	605	1011
357	348	127	562	5769	959	15	2013	623
357.5	388	172	352	5799	966	68	1729	1022

Depth (cm)	Hg	I	Ir	K	La	Mg	Mn	Mo
358	359	137	497	6269	991	66	862	1016
358.5	266	155	428	6219	883	4	1111	884
359	242	155	339	4717	829	56	965	945
359.5	313	125	468	4783	830	0	1663	1220
360	460	172	225	3682	800	0	1781	858
360.5	279	114	438	4056	788	32	2309	426
361	217	205	421	5164	898	0	2038	730
361.5	417	157	562	5438	778	0	2259	1019
362	113	168	156	5430	872	0	1222	734
362.5	213	180	336	5207	992	20	128	497
363	246	132	634	5359	1011	44	1677	537
363.5	436	146	459	5978	883	8	1496	130
364	68	164	373	6731	915	57	2442	0
364.5	146	188	40	5900	925	42	2250	692
365	430	181	142	6321	1056	35	1929	525
365.5	401	157	544	6178	909	27	2586	744
366	298	71	263	5627	886	20	469	652
366.5	310	162	529	7100	869	52	1301	715
367	164	118	406	4909	764	52	2225	712
367.5	53	103	206	5058	847	0	2560	875
368	338	138	615	5600	903	51	2084	518
368.5	478	93	655	9195	1340	83	0	
369	289	146	469	10347	1217	0	363	
369.5	799	164	515	9327	1252	29	0	
370	623	55	651	11057	1176	0	0	
370.5	311	102	663	10820	1257	44	0	
371	426	158	657	10424	1220	61	814	
371.5	537	150	727	11384	1164	21	536	
372	266	118	464	10557	1346	47	0	
372.5	387	101	290	9470	1266	83	0	
373	0	172	670	10040	1267	52	119	
373.5	273	81	740	10650	1238	0	215	
374	543	123	738	10090	1240	90	0	
374.5	357	146	458	8807	1165	11	0	
375	536	139	587	9471	1101	36	592	
375.5	398	188	584	10111	1278	24	0	
376	423	103	805	10513	1233	13	0	
376.5	761	46	572	11116	1116	20	470	
377	251	120	529	11427	1241	29	436	

Depth (cm)	Hg	I	Ir	K	La	Mg	Mn	Mo
377.5	541	219	617	11653	1151	0	1083	
378	570	217	516	11030	1228	0	0	
378.5	239	195	633	10323	1198	11	484	
379	410	202	382	11095	1223	51	0	
379.5	283	114	440	11158	1114	15	17	
380	196	115	617	10540	1150	0	1425	
380.5	309	140	716	10124	1080	84	729	
381	417	130	497	11192	1178	21	328	
381.5	168	171	382	7892	814	0	0	
382	548	127	543	9391	1113	37	313	
382.5	260	104	415	10119	1139	0	0	
383	472	167	836	10638	1132	11	0	
383.5	270	185	617	10535	1341	44	932	
384	506	222	757	11249	1242	31	769	
384.5	272	154	478	11321	1198	40	852	
385	518	122	547	11227	1269	18	1490	
385.5	473	158	451	11149	1218	7	61	
386	428	156	657	11072	1155	52	0	
386.5	765	105	149	12252	1238	67	782	
387	549	111	418	12590	1182	43	1265	
387.5	400	82	565	14264	1195	12	0	
388	498	188	845	14230	1229	37	1493	
388.5	251	156	603	13396	1207	38	0	
389	448	78	239	13471	1090	0	0	
389.5	506	186	557	13854	1146	0	1097	
390	485	167	659	11929	1160	45	0	
390.5	360	136	340	12276	1225	27	1552	
391	393	139	552	11314	1140	4	782	
391.5	234	167	501	11222	1228	0	0	
392	347	136	346	11593	1177	46	0	
392.5	397	71	668	11114	1135	0	310	
393	245	71	192	10961	1087	42	0	
393.5	460	182	805	10463	1022	30	483	
394	524	148	810	10408	1125	0	1365	
394.5	194	108	422	11312	1086	0	1034	
395	327	102	689	11659	1175	0	1222	
395.5	469	131	314	12395	1142	0	1143	
396	80	87	574	10399	894	24	1014	
396.5	549	138	507	10990	1196	12	106	

Depth (cm)	Hg	I	Ir	K	La	Mg	Mn	Mo
397	278	159	548	11192	1155	0	1637	
397.5	311	159	417	11689	1060	7	0	
398	274	110	518	12383	1016	67	0	
398.5	191	136	528	12198	874	43	456	
399	579	175	504	13001	1114	0	823	
399.5	301	149	476	13016	1088	29	909	
400	250	167	550	13511	1221	25	342	
400.5	353	105	693	13881	1098	33	944	
401	433	164	193	13046	1103	35	328	
401.5	247	108	608	11819	1251	69	444	
402	321	144	529	12658	1108	18	0	
402.5	295	76	361	13219	1146	0	255	
403	274	153	578	13299	1195	44	826	
403.5	502	167	543	13421	1111	41	78	
404	410	159	615	13809	1133	53	0	
404.5	437	159	348	14244	1122	27	705	
405	506	83	611	17972	963	44	594	
405.5	344	165	242	15229	1021	83	0	
406	206	183	296	14708	1116	7	1550	
406.5	216	94	388	14304	1085	14	0	
407	301	186	325	14255	1281	0	40	
407.5	214	164	348	15519	1105	41	0	
408	519	145	397	15216	1389	52	0	
408.5	520	59	489	15587	1089	30	1064	
409	374	121	547	15374	1154	0	0	
409.5	627	114	660	15879	1174	11	0	
410	184	125	514	15458	1135	33	457	
410.5	283	43	732	16368	1177	36	0	
411	633	112	658	16145	1249	22	0	
411.5	242	174	752	15651	1086	42	0	
412	243	46	304	16062	1182	35	230	
412.5	295	20	560	16876	1242	43	578	
413	376	0	391	15681	1197	97	902	
413.5	202	196	553	15550	1102	44	413	
414	235	82	472	15775	1043	42	924	
414.5	370	48	250	13255	850	29	703	
415	291	51	482	12083	866	34	1416	
415.5	136	117	434	12794	944	0	89	
416	185	148	517	15841	1054	52	0	

Depth (cm)	Hg	I	Ir	K	La	Mg	Mn	Mo
416.5	38	175	409	16140	1130	26	0	
417	457	144	791	15640	1191	14	1763	
417.5	32	84	260	15267	1151	18	17	
418	269	198	411	15207	1101	49	1540	
418.5	489	94	646	16195	1199	5	55	
419	289	176	502	16320	1192	7	290	
419.5	348	79	505	15057	1175	0	613	
420	272	207	510	16079	1154	5	715	
420.5	588	246	371	16322	1087	30	930	
421	382	200	552	16437	1178	0	0	
421.5	199	132	579	17055	1206	0	1565	
422	300	239	595	17124	1136	73	0	
422.5	475	245	468	18184	1105	0	0	
423	329	104	556	17106	1052	52	1572	
423.5	258	129	662	17208	1164	18	308	
424	590	58	299	16966	1195	14	861	
424.5	429	82	555	17269	1106	10	1344	
425	416	151	331	16860	1066	11	922	
425.5	145	197	695	16803	1114	0	0	
426	298	136	480	18046	1203	120	1068	
426.5	592	71	528	17374	1066	41	457	
427	602	218	397	17260	1166	0	1754	
427.5	437	117	376	17585	1034	96	369	
428	298	130	628	16443	1169	37	1294	
428.5	213	80	374	16585	1268	59	0	
429	121	134	279	14148	822	0	729	
429.5	297	120	140	13605	763	0	1062	
430	210	91	367	12419	695	39	0	
430.5	263	64	373	14294	754	10	1172	
431	235	62	271	8867	487	19	1138	

Table A 2.4 Cuobu XRF Geochemistry Ni – Rb

Depth (cm)	Ni	P	Pb	Pd	Pm	Pr	Pt	Rb
27	221	0		19	3337	1950	662	370
27.5	857	59		92	3150	452	836	427
28	1325	6		93	10947	1081	1041	908
28.5	1337	55		71	11470	1129	1233	1704
29	1185	23		79	10958	1297	1007	996
29.5	928	57		124	10007	892	928	871
30	1171	67		75	10944	975	1227	771
30.5	1256	68		73	10370	1259	797	974
31	1095	65		59	11221	926	1024	1116
31.5	1119	59		58	11200	1091	1413	1172
32	1189	84		121	11046	1207	1000	1031
32.5	1253	22		99	11600	899	1131	964
33	907	0		79	11645	886	1179	761
33.5	1232	0		133	10866	977	1493	924
34	1031	36		75	9174	1069	1596	995
34.5	1176	67		125	10621	1058	971	924
35	1357	34		139	11831	995	1307	782
35.5	1106	39		94	11101	1186	917	834
36	1093	67		93	10781	1097	1283	894
36.5	1284	76		81	10020	1081	1068	1201
37	1117	13		16	9778	1026	1276	1106
37.5	1116	27		61	11334	1143	1247	1003
38	1317	101		88	9708	958	650	1094
38.5	1129	39		101	10590	989	896	974
39	1168	51		59	10324	1317	969	920
39.5	1006	28		87	10513	1259	1132	981
40	1216	15		111	9749	997	1098	680
40.5	1188	33		157	11545	1354	1205	575
41	1055	0		88	10751	1114	1425	1096
41.5	1159	64		109	11603	1066	1066	1293
42	1007	93		109	10580	1155	1024	484
42.5	1294	25		171	10815	1141	1209	1134
43	1091	0		50	10532	1190	949	939
43.5	985	42		44	10527	926	1351	866
44	1183	46		120	9047	1220	1230	1520
44.5	1070	65		42	10558	1036	874	1324
45	954	0		21	9074	984	1191	1051
45.5	1197	39		119	9486	881	1017	1252

Depth (cm)	Ni	P	Pb	Pd	Pm	Pr	Pt	Rb
46	988	94		83	8840	1143	1178	1229
46.5	1136	31		90	9866	1089	1089	1361
47	1049	22		55	9256	913	1426	831
47.5	1075	28		72	7732	936	1207	1033
48	1062	64		73	8320	1115	1318	944
48.5	1208	0		29	9950	1184	1068	1084
49	1207	69		128	10276	1021	1206	794
49.5	1123	18		72	9626	1060	1017	1118
50	1143	7		65	10798	1081	1157	957
50.5	1018	58		97	10221	1385	910	1570
51	1186	20		135	9586	931	1005	1045
51.5	1186	62		84	9066	981	1206	568
52	1193	88		42	9613	1016	1110	1081
52.5	1151	59		92	10888	1021	1268	1263
53	995	27		38	9966	931	1176	1156
53.5	947	47		0	9072	1026	1130	1322
54	1169	53		137	9287	886	894	696
54.5	1257	51		127	11072	956	1035	1447
55	1321	65		75	10238	1263	1374	1061
55.5	991	43		124	9566	975	1401	1264
56	1162	28		69	10073	897	1196	1047
56.5	1130	5		69	8397	1184	943	1125
57	1276	0		110	10271	886	1014	1110
57.5	1277	34		80	8924	1018	879	1400
58	1226	69		61	10700	971	991	1377
58.5	1083	21		50	9112	927	1170	1119
59	742	47		59	7907	949	1149	1234
59.5	1073	65		57	10179	1028	995	1063
60	1176	72		46	8603	990	1262	999
60.5	1084	52		64	9532	1226	1021	1099
61	1122	60		41	9468	1037	1227	1137
61.5	1115	10		82	10218	1126	928	1195
62	1160	54		68	10016	1035	1140	1011
62.5	1002	36		101	8570	943	1382	1429
63	929	0		10	8761	967	1042	1016
63.5	1066	77		155	9810	921	1338	1009
64	1096	0		48	9675	890	1286	1003
64.5	1246	23		117	9586	1090	1087	863
65	1242	80		53	9763	1245	1205	1124

Depth (cm)	Ni	P	Pb	Pd	Pm	Pr	Pt	Rb
65.5	933	0		72	9442	1032	1104	1473
66	990	62		73	8821	1175	1061	993
66.5	1034	27		47	7467	1094	1136	1128
67	1090	55		35	9168	1147	1092	1026
67.5	1087	71		37	10738	1196	1115	1360
68	1071	48		99	10076	1228	1148	1179
68.5	926	35		67	9697	1038	1040	1445
69	1097	44		117	11031	1220	612	1246
69.5	1106	0		144	9658	1079	936	1173
70	986	0		69	9475	932	915	1502
70.5	1189	29		27	8947	946	1217	1272
71	1135	66		12	9268	1267	1177	1599
71.5	1188	102		99	10364	1334	1203	1313
72	1065	80		116	10137	1260	1412	1434
72.5	1205	27		92	9542	1219	1313	1908
73	1108	53		76	8395	1304	778	1132
73.5	948	0		98	10369	1030	1131	1530
74	849	63		100	5087	856	1091	1396
74.5	689	55		58	1604	387	342	1227
75	770	5		0	2157	480	818	975
75.5	739	7		0	5670	662	1010	773
76	1200	40		7	7810	967	729	1172
76.5	1047	33		44	8977	1227	862	1361
77	962	9		132	9506	1101	998	1209
77.5	1250	62		94	9298	1063	1119	1597
78	1033	65		44	8846	1042	1170	1303
78.5	1238	57		73	10055	1213	989	1456
79	1190	52		41	9919	1155	1113	1606
79.5	929	17		84	8963	1171	1049	2014
80	929	37		93	9871	988	1203	1817
80.5	1180	65		108	10744	915	1069	1784
81	1135	0		107	9110	1082	1407	1545
81.5	1124	9		69	9272	856	816	1380
82	1134	34		123	9326	995	914	1257
82.5	1088	29		28	10277	908	1064	1725
83	1114	15		10	8608	846	787	1407
83.5	511	28		0	1853	489	546	919
84	717	58		0	2626	660	888	563
84.5	738	7		0	3549	611	617	471

Depth (cm)	Ni	P	Pb	Pd	Pm	Pr	Pt	Rb
85	725	0		0	2955	716	769	561
85.5	723	12		0	2782	687	811	704
86	671	27		0	3968	629	973	900
86.5	692	0		0	3772	765	569	629
87	886	6		0	3229	729	380	675
87.5	941	5		0	3797	785	654	593
88	913	0		0	4407	766	642	780
88.5	888	34		27	4345	652	485	903
89	842	11		0	4141	762	584	567
89.5	724	13		44	3136	658	902	1212
90	706	10		0	2766	677	531	655
90.5	649	44		0	2901	658	362	1120
91	729	0		0	3815	541	473	622
91.5	1048	0		0	3807	757	882	768
92	989	0		0	5903	742	884	699
92.5	802	15		14	4918	699	551	1191
93	956	0		8	4753	784	797	1146
93.5	931	0		0	4806	857	949	1099
94	857	0		0	6568	757	615	1073
94.5	791	5		9	5703	1003	781	807
95	842	0		0	7157	760	616	953
95.5	701	37		25	5172	734	807	1077
96	894	0		0	6268	922	651	851
96.5	838	0		0	5072	809	906	868
97	595	0		11	6240	775	802	1210
97.5	782	0		14	6155	930	917	896
98	804	0		11	6822	666	685	535
98.5	610	63		30	6543	966	766	812
99	734	10		79	6335	825	828	852
99.5	682	0		51	7373	853	651	725
100	568	0		0	5289	866	612	947
100.5	670	39		0	5820	865	983	1036
101	570	11		25	5950	1032	779	709
101.5	420	0		0	7486	899	723	891
102	504	17		49	7034	1029	838	1142
102.5	667	0		69	8400	1069	811	772
103	585	0		38	8323	982	883	492
103.5	528	0		0	7813	1011	802	969
104	836	35		11	8895	925	1053	930

Depth (cm)	Ni	P	Pb	Pd	Pm	Pr	Pt	Rb
104.5	551	49		38	8119	1158	1070	905
105	352	7		7	7746	1181	663	581
105.5	457	6		39	8793	1000	882	871
106	304	0		43	8521	1059	920	822
106.5	462	0		54	8157	1042	854	1040
107	417	0		16	9334	968	1039	1032
107.5	720	0		14	6927	921	865	905
108	567	33		20	8354	1017	781	755
108.5	361	12		47	8975	1049	783	810
109	675	0		51	8864	953	671	1102
109.5	605	45		9	8075	1207	782	1018
110	619	0		39	8807	942	808	864
110.5	398	27		26	7429	873	876	1049
111	416	0		38	7981	1071	903	1120
111.5	321	8		53	6951	1097	1021	1185
112	410	0		5	6316	1067	868	882
112.5	480	18		47	6425	1189	840	810
113	445	0		35	7788	1138	866	952
113.5	575	10		66	7415	871	702	1051
114	435	23		60	7697	970	742	991
114.5	492	0		49	8280	1065	842	1282
115	458	16		0	7566	1069	786	1192
115.5	493	0		0	8183	1162	1068	1044
116	608	45		34	8545	836	969	753
116.5	432	35		56	7179	941	821	1052
117	321	39		62	8302	1067	1064	1007
117.5	553	19		33	6816	837	713	899
118	437	0		0	3760	828	586	689
118.5	493	0		6	4760	747	843	827
119	376	0		0	5467	757	719	762
119.5	534	0		0	7058	883	626	810
120	629	31		0	8549	940	759	1175
120.5	489	0		0	7501	1015	593	1312
121	571	14		37	8052	856	939	1642
121.5	526	28		0	6882	1037	962	1402
122	621	0		0	6798	985	986	1436
122.5	622	0		27	7288	875	1063	1420
123	815	0		80	7801	889	598	1052
123.5	790	16		0	7129	1009	821	1058

Depth (cm)	Ni	P	Pb	Pd	Pm	Pr	Pt	Rb
124	646	0		26	7089	1125	671	1124
124.5	593	75		66	7447	1096	713	1108
125	692	0		0	7340	896	953	943
125.5	689	61		21	6669	1045	844	754
126	743	0		53	7322	1287	806	1232
126.5	792	13		0	7517	1003	805	914
127	713	0		22	7879	1031	907	1097
127.5	711	0		44	7032	1027	814	916
128	846	0		35	7743	1012	853	819
128.5	745	0		8	6907	855	870	887
129	727	34		9	7787	1220	1162	698
129.5	425	6		0	7993	1073	925	670
130	451	29		31	6979	961	854	844
130.5	615	38		0	7099	974	794	1013
131	728	0		0	8207	1048	763	1036
131.5	860	0		24	8252	1086	870	1213
132	755	0		0	7546	964	922	1023
132.5	688	63		21	8348	1040	721	1015
133	692	0		7	8048	927	705	742
133.5	693	0		28	8083	1122	792	1353
134	716	11		0	6632	1083	969	919
134.5	710	0		0	7373	1094	1027	1180
135	735	18		36	9090	997	652	670
135.5	649	0		0	9036	1228	710	904
136	645	0		19	6690	998	637	1113
136.5	576	0		69	8306	935	809	986
137	235	0		39	7880	1074	666	1115
137.5	469	0		0	8452	1031	760	806
138	565	54		0	550	437	607	781
138.5	481	59		0	839	299	534	628
139	514	53		0	902	219	433	426
139.5	599	0		16	6028	896	708	971
140	670	0		0	7934	941	1096	1213
140.5	557	0		28	6891	949	721	1119
141	655	0		4	7504	1168	1174	991
141.5	418	0		38	6414	957	802	1150
142	565	18		34	7707	1057	684	1028
142.5	567	9		0	8597	964	912	874
143	524	13		0	8234	945	644	1202

Depth (cm)	Ni	P	Pb	Pd	Pm	Pr	Pt	Rb
143.5	462	0		14	7799	1033	762	999
144	731	0		30	6559	839	615	820
144.5	655	0		58	7367	1039	740	844
145	712	0		15	7527	966	874	827
145.5	691	0		47	7540	1008	956	913
146	585	0		40	8891	1046	956	1137
146.5	544	0		54	8351	1133	999	491
147	629	0		18	7287	1040	735	648
147.5	664	47		54	7833	1054	690	720
148	657	19		53	7813	954	818	1077
148.5	805	8		19	8639	1015	1023	1111
149	897	29		24	7255	1059	1005	903
149.5	876	0		0	7715	886	698	696
150	645	0		0	4808	812	706	833
150.5	481	37		0	2938	525	502	683
151	704	9		0	3446	596	585	584
151.5	749	0		0	3954	664	542	625
152	692	0		51	6793	969	922	570
152.5	714	0		0	7322	1110	878	583
153	706	14		46	8147	906	787	410
153.5	794	0	258		935	1313	328	851
154	880	0	244		1076	1302	354	748
154.5	827	8	389		967	1392	705	431
155	741	12	118		1104	1284	319	618
155.5	750	14	71		1084	1336	357	538
156	865	27	84		1089	1108	353	838
156.5	778	0	177		1052	1298	489	860
157	852	0	187		1104	1257	306	806
157.5	644	16	236		900	1290	553	676
158	768	0	331		889	1162	533	249
158.5	649	0	325		914	1178	400	558
159	710	22	206		757	1268	302	443
159.5	762	0	269		991	1267	366	778
160	626	54	185		904	1299	582	679
160.5	822	24	226		964	1304	487	298
161	838	14	215		897	1348	610	757
161.5	979	27	298		976	1259	656	791
162	887	7	74		922	1358	499	406
162.5	900	14	341		1047	1268	503	839

Depth (cm)	Ni	P	Pb	Pd	Pm	Pr	Pt	Rb
163	788	31	336		1067	1243	953	467
163.5	710	15	413		1030	1403	574	742
164	665	0	316		1134	1212	669	412
164.5	757	0	243		902	1357	419	611
165	799	36	239		1062	1277	466	610
165.5	748	20	284		1008	1323	638	170
166	784	0	406		1137	1298	555	438
166.5	890	0	345		1165	1278	773	635
167	779	0	329		960	1247	335	746
167.5	885	0	46		626	1289	465	559
168	820	34	197		709	590	478	823
168.5	715	34	170		439	485	145	518
169	643	46	302		248	627	435	365
169.5	655	6	282		504	943	175	543
170	629	25	255		1023	1257	246	553
170.5	712	0	365		932	1414	614	794
171	671	0	391		1071	1366	240	546
171.5	770	0	488		1106	1206	793	648
172	682	29	510		1009	1124	389	471
172.5	630	19	496		967	1243	420	269
173	621	74	402		1072	1335	194	574
173.5	602	0	477		959	1394	747	430
174	730	0	287		1167	1321	365	232
174.5	604	0	270		1019	1351	628	178
175	763	6	490		1070	1273	432	625
175.5	803	0	266		1117	1374	581	622
176	830	0	224		1089	1316	503	469
176.5	773	34	380		1074	1294	329	570
177	859	0	118		811	1363	416	758
177.5	640	0	252		794	1339	774	631
178	711	0	201		1054	1303	392	639
178.5	891	56	219		913	1229	539	745
179	760	0	515		828	1432	617	373
179.5	688	9	126		902	1258	571	411
180	668	35	174		1058	1288	434	763
180.5	896	0	408		1033	1334	528	697
181	949	0	273		1108	1344	417	553
181.5	879	0	385		936	1330	618	376
182	900	9	274		1052	1296	593	499

Depth (cm)	Ni	P	Pb	Pd	Pm	Pr	Pt	Rb
182.5	889	10	455		941	1349	404	437
183	830	0	130		772	1319	293	305
183.5	829	0	201		990	1297	569	366
184	779	0	533		787	1376	922	493
184.5	863	25	396		989	1285	495	424
185	845	50	369		1026	1331	713	530
185.5	869	0	224		735	1304	474	628
186	784	0	107		953	1261	600	604
186.5	674	15	268		769	1209	479	747
187	797	0	378		918	1315	591	482
187.5	692	0	152		1050	1354	295	461
188	696	5	406		1038	1319	526	957
188.5	707	0	401		957	1263	523	752
189	634	32	48		849	1278	326	411
189.5	738	4	75		1004	1348	346	532
190	814	64	342		1141	1274	761	823
190.5	824	0	233		668	1362	421	400
191	925	0	296		1020	1266	399	408
191.5	798	0	401		920	1229	706	604
192	719	0	122		1113	1342	287	862
192.5	766	25	293		1091	1327	674	437
193	842	0	434		1093	1377	517	1223
193.5	648	27	282		1150	1407	349	553
194	671	4	343		1031	1348	12	508
194.5	669	28	666		1049	1346	680	719
195	638	24	461		795	1428	453	468
195.5	592	15	439		1019	1331	652	485
196	990	0	206		1119	1219	685	518
196.5	1015	0	397		1080	1368	471	778
197	877	22	47		885	1427	431	682
197.5	927	0	287		1189	1317	497	778
198	917	0	87		938	1401	577	835
198.5	854	0	295		1059	1437	591	802
199	1077	22	295		1041	1429	550	691
199.5	861	0	275		1025	1398	252	793
200	793	0	233		949	1386	589	542
200.5	859	0	187		1260	1390	430	978
201	642	15	213		953	1403	593	500
201.5	814	0	408		987	1239	454	993

Depth (cm)	Ni	P	Pb	Pd	Pm	Pr	Pt	Rb
202	823	0	431		1027	1491	718	757
202.5	890	0	153		1001	1133	441	324
203	733	14	181		478	536	328	567
203.5	798	27	83		497	555	388	581
204	560	15	0		387	592	238	167
204.5	654	0	83		648	1162	335	441
205	813	39	407		1150	1251	613	787
205.5	738	0	337		950	1410	597	653
206	869	0	306		997	1345	375	525
206.5	735	11	370		741	1326	517	688
207	814	23	312		974	1394	673	727
207.5	844	33	122		1047	1414	497	680
208	729	7	558		1208	1399	815	389
208.5	844	14	360		868	1436	821	456
209	788	47	440		1093	1346	667	185
209.5	960	28	227		1046	1382	511	736
210	824	33	245		1191	1293	341	965
210.5	1009	0	231		983	1247	771	845
211	728	0	200		923	1387	447	363
211.5	864	0	343		1033	1379	636	788
212	801	57	226		926	1542	525	644
212.5	836	6	454		963	1452	354	672
213	718	10	242		938	1565	528	591
213.5	826	0	234		1144	1313	85	370
214	715	24	362		752	1182	287	537
214.5	913	5	195		733	1384	380	933
215	704	0	412		859	1406	528	976
215.5	642	34	176		789	1380	241	853
216	574	0	368		1017	1447	689	714
216.5	661	0	365		1061	1363	409	515
217	663	0	428		1017	1384	317	699
217.5	591	55	375		955	1449	794	677
218	607	39	430		1096	1289	525	657
218.5	787	43	420		1045	1421	414	724
219	832	0	186		911	1340	390	792
219.5	849	0	177		930	1306	515	708
220	937	34	341		813	1387	562	908
220.5	841	0	154		827	1272	615	773
221	885	50	140		892	1357	359	364

Depth (cm)	Ni	P	Pb	Pd	Pm	Pr	Pt	Rb
221.5	904	0	238		800	1303	642	671
222	900	7	231		774	1369	715	424
222.5	844	20	462		818	1407	574	488
223	849	71	444		971	1399	793	591
223.5	895	14	62		873	1339	579	586
224	811	50	236		587	945	307	507
224.5	822	0	104		955	1238	248	816
225	886	0	355		878	1396	599	597
225.5	1037	0	348		891	1316	738	750
226	941	50	185		757	1346	294	595
226.5	950	11	359		701	1195	345	593
227	980	0	527		940	1378	529	0
227.5	726	0	198		899	1298	614	805
228	863	13	144		905	1210	240	559
228.5	1009	52	113		1040	1229	408	748
229	945	20	272		844	1430	447	862
229.5	900	12	140		820	1286	465	572
230	826	0	348		841	1339	614	711
230.5	917	63	375		841	1287	367	392
231	761	12	391		882	1203	622	564
231.5	933	0		79	6290	1050	803	625
232	957	0		73	6139	958	1146	693
232.5	950	46		31	6386	972	888	825
233	886	0		0	4762	826	668	604
233.5	843	0		16	3141	635	579	812
234	973	30		37	6444	916	980	959
234.5	887	14		51	6448	1002	1023	858
235	735	25		22	6168	948	1018	833
235.5	877	14		16	7490	888	986	725
236	839	0		9	5673	942	1162	793
236.5	829	12		35	5623	883	1169	1026
237	823	0		32	6329	1034	903	1026
237.5	835	24		77	7113	1083	915	1076
238	784	28		76	6391	803	821	1147
238.5	817	25		4	6446	742	1179	725
239	709	0		52	5549	1063	1142	1089
239.5	981	0		0	5161	899	937	621
240	922	0		0	5448	674	808	623
240.5	992	14		7	5877	921	848	1028

Depth (cm)	Ni	P	Pb	Pd	Pm	Pr	Pt	Rb
241	698	0		26	5593	659	1009	659
241.5	785	43		45	6868	835	949	818
242	810	15		50	5467	1006	966	889
242.5	841	0		19	7037	857	989	1270
243	808	43		44	4848	796	963	855
243.5	745	71		28	4013	736	882	633
244	753	21		0	2691	547	729	359
244.5	774	30		0	2961	663	780	634
245	787	6		0	2954	575	424	623
245.5	860	0		27	4477	830	1244	421
246	784	0		4	5078	1017	988	802
246.5	799	4		26	5111	810	920	650
247	826	0		0	6927	953	1065	597
247.5	818	0		35	5892	1035	1152	870
248	936	56		11	5792	1033	1368	556
248.5	913	31		29	5715	848	1026	324
249	826	4		16	6149	906	1335	836
249.5	917	0		34	6971	905	1215	402
250	913	0		68	6345	999	1198	573
250.5	687	25		0	6369	875	899	741
251	748	49		11	7032	1018	801	777
251.5	744	0		16	5480	662	1005	754
252	695	29		10	5989	800	850	776
252.5	836	26		57	6688	1001	1027	941
253	934	42		0	6185	818	753	982
253.5	721	39		29	6060	776	1322	1045
254	708	5		24	4791	908	1081	925
254.5	693	0		60	7058	937	780	1029
255	618	0		12	6975	1002	1058	759
255.5	790	0		0	6109	953	870	903
256	646	22		0	5293	900	877	676
256.5	791	52		44	5356	982	1227	703
257	832	16		30	6555	890	617	548
257.5	967	0		24	6693	912	1377	840
258	767	7		28	5938	932	908	816
258.5	680	0		19	6164	827	1104	843
259	757	14		12	5953	806	888	868
259.5	868	0		42	5452	921	1170	1077
260	792	0		17	6422	846	1064	704

Depth (cm)	Ni	P	Pb	Pd	Pm	Pr	Pt	Rb
260.5	772	17		0	7135	932	1082	1173
261	973	5		30	7623	1251	822	918
261.5	972	0		0	6673	1219	770	663
262	923	0		0	7109	1229	910	783
262.5	847	0		23	8873	995	1403	507
263	719	25		7	8648	1541	1180	675
263.5	981	0		26	7845	1031	1065	694
264	932	54		12	7469	1117	964	925
264.5	1045	30		46	6822	1075	937	863
265	1075	0		0	6886	1211	1044	468
265.5	752	47		20	7437	1214	899	519
266	875	27		0	7578	1107	1101	708
266.5	963	0		0	7735	1240	1086	795
267	858	0		0	5911	965	1133	687
267.5	809	8		32	6281	1113	1043	661
268	883	0		0	5962	686	804	677
268.5	909	20		0	6292	1083	980	816
269	727	35		55	6704	1052	1038	681
269.5	868	22		0	6831	1282	812	947
270	908	5		0	5664	1025	704	932
270.5	719	0		0	7800	1180	1063	857
271	1042	36		17	7546	1142	846	542
271.5	880	0		36	7733	1137	861	539
272	701	22		6	6329	1237	824	738
272.5	933	14		0	7078	1084	952	737
273	625	11		0	7598	1157	1101	431
273.5	787	0		21	7170	1275	905	802
274	929	17		0	7509	1298	1163	1003
274.5	1005	0		0	8092	1539	1208	624
275	877	18		0	8065	1198	1001	743
275.5	1098	23		0	7341	1348	1081	482
276	1082	33		0	6873	1024	717	694
276.5	948	0		0	8396	1294	623	811
277	1034	0		0	7771	1127	1140	610
277.5	929	47		0	7219	1384	1213	644
278	898	0		11	8000	1233	1115	702
278.5	1004	0		0	6699	1155	891	886
279	971	55		30	6816	1191	1056	935
279.5	1075	0		0	6636	1277	753	591

Depth (cm)	Ni	P	Pb	Pd	Pm	Pr	Pt	Rb
280	992	10		7	5962	1087	911	668
280.5	872	37		0	6864	1383	947	795
281	1008	0		27	7116	1365	768	431
281.5	1209	0		0	7644	1174	794	933
282	1059	0		0	7698	1404	1158	929
282.5	921	28		0	7651	1417	1017	931
283	953	75		0	8584	1277	1201	423
283.5	1023	22		12	6966	1095	931	700
284	967	8		0	7954	1284	839	646
284.5	851	0		0	6878	1435	953	1219
285	907	0		32	8524	1375	805	821
285.5	909	0		7	7761	1246	870	934
286	909	0		0	6616	1120	1024	915
286.5	630	43		0	3150	751	641	478
287	556	6		0	1990	561	404	462
287.5	481	35		0	2514	598	482	478
288	658	0		0	5459	835	1001	743
288.5	869	0		0	7151	1259	976	462
289	1038	19		0	7591	1285	988	872
289.5	807	0		0	6488	1243	1054	604
290	1041	7		0	7336	1293	1091	651
290.5	1076	13		0	7144	1332	1127	466
291	1010	0		0	5998	1260	909	544
291.5	955	23		0	6626	1057	879	378
292	984	5		7	7125	1209	624	922
292.5	1100	0		15	7450	1166	834	377
293	859	27		0	6901	1310	725	1061
293.5	832	0		0	6344	1271	722	620
294	862	25		11	6835	1050	623	658
294.5	1062	0		0	7868	1492	762	684
295	929	16		0	7571	1387	745	767
295.5	907	0		0	6121	1129	922	1053
296	623	43		0	2949	899	947	542
296.5	582	0		0	2395	576	624	585
297	682	16		0	2780	486	520	615
297.5	883	84		0	3443	676	644	361
298	987	0		0	6710	1332	851	699
298.5	1057	0		0	6630	1188	842	541
299	807	0		0	7171	987	1036	545

Depth (cm)	Ni	P	Pb	Pd	Pm	Pr	Pt	Rb
299.5	1058	0		0	7030	1262	1255	817
300	796	0		0	6188	1144	714	603
300.5	983	0		0	6579	1277	882	611
301	930	0		0	5792	983	847	544
301.5	1005	14		0	6330	1106	926	676
302	865	0		4	7223	1235	816	435
302.5	926	37		0	5524	1108	642	665
303	807	56		0	5126	801	689	607
303.5	824	35		0	6711	1098	700	677
304	860	24		0	4866	1152	881	373
304.5	995	0		0	4992	1162	632	452
305	838	9		0	4577	907	702	479
305.5	908	0		0	3860	1093	857	851
306	1036	55		0	4476	861	857	551
306.5	1080	59		0	4400	964	977	384
307	903	32		0	4180	878	756	621
307.5	676	0	183		0	994	1160	714
308	946	35	115		0	1000	1149	1050
308.5	856	22	430		322	1046	858	1065
309	756	0	50		0	1023	978	815
309.5	752	40	311		0	1088	1133	1258
310	963	0	324		230	1004	1052	1066
310.5	772	16	385		0	1058	1277	949
311	830	0	314		0	877	1101	955
311.5	620	0	178		0	909	974	1033
312	925	13	571		115	960	1021	642
312.5	688	0	305		94	925	1064	958
313	744	0	531		403	1040	908	1031
313.5	578	11	398		0	1007	1244	350
314	761	9	180		670	1023	1052	705
314.5	586	0	384		250	905	1109	959
315	706	6	0		180	966	1051	383
315.5	657	0	482		0	931	1264	1024
316	546	4	55		0	1012	969	685
316.5	741	8	442		0	965	1257	706
317	602	0	162		0	871	1051	1053
317.5	601	46	241		744	965	1295	559
318	692	0	258		0	835	1223	852
318.5	526	45	0		0	930	871	1038

Depth (cm)	Ni	P	Pb	Pd	Pm	Pr	Pt	Rb
319	589	0	300		0	844	1014	721
319.5	739	0	385		0	760	1159	972
320	596	0	93		0	849	661	603
320.5	619	32	397		0	1054	1133	718
321	476	0	512		0	1176	1017	1081
321.5	773	26	460		0	813	1136	764
322	656	20	304		0	971	1138	983
322.5	645	0	249		0	973	1043	1370
323	474	0	355		0	894	803	1083
323.5	561	19	356		0	1023	923	580
324	415	38	556		0	976	1199	1259
324.5	616	0	0		0	880	678	992
325	748	0	0		0	1123	901	839
325.5	763	0	138		0	820	785	855
326	654	16	467		0	916	1213	1043
326.5	824	20	515		0	1044	881	667
327	742	0	432		0	875	973	1163
327.5	968	0	543		0	1007	1033	922
328	882	0	322		273	948	1074	1174
328.5	724	13	23		0	956	1057	505
329	563	11	366		0	802	786	987
329.5	870	13	12		0	925	858	786
330	697	35	188		0	906	1064	888
330.5	867	60	389		0	896	968	764
331	940	63	238		0	1062	1370	673
331.5	776	0	377		0	938	702	858
332	818	22	199		0	970	1015	590
332.5	740	37	93		0	1048	933	761
333	827	17	58		0	913	739	865
333.5	774	0	316		0	740	1061	813
334	820	0	470		0	1089	937	746
334.5	776	18	245		0	864	836	740
335	1152	27	58		0	779	902	800
335.5	843	50	0		0	195	367	535
336	767	82	0		0	99	255	305
336.5	662	45	0		0	57	274	370
337	718	76	0		0	688	801	616
337.5	830	0	348		0	1110	1198	1087
338	795	15	200		0	818	814	1234

Depth (cm)	Ni	P	Pb	Pd	Pm	Pr	Pt	Rb
338.5	742	7	335		0	795	824	847
339	837	0	0		0	1016	862	886
339.5	639	0	16		0	690	639	766
340	714	50	17		0	813	757	917
340.5	803	0	160		0	1060	893	1175
341	730	43	300		0	849	958	968
341.5	808	69	36		0	996	863	708
342	863	0	0		0	906	880	957
342.5	707	0	474		0	857	1009	491
343	639	0	98		0	959	611	844
343.5	749	55	181		0	815	863	526
344	690	0	160		0	1091	828	755
344.5	850	0	57		0	756	605	564
345	674	0	229		0	801	826	831
345.5	815	0	0		0	725	697	544
346	909	69	181		0	805	765	683
346.5	882	16	115		0	693	641	1097
347	750	22	8		0	852	645	867
347.5	640	13	127		0	793	944	651
348	803	31	0		0	661	803	500
348.5	715	0	0		0	682	800	726
349	907	24	0		0	821	926	674
349.5	847	0	0		0	675	680	767
350	712	61	61		0	624	790	372
350.5	829	66	104		0	667	862	251
351	745	13	0		0	813	529	392
351.5	728	0	0		0	525	556	768
352	763	43	214		0	576	728	715
352.5	786	21	0		0	675	933	930
353	791	5	0		0	470	862	638
353.5	659	45	0		0	221	634	91
354	564	98	21		0	173	556	521
354.5	510	45	0		0	322	322	491
355	709	0	0		0	850	1135	774
355.5	857	0	0		0	919	735	1140
356	805	24	0		0	544	581	524
356.5	517	42	90		0	767	746	496
357	799	0	0		0	708	746	683
357.5	799	39	98		0	783	673	839

Depth (cm)	Ni	P	Pb	Pd	Pm	Pr	Pt	Rb
358	775	34	0		0	701	952	628
358.5	760	0	0		0	653	754	553
359	708	50	0		0	221	583	810
359.5	690	72	0		0	379	837	417
360	781	35	0		0	193	695	615
360.5	810	19	223		0	403	815	772
361	776	60	120		0	334	688	473
361.5	788	27	0		0	475	882	620
362	660	36	0		0	389	556	719
362.5	718	43	0		0	509	360	472
363	818	16	11		0	661	769	334
363.5	817	0	412		0	486	854	673
364	947	12	377		0	646	705	889
364.5	820	36	0		0	754	718	694
365	907	30	102		0	646	700	926
365.5	789	74	0		0	738	920	710
366	814	32	0		0	809	547	699
366.5	735	41	91		0	888	601	824
367	820	38	0		0	636	854	350
367.5	786	54	72		0	705	548	449
368	850	54	0		0	469	857	557
368.5	411	0		0	3355	892	877	689
369	617	0		0	3926	1220	722	586
369.5	700	0		0	2834	1059	1023	700
370	362	0		11	4277	1227	988	777
370.5	694	27		20	3015	1157	856	784
371	522	0		0	3988	1132	932	552
371.5	822	42		39	3243	1086	1033	987
372	639	8		91	4382	1282	791	730
372.5	601	8		0	3341	1111	705	681
373	489	0		53	3049	1162	657	876
373.5	777	0		30	2642	1150	1173	694
374	634	75		0	2304	1180	917	665
374.5	453	59		0	2059	942	535	596
375	560	19		0	3726	961	614	818
375.5	629	30		0	3396	795	1042	468
376	629	0		0	2851	1250	1054	1261
376.5	706	9		0	3304	1176	822	1017
377	798	0		0	2722	1010	766	837

Depth (cm)	Ni	P	Pb	Pd	Pm	Pr	Pt	Rb
377.5	775	7		0	2570	1181	923	797
378	918	0		0	2811	1043	955	1270
378.5	807	28		0	3752	963	1216	856
379	718	49		0	2579	1125	655	1143
379.5	889	0		0	2662	1069	1336	972
380	695	51		57	2923	1166	723	818
380.5	877	42		21	2616	1033	1106	1037
381	728	24		0	3226	962	812	844
381.5	814	69		0	2067	1038	570	504
382	836	20		15	3213	1094	814	1098
382.5	753	10		0	2727	954	954	787
383	794	16		9	2207	1128	1283	1025
383.5	783	0		0	3609	931	936	873
384	798	0		0	3145	1055	1005	860
384.5	737	25		43	2765	1191	852	675
385	897	27		0	3359	1074	791	957
385.5	800	31		20	3186	1122	703	658
386	844	28		5	2921	1245	1103	730
386.5	754	0		5	2522	1234	840	1185
387	867	0		0	3206	1231	977	952
387.5	772	10		0	2590	1264	822	790
388	837	14		0	3187	1346	910	749
388.5	742	0		0	2240	1092	762	841
389	762	32		0	2638	1238	979	1163
389.5	779	36		0	3218	1220	684	1012
390	784	39		0	2925	1200	889	675
390.5	834	0		0	2680	959	895	1055
391	797	5		0	2605	1022	830	870
391.5	856	48		38	2239	946	599	844
392	673	0		0	1566	964	723	965
392.5	827	9		0	2375	987	1103	971
393	667	8		0	2492	998	652	1101
393.5	819	30		0	2293	790	900	996
394	872	26		0	3216	1167	1012	1182
394.5	901	15		0	3206	1027	926	706
395	792	34		0	2680	1031	927	942
395.5	694	61		0	2759	844	731	970
396	854	0		0	2295	1093	902	797
396.5	917	25		0	1920	800	777	726

Depth (cm)	Ni	P	Pb	Pd	Pm	Pr	Pt	Rb
397	779	0		0	2629	1043	559	936
397.5	812	37		0	1289	1243	743	1307
398	739	74		0	1930	1078	1016	587
398.5	908	0		0	3368	1151	754	917
399	730	0		0	2985	1016	643	1086
399.5	790	6		0	2912	1244	697	1235
400	774	35		0	1656	905	905	1211
400.5	800	32		0	2389	1019	682	1333
401	702	0		0	2438	1051	872	885
401.5	651	0		0	2054	1142	959	1151
402	743	46		0	2731	965	885	1189
402.5	734	0		0	2371	1064	736	996
403	970	0		0	2563	1115	906	1011
403.5	725	8		0	2051	1130	726	1161
404	740	0		0	2125	978	1014	1062
404.5	691	0		0	3324	996	769	1042
405	721	0		0	3138	1053	766	1216
405.5	724	46		0	409	1038	554	879
406	741	9		0	3668	1021	648	1296
406.5	790	24		0	3237	1076	754	919
407	825	18		0	2890	1238	753	1250
407.5	763	0		0	2832	1074	531	1134
408	872	34		0	2682	845	1072	1375
408.5	775	0		0	3837	1057	642	1165
409	874	0		0	3030	1105	827	1189
409.5	971	51		0	3135	1241	767	1774
410	1022	21		0	3176	977	791	1226
410.5	871	0		0	2465	1252	914	1295
411	817	0		0	2967	1084	768	1473
411.5	843	0		0	2105	1245	972	1344
412	789	23		7	1993	1182	568	1434
412.5	797	0		0	3437	1204	671	1348
413	890	13		0	2864	1049	668	1347
413.5	509	41		0	2093	1140	590	1165
414	684	26		0	2198	1022	664	1058
414.5	754	0		0	1440	901	588	928
415	753	0		0	1393	790	873	1184
415.5	613	15		0	2066	904	855	798
416	785	33		0	1995	1044	707	1217

Depth (cm)	Ni	P	Pb	Pd	Pm	Pr	Pt	Rb
416.5	768	39		0	2854	1067	528	1193
417	902	27		0	2663	1076	946	1212
417.5	771	0		0	1887	1049	788	1133
418	909	18		5	2806	1261	823	924
418.5	817	16		0	2204	1204	939	1295
419	835	15		0	3333	1019	525	1452
419.5	955	0		0	2986	1184	1022	1670
420	812	0		0	3187	1167	727	837
420.5	823	0		0	3595	1225	599	1184
421	746	54		0	3144	1240	719	1518
421.5	756	0		0	3499	1050	835	1376
422	677	0		14	2255	1168	796	1572
422.5	773	27		0	2859	1035	829	1221
423	694	0		0	3029	1016	611	1192
423.5	932	26		0	3021	1111	800	1469
424	816	25		0	2997	1120	1050	1444
424.5	787	0		0	3712	1267	877	1360
425	697	11		0	2434	1070	785	1018
425.5	860	16		0	2029	1048	942	1034
426	879	26		0	3387	1056	575	1292
426.5	855	0		0	2652	1059	774	1364
427	779	0		0	2992	1135	764	1419
427.5	879	20		0	2469	1223	910	1625
428	872	38		0	2911	1014	850	1428
428.5	876	24		0	2388	998	505	1643
429	655	20		0	1393	888	688	1216
429.5	653	0		0	1032	903	725	952
430	525	5		0	810	671	464	957
430.5	603	0		0	1831	828	706	981
431	438	56		0	11	540	885	1244

Table A 2.5 Cuobu XRF Geochemistry S – Tb

Depth (cm)	S	Sb	Sc	Se	Si	Sr	Ta	Tb
27	115	507	442	0	36	699	1436	688
27.5	287	119	106	0	251	1232	1481	98
28	558	262	499	147	510	1094	2522	864
28.5	585	321	360	15	505	1265	2931	850
29	777	314	357	478	633	1225	3197	854
29.5	598	223	359	349	535	776	3154	701
30	584	268	329	74	483	1273	2750	755
30.5	549	351	320	134	465	1132	2854	734
31	658	312	256	381	558	879	2821	786
31.5	658	229	303	536	493	1068	3201	651
32	688	257	379	343	517	1055	3098	775
32.5	725	275	286	489	628	1635	2771	873
33	617	241	338	308	465	1520	2455	756
33.5	610	251	329	0	569	1162	2838	637
34	656	328	354	4	537	1514	2498	869
34.5	702	323	308	107	497	1231	2646	750
35	849	339	387	94	721	858	2545	840
35.5	648	279	311	20	562	1177	2845	829
36	778	303	276	270	599	888	2765	854
36.5	751	232	333	89	619	1458	2996	821
37	877	255	385	621	843	1371	2779	754
37.5	763	334	323	623	628	1076	2641	786
38	838	251	324	272	723	1187	2957	700
38.5	853	267	318	401	780	1163	2623	810
39	1031	234	357	352	852	1140	3017	771
39.5	882	282	371	376	829	963	2925	895
40	832	241	292	282	674	1107	2933	852
40.5	1043	382	345	186	890	1528	2940	804
41	1066	290	346	0	936	1236	2719	802
41.5	1008	286	458	263	903	1172	2715	976
42	934	349	295	279	822	1007	2773	830
42.5	863	295	376	0	764	1168	2558	867
43	892	269	260	280	688	1563	2782	927
43.5	971	374	319	34	828	1315	2528	782
44	927	271	217	114	844	1441	2318	672
44.5	943	344	405	521	775	1373	2329	870
45	943	274	260	491	816	1533	2518	654
45.5	763	223	260	737	784	1232	2790	598

Depth (cm)	S	Sb	Sc	Se	Si	Sr	Ta	Tb
46	953	323	197	411	885	928	2528	610
46.5	823	296	238	226	787	1447	2387	770
47	886	226	277	0	872	1045	2487	644
47.5	891	340	225	173	747	1066	2369	732
48	805	242	266	308	720	1433	2577	738
48.5	967	267	278	229	780	1261	2689	755
49	856	380	298	0	917	1144	2569	701
49.5	747	349	292	357	737	981	2561	814
50	1008	277	355	303	961	1321	2741	862
50.5	1122	308	354	402	1173	1208	2622	944
51	991	305	248	434	970	1046	2376	856
51.5	1010	273	369	513	896	1491	2551	620
52	985	306	283	0	843	1441	2493	682
52.5	1058	209	262	0	872	1472	2146	624
53	1019	246	311	0	859	883	2791	642
53.5	1328	332	312	327	1091	1330	2734	809
54	847	205	218	261	656	1578	2520	718
54.5	836	239	320	234	807	1225	2644	592
55	1240	334	322	0	1386	1064	2567	747
55.5	1058	234	309	443	1051	825	2587	672
56	949	225	340	162	939	1347	2626	842
56.5	972	250	291	287	911	1273	2555	817
57	1075	257	351	91	1007	967	2638	750
57.5	830	286	254	0	875	1147	2785	754
58	822	338	279	0	906	1283	2460	752
58.5	1102	212	255	0	944	1211	2834	628
59	1107	314	261	128	1028	1590	2898	798
59.5	972	290	298	256	962	998	2492	624
60	1004	283	273	135	1174	1139	2844	903
60.5	1097	361	291	152	924	1727	2669	831
61	826	258	262	299	764	1793	2844	649
61.5	863	324	282	557	900	1169	2636	687
62	1173	310	332	268	1094	1412	2464	740
62.5	913	220	283	154	899	1226	2488	744
63	897	243	288	80	813	990	2483	700
63.5	981	181	353	217	994	1004	2876	692
64	964	315	241	55	952	1480	2546	706
64.5	1034	400	346	238	959	1565	2681	902
65	1063	369	318	90	1085	998	2491	765

Depth (cm)	S	Sb	Sc	Se	Si	Sr	Ta	Tb
65.5	1140	294	224	220	1043	1055	2499	686
66	1121	277	237	0	1143	1126	2498	663
66.5	956	329	269	0	1113	1274	2325	695
67	926	327	233	136	1059	1060	2192	707
67.5	1012	332	213	232	1209	1473	2584	635
68	1056	305	377	281	1218	1609	2458	918
68.5	972	333	321	382	1030	1049	2722	857
69	1001	303	336	807	1198	1237	2675	791
69.5	849	272	305	238	931	1224	2522	793
70	1064	323	288	156	1184	1580	2598	753
70.5	806	222	240	133	963	1709	2377	591
71	897	310	281	0	1082	1378	2463	700
71.5	1034	365	325	255	1183	1567	2304	960
72	1041	354	384	0	1302	1332	2794	824
72.5	1001	331	213	36	1496	1074	2280	663
73	1128	294	351	142	1466	1464	2578	840
73.5	1146	413	295	248	1625	1297	2693	877
74	937	392	231	0	1435	1564	2337	541
74.5	451	156	77	82	568	1329	1357	0
75	443	188	89	68	589	850	1442	0
75.5	608	213	173	0	732	526	1690	354
76	836	255	300	174	929	1162	2162	508
76.5	782	293	307	0	1041	1408	2773	572
77	844	241	334	213	1129	1028	2028	713
77.5	814	289	241	586	1050	1676	2263	787
78	811	278	212	498	1034	1587	2477	698
78.5	882	355	325	16	1124	1355	2619	735
79	936	325	344	103	1292	1336	2417	896
79.5	815	389	329	9	1066	1604	2225	902
80	950	379	307	348	1617	1515	2639	734
80.5	914	328	322	277	1203	1199	2617	840
81	789	249	282	0	1188	1239	2698	714
81.5	709	244	310	45	1242	962	2634	706
82	766	320	236	0	1156	1573	2396	724
82.5	848	311	250	82	1150	1771	2762	622
83	951	289	236	149	1710	1405	2519	646
83.5	930	154	162	0	308	932	1073	676
84	1097	184	128	45	343	1020	1128	676
84.5	1095	172	210	115	420	731	1296	639

Depth (cm)	S	Sb	Sc	Se	Si	Sr	Ta	Tb
85	1121	187	142	0	505	649	1464	522
85.5	1137	146	110	146	474	809	1195	700
86	1202	158	146	126	445	936	1315	434
86.5	1222	166	258	95	425	1018	1316	724
87	1206	206	257	143	408	949	1651	729
87.5	1061	198	244	318	478	743	1437	510
88	1146	222	223	151	518	1072	1329	552
88.5	1156	251	219	287	495	1237	1653	605
89	1219	179	195	151	533	681	1603	533
89.5	986	234	154	0	455	1052	1408	278
90	972	197	158	46	427	746	1243	295
90.5	858	249	132	48	425	539	1240	149
91	993	132	152	57	433	717	1324	298
91.5	1067	120	232	0	497	889	1688	621
92	1324	271	260	0	521	1053	1562	583
92.5	1343	281	215	99	612	509	1847	686
93	1329	236	262	259	609	965	1647	575
93.5	1350	248	217	20	571	743	1469	744
94	1302	222	330	25	471	1030	1863	697
94.5	1324	121	194	103	556	1334	1418	752
95	1367	293	179	22	510	1117	1545	792
95.5	1349	185	199	36	514	1018	1677	844
96	1467	202	240	224	424	532	1689	737
96.5	1211	182	177	14	470	963	1481	605
97	1657	234	188	0	521	644	1511	1023
97.5	1658	223	294	298	451	1177	1669	1059
98	1767	195	260	415	411	811	1466	1027
98.5	1837	304	148	253	519	655	1588	1086
99	1646	290	299	0	468	915	1719	985
99.5	1504	374	213	360	508	1036	1663	1040
100	1376	227	255	57	504	1191	1460	830
100.5	1516	237	213	0	532	732	1394	742
101	1703	287	269	112	392	400	1290	1208
101.5	1938	265	298	0	481	497	1598	1249
102	1989	337	340	211	495	657	1759	1215
102.5	1951	304	277	0	391	653	1527	1463
103	1880	241	234	671	351	865	1690	1244
103.5	1806	366	226	49	340	1023	1831	1276
104	1996	307	248	236	316	743	1691	1466

Depth (cm)	S	Sb	Sc	Se	Si	Sr	Ta	Tb
104.5	2238	249	212	149	490	1100	1514	1439
105	2295	255	293	0	458	668	1446	1626
105.5	2178	259	205	139	321	836	1484	1608
106	2271	256	235	302	528	981	1627	1340
106.5	2241	265	278	615	470	676	1859	1428
107	2194	320	275	445	420	565	1692	1333
107.5	1937	203	311	165	387	1347	1742	1476
108	2291	370	153	162	409	837	1635	1506
108.5	2417	314	258	161	451	595	1334	1620
109	1976	392	256	230	481	994	1832	1470
109.5	2043	329	293	304	755	1169	1745	1369
110	2023	224	263	101	445	1166	1671	1335
110.5	1952	329	171	242	445	793	1390	1273
111	1732	245	254	0	338	1158	1507	1241
111.5	1777	206	259	0	454	1112	1581	1475
112	1888	259	244	0	569	668	1583	1042
112.5	1948	272	273	78	684	706	1378	1352
113	1783	199	156	185	539	944	1583	1057
113.5	1656	293	279	84	484	1331	1580	1085
114	2173	376	263	0	554	1215	1462	1557
114.5	2122	321	296	118	524	430	1661	1626
115	2192	318	311	196	553	856	1458	1836
115.5	2284	256	281	0	532	633	1616	1651
116	1714	302	260	88	400	781	1565	1523
116.5	2010	292	236	425	539	1230	1354	1623
117	1994	374	232	153	492	1149	1500	1545
117.5	1668	279	277	337	537	1380	1498	1240
118	1505	220	151	80	512	623	1071	398
118.5	1672	203	202	0	464	921	1100	860
119	1508	374	213	0	540	981	1272	1013
119.5	1576	283	216	110	486	907	1531	1282
120	1711	300	273	0	575	1272	1582	1151
120.5	1688	203	253	144	636	1295	1462	1322
121	1799	236	313	195	772	1467	1462	998
121.5	1630	223	242	0	654	1034	1496	1186
122	1714	292	183	132	624	1162	1668	1240
122.5	1704	322	379	0	711	1047	1537	1271
123	1489	365	359	531	687	752	1730	1086
123.5	1461	231	287	257	663	1020	1697	1152

Depth (cm)	S	Sb	Sc	Se	Si	Sr	Ta	Tb
124	1508	261	269	221	564	1383	1842	1123
124.5	1585	403	261	592	614	1168	1778	1269
125	1467	279	308	524	701	1089	1530	892
125.5	1847	333	286	103	746	982	1601	1427
126	1667	281	265	251	721	1173	1888	1249
126.5	1539	340	202	184	611	540	1524	933
127	1479	266	266	257	513	757	1891	1216
127.5	1540	264	287	330	815	1160	1924	955
128	1503	233	266	0	666	865	1943	1118
128.5	1870	357	307	297	671	1200	1906	1175
129	1836	312	214	159	729	1200	1923	1243
129.5	1926	238	289	127	668	440	2010	1447
130	1819	271	252	300	687	878	1705	1440
130.5	1705	259	269	202	536	886	1636	1214
131	1656	289	313	188	706	992	2046	1193
131.5	1931	324	301	230	781	854	1964	1425
132	1772	249	253	162	875	838	1926	1444
132.5	1899	302	286	319	749	981	2033	1420
133	2132	303	303	209	831	960	1820	1493
133.5	2131	308	328	73	853	1191	1748	1434
134	1816	314	247	43	816	749	1618	1308
134.5	2192	316	244	61	858	675	1781	1420
135	2281	322	275	282	813	750	1779	1446
135.5	2439	344	236	419	854	975	1673	1512
136	1992	180	256	310	903	875	1672	1629
136.5	2584	300	321	229	809	706	1667	1674
137	2411	281	172	0	779	517	1672	2015
137.5	2361	258	314	49	918	587	1698	1787
138	1047	173	141	0	582	907	996	25
138.5	768	187	77	0	447	553	852	0
139	537	176	105	0	184	634	681	42
139.5	1677	249	283	0	569	497	1410	1176
140	2402	200	388	0	731	613	1550	1492
140.5	2334	325	242	191	831	1138	1826	1400
141	2049	282	227	0	707	1082	1569	1426
141.5	2178	268	195	339	716	1168	1743	1733
142	1946	402	250	0	744	998	1636	1355
142.5	2123	297	263	0	706	961	1333	1386
143	2128	245	174	7	1022	792	1455	1553

Depth (cm)	S	Sb	Sc	Se	Si	Sr	Ta	Tb
143.5	1998	353	304	0	718	831	1730	1672
144	1947	187	330	466	812	965	1762	1800
144.5	1980	296	291	454	696	672	1913	1361
145	1945	252	344	0	799	1356	1782	1608
145.5	1961	368	348	17	758	856	1661	1528
146	2168	315	222	81	785	871	1811	1497
146.5	2323	262	315	59	771	467	1866	1784
147	2236	233	337	73	714	863	1812	1533
147.5	2559	310	324	0	713	852	1554	1642
148	2262	292	243	216	726	1129	1809	1571
148.5	2110	311	212	0	721	988	1723	1548
149	1933	314	402	130	724	725	1631	1400
149.5	1618	253	351	291	734	820	1885	1037
150	1247	165	230	383	754	1036	1494	911
150.5	949	186	187	331	452	1072	1567	373
151	978	156	194	56	558	710	1367	365
151.5	873	189	162	435	428	805	1344	640
152	1785	238	235	148	760	654	1766	1306
152.5	2188	326	231	536	721	953	1761	1617
153	2486	320	326	11	743	463	1826	1865
153.5	1757		287	210	1002	703	83	2613
154	1728		181	241	845	1011	268	2705
154.5	1481		249	276	833	779	229	2140
155	1644		269	69	860	1103	303	2536
155.5	1579		303	0	700	519	299	2740
156	1419		355	155	823	1010	343	2411
156.5	1504		278	266	743	758	253	2139
157	1824		275	154	660	622	208	2683
157.5	2099		324	248	651	552	215	3422
158	2289		212	128	560	860	301	3296
158.5	1952		244	10	465	405	142	3273
159	1779		275	283	503	724	257	2956
159.5	1800		297	297	475	573	259	2528
160	1703		275	291	514	698	210	3702
160.5	1442		215	108	462	383	317	3500
161	1560		282	0	585	555	109	2931
161.5	1417		280	271	548	445	290	2274
162	1300		280	153	618	742	188	2161
162.5	1450		289	0	580	851	402	3088

Depth (cm)	S	Sb	Sc	Se	Si	Sr	Ta	Tb
163	1637		194	369	607	525	362	3054
163.5	1633		211	222	594	523	241	4045
164	1444		378	151	555	562	316	3484
164.5	1536		318	149	673	884	293	3185
165	1403		313	196	636	813	217	2339
165.5	1458		259	33	642	840	288	2242
166	1434		269	179	680	867	352	3383
166.5	1556		226	580	531	983	123	3149
167	1330		386	85	606	663	124	2674
167.5	1376		245	461	567	689	268	2222
168	1028		272	282	353	956	167	671
168.5	623		130	0	121	410	71	236
169	852		188	108	230	852	44	1029
169.5	1241		193	0	303	416	194	1943
170	1882		241	305	490	868	174	3088
170.5	1942		299	201	557	748	152	3349
171	1766		255	381	507	871	277	3119
171.5	1692		197	91	494	759	163	2378
172	1862		296	144	480	833	94	3143
172.5	1972		320	168	398	542	256	4034
173	2373		267	337	548	1016	292	3739
173.5	2299		271	432	509	707	99	3554
174	2451		328	369	629	675	205	3656
174.5	2176		229	469	537	822	249	3668
175	1989		267	67	554	570	258	3490
175.5	2141		266	331	669	288	246	3134
176	2047		321	412	670	641	250	2697
176.5	2090		388	402	551	675	377	3240
177	1901		372	66	546	732	282	2776
177.5	1814		283	198	556	566	187	2845
178	1841		327	87	632	610	231	3293
178.5	1509		221	296	592	769	309	2340
179	1628		271	231	520	647	259	2675
179.5	1556		221	217	535	161	186	2517
180	1644		234	454	546	614	214	2635
180.5	1565		311	354	501	769	290	2969
181	1445		269	0	611	914	164	2254
181.5	1419		213	383	597	444	388	2558
182	1406		314	196	404	812	307	2674

Depth (cm)	S	Sb	Sc	Se	Si	Sr	Ta	Tb
182.5	1516		220	692	574	457	313	2378
183	1592		186	207	545	784	234	2405
183.5	1771		330	122	486	502	146	2627
184	1883		304	283	608	852	298	3022
184.5	1967		398	365	496	496	326	2918
185	1981		263	243	576	395	347	2587
185.5	1666		233	283	411	865	249	2844
186	1723		313	470	460	832	301	2353
186.5	1531		199	207	537	972	96	2026
187	1939		297	250	421	1187	190	3007
187.5	2173		289	115	494	346	206	3077
188	2342		340	328	413	775	126	3337
188.5	2038		297	651	391	842	124	3025
189	1692		320	193	456	451	213	3886
189.5	1585		314	383	451	623	159	2316
190	2096		298	290	531	722	407	3044
190.5	1459		210	137	404	442	373	2437
191	1710		315	151	629	757	205	2497
191.5	1669		275	407	786	811	219	2636
192	1762		323	82	779	815	90	2721
192.5	2027		167	50	859	576	179	2272
193	1781		319	82	616	727	241	3788
193.5	1962		347	510	607	950	235	3770
194	1956		292	210	491	495	180	3338
194.5	3549		190	66	473	461	246	4685
195	3286		238	193	529	717	347	3597
195.5	2351		330	360	691	472	192	3452
196	1717		332	137	824	847	289	2250
196.5	1746		263	209	843	1024	275	2394
197	1685		216	532	846	906	234	2171
197.5	1634		301	369	1008	718	415	2558
198	1620		251	393	788	651	200	2205
198.5	1659		222	0	871	637	203	2888
199	1593		204	348	712	924	377	1761
199.5	1765		355	381	824	744	225	2340
200	1893		338	19	858	893	170	2384
200.5	1915		455	22	765	1101	242	1642
201	2052		306	281	640	1062	236	2508
201.5	1689		399	294	493	836	406	2429

Depth (cm)	S	Sb	Sc	Se	Si	Sr	Ta	Tb
202	1963		357	291	572	797	384	3563
202.5	1565		268	60	424	847	143	1863
203	893		145	15	211	665	19	255
203.5	804		181	0	227	362	79	449
204	602		92	187	248	610	124	482
204.5	1425		191	153	431	1041	35	2007
205	1753		305	178	584	935	300	2814
205.5	1831		251	175	605	710	189	3004
206	1957		259	562	584	666	428	2913
206.5	2348		217	406	490	979	238	2299
207	2147		258	472	716	721	225	2250
207.5	1726		333	244	678	957	234	2991
208	1610		299	196	430	604	395	3182
208.5	2187		329	393	508	705	269	2709
209	2202		286	95	520	1029	233	2714
209.5	1817		460	303	680	574	374	2729
210	1642		338	191	679	704	336	2380
210.5	1614		292	179	594	900	98	2554
211	1935		380	197	486	278	208	3462
211.5	1629		242	166	593	922	465	2384
212	1797		301	207	598	840	328	2089
212.5	1974		254	139	416	962	313	3271
213	2156		291	136	512	1040	244	2967
213.5	1871		269	243	260	692	315	3172
214	1601		299	0	289	616	401	3123
214.5	1705		282	172	249	637	337	3140
215	1955		332	409	346	781	226	3639
215.5	1849		253	358	448	881	284	2938
216	2173		388	336	448	723	302	3123
216.5	2738		238	321	454	796	322	3851
217	2701		401	23	461	738	331	3670
217.5	2719		351	218	391	833	183	2886
218	2053		296	278	336	704	310	3203
218.5	2038		361	248	230	897	212	3118
219	1915		226	314	400	883	366	3094
219.5	1762		265	438	411	854	416	2930
220	1615		259	287	405	870	460	2563
220.5	1501		225	255	346	852	299	2239
221	1520		197	131	305	791	404	2631

Depth (cm)	S	Sb	Sc	Se	Si	Sr	Ta	Tb
221.5	1704		335	449	387	1202	297	2809
222	1564		346	9	331	879	332	2231
222.5	1958		239	280	429	1032	327	3019
223	1999		285	456	432	795	339	2300
223.5	1871		340	56	384	913	366	2162
224	1284		265	160	357	610	289	1613
224.5	1515		278	465	176	860	260	2204
225	1648		287	597	362	681	292	2721
225.5	1325		263	85	407	794	240	1931
226	1453		290	344	447	595	273	2352
226.5	1209		289	97	341	483	291	2393
227	1313		242	152	320	410	328	2579
227.5	1287		317	382	295	718	306	2333
228	1296		269	275	303	825	211	1885
228.5	1281		268	98	350	507	347	1862
229	1376		360	0	343	800	328	2568
229.5	1309		209	0	319	649	249	2094
230	1298		252	142	292	417	329	1847
230.5	1467		384	291	392	761	169	1655
231	1703		337	76	451	965	106	1764
231.5	187	146	298	250	69	753	2267	378
232	184	272	296	185	12	1017	2202	492
232.5	215	215	303	236	0	926	2005	476
233	204	76	283	0	23	352	2103	424
233.5	175	114	190	145	67	525	1345	234
234	214	193	239	231	25	1175	2223	417
234.5	219	159	351	287	13	885	1962	449
235	203	185	228	192	35	1145	2053	428
235.5	179	113	238	156	0	986	1803	197
236	192	95	188	113	52	790	2021	375
236.5	179	92	270	336	40	1079	2041	369
237	292	165	319	132	57	1016	2240	545
237.5	226	166	261	119	0	799	2039	506
238	251	170	250	378	0	868	2062	364
238.5	183	113	269	308	0	1030	1768	143
239	176	158	266	252	59	1002	1936	156
239.5	256	113	266	210	36	621	1728	397
240	233	83	274	5	10	928	1725	406
240.5	218	160	273	252	43	910	1879	561

Depth (cm)	S	Sb	Sc	Se	Si	Sr	Ta	Tb
241	193	150	186	0	20	1161	2024	431
241.5	212	199	291	228	7	1360	2016	486
242	151	199	259	277	12	1251	1958	475
242.5	137	140	313	453	36	861	2177	350
243	158	148	223	351	15	912	1776	61
243.5	105	86	226	61	20	922	1738	0
244	83	41	137	244	30	620	1502	0
244.5	63	71	98	167	0	551	1608	58
245	56	85	206	18	0	458	1383	138
245.5	136	118	220	434	22	754	1870	225
246	162	144	201	23	19	673	2099	520
246.5	171	97	252	350	0	1016	2363	476
247	133	107	249	77	0	613	2165	448
247.5	111	85	319	178	0	1039	2065	404
248	177	119	282	494	12	556	1955	258
248.5	148	109	225	304	32	762	2206	244
249	93	160	201	195	0	1247	2070	308
249.5	66	80	260	286	26	604	2204	304
250	166	110	208	261	40	1003	1978	311
250.5	127	62	244	238	0	970	2092	377
251	147	115	239	631	52	1375	1849	317
251.5	114	120	218	316	29	1001	1841	299
252	131	66	210	371	8	1200	1911	240
252.5	117	176	142	464	26	1160	2052	215
253	129	28	304	578	0	772	2058	237
253.5	127	65	291	192	17	656	1730	233
254	131	84	209	343	25	1514	1870	244
254.5	98	107	304	212	100	1051	2028	354
255	124	142	233	312	0	758	1654	461
255.5	152	115	178	268	23	910	2133	336
256	149	115	280	114	28	915	2060	459
256.5	161	133	262	224	4	771	1981	380
257	140	157	311	681	0	672	2333	352
257.5	142	178	249	302	0	973	1932	290
258	107	106	179	141	46	789	1957	219
258.5	133	125	194	423	14	802	2087	365
259	113	106	285	136	27	722	1982	353
259.5	173	161	241	178	58	900	2022	122
260	241	133	205	182	54	858	2019	248

Depth (cm)	S	Sb	Sc	Se	Si	Sr	Ta	Tb
260.5	407	130	321	433	105	739	2336	175
261	620	140	222	642	174	943	2285	422
261.5	949	180	248	520	372	858	2050	350
262	909	235	209	310	478	948	2154	316
262.5	1232	292	305	94	391	968	1828	554
263	1468	295	390	104	420	1156	1816	442
263.5	1258	220	311	226	531	1086	1940	616
264	1131	292	280	550	537	865	2281	571
264.5	1109	288	320	290	512	632	2061	400
265	942	238	324	102	502	689	2266	375
265.5	1033	189	369	369	405	782	1880	498
266	843	193	313	495	415	613	2178	477
266.5	912	239	293	322	462	762	2457	207
267	937	206	236	131	370	576	2015	383
267.5	952	207	355	201	307	834	1798	536
268	733	196	237	203	220	803	1496	274
268.5	838	183	236	318	336	610	2248	378
269	847	248	249	363	338	936	2239	332
269.5	1035	241	290	362	546	746	2347	452
270	963	192	288	298	397	998	2064	497
270.5	1082	283	354	394	369	1189	2057	375
271	880	228	342	421	336	1005	2424	611
271.5	936	220	293	420	348	933	2211	609
272	1017	166	344	189	377	1317	1946	623
272.5	1492	314	365	536	313	659	1965	797
273	1453	256	274	226	354	927	2078	417
273.5	1468	270	313	115	446	933	2004	634
274	1520	327	327	197	353	677	2052	680
274.5	1138	329	318	200	291	721	2511	428
275	1291	240	405	478	369	1014	2499	560
275.5	1279	342	440	321	454	925	2299	728
276	1000	300	387	79	433	650	2245	730
276.5	1073	276	451	367	362	845	2546	618
277	1039	322	310	322	352	969	2164	714
277.5	1192	213	347	207	448	805	2123	647
278	1162	270	353	172	431	926	2180	712
278.5	1082	280	346	609	324	1138	1974	634
279	1109	261	350	115	361	1035	2288	627
279.5	910	229	381	380	436	933	2225	671

Depth (cm)	S	Sb	Sc	Se	Si	Sr	Ta	Tb
280	996	247	315	499	381	1210	2215	599
280.5	929	208	377	0	407	616	2193	544
281	1112	286	443	356	387	789	2217	734
281.5	1096	314	393	575	545	1072	2367	692
282	1127	260	372	302	584	1131	2086	681
282.5	1227	287	452	358	590	857	2254	749
283	1413	366	337	181	564	686	2069	707
283.5	1321	345	328	343	564	1165	2122	830
284	1227	382	298	198	548	643	2084	728
284.5	1124	280	357	197	532	553	2068	865
285	1183	304	396	473	542	698	2192	662
285.5	1184	222	415	92	371	888	2030	869
286	1585	300	253	317	395	938	2329	897
286.5	774	218	176	184	341	902	1059	49
287	575	203	121	79	265	814	1117	0
287.5	459	154	156	178	156	666	720	168
288	787	235	230	0	231	992	1483	460
288.5	1278	287	413	154	380	1084	1981	860
289	1059	247	395	274	494	922	2301	620
289.5	996	196	369	131	466	796	1984	837
290	907	286	343	145	393	692	2199	651
290.5	945	246	301	81	408	672	1764	837
291	739	198	364	41	469	880	2075	742
291.5	1006	227	398	9	460	815	2198	855
292	895	297	419	234	404	423	2234	731
292.5	1025	233	358	411	460	818	2180	722
293	1328	231	392	291	528	543	1807	680
293.5	1455	318	369	139	681	556	1901	626
294	1112	263	388	352	488	947	1958	578
294.5	988	234	359	354	581	1123	2144	565
295	1068	223	345	37	549	971	1971	633
295.5	1341	265	328	81	608	781	1894	731
296	1100	179	200	339	521	855	1323	221
296.5	715	199	187	0	532	889	1242	146
297	569	227	166	0	446	520	1175	35
297.5	532	149	136	155	511	504	1352	103
298	1029	225	375	227	691	915	2213	436
298.5	886	241	298	42	549	515	2238	494
299	1149	261	290	0	639	844	1843	393

Depth (cm)	S	Sb	Sc	Se	Si	Sr	Ta	Tb
299.5	1217	235	306	372	613	833	1958	716
300	1666	185	331	310	768	1220	1950	628
300.5	1541	240	360	14	658	872	1812	538
301	1141	243	309	315	494	927	2121	460
301.5	1273	255	377	303	561	535	1785	553
302	1808	281	278	180	473	650	1870	550
302.5	1322	208	249	224	633	909	1780	448
303	1069	119	315	395	311	991	1764	392
303.5	1636	206	217	291	356	734	1816	507
304	1192	191	286	268	392	738	1709	567
304.5	999	184	244	239	397	530	1804	488
305	908	180	275	338	369	1057	1568	330
305.5	1074	95	276	180	342	1051	1665	389
306	854	189	301	332	337	1211	1782	383
306.5	1015	257	195	7	416	631	1698	381
307	823	207	152	155	368	1051	1704	346
307.5	1073	250	314	249	675	598	1923	1390
308	1082	272	339	166	630	745	2217	1248
308.5	1104	140	227	286	631	1300	2163	1148
309	1166	223	227	219	650	467	2159	1348
309.5	1233	231	281	387	515	607	1898	1411
310	1138	235	257	73	496	1526	2190	1471
310.5	1125	247	182	227	792	1009	2153	1276
311	1249	310	364	356	878	867	2017	1432
311.5	1091	249	315	178	817	1068	1870	1470
312	1072	214	300	630	763	977	2235	1481
312.5	1007	142	209	421	558	892	1811	1135
313	1152	193	242	434	530	1187	2262	1385
313.5	1291	216	219	485	528	750	1681	1648
314	1225	260	279	108	570	944	1681	1122
314.5	1147	186	222	180	562	868	1802	1548
315	1063	237	285	220	526	987	2190	1466
315.5	1255	252	349	482	594	1124	1831	1836
316	1207	213	303	351	540	772	1642	1893
316.5	1226	160	252	296	622	1253	1976	1450
317	1387	230	263	210	599	837	1712	1717
317.5	1398	317	295	241	615	919	1925	1549
318	1710	210	200	496	705	1281	1853	1427
318.5	1385	244	333	287	677	513	1933	1761

Depth (cm)	S	Sb	Sc	Se	Si	Sr	Ta	Tb
319	1598	213	308	151	661	874	1885	1464
319.5	1779	265	381	0	555	1111	1688	1900
320	1657	267	292	239	645	719	1881	1904
320.5	1528	206	270	229	689	672	1770	1822
321	1529	415	304	245	626	835	1900	1657
321.5	1460	235	244	511	502	1318	1811	1578
322	1508	232	388	385	605	919	1782	1968
322.5	1418	239	340	325	491	1035	1883	1861
323	1495	226	399	487	594	997	2044	1938
323.5	1396	238	335	446	594	1034	1865	2157
324	1401	291	276	21	604	847	1940	1998
324.5	1590	227	266	506	644	851	1784	1926
325	1470	221	334	107	694	670	1937	1923
325.5	1205	207	189	508	843	927	2112	1558
326	1314	226	363	317	828	1036	1881	1615
326.5	1044	183	332	364	724	749	1853	1419
327	951	175	281	264	695	1038	1984	1437
327.5	940	234	323	505	699	1094	2082	1097
328	927	268	386	465	771	713	2168	1230
328.5	1160	133	311	195	778	763	1934	1508
329	1166	320	402	362	738	659	1877	1804
329.5	1090	265	290	119	570	638	2013	1756
330	1264	297	317	184	569	801	1647	1736
330.5	1355	223	224	485	679	1074	1725	1513
331	1135	226	357	616	827	904	1881	1271
331.5	1114	172	227	459	800	985	2074	1379
332	1421	252	217	386	844	825	1888	1749
332.5	1222	230	311	0	786	867	1600	1476
333	1076	286	338	134	746	782	2083	1262
333.5	1289	281	368	499	840	948	1917	1779
334	1091	211	258	302	825	919	1869	1591
334.5	1073	250	404	656	796	648	1752	1586
335	1219	240	344	291	1051	1034	1848	1315
335.5	325	199	128	0	188	623	613	23
336	119	201	94	0	18	705	238	0
336.5	113	182	84	45	59	544	211	17
337	726	220	207	377	558	1011	1400	902
337.5	1342	240	318	290	1033	1182	1796	1585
338	1168	279	394	320	848	766	1757	1449

Depth (cm)	S	Sb	Sc	Se	Si	Sr	Ta	Tb
338.5	1324	267	294	108	786	964	1807	1560
339	1235	170	299	240	832	748	1534	2002
339.5	1374	229	336	0	851	914	1864	1518
340	1568	293	282	172	715	722	1614	1605
340.5	1311	296	366	0	878	1063	1888	1835
341	1323	259	337	500	922	667	1580	1442
341.5	1312	336	352	181	833	1026	1839	1318
342	1307	248	354	256	819	1096	1723	1341
342.5	1199	230	358	0	892	1199	1398	1451
343	1450	134	225	140	666	1029	1745	1858
343.5	1264	246	305	160	759	643	1600	1677
344	1451	281	320	174	683	761	1414	1705
344.5	1440	180	306	12	818	843	1684	1467
345	1429	221	241	69	719	810	1653	1518
345.5	1280	250	128	297	725	752	1567	1437
346	1159	198	346	617	855	749	1687	1174
346.5	1089	259	336	65	794	865	1619	1093
347	1235	330	346	521	754	661	2010	1352
347.5	1394	256	297	0	702	1016	1649	1714
348	1165	266	345	115	643	819	1498	1316
348.5	1062	147	337	192	730	954	1425	1103
349	1039	223	215	170	722	739	1319	1125
349.5	1149	192	210	297	673	607	1490	1148
350	1504	242	309	40	586	578	1404	1433
350.5	1561	236	236	140	595	750	1456	1604
351	1044	294	342	386	701	1023	1588	1151
351.5	959	190	268	560	548	1043	1342	1391
352	1050	222	249	184	561	710	1528	1336
352.5	1055	211	226	85	535	677	1453	1576
353	561	214	222	51	365	841	968	445
353.5	556	194	76	0	253	628	597	373
354	594	175	151	194	322	597	788	416
354.5	652	194	192	53	490	116	672	805
355	961	92	240	0	771	750	1532	1272
355.5	1127	236	284	106	763	818	1806	1553
356	1010	236	305	527	559	1055	1479	1107
356.5	1356	218	327	147	577	605	1203	1502
357	975	114	232	78	576	670	1400	1187
357.5	853	213	281	162	564	1039	1402	1214

Depth (cm)	S	Sb	Sc	Se	Si	Sr	Ta	Tb
358	1028	190	269	50	596	576	1379	1320
358.5	847	221	156	234	486	596	1404	1236
359	632	122	170	95	392	397	1118	1098
359.5	770	186	235	0	383	769	961	1295
360	853	157	150	94	271	808	1143	1145
360.5	621	127	246	41	402	1184	1033	643
361	682	120	187	0	408	700	1421	1119
361.5	891	192	262	81	352	888	1186	1338
362	763	174	248	256	472	864	1217	1238
362.5	992	142	198	453	398	937	1368	1313
363	937	187	108	274	513	858	1413	1007
363.5	813	100	119	0	571	977	1473	925
364	783	155	168	359	583	954	1429	947
364.5	840	199	305	207	598	910	1361	853
365	900	131	283	224	553	716	1539	1274
365.5	1051	284	254	44	532	875	1351	1158
366	1009	248	245	51	636	876	1247	1121
366.5	1007	128	266	604	699	1009	1329	1170
367	766	228	292	33	396	703	1201	980
367.5	755	223	211	80	446	609	1251	841
368	718	209	314	114	529	773	1395	865
368.5	1959	294	321	278	834	883	1593	2195
369	1666	214	305	197	901	930	1960	1761
369.5	1639	240	353	113	844	1063	1657	1663
370	2220	271	351	619	861	974	1655	2462
370.5	1896	332	334	403	926	853	2213	1725
371	2118	245	298	141	878	878	1801	1706
371.5	1833	297	399	399	1027	1459	1809	1334
372	2059	282	351	0	896	1066	1620	2263
372.5	2126	288	334	259	822	761	1483	2116
373	1799	243	370	223	916	1041	1852	1760
373.5	1740	290	393	389	875	981	1877	1358
374	2139	274	314	157	831	1033	1964	1757
374.5	1576	208	357	231	798	929	1676	1524
375	2023	222	336	258	900	736	1713	2013
375.5	1836	242	242	56	862	762	1501	1760
376	1695	228	288	418	927	1242	1822	1529
376.5	1738	315	352	93	1019	1235	2004	1605
377	1555	326	301	645	1099	1220	1984	1325

Depth (cm)	S	Sb	Sc	Se	Si	Sr	Ta	Tb
377.5	1511	193	360	377	1032	858	2016	1117
378	1435	159	312	304	1026	1051	1975	1096
378.5	1343	150	335	141	955	953	1872	1176
379	1290	193	351	197	936	857	2098	1034
379.5	1226	221	325	67	997	1193	2225	1031
380	1184	267	316	292	987	1201	2044	971
380.5	1244	275	341	294	1025	1293	1991	994
381	1365	257	261	184	1109	1215	2016	1084
381.5	977	176	219	418	772	683	1795	790
382	1364	240	381	416	1013	1001	2107	825
382.5	1420	244	443	502	962	889	1769	1169
383	1446	223	306	0	1012	881	2047	1155
383.5	1543	247	369	133	1068	851	2286	977
384	1520	248	302	482	1110	1123	2304	1104
384.5	1452	275	314	159	1013	1007	2058	1256
385	1441	281	387	307	1033	667	2184	1043
385.5	1491	278	268	284	951	1181	1962	1103
386	1562	279	342	28	1065	1010	1880	1339
386.5	1572	326	417	266	1006	1299	1940	1333
387	1599	296	417	126	1114	1114	2106	1010
387.5	1541	290	356	348	1253	965	2317	1264
388	1551	252	325	0	1167	1036	2112	1091
388.5	1576	241	294	244	1075	1074	2009	1164
389	1571	291	324	51	1111	1092	1964	1140
389.5	1680	185	320	174	1472	871	2032	1199
390	1425	277	376	366	1211	1517	1916	931
390.5	1520	210	307	523	1049	1029	1693	988
391	1532	200	363	264	932	1196	1793	996
391.5	1564	283	331	291	1114	882	1794	1113
392	1488	269	206	637	1043	898	1787	929
392.5	1462	266	356	262	1051	1273	2013	1046
393	1501	285	286	166	1082	1059	1851	947
393.5	1372	130	280	0	1013	952	1883	875
394	1278	259	383	301	1058	800	1919	825
394.5	1373	234	394	272	1138	727	1959	792
395	1370	230	281	229	1060	959	1930	879
395.5	1489	172	352	409	1232	1039	1804	890
396	1273	227	368	311	970	1030	1899	731
396.5	1445	203	304	77	1121	681	1900	1025

Depth (cm)	S	Sb	Sc	Se	Si	Sr	Ta	Tb
397	1451	250	346	109	1033	1022	1702	1025
397.5	1571	292	273	504	1072	1027	1935	980
398	1544	233	302	220	971	1267	1785	834
398.5	1314	270	286	170	966	1388	1725	1073
399	1430	221	304	591	981	1148	1819	1150
399.5	1678	252	317	298	1017	1159	1944	1046
400	1823	280	326	360	1061	1455	1733	949
400.5	1876	237	378	464	980	1286	1934	1067
401	1568	242	271	233	1043	1011	1814	1207
401.5	1392	306	338	127	941	953	2014	1179
402	1468	192	307	322	1021	929	1799	998
402.5	1619	211	349	391	1143	840	1744	951
403	1610	276	315	26	1177	742	1826	1007
403.5	1589	244	396	283	1174	1128	1835	1076
404	1434	348	358	412	1195	1506	1593	997
404.5	1559	225	346	151	1177	1543	1744	1321
405	1890	277	310	0	1893	1371	1759	1295
405.5	1680	298	324	542	1934	1190	1736	1291
406	1345	181	287	473	1479	1175	1816	865
406.5	1335	255	358	520	1464	1412	1843	1120
407	1558	235	369	0	1441	1259	2029	1154
407.5	1538	227	346	436	1476	1183	2046	1012
408	1630	292	360	0	1620	1126	1456	991
408.5	1745	326	288	267	1646	1201	1903	958
409	1697	260	324	129	1707	1340	2001	948
409.5	1865	284	381	534	1676	1631	1880	1272
410	1776	271	363	406	1558	1409	1993	1062
410.5	1744	321	245	254	1654	1084	1918	983
411	1888	271	366	430	1809	1058	2172	1143
411.5	1950	286	261	308	1692	1181	1613	1240
412	1721	249	356	420	1644	1279	1954	1272
412.5	1914	357	313	80	1687	1492	1858	1110
413	2068	378	278	242	1671	1229	1930	1059
413.5	1827	219	397	325	1629	1427	1804	1136
414	1879	316	210	31	1728	971	1852	1032
414.5	1467	267	278	271	1436	1097	1452	686
415	1362	267	301	0	1260	1014	1366	648
415.5	1360	272	293	157	1493	934	1158	732
416	1846	236	387	331	1668	1072	1697	1187

Depth (cm)	S	Sb	Sc	Se	Si	Sr	Ta	Tb
416.5	1859	308	374	599	1638	934	1847	999
417	1824	333	447	240	1676	1051	1862	1104
417.5	1763	298	261	399	1577	1364	1807	1160
418	1776	278	321	305	1528	942	1908	1277
418.5	1813	312	346	400	1566	975	1985	1135
419	1870	275	335	310	1526	1080	1976	1111
419.5	1798	368	384	213	1544	980	2013	1135
420	2105	224	368	188	1525	1357	1834	1226
420.5	1813	257	346	357	1550	844	1771	1116
421	1814	229	363	260	1631	1164	1941	1178
421.5	1965	242	365	484	1660	1126	1945	1212
422	1836	263	293	244	1555	1504	1774	1155
422.5	1978	346	382	323	1642	1204	1887	1340
423	1821	282	311	331	1736	1108	1735	974
423.5	1945	323	358	276	1750	1286	1909	1035
424	2008	367	294	39	1748	1531	1841	1148
424.5	2098	328	352	494	1794	1011	1910	1031
425	2135	299	414	92	1886	950	2028	969
425.5	2014	185	367	6	1789	912	1875	1023
426	1731	330	345	340	1877	1158	1737	1198
426.5	1692	273	393	457	1815	1393	1749	1063
427	1801	251	307	260	1865	1196	1811	1195
427.5	1821	271	367	308	1837	1210	1602	1183
428	1928	324	372	183	1870	1314	1675	1042
428.5	1998	387	344	510	1861	1375	1777	1191
429	1589	293	276	39	1724	1378	1365	926
429.5	1667	281	209	0	1528	1169	1228	742
430	1406	207	252	383	1431	771	1176	791
430.5	1654	189	205	385	1917	1075	1290	701
431	1007	154	203	148	989	872	970	522

Table A 2.6 Cuobu XRF geochemistry Te – Zn

Depth (cm)	Te	Tl	Tm	V	W	Y	Zn
27		88	185	529	1782	0	18635
27.5		40	69	1389	2138	486	30
28		180	609	2712	4291	181	224
28.5		0	699	2730	4369	0	65
29		398	440	2590	4479	363	156
29.5		295	427	2617	4130	98	135
30		217	528	2735	4278	291	295
30.5		175	649	2552	4327	90	0
31		478	637	2735	4197	113	0
31.5		573	571	2684	4569	0	474
32		369	691	2577	4336	214	22
32.5		221	540	2785	4118	159	72
33		111	514	2620	3941	565	156
33.5		398	425	2620	4102	95	15
34		292	693	2583	3917	179	103
34.5		115	554	2642	4160	0	0
35		52	649	2705	4294	323	123
35.5		93	705	2619	4257	246	40
36		269	542	2677	4443	513	281
36.5		169	537	2705	4071	0	85
37		253	414	2703	4224	472	18
37.5		333	867	2726	4130	242	60
38		80	522	2608	4258	183	221
38.5		66	689	2833	4114	419	117
39		91	542	2627	4286	91	81
39.5		675	841	2821	4368	239	328
40		447	589	2592	4160	272	202
40.5		259	622	2574	4184	606	133
41		188	511	2761	4115	324	223
41.5		88	542	2886	4275	86	199
42		193	670	2712	4401	666	108
42.5		177	538	2769	4360	861	284
43		182	704	2844	3927	157	429
43.5		374	481	2556	4078	651	49
44		333	545	2464	4155	425	112
44.5		265	496	2432	3980	0	190
45		215	439	2323	3914	20	58
45.5		354	319	2461	3946	0	141

Depth (cm)	Te	Tl	Tm	V	W	Y	Zn
46		394	504	2329	3924	191	57
46.5		85	517	2503	3943	180	178
47		255	436	2336	3961	0	132
47.5		195	472	2249	3936	0	17
48		259	517	2271	4013	414	25
48.5		213	541	2437	4062	0	0
49		226	463	2555	3993	50	60
49.5		0	735	2782	3954	0	110
50		36	567	2723	4056	484	143
50.5		417	612	2410	4262	288	207
51		549	644	2810	4110	203	171
51.5		122	479	2410	3894	543	0
52		399	407	2380	3945	0	0
52.5		227	560	2548	4094	321	379
53		54	480	2708	4070	738	41
53.5		402	418	2487	4018	504	0
54		207	514	2594	3910	261	0
54.5		610	289	2660	4385	203	256
55		179	539	2498	4454	0	120
55.5		420	618	2537	4218	225	349
56		0	409	2784	4077	292	159
56.5		166	582	2348	4028	0	80
57		188	548	2704	4091	402	0
57.5		183	296	2455	4194	313	133
58		5	646	2727	4094	169	0
58.5		351	506	2517	4159	164	270
59		327	320	2620	4056	345	83
59.5		354	518	2375	4092	312	271
60		489	446	2474	4131	0	214
60.5		557	706	2454	4162	206	322
61		180	397	2404	3925	107	45
61.5		433	588	2487	4097	0	219
62		169	607	2781	3990	360	166
62.5		289	460	2477	4055	450	79
63		83	415	2386	3780	266	0
63.5		286	546	2770	3876	329	0
64		438	411	2456	3930	431	244
64.5		188	524	2644	3877	145	106
65		302	627	2442	4055	614	17

Depth (cm)	Te	Tl	Tm	V	W	Y	Zn
65.5		149	510	2727	4077	108	0
66		216	497	2457	3897	0	0
66.5		0	429	2372	3668	370	17
67		104	443	2517	4116	359	157
67.5		24	312	2418	4115	417	114
68		263	620	2442	4240	187	214
68.5		229	513	2564	3959	345	91
69		224	457	2403	4135	0	35
69.5		398	373	2606	3937	432	145
70		353	588	2582	3687	139	4
70.5		199	508	2439	3948	156	222
71		449	469	2401	4007	0	279
71.5		334	683	2597	3994	535	53
72		308	629	2611	4184	587	193
72.5		97	628	2306	4317	86	436
73		433	527	2404	3901	97	363
73.5		109	560	2707	4285	74	464
74		69	215	2272	3452	232	36
74.5		12	0	1232	1983	327	0
75		157	0	1359	2111	28	96
75.5		390	417	1786	2716	208	322
76		0	368	2048	3459	410	215
76.5		263	407	2331	3968	247	192
77		182	635	2413	3914	308	161
77.5		226	512	2628	4009	264	368
78		500	511	2397	3957	349	231
78.5		122	476	2371	4099	0	149
79		134	766	2502	4165	420	127
79.5		163	714	2574	4078	593	129
80		231	481	2483	4347	326	183
80.5		407	513	2520	4099	736	113
81		218	505	2501	3805	451	373
81.5		68	607	2500	3979	79	223
82		288	512	2532	4004	0	358
82.5		277	479	2520	4268	74	342
83		122	557	2561	3725	0	447
83.5		0	574	1321	1973	487	33
84		21	405	1304	1802	80	344
84.5		0	437	1589	2109	178	270

Depth (cm)	Te	Tl	Tm	V	W	Y	Zn
85		0	501	1536	2234	289	267
85.5		0	603	1614	2166	179	281
86		13	463	1793	2222	468	120
86.5		84	482	1674	2168	293	280
87		0	390	1621	2387	0	149
87.5		0	669	1584	2277	169	94
88		73	538	1587	2308	136	392
88.5		0	575	1648	2339	359	302
89		0	530	1555	2403	377	356
89.5		25	177	1286	2287	553	184
90		0	380	1172	1977	408	266
90.5		52	199	1181	1949	406	94
91		0	425	1412	1979	226	0
91.5		0	645	1540	2318	215	242
92		0	519	1850	2750	156	295
92.5		118	510	1763	2804	181	530
93		0	688	1814	2741	0	217
93.5		203	782	1769	2595	91	395
94		69	599	2075	2782	667	342
94.5		183	929	1696	2574	332	264
95		0	673	1776	2486	76	169
95.5		26	787	1937	2790	496	372
96		0	722	1912	2666	398	327
96.5		167	730	1562	2400	176	240
97		17	622	2182	2539	167	99
97.5		199	807	2076	2513	680	345
98		100	865	2358	2605	19	309
98.5		88	802	2198	2819	128	433
99		0	980	2148	2869	463	235
99.5		131	804	2132	2916	88	215
100		152	697	1785	2447	275	131
100.5		350	586	1803	2454	88	270
101		129	959	2059	2404	203	164
101.5		136	976	2185	2573	188	278
102		253	695	2459	2700	0	195
102.5		54	909	2222	2756	207	61
103		117	797	2275	2931	219	165
103.5		424	799	2303	2973	342	104
104		406	876	2482	2827	39	194

Depth (cm)	Te	Tl	Tm	V	W	Y	Zn
104.5		339	733	2293	2718	0	170
105		432	825	2387	2526	201	109
105.5		345	786	2508	2435	328	34
106		203	631	2459	2721	216	183
106.5		589	825	2575	2781	0	359
107		570	875	2767	2801	326	314
107.5		449	910	2705	2815	277	136
108		369	858	3019	2748	201	206
108.5		233	1068	3101	2624	39	109
109		412	863	2775	2854	0	356
109.5		436	775	2378	2904	219	473
110		293	792	2504	2805	343	122
110.5		402	750	2751	2730	127	207
111		422	796	2661	2582	0	156
111.5		277	973	2604	2675	61	110
112		373	744	2451	2577	10	195
112.5		42	872	2432	2427	0	62
113		113	485	2346	2587	159	312
113.5		52	899	2546	2865	197	235
114		189	1008	2866	2870	189	250
114.5		323	812	2751	2798	0	162
115		393	852	2854	2583	277	377
115.5		341	835	2841	2512	0	98
116		292	947	2844	2870	121	242
116.5		180	885	2632	2574	121	26
117		325	928	2729	2775	142	387
117.5		408	844	2305	2637	245	482
118		38	311	1772	1973	0	232
118.5		190	559	2125	1968	230	233
119		58	749	2160	2020	119	498
119.5		135	782	2558	2627	202	412
120		159	881	2719	2768	0	273
120.5		273	825	2733	2573	0	247
121		137	717	2848	2707	72	463
121.5		51	692	2639	2800	54	0
122		151	929	2618	2685	271	90
122.5		76	957	2798	2730	94	167
123		165	767	2333	2948	553	283
123.5		192	815	2300	3105	166	375

Depth (cm)	Te	Tl	Tm	V	W	Y	Zn
124		335	690	2124	2855	56	297
124.5		453	907	2272	2953	390	380
125		328	785	2192	3111	394	365
125.5		176	986	2122	2848	427	415
126		211	769	2189	2983	210	116
126.5		19	804	2197	3050	54	127
127		123	682	2133	2947	110	254
127.5		252	855	2109	3046	203	323
128		359	778	2229	2902	0	250
128.5		290	766	2339	2898	0	114
129		324	968	2348	3002	0	276
129.5		219	831	2438	3017	0	347
130		301	890	2270	2915	199	165
130.5		251	781	2263	2763	228	130
131		296	612	2237	2932	320	148
131.5		246	899	2292	2819	148	225
132		364	834	2404	2955	178	268
132.5		310	770	2302	2946	0	422
133		410	858	2449	2933	173	312
133.5		71	881	2365	2892	140	62
134		60	797	2336	3027	391	311
134.5		178	848	2590	2923	0	201
135		243	853	2760	2613	0	171
135.5		264	785	2543	2950	0	218
136		274	987	2572	2756	288	252
136.5		223	732	2681	2635	103	136
137		13	753	2693	2709	66	236
137.5		226	914	2798	2777	352	212
138		0	0	1063	1505	264	71
138.5		0	0	918	1201	593	0
139		37	46	822	976	249	20
139.5		98	666	2061	2516	0	369
140		479	1022	2882	2864	568	338
140.5		337	761	3020	2784	0	204
141		384	721	2989	2637	331	353
141.5		291	765	2836	2841	403	488
142		0	759	2726	2609	0	0
142.5		0	925	2631	2638	386	201
143		388	1004	2656	2718	59	212

Depth (cm)	Te	Tl	Tm	V	W	Y	Zn
143.5		280	983	2606	2819	236	357
144		309	756	2439	3047	374	338
144.5		278	844	2325	2872	0	338
145		209	849	2370	2869	559	158
145.5		390	910	2684	2797	537	131
146		299	929	2613	2844	91	163
146.5		409	943	2748	2976	126	456
147		153	929	2682	2788	40	0
147.5		244	1056	2829	2763	0	167
148		500	948	2910	2922	422	375
148.5		316	992	2575	2884	0	386
149		130	902	2403	2877	267	229
149.5		119	771	2218	2830	200	252
150		117	651	1747	2521	327	156
150.5		270	170	1337	1992	377	0
151		118	444	1259	2102	396	247
151.5		96	560	1353	2158	395	170
152		368	926	2317	3065	677	139
152.5		347	1111	2540	3118	432	327
153		122	979	2793	2836	31	330
153.5	222	384	1446	1822	1874	286	55
154	264	554	1494	1854	1812	102	195
154.5	267	344	1083	1749	1690	195	89
155	218	216	1353	1624	1892	126	74
155.5	171	336	1329	1600	1899	0	73
156	256	502	1158	1650	1917	269	133
156.5	180	274	1354	1682	2041	0	178
157	284	466	1277	1803	1894	261	268
157.5	210	355	1717	1799	1711	260	106
158	196	669	1813	2026	1506	376	355
158.5	293	159	1837	1926	1757	182	124
159	142	562	1821	2157	1741	357	0
159.5	183	466	1691	1940	1784	68	162
160	212	594	1639	1947	2005	0	0
160.5	290	410	1338	1718	2024	76	160
161	303	472	1318	1964	1935	120	149
161.5	255	896	1106	1780	1842	0	115
162	148	292	1104	1716	2114	309	112
162.5	162	263	1270	1791	2018	140	169

Depth (cm)	Te	Tl	Tm	V	W	Y	Zn
163	250	604	1627	1933	1842	61	311
163.5	232	173	1643	1772	2108	414	68
164	301	203	1673	1883	2236	0	0
164.5	180	514	1605	1948	2144	147	176
165	172	199	1460	1751	1974	183	99
165.5	304	175	1223	1700	2055	72	153
166	249	277	1460	1889	2106	149	265
166.5	253	611	1587	1918	2186	536	104
167	252	301	1240	1766	2088	641	0
167.5	154	447	1258	1803	2000	434	235
168	170	534	542	1022	1385	494	85
168.5	149	84	275	744	882	182	151
169	180	570	443	1060	1110	173	96
169.5	211	383	1032	1388	1391	351	41
170	125	677	1890	2088	1879	396	0
170.5	209	272	1719	1798	2088	492	121
171	320	656	1786	1811	2004	467	132
171.5	213	565	1658	1775	1931	402	32
172	200	332	1732	1902	1606	107	50
172.5	197	623	2169	2049	1864	217	217
173	182	515	2280	2077	1971	131	0
173.5	266	795	2032	1963	1889	0	0
174	196	589	2045	1960	1907	76	0
174.5	195	712	1902	2207	2077	0	97
175	239	449	1668	2020	2211	219	37
175.5	247	784	1790	1967	2051	84	77
176	249	476	1497	1996	1895	82	182
176.5	292	583	1973	2073	2095	520	228
177	193	594	1797	2142	1946	208	0
177.5	206	498	1741	2022	2083	190	70
178	356	523	1844	2018	2061	312	0
178.5	174	754	1400	1804	2057	325	187
179	242	454	1662	1916	2077	108	98
179.5	218	410	1635	1846	2015	90	103
180	177	798	1702	1897	1862	153	0
180.5	209	566	1473	1867	2004	257	0
181	198	510	1262	1558	1676	177	336
181.5	127	121	1403	1849	2162	192	0
182	176	495	1378	1940	2113	0	224

Depth (cm)	Te	Tl	Tm	V	W	Y	Zn
182.5	149	622	1466	1705	2021	0	13
183	254	291	1578	2020	2016	287	17
183.5	240	647	1489	2017	2099	231	125
184	180	443	1656	1668	2122	25	346
184.5	194	626	1779	1975	2156	298	173
185	174	676	1436	1969	1986	163	304
185.5	237	567	1688	2085	1846	95	80
186	241	597	1613	1830	2101	561	86
186.5	83	625	1365	1630	1905	426	13
187	181	532	1706	1743	1832	472	107
187.5	226	343	1858	1908	1851	224	0
188	159	652	2053	2097	2039	175	0
188.5	253	589	1799	2195	1818	504	113
189	222	392	1927	2150	2132	79	0
189.5	218	515	1576	1901	1763	437	0
190	248	897	1583	1900	1988	342	233
190.5	244	327	1431	2197	1857	82	43
191	280	379	1754	2103	2243	71	0
191.5	185	511	1501	1908	1775	322	136
192	191	397	1383	1843	1984	104	0
192.5	279	300	1347	2020	2101	267	170
193	184	658	1910	1972	1987	0	133
193.5	274	983	2111	2137	2028	268	352
194	255	427	2309	2393	1782	0	0
194.5	196	788	2838	2856	2030	200	440
195	216	695	2354	2688	2140	239	346
195.5	140	643	1839	2361	2192	175	166
196	288	711	1222	1922	2207	395	45
196.5	259	223	1183	1812	2325	16	67
197	134	548	1221	1778	2205	131	0
197.5	278	879	1457	1942	2239	626	251
198	216	634	1201	1889	2033	389	107
198.5	342	456	1453	1829	2176	391	28
199	276	879	1126	1774	1935	104	155
199.5	298	480	1424	1932	2204	212	46
200	209	390	1720	2137	1894	0	74
200.5	345	614	1435	1796	2050	172	179
201	240	291	1840	2189	2191	242	52
201.5	221	549	1758	1989	1887	378	190

Depth (cm)	Te	Tl	Tm	V	W	Y	Zn
202	218	822	1798	2045	2129	211	146
202.5	243	30	1429	1620	1797	387	35
203	160	367	588	961	1043	785	194
203.5	106	292	437	864	1160	344	70
204	130	0	512	881	921	467	11
204.5	266	490	1241	1804	1833	401	0
205	288	385	1647	2084	1981	200	0
205.5	180	768	1761	2055	2035	80	249
206	213	473	1887	2071	2243	139	0
206.5	184	564	1795	2452	2221	0	27
207	208	479	1840	2174	2282	495	141
207.5	245	395	1605	1997	2103	21	48
208	303	563	1930	2028	2357	174	279
208.5	298	591	2096	2340	1973	420	263
209	201	670	1854	2093	2109	351	213
209.5	263	522	1568	1957	1857	46	267
210	291	662	1387	1773	2074	0	224
210.5	287	384	1374	1930	2034	31	106
211	202	742	2206	2268	1859	289	17
211.5	280	347	1636	1801	1998	208	211
212	375	540	1504	1865	2386	327	0
212.5	211	413	1924	2047	1974	152	145
213	168	384	1925	2224	2168	352	125
213.5	255	669	1929	1944	1840	63	9
214	276	306	1871	2004	1635	423	98
214.5	262	587	2113	2048	1929	144	243
215	276	540	2158	1960	1930	200	120
215.5	270	607	1972	1885	1963	10	185
216	298	593	2503	2240	1904	132	165
216.5	194	519	2730	2119	1808	0	189
217	284	773	2612	2216	1770	250	294
217.5	265	587	2881	2428	1783	78	134
218	219	498	2387	2188	2211	85	188
218.5	308	665	2213	2024	2177	303	317
219	301	378	1873	2074	2081	429	148
219.5	347	452	1505	1798	2141	317	153
220	174	690	1536	1861	1877	57	336
220.5	286	489	1566	1975	2037	46	81
221	156	586	1619	1963	1898	267	258

Depth (cm)	Te	Tl	Tm	V	W	Y	Zn
221.5	286	740	1553	2178	1952	463	13
222	391	469	1506	1997	1983	582	174
222.5	114	671	1812	2168	2125	314	223
223	175	448	1620	1960	1990	562	352
223.5	312	431	1544	1853	2018	74	241
224	246	343	1054	1217	1339	0	75
224.5	52	176	1562	1660	1955	346	0
225	308	329	1539	1808	2123	0	6
225.5	214	376	1242	1744	2014	150	250
226	267	411	1353	1773	2159	276	0
226.5	195	499	1198	1703	1881	398	201
227	169	242	1382	1649	2024	121	145
227.5	228	425	1579	1802	1995	195	7
228	151	348	1324	1958	1959	279	0
228.5	277	111	1232	1558	1936	0	97
229	206	514	1374	1704	2009	338	0
229.5	184	536	1460	1781	1878	49	0
230	192	555	1305	1766	2011	73	206
230.5	188	349	1257	1459	2077	0	0
231	252	447	1274	1589	2003	351	95
231.5		285	483	1277	3118	247	289
232		358	316	1188	3042	202	0
232.5		248	636	1253	3102	408	293
233		43	468	1138	2618	257	155
233.5		125	308	851	2111	325	144
234		337	488	1358	2940	197	318
234.5		332	585	1206	2959	0	187
235		130	543	1494	3040	153	0
235.5		498	475	1344	2878	0	205
236		413	596	1366	3049	213	141
236.5		356	382	1243	2906	0	6
237		552	594	1440	3049	0	405
237.5		589	665	1305	2938	232	147
238		163	492	1283	3047	174	159
238.5		416	448	1116	2732	151	79
239		304	360	926	2894	148	217
239.5		264	528	1163	2840	77	368
240		25	429	1375	2533	130	154
240.5		340	800	1484	2883	104	70

Depth (cm)	Te	Tl	Tm	V	W	Y	Zn
241		219	415	1427	2719	230	0
241.5		191	558	1584	2965	548	211
242		344	616	1278	2812	161	0
242.5		462	273	1206	2955	0	160
243		156	375	1045	2653	393	229
243.5		166	188	807	2422	51	243
244		276	268	888	2258	143	93
244.5		226	221	921	2094	635	71
245		24	249	810	1862	108	15
245.5		418	387	1129	2834	256	271
246		416	489	1182	3114	336	146
246.5		436	461	1332	2852	0	0
247		285	436	1224	2798	109	108
247.5		445	454	1265	2753	575	54
248		583	494	1017	2751	15	193
248.5		201	431	1260	2994	0	0
249		506	364	1121	2997	213	80
249.5		398	370	1219	3044	179	267
250		447	468	1184	2871	67	118
250.5		367	394	1111	2994	82	0
251		425	514	981	2876	224	0
251.5		596	260	1144	2789	269	98
252		232	289	1099	2706	198	0
252.5		563	386	946	3034	0	97
253		375	347	1163	2847	0	196
253.5		432	364	1094	2633	104	0
254		290	587	1218	2912	395	93
254.5		231	401	1254	2956	0	0
255		160	312	1147	2692	279	0
255.5		375	412	1164	2970	58	214
256		369	505	1217	2804	61	0
256.5		535	377	1305	2908	85	226
257		81	498	1242	2874	0	0
257.5		502	392	1382	3067	0	150
258		395	247	1251	3084	295	0
258.5		313	383	1347	2757	408	24
259		63	412	1216	2845	27	0
259.5		527	227	1007	2793	0	316
260		256	381	1317	3024	0	96

Depth (cm)	Te	Tl	Tm	V	W	Y	Zn
260.5		547	358	1424	2990	437	111
261		555	453	1386	3131	173	377
261.5		561	553	1265	2978	0	192
262		288	367	1253	3060	62	101
262.5		361	737	1797	2965	177	236
263		486	842	1663	3118	0	108
263.5		449	724	1683	3021	191	336
264		422	569	1556	3218	41	102
264.5		294	586	1526	3014	29	393
265		340	497	1452	3128	0	287
265.5		426	688	1634	2929	566	131
266		255	381	1531	2918	139	108
266.5		328	282	1336	3133	225	85
267		280	479	1502	2833	0	216
267.5		273	410	1518	2806	0	0
268		331	335	1544	2443	60	134
268.5		629	547	1376	2639	304	168
269		367	369	1431	2960	407	0
269.5		548	379	1567	3250	0	47
270		393	386	1537	2963	149	41
270.5		507	372	1627	3133	395	0
271		454	391	1547	2989	231	292
271.5		388	615	1703	3125	169	120
272		322	410	1474	2794	49	0
272.5		603	536	2067	2924	266	242
273		416	279	1673	2933	205	169
273.5		393	468	1769	3058	468	0
274		431	679	1957	3192	0	196
274.5		483	392	1415	3214	205	26
275		395	471	1732	3339	95	9
275.5		326	520	1820	3405	265	341
276		391	628	1770	3141	184	327
276.5		232	449	1689	3143	0	81
277		230	650	1776	3040	132	74
277.5		347	696	1450	3305	206	209
278		362	736	1607	3301	0	46
278.5		244	667	1731	3083	0	181
279		335	584	1500	3293	167	274
279.5		206	575	1715	3396	115	192

Depth (cm)	Te	Tl	Tm	V	W	Y	Zn
280		416	576	1733	3221	241	359
280.5		132	532	1553	3086	169	34
281		261	777	1697	3132	403	92
281.5		337	579	1696	3337	0	164
282		406	536	1498	3069	110	28
282.5		13	713	1874	3287	0	294
283		372	619	1861	3379	0	153
283.5		288	595	1951	3340	229	168
284		191	439	1592	2957	65	71
284.5		498	653	1764	3078	0	191
285		331	607	1839	3190	126	237
285.5		377	767	1757	3179	272	278
286		322	608	2059	3037	342	301
286.5		0	230	980	1752	448	0
287		89	63	712	1564	310	0
287.5		243	151	764	1237	140	31
288		257	288	1280	2407	339	194
288.5		243	717	1847	3053	416	288
289		265	473	1630	3160	0	274
289.5		39	585	1690	2731	242	88
290		188	618	1834	3171	217	161
290.5		279	609	1504	2794	250	344
291		4	645	1766	2957	209	0
291.5		197	664	1869	3013	32	93
292		202	573	1840	3137	0	190
292.5		372	514	2058	2939	372	397
293		226	842	2025	2868	78	81
293.5		111	716	1885	2719	285	64
294		192	642	1779	3072	439	115
294.5		286	649	1574	3198	0	281
295		145	547	1816	3017	196	110
295.5		33	728	1795	2747	279	158
296		66	296	1183	2224	455	113
296.5		0	198	1057	1842	222	0
297		0	137	996	1653	460	0
297.5		0	242	987	2038	190	106
298		369	424	1340	3060	325	187
298.5		567	501	1496	3197	376	204
299		284	714	1869	2649	263	137

Depth (cm)	Te	Tl	Tm	V	W	Y	Zn
299.5		243	731	1836	2959	158	194
300		141	735	1781	2930	352	78
300.5		261	665	1838	2795	350	197
301		134	603	1767	2861	274	0
301.5		240	672	1914	2730	306	338
302		254	634	2107	2689	200	352
302.5		215	367	1246	2522	388	204
303		264	421	1566	2428	322	198
303.5		0	618	2006	2556	153	236
304		237	584	1705	2761	98	86
304.5		38	506	1340	2564	96	128
305		0	430	1613	2387	525	77
305.5		0	477	1415	2375	283	286
306		204	416	1450	2483	438	179
306.5		271	513	1466	2350	257	349
307		0	290	1560	2289	266	26
307.5	66	297	538	1673	2987	76	161
308	150	473	532	1641	3107	39	71
308.5	147	487	273	1794	2889	419	175
309	133	567	490	1672	3044	290	53
309.5	70	474	479	1698	2810	0	254
310	93	353	284	2005	3022	263	0
310.5	167	383	409	1982	2897	0	186
311	79	293	503	2125	3047	0	55
311.5	37	144	407	1855	2735	285	53
312	163	536	589	2028	3062	109	269
312.5	219	566	507	1728	2978	134	0
313	178	624	362	1807	2908	161	183
313.5	178	375	577	1933	2753	0	0
314	166	468	520	1819	2893	55	283
314.5	230	689	643	2060	2689	200	163
315	185	598	442	2120	2841	233	317
315.5	116	424	541	2177	2757	255	174
316	108	401	616	2179	2496	169	297
316.5	212	336	415	1973	2931	173	122
317	170	392	388	2140	2718	45	67
317.5	118	522	338	2014	2782	0	309
318	225	517	567	2101	2545	401	198
318.5	187	414	372	1993	3105	144	92

Depth (cm)	Te	Tl	Tm	V	W	Y	Zn
319	156	336	385	2201	2702	0	190
319.5	181	582	515	2306	2759	379	431
320	0	265	559	2313	2440	0	26
320.5	126	375	417	2218	2806	312	224
321	86	391	393	1933	2735	0	0
321.5	235	386	465	1886	2768	160	122
322	66	572	448	2125	2461	389	266
322.5	103	692	452	2047	2427	421	249
323	70	642	301	1985	2734	232	121
323.5	76	446	425	1812	2728	101	0
324	59	465	421	1899	2734	0	33
324.5	141	551	520	2002	2809	204	37
325	135	184	368	1831	2568	0	108
325.5	154	253	510	1759	2808	48	24
326	42	426	436	1739	2740	129	156
326.5	151	89	712	1690	2731	339	50
327	168	249	502	1728	2807	0	66
327.5	83	278	517	1572	2930	0	280
328	90	319	330	1691	2889	168	51
328.5	54	269	520	1769	2602	73	50
329	0	303	448	1995	2479	151	0
329.5	144	436	453	1726	2661	13	90
330	117	343	466	1927	2627	146	176
330.5	315	551	392	2074	2810	198	438
331	19	198	467	1926	3190	0	76
331.5	132	227	375	2069	2936	53	140
332	241	556	483	2386	2856	440	389
332.5	133	247	572	1916	2550	197	0
333	41	302	522	1741	2511	235	101
333.5	0	385	500	2096	2687	409	136
334	151	358	675	2074	2662	316	469
334.5	38	240	580	2241	2677	0	208
335	75	74	464	2005	2826	486	153
335.5	6	0	31	507	813	566	22
336	71	0	0	250	420	768	13
336.5	54	0	0	293	468	382	5
337	51	86	357	1380	2100	148	12
337.5	108	368	376	1994	2890	21	228
338	0	280	543	2326	2657	400	165

Depth (cm)	Te	Tl	Tm	V	W	Y	Zn
338.5	184	362	398	2318	2606	183	0
339	165	316	540	2020	2489	182	294
339.5	57	396	426	2188	2414	230	129
340	126	336	509	1866	2255	344	287
340.5	42	302	538	2130	2645	365	281
341	96	97	532	2005	2384	0	88
341.5	96	365	544	2039	2483	72	177
342	83	270	471	2093	2386	146	197
342.5	56	219	550	1706	2351	358	42
343	211	360	452	1969	2486	231	187
343.5	148	189	453	1748	2408	132	90
344	11	196	490	2127	2236	378	0
344.5	0	46	478	2179	2516	271	247
345	131	30	446	2177	2211	266	212
345.5	131	52	441	2065	2234	189	175
346	82	156	555	1798	2456	118	313
346.5	78	0	384	1662	2285	346	0
347	0	240	341	1825	2521	203	107
347.5	11	85	331	2129	2154	0	178
348	15	146	480	1866	2318	0	154
348.5	115	84	547	1731	2222	166	54
349	68	0	351	1633	2240	82	0
349.5	77	0	367	1829	2102	0	0
350	11	97	316	2094	2178	0	86
350.5	74	323	478	2113	2247	358	230
351	10	22	336	1699	1950	409	113
351.5	24	0	364	1849	2061	264	55
352	100	245	494	1874	2319	321	298
352.5	95	0	587	1779	2140	302	79
353	0	0	47	846	1532	492	172
353.5	141	0	128	815	1146	501	122
354	8	34	137	988	1158	14	61
354.5	96	61	307	1041	1247	195	0
355	120	79	527	1449	2452	0	195
355.5	104	263	323	1846	2706	374	81
356	20	138	494	1797	2076	267	210
356.5	0	144	233	1707	2027	171	211
357	147	0	410	1524	2046	155	139
357.5	26	66	366	1530	2012	488	24

Depth (cm)	Te	Tl	Tm	V	W	Y	Zn
358	0	73	445	1578	2105	251	73
358.5	17	0	221	1453	1856	241	118
359	59	0	274	1418	1743	204	24
359.5	0	12	365	1396	1760	455	72
360	35	0	161	1496	1659	110	151
360.5	46	0	242	1009	1646	601	51
361	81	43	373	1380	1692	627	208
361.5	47	86	308	1350	1841	485	265
362	51	0	429	1545	1706	226	140
362.5	169	144	390	1400	1898	592	226
363	173	125	353	1527	2061	122	105
363.5	164	67	187	1402	1887	305	129
364	100	143	424	1379	2105	397	192
364.5	19	0	369	1230	2130	280	219
365	125	0	420	1421	1944	324	89
365.5	59	106	469	1832	1994	82	238
366	49	27	361	1781	1924	244	100
366.5	79	0	334	1442	2122	0	0
367	0	0	401	1334	1865	532	190
367.5	18	0	155	1259	1813	526	31
368	12	101	392	1438	1909	13	49
368.5		286	786	2277	2671	495	80
369		141	486	2158	2645	208	119
369.5		202	413	2093	2753	245	122
370		0	281	2566	2406	175	0
370.5		201	230	2263	2914	358	375
371		189	365	2592	2696	30	386
371.5		122	511	2297	2783	264	305
372		20	481	2067	2474	440	167
372.5		118	477	2126	2670	174	206
373		0	404	2282	2940	0	88
373.5		180	161	2192	2695	0	283
374		159	235	2339	2821	193	449
374.5		220	229	2064	2275	249	7
375		278	185	2216	2445	298	168
375.5		354	234	2098	2345	10	331
376		258	274	1906	2558	297	333
376.5		305	101	2307	2880	0	353
377		100	308	2060	2834	416	337

Depth (cm)	Te	Tl	Tm	V	W	Y	Zn
377.5		308	409	1824	3046	118	388
378		183	363	1974	2911	203	433
378.5		69	278	2008	2905	344	117
379		205	308	1608	2778	252	147
379.5		184	98	1871	3013	384	402
380		0	336	1644	2978	192	0
380.5		277	280	1704	2831	341	247
381		94	380	1656	2878	15	224
381.5		0	254	1444	2529	328	99
382		117	276	1613	2795	155	332
382.5		286	276	2154	2881	303	126
383		200	289	1746	2840	0	430
383.5		272	211	1998	2892	393	258
384		217	276	1829	2943	105	287
384.5		235	270	2031	3047	388	223
385		40	267	2067	3040	331	403
385.5		90	414	1858	2919	238	153
386		245	392	1969	2988	13	201
386.5		29	346	1822	2942	231	421
387		232	212	1769	3016	588	252
387.5		274	178	1796	3098	0	401
388		16	142	1603	3057	303	432
388.5		0	368	1677	2745	460	205
389		135	325	1496	3055	249	496
389.5		303	314	1772	2772	175	448
390		36	435	1567	2596	191	159
390.5		91	310	1797	2786	11	157
391		34	354	1695	2760	491	309
391.5		184	368	1797	2797	232	232
392		9	324	1647	2850	582	364
392.5		352	371	1554	2918	248	370
393		51	213	1601	2779	68	0
393.5		229	293	1663	2656	291	158
394		155	311	1499	2599	126	270
394.5		135	282	1628	2732	342	204
395		190	277	1603	2792	112	239
395.5		96	203	1914	2506	161	168
396		0	152	1475	2711	223	204
396.5		240	210	1772	2868	460	278

Depth (cm)	Te	Tl	Tm	V	W	Y	Zn
397		0	314	1632	2630	366	58
397.5		89	363	1463	2637	226	328
398		25	270	1771	2820	399	375
398.5		48	408	1878	2709	450	155
399		151	193	1891	2732	185	334
399.5		135	168	1414	2504	109	0
400		56	360	1683	2835	387	137
400.5		31	302	1711	2671	281	156
401		0	421	1871	2723	353	481
401.5		263	213	1755	2705	202	349
402		65	133	1792	2705	0	197
402.5		0	193	1655	2521	0	153
403		248	368	1571	2948	35	161
403.5		18	401	1350	2693	439	412
404		260	403	1884	2795	131	452
404.5		57	151	1914	2557	258	202
405		21	237	2291	2805	189	356
405.5		167	334	1463	2339	566	200
406		9	192	1811	2693	0	245
406.5		167	208	1840	3109	364	304
407		221	293	1855	2894	362	240
407.5		233	283	1921	2966	141	353
408		28	316	1788	3052	55	486
408.5		0	286	1899	2823	131	268
409		203	238	1709	2897	0	259
409.5		322	331	1700	2972	305	636
410		334	329	1743	2968	174	527
410.5		83	276	1582	3016	105	377
411		261	253	1805	2994	0	480
411.5		140	340	1628	2707	275	411
412		190	368	1627	2917	306	513
412.5		226	299	1405	2702	471	487
413		0	345	1729	2605	129	287
413.5		0	220	1594	2738	0	347
414		0	355	1592	2801	168	161
414.5		0	277	1412	2384	302	403
415		0	201	1438	2188	201	284
415.5		0	297	1404	2277	391	292
416		0	393	1762	2663	0	130

Depth (cm)	Te	Tl	Tm	V	W	Y	Zn
416.5		0	457	1836	2829	142	302
417		167	327	1632	2758	0	298
417.5		59	333	1896	2811	84	232
418		75	192	1820	2900	167	497
418.5		287	312	1594	3045	409	452
419		334	251	1804	2808	193	545
419.5		384	353	1801	2875	509	416
420		121	210	1903	2935	278	343
420.5		0	215	1858	2773	0	313
421		252	271	1960	2935	312	456
421.5		141	279	1778	2642	0	441
422		247	387	1934	2846	270	422
422.5		114	258	1918	2933	369	362
423		152	482	1785	2752	262	587
423.5		159	394	1736	3081	316	345
424		156	268	1670	3102	342	451
424.5		85	274	1562	2931	69	545
425		0	161	1622	2767	402	551
425.5		126	333	1822	2821	344	481
426		14	351	1860	2925	309	530
426.5		114	221	1731	2852	357	388
427		48	187	1930	2834	187	538
427.5		172	299	1669	2919	122	595
428		105	267	1718	2871	76	447
428.5		49	358	1700	2840	746	410
429		0	276	1358	2354	590	367
429.5		42	264	1346	2091	379	286
430		186	308	1312	1711	188	271
430.5		163	270	1213	1978	47	280
431		0	125	951	1841	500	203

Appendix 3: Galang Co age model produced by Bacon® with composite depths vs. mean age.

Table A 3.1: Galang Co Depth vs. Mean Age (BP) for composite core.

Depth (cm)	Mean Age (BP)	Depth (cm)	Mean Age (BP)
1	-62.9	35	141.9
2	-60.8	36	210.3
3	-58.6	37	277.2
4	-56.5	38	344
5	-54.4	39	410.7
6	-52.6	40	477.8
7	-50.9	41	540.5
8	-49.2	42	604.3
9	-47.4	43	667.8
10	-45.7	44	731
11	-44.1	45	792.7
12	-42.5	46	856.8
13	-40.9	47	920.6
14	-39.2	48	984.3
15	-37.6	49	1047.6
16	-33.5	50	1110.8
17	-29.4	51	1178.4
18	-25.4	52	1246.3
19	-21.3	53	1313.6
20	-17.3	54	1381.2
21	-9.3	55	1448.7
22	-1.3	56	1516
23	6.7	57	1584.8
24	14.7	58	1653
25	22.6	59	1721.1
26	33.9	60	1789.4
27	45	61	1855.3
28	55.9	62	1922.1
29	66.9	63	1988.6
30	77.8	64	2054.9
31	90.9	65	2121
32	103.8	66	2179.8
33	116.4	67	2238.3
34	129.2	68	2297.4

Depth (cm)	Mean Age (BP)
69	2355.9
70	2414.3
71	2485.8
72	2556.9
73	2628.8
74	2700.7
75	2772.8
76	2836.3
77	2900.3
78	2964.5
79	3028.6
80	3091.5
81	3150.8
82	3210.9
83	3271.8
84	3332.9
85	3393.6
86	3433.5
87	3472.5
88	3511.3
89	3550.2
90	3588.5
91	3629.3
92	3669.8
93	3710.2
94	3750.5
95	3791.5
96	3831.1
97	3870.6
98	3910.4
99	3950.3
100	3989.9
101	4036.2
102	4082.1
103	4128.2
104	4172.5
105	4216.8
106	4261.9
107	4306

Depth (cm)	Mean Age (BP)
108	4351.9
109	4397.1
110	4442.2
111	4485.7
112	4529.3
113	4572.7
114	4616.2
115	4659.4
116	4700.6
117	4741.6
118	4783
119	4824.7
120	4865.5
121	4905.5
122	4945.4
123	4986.1
124	5026.4
125	5067.7
126	5115.2
127	5163.4
128	5211
129	5259
130	5306.3
131	5349.4
132	5392.4
133	5436.3
134	5479.9
135	5524.2
136	5565.8
137	5608.4
138	5650.8
139	5694.1
140	5737.4
141	5764.3
142	5791.3
143	5818.2
144	5845.5
145	5872.4
146	5903.2

Depth (cm)	Mean Age (BP)
147	5934.8
148	5966.3
149	5997.9
150	6029.6
151	6081.2
152	6132.7
153	6184.2
154	6235.8
155	6287.3
156	6338.1
157	6389.4
158	6440.5
159	6491.5
160	6542.5
161	6583.7
162	6625.9
163	6667.8
164	6709.5
165	6750.9
166	6781.5
167	6812.4
168	6843.3
169	6873.4
170	6904.4
171	6933.1
172	6961.9
173	6991.1
174	7020
175	7048.5
176	7075.9
177	7103.7
178	7131.1
179	7158.7
180	7185.8
181	7202.6
182	7219.1
183	7235.8
184	7252.6
185	7269

Depth (cm)	Mean Age (BP)
186	7285.5
187	7302.3
188	7319.1
189	7335.6
190	7352.2
191	7369
192	7385.9
193	7402.7
194	7419.7
195	7436.7
196	7453
197	7469.8
198	7487.2
199	7504.6
200	7521.9
201	7537.9
202	7553.9
203	7569.7
204	7585.6
205	7601.5
206	7616.5
207	7631.3
208	7646.2
209	7661.1
210	7676.2
211	7691
212	7705.9
213	7720.8
214	7735.6
215	7750.4
216	7765
217	7779.9
218	7794.8
219	7809.6
220	7824.4
221	7840
222	7855.6
223	7871.4
224	7886.3

Depth (cm)	Mean Age (BP)
225	7901
226	7917.7
227	7934.3
228	7949.6
229	7964.4
230	7979.2
231	8013.5
232	8047.9
233	8082.1
234	8115.8
235	8148.2
236	8230.7
237	8313.5
238	8393.8
239	8474
240	8554.5
241	8649.3
242	8743.7
243	8838.4
244	8932.7
245	9027.2
246	9127.9
247	9229.7
248	9332
249	9433.7
250	9536.1
251	9624.1
252	9713
253	9801.9
254	9891.1
255	9979.8
256	10072.8
257	10166.3
258	10259.6
259	10352.5
260	10446.4

Depth (cm)	Mean Age (BP)
261	10536.9
262	10629.3
263	10721.3
264	10813.7
265	10904.9
266	10993.9
267	11084.6
268	11176.4
269	11268.2
270	11358.6
271	11422.3
272	11485.7
273	11548.9
274	11610.6
275	11671.1
276	11721.9
277	11772.3
278	11819.8
279	11865.6
280	11671.1
281	11721.9
282	11772.3
283	11819.8
284	11865.6
285	11911.7
286	11958.3
287	12004.1
288	12050.3
289	12096
290	12141.9
291	12189.6
292	12234.2
293	12279.5
294	12326.3
295	12374.4

Appendix 4: Galang Co XRF Geochemistry

Table A 4.1 Galang Co XRF Geochemistry Al – Br

Depth (cm)	Al	Ag	Ar	As	Au	Ba	Bi	Br
14.25	85		15491	0	209		0	350
14.75	57		11980	0	215		0	241
15.25	126		4181	95	637		351	865
15.75	85		4350	312	627		315	291
16.25	77		5519	463	681		392	320
16.75	87		7979	230	578		118	550
17.25	106		8086	423	532		303	162
17.75	114		7361	321	692		563	519
18.25	104		6597	536	505		366	447
18.75	112		4813	422	649		315	727
19.25	116		4437	405	671		681	271
19.75	75		4040	419	676		351	387
20.25	119		3913	291	593		337	0
20.75	153		4623	473	464		314	411
21.25	115		4632	773	514		640	150
21.75	110		4676	488	693		483	309
22.25	97		4905	358	561		264	501
22.75	108		4260	544	541		249	373
23.25	120		4100	410	571		416	378
23.75	102		5041	548	857		449	343
24.25	116		5515	708	578		468	413
24.75	122		4496	458	619		482	566
25.25	74		5041	483	732		389	671
25.75	124		4530	405	574		194	270
26.25	118		4755	459	656		279	0
26.75	117		5269	716	620		436	301
27.25	159		5164	513	653		369	467
27.75	150		4972	96	480		169	539
28.25	132		5964	112	570		162	429
28.75	157		5569	371	533		293	545
29.25	140		4498	380	376		379	268
29.75	132		4799	445	507		417	320
30.25	94		5557	281	595		480	636
30.75	125		5153	503	516		359	648
31.25	87		5753	316	431		468	437
31.75	112		5620	702	642		383	581

Depth (cm)	Al	Ag	Ar	As	Au	Ba	Bi	Br
32.25	110		4908	242	518		335	165
32.75	112		4697	656	432		377	295
33.25	143		4799	340	366		436	389
33.75	144		5173	390	596		347	507
34.25	53		5015	333	471		306	265
34.75	86		4576	436	665		426	520
35.25	103		5035	216	533		103	67
35.75	138		5010	497	489		400	523
36.25	112		5339	431	596		463	0
36.75	76		5565	510	537		331	640
37.25	103		5850	615	628		295	635
37.75	155		5444	570	728		594	673
38.25	116		5323	409	509		516	322
38.75	141		5645	502	652		663	372
39.25	146		5205	531	698		285	453
39.75	175		5000	611	578		424	299
40.25	100		5215	395	715		473	396
40.75	77		5305	384	395		333	276
41.25	104		5249	434	486		273	223
41.75	129		5443	379	474		306	260
42.25	137		5513	567	548		160	412
42.75	47		5167	488	545		271	205
43.25	164		5652	724	446		224	797
43.75	173		5569	730	653		770	60
44.25	116		5518	460	709		191	338
44.75	149		6250	258	733		263	494
45.25	136		6187	625	442		479	337
45.75	126		6166	470	484		280	68
46.25	171		6112	357	544		362	576
46.75	108		5946	347	374		412	119
47.25	105		6451	622	349		599	75
47.75	132		6459	735	630		464	451
48.25	98		5967	580	370		540	373
48.75	131		6295	349	565		340	661
49.25	95		6345	290	535		232	449
49.75	128		6115	589	514		344	298
50.25	141		5963	489	408		556	259
50.75	69		6323	564	360		256	322
51.25	116		6233	408	411		358	83

Depth (cm)	Al	Ag	Ar	As	Au	Ba	Bi	Br
51.75	113		6192	330	496		145	365
52.25	134		6770	633	548		208	245
52.75	111		6969	364	270		305	475
53.25	203		6155	183	227		225	468
53.75	173		7030	217	511		175	240
54.25	182		7195	334	216		348	633
54.75	131		6945	274	396		286	287
55.25	141		7585	31	386		325	233
55.75	158		7306	210	219		133	673
56.25	108		7473	349	659		275	805
56.75	165		7375	431	377		171	492
57.25	166		7736	557	401		484	636
57.75	114		7265	248	483		311	378
58.25	119		7535	542	555		455	357
58.75	66		7814	586	265		506	226
59.25	163		7585	296	429		369	425
59.75	110		7234	442	407		187	324
60.25	125		7886	575	281		522	271
60.75	97		7052	563	517		338	171
61.25	99		7689	453	406		259	0
61.75	234		7488	694	785		487	280
62.25	136		7539	346	408		281	117
62.75	117		7731	579	545		351	213
63.25	149		8161	630	481		392	0
63.75	118		8120	339	448		68	50
64.25	80		8395	535	401		337	26
64.75	160		7835	489	628		442	72
65.25	107		8595	691	180		407	99
65.75	125		8234	619	384		443	253
66.25	127		8452	482	232		296	0
66.75	96		8677	409	684		175	112
67.25	134		8644	488	462		486	158
67.75	164		8744	426	420		322	14
68.25	84		8983	306	484		556	0
68.75	78		9003	540	448		410	161
69.25	145		8628	364	449		222	0
69.75	161		9013	362	285		108	102
70.25	114		8571	110	668		201	285
70.75	124		8589	260	473		325	0

Depth (cm)	Al	Ag	Ar	As	Au	Ba	Bi	Br
71.25	132		8833	407	312		117	0
71.75	134		8936	127	342		328	309
72.25	107		8899	31	587		7	177
72.75	172		9206	316	311		190	469
73.25	113		9240	279	330		204	418
73.75	151		9024	274	448		263	512
74.25	168		9305	436	623		340	447
74.75	116		9359	127	449		262	723
75.25	122		9331	139	726		261	419
75.75	122		9208	185	234		241	465
76.25	134		9267	365	504		134	434
76.75	167		9672	235	560		127	532
77.25	42		9562	156	395		291	577
77.75	86		9439	312	419		60	250
78.25	127		9092	0	508		0	311
78.75	130		9453	197	477		249	420
79.25	127	0	8084	245	347	41	282	180
79.75	135	12	8532	535	429	0	133	514
80.25	131	43	9321	508	502	0	265	435
80.75	87	0	9258	138	317	87	80	459
81.25	121	47	9306	289	452	184	267	353
81.75	158	0	9989	425	602	0	89	896
82.25	90	25	8978	330	580	233	324	639
82.75	175	52	7361	587	516	0	588	506
83.25	142	61	7949	372	737	81	223	499
83.75	158	14	7751	475	531	37	316	718
84.25	171	0	8704	213	538	220	380	983
84.75	151	0	8104	333	404	0	433	712
85.25	119	7	7485	542	568	435	438	713
85.75	158	96	8129	365	554	154	472	584
86.25	131	0	7851	311	542	0	363	593
86.75	106	0	8383	430	377	163	310	518
87.25	145	0	8838	220	496	0	297	551
87.75	176	0	9070	303	377	270	338	834
88.25	103	0	9327	490	551	0	448	914
88.75	167	0	9185	428	215	122	233	809
89.25	71	72	8996	917	623	145	341	720
89.75	175	0	8804	812	835	0	355	844
90.25	159	138	8500	929	536	124	288	321

Depth (cm)	Al	Ag	Ar	As	Au	Ba	Bi	Br
90.75	139	103	8982	745	523	0	210	144
91.25	182	420	7904	0	228	162	0	75
91.75	253	503	7902	0	0	0	0	0
92.25	221	372	8107	386	217	0	0	0
92.75	156	420	8353	346	331	58	0	0
93.25	170	219	8695	1005	402	0	134	140
93.75	159	83	8345	785	552	40	237	0
94.25	122	35	8266	784	731	158	424	239
94.75	123	0	8352	953	647	0	548	280
95.25	91	7	8327	521	564	0	126	408
95.75	145	0	8785	572	523	0	492	356
96.25	185	0	9174	553	655	156	284	567
96.75	116	0	8929	689	489	350	421	419
97.25	188	118	8623	344	413	231	388	310
97.75	120	71	8735	620	546	608	562	144
98.25	150	22	8839	429	564	324	368	274
98.75	233	0	8891	307	619	0	395	558
99.25	109	0	8277	620	442	221	221	249
99.75	155	0	7594	404	694	170	360	242
100.25	149	0	7789	641	694	91	302	85
100.75	165	7	7595	701	482	0	408	283
101.25	130	4	7575	758	570	101	572	249
101.75	180	45	7465	585	593	102	416	230
102.25	161	82	7188	408	216	34	219	454
102.75	166	0	7429	448	597	306	237	62
103.25	111	31	7839	332	546	537	186	509
103.75	87	21	7622	632	429	584	237	813
104.25	168	0	7510	389	586	0	359	682
104.75	123	30	7921	175	463	557	187	675
105.25	138	0	8042	497	344	516	249	602
105.75	124	82	7609	195	637	0	497	859
106.25	148	0	8033	213	539	96	356	581
106.75	136	0	8554	408	435	32	427	472
107.25	141	29	8322	357	372	131	270	754
107.75	138	0	7726	333	777	214	369	950
108.25	138	34	8619	462	554	0	151	925
108.75	111	0	8275	95	501	97	225	581
109.25	129	0	8384	289	521	73	241	868
109.75	101	0	8577	619	602	333	372	948

Depth (cm)	Al	Ag	Ar	As	Au	Ba	Bi	Br
110.25	127	0	8464	308	413	129	299	679
110.75	122	0	8457	323	363	0	230	525
111.25	125	0	8341	486	670	184	453	880
111.75	129	0	8036	524	525	194	537	1048
112.25	78	50	8546	440	665	571	563	644
112.75	102	0	8426	532	439	559	208	540
113.25	142	0	8584	180	612	0	420	909
113.75	118	0	8537	410	368	188	303	686
114.25	140	17	8328	424	523	436	529	653
114.75	120	25	8655	306	484	627	344	752
115.25	190	0	8610	550	542	499	402	690
115.75	156	0	8212	490	466	308	54	605
116.25	201	0	8412	591	502	234	494	607
116.75	182	31	8082	293	533	0	573	817
117.25	137	0	7746	681	455	68	306	1025
117.75	153	0	8096	440	667	0	357	713
118.25	145	0	7440	582	463	201	276	458
118.75	220	0	7222	402	630	348	399	545
119.25	80	52	7776	382	463	0	275	1057
119.75	99	59	7291	554	487	215	532	883
120.25	123	0	11395	112	423	0	0	1018
120.75	93	0	14257	0	384	0	0	494
121.25	24	0	14437	0	204	6	0	377
121.75	65	0	14991	0	271	49	0	501
122.25	106	0	6721	255	483	19	101	599
122.75	140	0	6396	542	487	255	547	972
123.25	153	0	7544	346	500	163	454	691
123.75	155	30	7278	468	597	186	480	598
124.25	127	0	7757	490	579	1010	278	562
124.75	121	0	8323	405	280	741	309	127
125.25	136	0	8110	366	589	74	5	532
125.75	142	0	7837	303	474	134	334	413
126.25	123	0	8191	292	395	674	148	397
126.75	121	0	8321	557	325	171	440	468
127.25	157	0	8169	636	383	793	285	179
127.75	151	0	8137	517	601	9	444	198
128.25	111	0	9040	518	459	814	307	345
128.75	192	0	8365	188	503	1251	284	97
129.25	147	0	8504	380	288	356	501	759

Depth (cm)	Al	Ag	Ar	As	Au	Ba	Bi	Br
129.75	143	0	8225	592	464	235	377	601
130.25	117	0	8085	708	343	825	448	603
130.75	137	0	8379	742	411	490	267	877
131.25	121	0	8701	754	288	144	432	445
131.75	120	0	8445	709	405	214	482	636
132.25	170	0	8372	673	446	0	275	767
132.75	156	0	8802	703	469	539	134	567
133.25	105	0	9230	479	508	0	215	834
133.75	140	85	9277	512	638	0	346	549
134.25	104	0	9598	422	396	226	459	814
134.75	166	0	9645	643	537	0	387	907
135.25	110	151	9421	821	590	0	461	533
135.75	160	6	9310	659	447	392	367	996
136.25	129	25	9194	690	635	122	320	776
136.75	100	0	9463	426	513	0	505	678
137.25	122	0	9880	728	476	0	353	662
137.75	143	25	9409	515	782	0	293	383
138.25	162	150	9334	634	576	0	250	719
138.75	122	0	10042	1044	638	0	348	756
139.25	109	13	9977	847	569	0	208	572
139.75	205	15	9828	584	466	86	219	1176
140.25	146	0	10248	920	537	0	177	917
140.75	156	29	10168	681	654	13	119	486
141.25	131	0	10190	720	592	0	32	784
141.75	179	0	10589	417	509	371	106	379
142.25	99	0	10256	566	730	426	33	429
142.75	172	0	9939	473	346	34	306	543
143.25	100	0	9979	594	395	0	617	305
143.75	131	0	9965	1067	603	54	188	657
144.25	113	0	9898	1205	447	0	539	0
144.75	176	0	9726	1174	517	484	321	119
145.25	196	0	10289	706	684	1122	416	0
145.75	321	0	10038	503	558	2853	221	125
146.25	329	0	10243	724	530	2199	440	18
146.75	310	0	10430	265	466	1987	350	0
147.25	345	0	10445	532	610	2455	450	0
147.75	217	0	10068	746	667	1633	251	460
148.25	137	20	8976	474	353	183	240	879
148.75	113	0	8875	581	446	142	319	1157

Depth (cm)	Al	Ag	Ar	As	Au	Ba	Bi	Br
149.25	125	59	8637	711	533	0	24	784
149.75	106	0	8518	737	616	0	524	992
150.25	157	0	8518	424	727	0	513	833
150.75	157	0	8619	721	715	170	393	909
151.25	167	0	8494	503	522	0	358	667
151.75	178	22	8182	723	327	153	459	510
152.25	232	0	8254	715	665	0	473	591
152.75	193	0	8607	760	642	471	273	100
153.25	171	0	8369	975	551	951	528	615
153.75	163	21	8459	743	608	0	441	438
154.25	108	27	8716	838	563	0	586	350
154.75	138	0	10199	450	374	0	269	30
155.25	112	44	12803	0	388	378	0	134
155.75	49	0	14433	0	203	269	0	178
156.25	53	0	16089	0	133	109	0	41
156.75	89	18	15579	0	292	204	0	129
157.25	125	104	7000	392	375	373	120	491
157.75	159	86	6814	465	784	296	539	378
158.25	130	88	7490	348	578	549	589	548
158.75	168	50	7845	313	699	511	346	633
159.25	140	81	7847	214	399	1097	70	102
159.75	107	0	8034	497	592	131	345	502
160.25	111	6	7666	179	481	492	131	203
160.75	158	60	7724	626	618	132	303	517
161.25	137	77	7366	910	631	44	471	323
161.75	108	195	7126	317	516	411	339	155
162.25	150	27	7250	625	430	254	372	570
162.75	176	116	6927	363	874	0	337	354
163.25	149	0	7226	447	746	0	713	339
163.75	127	114	6798	394	845	375	142	949
164.25	99	66	6146	640	791	166	387	95
164.75	157	94	6276	780	893	175	428	52
165.25	107	120	5409	570	723	0	598	602
165.75	127	268	7407	0	542	0	0	1085
166.25	49	66	17079	0	241	0	0	362
166.75	91	57	12136	0	311	79	0	17
167.25	131	48	7229	128	946	132	42	506
167.75	101	43	7506	481	948	57	299	378
168.25	146	83	7119	654	730	65	305	431

Depth (cm)	Al	Ag	Ar	As	Au	Ba	Bi	Br
168.75	146	98	7402	601	581	788	576	480
169.25	183	83	7476	536	718	2098	366	318
169.75	131	0	7715	491	564	818	330	0
170.25	140	93	7044	521	358	2028	412	116
170.75	176	35	7016	200	432	4144	385	214
171.25	186	152	7410	575	764	2324	346	398
171.75	118	86	7459	240	663	2114	176	242
172.25	145	0	8776	350	646	1041	451	586
172.75	163	13	9678	435	459	1721	163	427
173.25	128	0	11152	224	324	707	144	369
173.75	113	0	14220	141	444	476	87	69
174.25	112	0	11520	380	449	298	0	0
174.75	156	4	7502	36	614	154	96	396
175.25	170		8191	676	567		727	190
175.75	116		7965	478	599		483	361
176.25	118		7595	798	573		389	226
176.75	117		7172	389	556		409	138
177.25	148		7441	649	630		382	345
177.75	161		7168	712	538		307	446
178.25	131		9396	434	511		308	242
178.75	121		12739	0	440		0	0
179.25	90		13100	13	451		0	0
179.75	53		15612	0	226		0	99
180.25	102		6170	378	680		242	176
180.75	185		7054	345	496		433	362
181.25	174		7373	319	616		696	193
181.75	134		6711	883	870		643	785
182.25	143		6959	272	774		492	658
182.75	117		7283	9	804		493	978
183.25	91		6276	522	707		528	783
183.75	140		7197	216	698		547	866
184.25	85		7201	242	910		716	656
184.75	147		7188	367	836		267	442
185.25	147		6754	486	604		354	804
185.75	133		5652	330	624		207	877
186.25	134		6567	378	850		554	836
186.75	117		6581	800	699		422	268
187.25	100		6365	730	492		435	331
187.75	106		6858	523	576		531	419

Depth (cm)	Al	Ag	Ar	As	Au	Ba	Bi	Br
188.25	204		7192	826	714		316	482
188.75	151		7641	740	753		504	136
189.25	104		8306	332	524		419	154
189.75	71		8208	446	569		512	630
190.25	137		8093	506	420		143	765
190.75	134		8154	731	707		562	554
191.25	124		9021	361	522		410	965
191.75	145		8544	593	463		460	548
192.25	165		8509	853	583		492	284
192.75	85		8729	418	492		592	415
193.25	178		8322	701	583		411	452
193.75	134		7523	464	416		438	153
194.25	135		7768	663	755		399	378
194.75	127		7116	358	739		299	208
195.25	158		7000	611	625		717	304
195.75	169		7026	493	792		95	583
196.25	162		6540	493	761		387	428
196.75	183		6945	321	559		295	662
197.25	63		7955	365	766		331	591
197.75	126		7511	377	644		619	493
198.25	153		8229	657	414		625	764
198.75	141		9549	402	651		336	441
199.25	66		8970	438	632		382	599
199.75	124		9166	496	376		321	206
200.25	154		9180	321	439		231	164
200.75	162		7914	558	645		638	162
201.25	156		8747	287	659		398	121
201.75	83		11506	260	416		0	19
202.25	83		16158	0	337		0	0
202.75	62		15322	0	90		0	0
203.25	87		14281	54	585		27	235
203.75	101		7301	573	400		329	102
204.25	156		7476	423	491		376	273
204.75	106		7260	333	343		529	120
205.25	122		6558	493	866		489	73
205.75	163		7980	496	616		414	164
206.25	121		8852	530	506		250	700
206.75	149		8593	438	690		200	63
207.25	163		7985	782	690		528	450

Depth (cm)	Al	Ag	Ar	As	Au	Ba	Bi	Br
207.75	179		9387	525	320		288	56
208.25	159		9016	744	613		308	98
208.75	90		8042	572	680		454	350
209.25	117		7945	891	746		539	434
209.75	105		7688	489	691		320	219
210.25	174		8170	499	624		156	146
210.75	114		8374	237	621		291	317
211.25	144		9302	642	526		186	483
211.75	112		9038	151	463		127	503
212.25	123		8792	423	642		464	421
212.75	166		8672	603	469		378	461
213.25	88		8385	211	461		274	415
213.75	123		9034	442	461		429	209
214.25	119		8820	406	629		436	422
214.75	135		8227	143	677		352	594
215.25	101		7870	415	608		264	521
215.75	104		7543	331	649		370	0
216.25	131		8375	265	916		114	167
216.75	142		7798	331	733		634	479
217.25	137		7758	427	672		425	318
217.75	149		7953	218	789		636	253
218.25	150		8205	570	621		265	294
218.75	138		7208	827	534		531	315
219.25	179		6864	664	856		503	269
219.75	162		7179	9	503		410	638
220.25	74		6489	663	838		364	0
220.75	178		8079	361	660		243	484
221.25	137		8490	402	612		736	930
221.75	126		8764	499	563		354	264
222.25	96		10227	396	546		301	43
222.75	122		8008	324	497		462	145
223.25	200		7022	687	478		106	286
223.75	132		6597	1244	421		334	310
224.25	145		6221	1232	883		463	197
224.75	182		5884	823	898		651	173
225.25	70		6117	512	612		448	539
225.75	170		6716	413	678		538	135
226.25	129		6274	369	507		266	112
226.75	196		7045	240	733		217	723

Depth (cm)	Al	Ag	Ar	As	Au	Ba	Bi	Br
227.25	122		8567	403	884		268	529
227.75	122		8495	290	850		236	432
228.25	153		8047	829	455		460	288
228.75	180		8509	462	768		496	266
229.25	180		8862	596	493		313	224
229.75	118		8738	545	406		511	0
230.25	120		12550	189	483		0	0
230.75	53		15756	0	317		0	0
231.25	22		15447	0	139		0	0
231.75	117		10948	187	442		371	513
232.25	103		8185	320	590		373	0
232.75	176		8104	515	679		263	205
233.25	129		8507	301	601		161	427
233.75	118		8783	531	500		684	403
234.25	196		7880	845	581		577	438
234.75	144		9105	496	575		389	467
235.25	168		8899	524	529		482	312
235.75	104		7391	488	348		357	0
236.25	163		8349	441	364		412	207
236.75	193		7972	256	451		177	183
237.25	129		8797	216	419		206	217
237.75	115		8379	464	406		525	662
238.25	137		8280	613	649		473	368
238.75	137		8231	390	665		350	0
239.25	125		8026	477	472		463	107
239.75	181		7347	465	783		454	276
240.25	124		8653	453	438		539	485
240.75	133		7822	223	419		214	311
241.25	71		6341	542	585		265	147
241.75	163		6007	482	817		78	831
242.25	58		6016	401	761		401	957
242.75	174	0	7982	307	374	940	496	95
243.25	140	0	7290	304	676	304	254	0
243.75	131	0	8477	303	518	854	393	213
244.25	162	0	8646	0	537	871	507	33
244.75	186	55	8758	689	524	750	210	25
245.25	165	0	8260	852	627	812	401	0
245.75	163	28	7297	33	610	1067	526	0
246.25	133	0	9310	421	456	758	507	299

Depth (cm)	Al	Ag	Ar	As	Au	Ba	Bi	Br
246.75	145	0	8164	706	626	551	581	402
247.25	124	0	8870	1002	514	286	641	116
247.75	138	0	8145	402	381	718	681	200
248.25	204	0	8091	523	355	498	532	45
248.75	121	0	8529	770	571	653	611	132
249.25	111	0	9046	776	368	1036	376	180
249.75	157	0	9628	244	445	682	546	331
250.25	151	0	9404	582	475	705	314	223
250.75	155	0	9020	560	427	743	410	12
251.25	205	189	8424	520	591	661	648	427
251.75	125	175	8193	858	208	657	385	86
252.25	154	298	8013	1230	587	520	695	502
252.75	190	19	8123	1400	574	675	568	148
253.25	149	248	7929	1333	509	744	732	512
253.75	151	260	7686	1061	633	754	644	147
254.25	86	229	7721	616	820	496	592	151
254.75	122	194	7645	1158	520	182	710	496
255.25	141	225	8131	1230	389	478	496	294
255.75	168	293	8070	856	429	598	416	13
256.25	95	472	8087	1102	514	338	884	304
256.75	124	129	9422	861	647	467	442	187
257.25	210	33	10616	356	399	413	375	230
257.75	114	46	10800	449	487	577	392	247
258.25	96	0	9379	715	446	28	446	143
258.75	139	0	8444	628	855	484	484	22
259.25	134	0	9689	988	659	221	427	0
259.75	108	0	9145	463	548	356	437	0
260.25	140	0	9971	269	793	332	509	248
260.75	167	0	7399	521	552	499	396	744
261.25	167	0	8925	614	294	627	487	170
261.75	93	0	8993	534	331	898	232	120
262.25	129	269	8562	788	506	555	467	0
262.75	112	161	8100	722	821	630	638	291
263.25	175	288	7211	942	620	369	673	213
263.75	121	203	6600	1159	617	0	520	145
264.25	144	46	7470	662	736	610	676	0
264.75	144	347	7362	1030	637	599	649	143
265.25	131	21	7458	436	499	545	454	0
265.75	118	16	7279	697	596	547	720	237

Depth (cm)	Al	Ag	Ar	As	Au	Ba	Bi	Br
266.25	163	226	7529	805	519	264	545	95
266.75	185	260	7768	517	563	342	584	74
267.25	186	33	7947	549	634	796	455	152
267.75	159	0	8020	295	541	367	483	405
268.25	147	0	8595	777	492	779	406	218
268.75	142	0	8566	567	482	506	470	134
269.25	142	0	8072	108	562	766	477	0
269.75	149	0	9326	117	198	1009	198	71
270.25	152	0	8880	0	0	1671	0	155
270.75	137	107	9208	0	239	1241	40	85
271.25	168	269	8476	0	0	710	0	539
271.75	221	404	7598	0	0	655	0	537
272.25	196	484	7930	0	0	596	0	207
272.75	261	617	7694	0	0	578	0	518
273.25	162	272	8413	0	68	487	0	565
273.75	146	299	8441	0	568	548	328	858
274.25	108	414	8391	790	708	285	251	649
274.75	141	0	12651	1013	918	268	331	514
275.25	128	0	12798	310	369	0	15	0
275.75	98	0	13529	644	492	0	142	0
276.25	92	0	12166	405	613	19	57	146
276.75	111	36	9913	1102	405	82	336	0
277.25	126	545	6856	947	649	176	490	19
277.75	142	356	7129	796	858	272	625	410
278.25	178	517	7433	699	607	145	560	163
278.75	147	171	7664	937	724	387	663	273
279.25	185	52	7929	765	739	385	741	251
279.75	156	0	7756	1316	804	359	466	483
280.25	97	0	7130	1249	606	248	491	0
280.75	93	246	7060	1254	606	7	434	89
281.25	154	110	6860	1072	829	0	571	44
281.75	125	148	5992	1206	985	99	420	256
282.25	123	8	6958	1064	792	182	634	460
282.75	173	141	7026	1001	756	62	578	443
283.25	124	270	7497	1111	814	69	800	595
283.75	139	508	6019	1255	726	115	646	0
284.25	168	816	6173	1095	714	136	758	311
284.75	115	823	6635	740	661	132	522	120
285.25	136	397	7143	801	661	0	559	298

Depth (cm)	Al	Ag	Ar	As	Au	Ba	Bi	Br
285.75	139	7	7156	762	637	147	486	0
286.25	147	44	7938	1177	550	0	380	574
286.75	145	0	7261	475	896	318	288	385
287.25	166	153	7688	0	308	517	136	633
287.75	266	628	7209	0	0	453	0	484
288.25	190	227	7765	0	0	1291	0	163
288.75	145	0	8521	430	375	1845	131	324
289.25	184	0	8865	527	234	2139	402	418
289.75	128	41	8690	543	419	1863	481	195
290.25	157	0	9378	227	425	766	490	126
290.75	183	0	6279	419	279	1172	359	121
291.25	155	0	8574	348	501	1785	534	475
291.75	159	0	8647	205	450	1406	315	330
292.25	173	0	8377	0	329	1136	461	235
292.75	232	0	9701	113	277	1513	239	359
293.25	137	0	10173	249	413	1198	266	260
293.75	199	46	10271	147	249	1465	384	12

Table A 4.2 Galang Co XRF Geochemistry Ca – Hf

Depth (cm)	Ca	Cl	Co	Cu	Eu	Ga	Ge	Hf
14.25	18937	103	517	328	61	400	143	154
14.75	26260	45	361	450	927	472	233	186
15.25	45327	116	851	525	2313	441	476	177
15.75	48633	74	819	640	3657	383	113	177
16.25	56344	19	1282	646	3494	410	87	204
16.75	51547	66	1108	541	3376	210	172	211
17.25	43389	106	1201	637	2891	322	173	207
17.75	44202	37	964	601	3202	587	26	159
18.25	42918	57	1184	762	2077	684	300	181
18.75	46318	90	1025	630	3047	525	368	239
19.25	43096	56	1057	526	3555	785	264	105
19.75	44064	0	1218	629	3281	378	0	217
20.25	44929	90	987	395	4035	647	369	116
20.75	46652	15	1522	460	3129	575	133	162
21.25	46213	55	1304	596	3855	531	6	167
21.75	43905	57	1216	585	3239	596	200	251
22.25	45489	66	1340	617	3846	265	552	164
22.75	43730	18	1239	407	2871	605	239	241
23.25	43602	16	1131	550	3505	609	577	100
23.75	49754	43	1436	497	3863	642	352	317
24.25	47903	95	1575	456	3709	647	429	230
24.75	51304	49	1387	511	3784	551	313	270
25.25	54481	81	1593	488	3402	565	307	188
25.75	52322	49	1439	504	3357	353	286	88
26.25	54949	59	1480	543	3526	480	162	212
26.75	56879	68	1446	651	3880	627	258	211
27.25	56899	63	1392	674	3366	815	155	278
27.75	57889	66	1138	540	3162	606	340	249
28.25	59036	40	1245	375	3105	368	209	277
28.75	54239	56	1046	559	2656	134	98	221
29.25	53139	5	756	589	2284	472	526	247
29.75	55598	38	826	630	2462	541	267	139
30.25	51123	104	788	781	2666	666	447	259
30.75	52365	54	942	790	2605	762	339	229
31.25	54830	53	913	516	2913	357	262	126
31.75	52610	48	1269	686	2692	259	140	398
32.25	54221	63	1126	689	3149	491	263	140
32.75	53089	18	799	741	3277	349	441	182

Depth (cm)	Ca	Cl	Co	Cu	Eu	Ga	Ge	Hf
33.25	53297	47	918	343	2872	450	336	188
33.75	50688	24	712	695	2873	716	589	76
34.25	44459	15	793	554	2492	531	539	325
34.75	46340	12	793	700	2813	613	509	251
35.25	46711	57	700	718	2867	236	317	141
35.75	42804	13	912	829	2319	427	550	205
36.25	45971	26	846	760	2226	624	356	330
36.75	44031	55	645	742	2853	262	396	170
37.25	45213	35	1014	749	2345	535	339	307
37.75	44970	25	1207	524	3204	387	210	194
38.25	47409	0	1106	549	3625	216	281	136
38.75	51414	14	1256	860	3659	383	0	53
39.25	52535	25	1326	682	3459	577	339	213
39.75	55706	23	1441	371	3640	578	505	233
40.25	58763	52	1776	522	3427	479	108	219
40.75	60557	62	1728	540	3564	420	353	128
41.25	61740	52	1483	664	3194	383	157	130
41.75	61526	77	1330	571	2796	341	286	266
42.25	56731	60	1358	706	3273	151	419	278
42.75	57867	64	1230	661	2807	593	276	90
43.25	55396	38	1144	951	2360	717	537	299
43.75	53853	10	1037	592	2107	709	91	215
44.25	57956	21	947	728	2539	545	229	201
44.75	60781	85	797	721	3288	342	17	233
45.25	61936	75	1081	598	2850	520	429	212
45.75	63916	24	1096	721	2748	503	262	277
46.25	63609	47	1004	537	3362	80	478	246
46.75	64640	63	1324	609	1965	203	384	223
47.25	70552	82	1155	643	3223	396	113	178
47.75	68747	82	1540	803	2600	515	422	267
48.25	65910	44	1227	708	2763	637	530	243
48.75	66637	50	1157	786	2684	708	606	196
49.25	64400	29	1100	690	2588	488	426	260
49.75	63898	77	1109	765	3380	636	397	247
50.25	62835	53	1149	792	2869	322	152	194
50.75	69343	47	1482	466	2976	287	365	249
51.25	69394	74	1238	428	2694	602	510	312
51.75	72924	55	1353	726	3020	409	381	234
52.25	75811	81	1320	498	3150	380	106	238

Depth (cm)	Ca	Cl	Co	Cu	Eu	Ga	Ge	Hf
52.75	89138	73	1455	640	2085	492	331	101
53.25	102910	79	988	440	1955	533	610	168
53.75	102671	49	916	594	1203	532	222	218
54.25	105465	72	1014	478	1486	383	364	337
54.75	96442	97	693	638	2241	874	335	173
55.25	94145	92	809	677	2467	692	0	130
55.75	83408	77	604	478	2109	466	286	248
56.25	73891	38	608	941	2683	671	155	162
56.75	58230	36	635	734	1936	124	597	289
57.25	50620	66	542	820	2476	752	579	241
57.75	44880	54	710	819	2173	221	283	203
58.25	44206	57	921	765	1997	665	422	292
58.75	45737	0	762	532	2780	270	546	295
59.25	43215	44	702	654	2616	517	395	238
59.75	39201	38	829	763	2634	675	490	230
60.25	52759	69	706	565	2754	396	756	253
60.75	62287	75	829	620	2719	362	239	252
61.25	59518	59	907	503	3099	389	148	234
61.75	45942	28	1411	718	3318	300	135	247
62.25	46641	83	1183	499	3880	324	268	291
62.75	53789	17	1248	470	3143	555	425	398
63.25	51527	60	1057	617	2647	749	343	354
63.75	48707	28	1285	556	2829	300	35	189
64.25	43449	54	1340	396	3692	462	353	193
64.75	37041	61	916	663	3610	469	371	270
65.25	45545	43	992	577	3424	581	661	341
65.75	45272	20	1144	402	2981	510	640	206
66.25	34750	39	910	937	3629	530	420	241
66.75	42461	5	1069	667	3839	459	175	300
67.25	42629	30	1020	670	3478	765	296	424
67.75	61993	65	755	742	3292	784	427	200
68.25	50396	50	1074	543	3236	258	17	342
68.75	40045	26	985	675	3687	404	404	352
69.25	35007	0	1162	651	3508	272	93	390
69.75	38827	17	1087	712	3056	487	370	335
70.25	38793	49	935	685	2791	324	204	261
70.75	37423	33	1082	466	3098	201	360	356
71.25	46071	37	1193	658	3203	555	224	369
71.75	39303	12	713	902	2656	570	129	152

Depth (cm)	Ca	Cl	Co	Cu	Eu	Ga	Ge	Hf
72.25	54185	46	787	704	2446	198	140	244
72.75	68099	52	961	579	3052	311	287	335
73.25	62539	65	854	458	2648	334	537	463
73.75	42711	46	508	908	2905	615	524	295
74.25	40190	19	387	758	3058	568	677	202
74.75	40957	39	898	781	1971	384	587	361
75.25	40947	77	268	872	2687	507	61	375
75.75	45632	23	515	747	2959	404	326	133
76.25	50611	59	827	674	2855	616	70	266
76.75	53128	57	674	938	2843	560	284	268
77.25	71054	75	927	477	2504	182	464	248
77.75	86706	65	963	594	2505	559	307	298
78.25	88458	21	986	527	2547	435	112	382
78.75	90307	63	1081	336	2920	533	474	375
79.25	80214	107	1032	476	3530	793	404	208
79.75	74335	140	1127	487	2387	328	61	364
80.25	63322	168	907	565	2121	456	270	314
80.75	70152	224	1083	359	1733	415	0	236
81.25	64790	112	1024	602	1991	470	156	287
81.75	62392	122	927	812	2366	516	125	153
82.25	67755	50	1105	699	1590	657	327	374
82.75	85921	58	1358	622	3297	169	278	176
83.25	81513	74	1236	528	2831	90	175	382
83.75	88756	41	1080	582	3341	430	94	271
84.25	91578	95	1134	501	3648	452	283	320
84.75	88114	114	1246	635	3658	481	547	143
85.25	90527	98	962	568	3407	554	224	296
85.75	92446	105	1084	918	3035	874	480	336
86.25	86550	68	749	871	2870	524	328	265
86.75	88303	90	985	647	2518	106	135	160
87.25	86376	67	912	631	2210	297	63	329
87.75	79612	79	801	550	2862	487	454	194
88.25	75794	109	1007	867	2763	146	409	308
88.75	67249	115	985	753	2823	678	505	331
89.25	51774	81	866	651	3160	411	621	353
89.75	47439	74	938	825	3351	624	401	216
90.25	67142	26	942	488	3155	0	227	385
90.75	148962	45	807	472	2036	419	9	328
91.25	509538	227	791	0	1852	0	0	356

Depth (cm)	Ca	Cl	Co	Cu	Eu	Ga	Ge	Hf
91.75	620346	210	1114	0	2020	0	0	246
92.25	414909	129	1422	348	2866	367	0	309
92.75	360186	146	1737	110	2264	0	0	190
93.25	167792	81	2011	564	3383	202	0	145
93.75	119978	43	2193	222	4017	51	46	176
94.25	66303	40	1887	542	4286	414	35	142
94.75	42101	52	2018	634	4031	443	163	277
95.25	42274	44	1897	425	3403	529	133	366
95.75	46602	79	1745	770	3965	614	416	135
96.25	51722	46	1737	299	3448	663	124	295
96.75	63190	47	1866	503	2734	242	173	99
97.25	70101	71	1640	639	3462	338	0	175
97.75	75519	91	2205	485	2600	380	180	277
98.25	76635	96	1766	540	3029	685	128	198
98.75	78082	86	2077	392	3341	369	166	222
99.25	68747	75	1786	627	3305	421	363	262
99.75	72375	49	1694	590	3024	451	0	276
100.25	80604	37	1711	671	3387	373	85	174
100.75	81376	104	1652	596	2940	469	245	247
101.25	82034	65	1442	504	2789	440	109	324
101.75	78499	71	1534	578	2977	480	141	225
102.25	81127	105	1416	443	3056	320	263	284
102.75	88112	69	1687	595	3041	212	0	238
103.25	87862	52	1552	556	3031	530	237	221
103.75	89829	70	1677	682	3288	368	225	348
104.25	86263	73	1422	680	3070	248	173	307
104.75	82555	52	1163	788	3304	145	79	102
105.25	82717	28	1238	529	2630	364	471	389
105.75	81953	82	1830	744	2870	537	309	246
106.25	78805	33	1323	611	3454	537	41	207
106.75	82664	71	1147	797	3070	576	0	82
107.25	79942	60	1034	655	2966	433	274	254
107.75	80204	58	1315	813	3199	490	63	201
108.25	78926	51	1076	696	2482	534	184	439
108.75	80008	58	1063	863	2263	444	298	258
109.25	83658	57	968	805	2436	419	364	278
109.75	82529	74	977	606	2407	569	313	132
110.25	80346	54	1014	621	2936	164	280	275
110.75	83515	54	1000	586	2727	184	441	315

Depth (cm)	Ca	Cl	Co	Cu	Eu	Ga	Ge	Hf
111.25	83496	57	1219	639	2488	508	367	386
111.75	81746	47	1035	640	2530	489	394	194
112.25	77994	32	1513	641	1588	409	305	310
112.75	76286	74	1231	555	2588	452	403	226
113.25	84036	111	965	681	3029	346	527	489
113.75	87381	87	989	692	2859	422	289	153
114.25	89090	75	1176	707	2744	641	420	251
114.75	86136	56	1031	806	2751	507	202	318
115.25	78929	47	1149	650	2330	611	368	359
115.75	82416	40	1090	599	2386	355	217	303
116.25	79510	31	1103	723	2666	428	319	282
116.75	75169	86	1022	719	2969	430	475	270
117.25	76238	50	1206	661	2342	500	390	243
117.75	77297	103	1156	565	1903	362	0	194
118.25	81904	6	1175	658	2056	295	255	158
118.75	85497	23	993	624	2696	711	91	265
119.25	84702	51	981	700	3145	515	212	233
119.75	78979	0	1101	708	3217	564	112	203
120.25	54061	33	609	554	586	358	276	327
120.75	26472	35	249	391	0	268	143	218
121.25	18417	41	207	335	0	327	100	228
121.75	18786	9	245	304	49	345	192	104
122.25	39142	20	531	457	1389	485	234	246
122.75	72194	87	1109	591	2989	441	402	163
123.25	79511	52	1521	752	2202	261	211	88
123.75	89135	93	1407	796	2768	682	591	227
124.25	113939	73	1478	625	3084	436	289	345
124.75	108169	95	1691	390	2791	79	352	171
125.25	114750	53	1508	750	2489	308	138	168
125.75	112933	80	1449	530	2158	96	203	149
126.25	115873	76	1399	455	2189	181	225	379
126.75	116965	120	1536	717	2387	474	296	161
127.25	120070	78	1432	579	2416	263	25	83
127.75	96156	81	1686	732	2518	812	156	146
128.25	92365	51	2118	425	2380	899	470	224
128.75	111007	64	1830	754	2143	325	71	60
129.25	114433	75	1265	742	1940	556	401	230
129.75	107232	92	1144	667	2368	405	289	207
130.25	98497	63	1285	719	2076	358	382	211

Depth (cm)	Ca	Cl	Co	Cu	Eu	Ga	Ge	Hf
130.75	88829	65	1145	586	2645	497	416	189
131.25	90498	86	1081	701	2156	630	256	273
131.75	82770	52	1227	515	2419	485	197	286
132.25	81580	50	1079	820	2036	373	429	211
132.75	83955	101	1230	785	1874	546	325	142
133.25	98968	52	1210	855	1794	428	487	227
133.75	98969	86	904	715	2485	630	242	393
134.25	92556	67	1253	695	1425	319	311	323
134.75	84917	68	1285	661	2352	553	262	350
135.25	79767	26	1294	725	2148	629	308	319
135.75	81112	54	1202	655	2342	508	182	217
136.25	85151	45	1268	752	2013	324	269	299
136.75	80180	75	1120	774	2701	359	82	273
137.25	76682	41	1303	658	2702	219	446	321
137.75	72843	67	1419	831	2554	566	0	275
138.25	65811	7	1346	687	2168	511	0	278
138.75	62810	18	990	714	2823	458	292	363
139.25	62403	34	1081	738	2891	407	328	324
139.75	63394	0	1286	656	2195	433	155	352
140.25	62112	17	1108	808	2476	360	431	212
140.75	61853	50	1177	661	2991	471	0	213
141.25	62113	8	1624	827	1518	156	207	240
141.75	64599	64	1379	513	2410	352	205	319
142.25	67940	18	1715	687	2229	437	311	344
142.75	68128	73	1354	472	2561	285	90	194
143.25	62568	11	1747	523	2160	494	272	361
143.75	46999	75	1775	722	3161	756	150	313
144.25	44604	36	1967	573	3444	619	307	249
144.75	54038	78	2567	599	2743	459	180	189
145.25	62900	110	2569	405	3403	779	0	272
145.75	88099	154	2823	646	2185	623	249	148
146.25	92803	159	2823	922	1913	503	460	178
146.75	102751	162	2809	774	1960	538	341	235
147.25	91768	113	2651	800	1792	660	329	247
147.75	69466	114	1674	1045	2599	807	149	279
148.25	61535	56	964	743	3066	418	146	207
148.75	60268	47	1135	682	2418	464	390	428
149.25	58104	9	1275	632	2819	221	160	298
149.75	56608	54	1232	782	2864	711	549	401

Depth (cm)	Ca	Cl	Co	Cu	Eu	Ga	Ge	Hf
150.25	52808	62	1312	630	2934	671	299	296
150.75	50939	0	1164	713	3230	366	139	291
151.25	46844	37	1301	512	3356	377	56	258
151.75	49287	64	1354	749	2533	511	171	300
152.25	62528	93	1630	669	2660	726	196	371
152.75	80540	69	1399	616	2709	296	419	364
153.25	61615	44	1293	648	2845	214	287	134
153.75	56287	50	1217	867	2876	460	152	287
154.25	49407	68	1158	880	2651	451	375	289
154.75	45180	0	843	877	1904	548	452	260
155.25	20766	44	400	799	0	491	302	249
155.75	14451	40	160	463	0	452	110	191
156.25	7452	7	85	416	0	411	268	187
156.75	9881	9	217	478	0	172	36	120
157.25	30413	40	385	616	1381	241	575	206
157.75	48046	36	771	784	2648	356	209	348
158.25	45350	14	1027	829	2438	721	499	301
158.75	50508	5	764	983	2283	175	315	242
159.25	52454	0	766	632	2330	198	528	332
159.75	56706	72	942	760	2328	376	645	349
160.25	58273	31	650	745	2522	185	331	216
160.75	52409	32	676	1045	3304	375	426	329
161.25	49129	73	736	979	2769	556	194	197
161.75	52760	50	787	989	3092	431	39	259
162.25	48287	0	494	1046	2229	196	318	110
162.75	41723	0	394	784	2171	228	243	295
163.25	38022	0	157	913	2194	309	120	367
163.75	43789	0	331	919	2493	461	285	384
164.25	37944	0	310	1183	2174	628	729	281
164.75	35946	0	547	932	1769	726	441	273
165.25	32931	18	201	1112	2139	396	317	321
165.75	36512	34	251	1061	1729	421	494	419
166.25	9850	35	121	265	63	194	116	136
166.75	16632	23	23	430	42	302	72	233
167.25	41519	58	261	1096	2298	267	443	382
167.75	45318	5	293	1018	2525	478	666	330
168.25	52613	20	764	849	2613	641	434	351
168.75	51116	51	877	840	2677	433	422	330
169.25	56682	37	718	733	2158	476	265	255

Depth (cm)	Ca	Cl	Co	Cu	Eu	Ga	Ge	Hf
169.75	57126	59	990	703	2503	144	331	161
170.25	53845	70	1012	966	1939	829	332	254
170.75	55170	54	925	909	2417	383	330	223
171.25	51324	32	864	947	2388	254	646	380
171.75	53423	38	876	796	2148	315	219	173
172.25	54057	52	750	994	2323	592	183	223
172.75	51590	56	568	580	2626	229	524	300
173.25	43339	36	664	695	1454	556	269	306
173.75	29177	0	570	492	671	602	151	243
174.25	34510	6	385	956	1271	404	136	283
174.75	45540	131	705	620	1571	521	535	315
175.25	49019	0	604	727	3051	671	171	250
175.75	47303	0	757	912	2897	575	441	357
176.25	47297	29	509	966	3482	486	527	275
176.75	45483	6	476	831	3251	330	471	252
177.25	48248	0	572	1034	3353	291	361	249
177.75	45936	7	471	795	3279	129	438	253
178.25	45124	43	564	1020	2492	482	109	290
178.75	19942	79	263	679	117	463	162	203
179.25	20207	64	268	704	286	424	166	319
179.75	13286	46	203	398	0	260	262	179
180.25	37517	24	388	730	2499	686	428	327
180.75	53413	19	549	869	3198	375	271	182
181.25	48303	15	509	1047	3519	306	246	182
181.75	43102	0	287	856	2985	139	567	303
182.25	46032	0	206	1105	2555	497	533	242
182.75	52781	0	466	800	2472	377	320	394
183.25	46760	19	340	854	2205	540	410	357
183.75	49523	9	248	914	2751	442	72	151
184.25	51413	0	219	762	2319	147	465	287
184.75	49618	0	197	944	2502	285	330	258
185.25	49420	7	72	1161	2571	364	434	341
185.75	50589	0	372	970	2099	239	317	278
186.25	58767	0	301	755	3439	524	115	123
186.75	57795	15	587	799	2714	231	522	372
187.25	63556	20	432	761	3576	401	477	244
187.75	63110	0	442	679	3350	292	211	356
188.25	60260	48	415	823	2959	359	503	385
188.75	63400	0	556	917	2956	372	274	183

Depth (cm)	Ca	Cl	Co	Cu	Eu	Ga	Ge	Hf
189.25	58620	0	280	793	3658	357	140	350
189.75	60254	0	508	871	2911	425	350	136
190.25	59634	11	433	750	3573	514	688	258
190.75	58838	0	658	1106	3000	650	433	328
191.25	59066	77	495	972	3530	328	491	434
191.75	59498	18	417	1018	2753	671	408	345
192.25	60085	49	470	718	2995	626	541	174
192.75	57643	17	574	823	3208	643	314	202
193.25	58894	38	284	1072	3583	647	539	272
193.75	66668	6	438	678	3083	357	496	192
194.25	62188	0	385	795	2898	319	477	390
194.75	63633	0	444	860	2803	591	218	386
195.25	62492	0	474	650	3329	822	613	269
195.75	51883	0	252	837	3047	447	730	328
196.25	53842	0	161	778	3104	519	346	294
196.75	55546	19	322	939	2881	179	428	330
197.25	60152	12	302	814	2912	111	280	243
197.75	58281	0	368	979	2910	537	273	214
198.25	58994	7	452	844	2700	464	490	408
198.75	54486	0	450	772	3295	437	172	260
199.25	56887	15	335	940	3137	708	577	109
199.75	58281	0	565	933	2661	382	606	358
200.25	60908	23	465	808	3710	108	437	290
200.75	57237	38	373	836	2973	262	347	345
201.25	59241	22	576	814	3322	266	17	329
201.75	49133	51	455	926	1210	534	331	367
202.25	16911	66	212	337	0	562	14	204
202.75	9610	90	204	433	0	304	194	140
203.25	15715	39	87	481	0	243	267	222
203.75	41819	202	192	661	1994	451	532	314
204.25	63698	135	464	994	2481	240	678	193
204.75	65479	61	547	685	3443	428	278	163
205.25	69372	29	362	772	2714	322	404	226
205.75	63066	23	480	762	2968	605	369	350
206.25	63250	25	708	869	2705	453	590	167
206.75	57923	39	530	702	2559	423	213	292
207.25	61613	32	417	874	3106	328	526	255
207.75	57617	65	545	766	3323	260	426	273
208.25	52535	50	310	912	2675	581	286	311

Depth (cm)	Ca	Cl	Co	Cu	Eu	Ga	Ge	Hf
208.75	57211	25	516	958	2366	551	379	284
209.25	61054	7	526	994	2624	454	386	415
209.75	60050	48	555	727	2805	307	397	323
210.25	62384	4	387	926	3291	403	201	364
210.75	63673	37	529	687	2892	379	585	370
211.25	59942	52	309	1029	2524	411	492	242
211.75	53966	75	264	738	2362	476	498	282
212.25	65008	64	561	696	3629	373	245	140
212.75	62807	73	496	557	3698	674	658	317
213.25	59733	0	551	945	2542	638	689	353
213.75	56930	13	320	517	2670	351	541	242
214.25	56053	0	218	845	3090	576	378	410
214.75	53362	0	146	890	2200	137	376	400
215.25	51758	0	207	971	1611	378	517	385
215.75	53862	0	54	1055	2131	419	206	222
216.25	54441	35	92	970	2035	622	229	416
216.75	54127	41	196	1135	2019	575	307	377
217.25	52994	0	164	1126	2266	590	525	395
217.75	55213	0	410	1099	2850	524	605	233
218.25	53020	0	400	990	3058	312	342	124
218.75	55107	22	327	729	3180	544	453	123
219.25	45880	8	350	695	3347	619	587	330
219.75	45264	0	352	881	2753	445	392	319
220.25	41147	0	261	918	2777	558	385	221
220.75	40018	0	504	784	2643	544	539	331
221.25	39643	0	569	1004	2974	1038	808	243
221.75	46233	13	259	748	3819	404	548	394
222.25	76340	52	842	833	2887	365	343	248
222.75	64122	85	631	602	3559	242	160	202
223.25	55817	5	351	674	3187	145	455	289
223.75	56746	0	341	555	2721	326	517	234
224.25	50741	0	486	1051	2180	434	506	281
224.75	68102	40	310	991	3168	694	550	217
225.25	62018	10	679	883	2659	218	596	192
225.75	75059	53	322	902	3068	544	216	321
226.25	55720	0	333	897	2362	234	632	163
226.75	49494	0	313	1134	2181	0	360	106
227.25	51485	0	496	1137	2857	392	401	302
227.75	55882	0	192	833	2962	600	217	377

Depth (cm)	Ca	Cl	Co	Cu	Eu	Ga	Ge	Hf
228.25	58827	0	478	1038	2759	721	366	257
228.75	50652	12	519	918	4249	469	278	281
229.25	53911	64	1056	985	3563	532	133	325
229.75	52565	43	748	760	4096	165	231	273
230.25	40987	13	646	798	755	597	186	235
230.75	23954	31	224	523	0	427	133	187
231.25	15512	66	179	358	0	313	104	111
231.75	36042	18	313	474	1013	303	473	0
232.25	66632	61	591	824	2963	377	398	198
232.75	62194	65	684	911	2550	634	174	423
233.25	63112	44	358	798	3399	174	356	261
233.75	66089	76	471	781	3299	469	358	267
234.25	65384	13	524	703	3882	263	526	198
234.75	73513	80	784	668	3956	392	474	279
235.25	86538	0	632	680	2771	367	318	205
235.75	79983	34	611	766	2582	269	610	297
236.25	74595	45	413	604	2782	503	329	187
236.75	76539	55	415	826	2820	451	433	340
237.25	73503	64	595	635	3101	147	291	197
237.75	75595	0	352	652	3560	353	615	245
238.25	72789	10	440	865	2314	595	587	378
238.75	70698	0	400	722	3542	568	64	253
239.25	58649	0	371	908	3039	255	188	180
239.75	58269	44	511	1044	3562	582	536	288
240.25	71600	45	403	903	3186	575	411	309
240.75	80093	78	527	664	2427	380	303	129
241.25	58343	36	387	688	2576	465	366	276
241.75	52799	61	293	956	2114	328	578	266
242.25	50672	4	167	954	2673	792	399	355
242.75	96619	12	1108	768	3763	511	245	427
243.25	94526	5	1171	832	4194	533	358	532
243.75	104211	32	1174	1018	3870	770	168	411
244.25	93638	41	1096	696	3721	259	582	576
244.75	102767	21	1217	632	4449	317	525	558
245.25	105089	36	1196	657	3827	828	561	592
245.75	121177	31	1170	542	3698	750	271	568
246.25	95192	0	754	918	3698	428	807	419
246.75	65010	0	752	1225	3003	520	735	727
247.25	78308	20	773	1114	4310	852	473	665

Depth (cm)	Ca	Cl	Co	Cu	Eu	Ga	Ge	Hf
247.75	81838	55	656	807	3412	565	399	319
248.25	70016	0	719	936	3598	703	898	696
248.75	75400	0	725	950	4394	730	371	562
249.25	87246	19	1084	683	4837	706	404	557
249.75	87132	0	1060	1039	4024	587	163	492
250.25	85060	13	1091	761	3891	362	322	305
250.75	97800	7	834	621	4443	344	374	413
251.25	90223	12	999	598	4441	466	420	563
251.75	68615	0	1357	961	4390	533	488	431
252.25	59695	0	1031	1002	4254	454	352	412
252.75	53139	14	995	973	4575	669	422	427
253.25	54434	0	944	807	4846	471	697	650
253.75	51747	0	1101	930	4438	781	596	671
254.25	50435	0	965	1215	5068	628	456	275
254.75	47959	0	1295	832	4295	261	294	289
255.25	48255	0	1047	993	4394	592	300	556
255.75	49417	0	1178	981	3468	250	386	394
256.25	51233	0	1217	1102	4324	607	491	532
256.75	53216	0	980	1081	3790	743	535	538
257.25	64896	6	1059	824	4117	819	379	374
257.75	73436	41	958	773	3354	652	207	262
258.25	78871	0	651	708	3365	698	634	447
258.75	104577	9	836	816	3410	744	455	515
259.25	70111	33	679	821	2566	294	461	468
259.75	73056	0	702	837	2252	445	428	406
260.25	87063	0	802	926	3265	694	499	505
260.75	76218	16	999	796	3893	539	828	495
261.25	87800	53	889	659	4230	359	630	465
261.75	75115	0	982	719	4159	547	235	515
262.25	70208	0	872	950	3697	470	476	467
262.75	58863	0	1010	943	3125	796	406	678
263.25	53778	0	842	825	3254	982	880	541
263.75	52198	0	937	1012	3961	545	724	533
264.25	54100	0	865	843	4070	628	248	552
264.75	56114	0	957	975	4066	458	485	587
265.25	54957	0	754	1011	4061	426	245	668
265.75	55781	0	638	1094	3966	775	521	577
266.25	60579	0	721	735	3938	394	501	683
266.75	60960	0	781	938	4499	606	513	470

Depth (cm)	Ca	Cl	Co	Cu	Eu	Ga	Ge	Hf
267.25	65490	0	968	1036	4756	556	574	401
267.75	70555	0	928	1208	4520	778	491	447
268.25	86239	27	1265	718	4171	541	626	487
268.75	103293	40	1074	829	4434	667	169	449
269.25	150261	0	796	924	3881	367	416	396
269.75	181437	17	1235	542	3915	653	376	440
270.25	329379	56	1266	332	2959	0	8	260
270.75	607306	40	1041	400	2878	0	0	351
271.25	1016696	63	852	0	1644	0	0	229
271.75	1105500	74	702	0	1656	0	0	312
272.25	1018303	79	859	0	1286	0	0	400
272.75	1236244	74	895	0	1007	0	0	320
273.25	916648	16	654	83	1558	0	0	325
273.75	506881	25	626	409	2585	0	341	421
274.25	223402	0	793	791	2763	155	539	552
274.75	91223	6	345	760	814	446	152	232
275.25	53707	15	253	278	0	254	392	28
275.75	43638	53	225	563	0	333	398	0
276.25	42337	64	304	474	198	65	308	88
276.75	60895	26	487	691	930	401	370	258
277.25	86953	0	648	1026	3012	793	432	405
277.75	80731	0	623	935	3321	503	343	443
278.25	71572	0	772	1073	3844	830	372	620
278.75	67957	0	803	891	3345	572	618	795
279.25	66481	0	869	945	3391	797	720	753
279.75	65378	0	809	1184	2982	256	476	529
280.25	63583	0	937	1062	2796	566	739	698
280.75	63552	0	598	925	3700	570	485	526
281.25	64682	0	827	933	3401	644	484	582
281.75	59114	0	631	846	3200	890	334	541
282.25	58399	9	717	956	3627	857	791	682
282.75	60695	0	804	823	3732	356	531	591
283.25	65170	0	869	872	2795	590	401	517
283.75	66254	7	739	887	3242	440	495	544
284.25	69679	0	677	728	3983	260	312	601
284.75	78357	0	721	1030	3413	301	542	603
285.25	84040	0	638	945	3524	437	596	523
285.75	84082	0	785	850	2867	585	308	823
286.25	101430	0	776	1043	2259	797	666	664

Depth (cm)	Ca	Cl	Co	Cu	Eu	Ga	Ge	Hf
286.75	98998	0	723	1036	2874	270	439	636
287.25	476245	0	746	439	3328	11	201	431
287.75	1215259	68	755	0	1376	0	0	323
288.25	828785	100	816	0	1022	0	0	287
288.75	163474	29	1613	630	4134	700	205	356
289.25	93039	99	1952	692	3921	644	265	291
289.75	95706	29	1771	823	4818	556	98	373
290.25	88297	18	1711	635	3460	596	60	393
290.75	88520	34	1546	702	2882	636	485	417
291.25	103402	24	1511	582	3759	664	330	493
291.75	138440	55	1543	399	3258	484	222	395
292.25	135872	36	1576	566	2947	654	302	248
292.75	118498	25	1612	581	2515	478	147	347
293.25	141802	0	1395	627	2733	496	293	241
293.75	148087	0	1361	634	2814	435	149	105

Table A 4.3 Galang Co XRF Geochemistry Hg – Mo

Depth (cm)	Hg	I	Ir	K	La	Mg	Mn	Mo
14.25	0	247	72	3304	533	13	3898	0
14.75	25	187	85	4632	501	25	2738	0
15.25	118	326	401	10350	1066	0	4279	0
15.75	533	360	667	11384	1081	0	4581	0
16.25	573	374	664	11838	1137	0	4115	0
16.75	247	417	374	10852	1154	0	4578	153
17.25	401	429	413	9997	1104	0	3474	0
17.75	588	376	202	9814	1001	24	3358	118
18.25	161	456	259	9444	1141	0	5453	296
18.75	223	316	394	11474	1089	9	4725	32
19.25	467	288	218	9361	987	5	3341	317
19.75	662	355	620	9696	1117	0	3995	71
20.25	620	354	410	9717	1078	0	2904	0
20.75	517	418	392	10926	1137	82	4873	0
21.25	836	429	435	10055	1093	0	3110	0
21.75	416	354	269	9738	1163	21	4240	175
22.25	297	425	637	9456	1133	0	4328	250
22.75	357	427	481	9881	1184	0	5506	438
23.25	388	383	347	8963	1087	0	3806	215
23.75	406	354	463	10466	1101	0	4183	207
24.25	273	408	273	10079	1308	0	4039	125
24.75	351	301	538	11493	1249	35	3696	63
25.25	371	384	407	12541	1225	0	4407	175
25.75	465	346	557	11460	1082	6	3755	0
26.25	921	415	582	11829	1161	0	4634	53
26.75	548	497	509	12634	1248	8	3657	72
27.25	582	398	282	12988	1146	17	4175	187
27.75	409	422	371	13007	1094	0	6878	159
28.25	151	374	547	13781	1271	22	4806	134
28.75	491	367	821	11740	1075	38	5537	0
29.25	334	283	603	11363	1060	0	5195	57
29.75	525	392	412	12781	1070	56	4442	341
30.25	339	422	174	12020	1025	0	4782	63
30.75	376	389	387	12369	1113	26	5530	119
31.25	263	403	524	12616	1186	0	4955	0
31.75	457	382	502	12107	1193	0	4894	17
32.25	360	403	228	12211	1076	33	4754	0
32.75	293	339	360	13039	1077	44	4447	7

Depth (cm)	Hg	I	Ir	K	La	Mg	Mn	Mo
33.25	299	422	479	13064	1089	0	4375	417
33.75	240	449	421	12716	1281	11	4256	93
34.25	427	349	693	9706	1186	55	4409	49
34.75	297	386	290	10957	1005	45	4593	96
35.25	620	335	682	11340	1170	0	4256	59
35.75	191	358	507	9913	1084	72	5811	396
36.25	572	460	367	10558	1193	20	4881	0
36.75	297	413	597	10081	1154	0	5192	92
37.25	462	401	349	9808	1279	63	5456	38
37.75	578	483	551	9524	1128	0	4620	0
38.25	717	364	689	10777	1224	0	4366	81
38.75	559	351	486	12384	1174	25	3921	51
39.25	390	377	537	11815	1210	0	4264	175
39.75	252	383	349	12873	1250	11	4070	276
40.25	496	387	501	13277	1155	22	4114	356
40.75	583	403	533	12612	1207	0	4683	230
41.25	680	452	664	13778	1318	0	5098	218
41.75	575	444	480	14723	1156	26	4554	297
42.25	387	372	839	12518	1199	21	4294	0
42.75	344	398	471	14207	1223	9	4781	0
43.25	284	387	498	13813	1065	0	6322	121
43.75	558	428	376	12331	1066	14	6745	0
44.25	488	353	561	14600	1076	0	5704	0
44.75	532	435	623	14707	1162	0	3901	137
45.25	363	398	547	14964	1204	20	5301	0
45.75	440	376	387	16087	1209	0	5612	122
46.25	287	559	934	15182	1310	17	3452	0
46.75	360	355	577	15245	1224	9	5758	292
47.25	597	419	453	17367	1360	20	3757	159
47.75	308	459	566	16183	1297	0	5787	128
48.25	423	362	425	14886	1222	0	5348	152
48.75	218	388	563	14620	1247	17	4994	166
49.25	244	427	585	13891	1282	35	5961	21
49.75	280	412	367	13405	1226	36	4582	0
50.25	488	476	663	13954	1297	25	5008	0
50.75	531	439	616	15821	1316	0	5355	0
51.25	325	427	448	16228	1204	65	4546	272
51.75	336	437	427	19093	1165	27	4816	359
52.25	497	426	729	20669	1327	0	4519	0

Depth (cm)	Hg	I	Ir	K	La	Mg	Mn	Mo
52.75	442	399	510	30409	1153	24	5155	160
53.25	159	302	374	42191	1051	46	3378	137
53.75	314	360	491	37006	1211	0	7160	106
54.25	258	312	532	37411	1196	63	6014	179
54.75	367	358	360	29091	1100	0	5100	283
55.25	376	406	353	27305	1233	0	5095	0
55.75	176	434	448	23329	1104	47	5008	459
56.25	295	510	413	16406	1218	33	4307	179
56.75	216	368	829	17527	1252	34	5762	316
57.25	0	389	316	20211	1207	55	4184	0
57.75	241	341	535	17355	1290	22	5535	0
58.25	242	407	368	18264	1235	11	5487	281
58.75	269	262	559	18805	1233	0	4202	66
59.25	286	405	457	19095	1069	61	4356	0
59.75	271	408	392	17712	1209	0	4132	339
60.25	0	457	390	17337	1158	31	4407	531
60.75	437	433	690	12379	1239	0	4977	0
61.25	418	457	544	14824	1233	0	3425	0
61.75	403	360	613	12117	1150	38	4734	82
62.25	404	361	594	12567	1237	0	3125	4
62.75	123	475	431	12970	1279	0	4387	0
63.25	407	447	287	13376	1089	0	4094	0
63.75	415	379	472	13977	1185	0	3642	452
64.25	459	350	382	12833	1208	0	3297	0
64.75	254	405	422	10846	1104	54	3592	0
65.25	97	390	443	11880	1228	10	3285	298
65.75	45	398	476	11122	1143	60	4131	0
66.25	339	431	568	9791	1213	0	3959	200
66.75	544	338	491	7320	1123	31	2745	185
67.25	426	380	331	8172	1238	11	3683	111
67.75	486	482	525	7174	1172	0	3533	0
68.25	440	445	601	7283	1289	18	3823	41
68.75	309	440	425	7050	1182	24	2926	0
69.25	452	361	499	7412	1091	5	3733	0
69.75	286	416	359	6990	1119	0	4161	0
70.25	204	499	429	7676	1203	72	4277	0
70.75	488	350	652	6948	1128	0	3566	434
71.25	450	498	600	6983	1197	0	3507	0
71.75	212	394	339	6887	1131	9	3756	89

Depth (cm)	Hg	I	Ir	K	La	Mg	Mn	Mo
72.25	243	338	782	8564	1188	22	5016	255
72.75	149	393	426	7956	1340	0	3578	0
73.25	119	322	409	9707	1132	26	4437	0
73.75	149	372	397	10303	1172	18	3131	142
74.25	32	372	414	11571	1068	48	3519	176
74.75	23	385	551	12697	1115	7	5480	239
75.25	425	373	555	12892	1161	66	4027	397
75.75	72	289	470	17952	1209	0	2872	195
76.25	240	344	314	20595	1158	44	3783	53
76.75	309	413	517	20863	1175	31	2959	545
77.25	106	371	607	23960	1113	0	4084	43
77.75	441	378	483	23140	1110	0	3562	0
78.25	479	349	463	23242	1242	0	4539	0
78.75	270	321	415	25426	1131	6	4384	54
79.25	499	389	153	16165	1100	23	1117	0
79.75	572	472	554	12796	995	18	1879	142
80.25	339	450	340	9950	912	21	1675	0
80.75	407	478	324	12025	960	0	2427	232
81.25	399	486	327	11820	1024	15	1131	121
81.75	338	488	378	9668	947	13	1319	476
82.25	145	421	252	11572	992	6	3299	180
82.75	500	540	557	14706	1252	44	1453	0
83.25	759	505	768	12726	1331	27	3103	208
83.75	593	498	552	16027	1322	0	3335	106
84.25	457	523	636	19250	1293	6	4335	0
84.75	210	529	572	18008	1347	47	5587	347
85.25	322	549	541	17765	1238	32	10719	109
85.75	461	506	447	18381	1255	21	8099	162
86.25	451	628	311	14877	1295	14	6042	89
86.75	347	518	740	17083	1325	0	5673	228
87.25	521	535	656	17161	1259	0	4521	253
87.75	187	457	559	13553	1146	0	2079	107
88.25	177	506	683	14350	1254	35	2832	300
88.75	166	533	403	14067	1359	19	1917	396
89.25	144	527	620	11416	1285	26	1421	33
89.75	403	458	399	10776	1178	10	2138	664
90.25	474	478	885	9399	1275	67	1563	656
90.75	404	469	529	7225	1208	0	1173	129
91.25	252	97	791	5186	849	0	1453	0

Depth (cm)	Hg	I	Ir	K	La	Mg	Mn	Mo
91.75	548	302	864	4882	884	0	1067	0
92.25	685	337	556	5673	1010	27	0	0
92.75	635	372	795	6307	1007	9	1155	293
93.25	809	572	555	7458	1207	33	737	0
93.75	721	570	662	9744	1248	0	0	271
94.25	757	467	533	11106	1471	24	86	74
94.75	604	503	574	14177	1395	14	681	327
95.25	671	476	629	12963	1204	25	1833	290
95.75	548	523	452	12987	1292	38	1595	0
96.25	470	507	165	14938	1253	0	3131	281
96.75	455	432	566	16966	1226	0	6755	0
97.25	618	471	614	17388	1175	9	8433	175
97.75	647	400	446	19946	1256	0	4438	105
98.25	543	523	458	20865	1216	0	3569	155
98.75	574	504	469	18852	1351	0	2671	0
99.25	411	546	511	15719	1224	30	2019	67
99.75	802	490	523	17317	1163	29	2382	466
100.25	742	491	586	22273	1224	36	2379	0
100.75	601	599	379	19135	1256	0	2926	92
101.25	759	523	325	17539	1230	0	2392	16
101.75	615	440	525	16410	1218	0	3214	0
102.25	478	473	373	17347	1256	50	3573	235
102.75	840	530	695	19081	1334	0	4566	0
103.25	422	464	659	19722	1340	31	4516	133
103.75	566	603	561	19618	1281	0	3726	19
104.25	597	486	662	18312	1164	0	6169	273
104.75	559	465	798	17582	1199	57	3070	135
105.25	258	519	466	18755	1251	41	2074	304
105.75	537	546	542	17884	1333	0	2562	280
106.25	610	513	556	16495	1090	0	1067	381
106.75	636	558	623	19130	1187	0	2991	267
107.25	473	635	590	15529	1345	0	1594	325
107.75	496	495	552	15764	1286	10	1421	287
108.25	601	499	423	16388	1141	45	2314	323
108.75	374	529	677	15721	1290	34	3123	0
109.25	350	543	734	15860	1226	0	2971	0
109.75	316	500	529	16301	1181	7	3070	313
110.25	338	572	697	16209	1226	11	1130	106
110.75	380	545	674	16532	1260	0	2388	81

Depth (cm)	Hg	I	Ir	K	La	Mg	Mn	Mo
111.25	438	637	563	15033	1394	0	2953	269
111.75	348	542	510	16284	1201	0	3555	125
112.25	440	459	510	16405	1238	77	6110	190
112.75	403	549	631	18726	1190	6	4082	0
113.25	228	643	512	18504	1254	0	1732	256
113.75	298	470	583	18649	1147	0	1942	153
114.25	465	538	477	18659	1230	19	1947	285
114.75	276	514	499	16694	1255	17	1277	315
115.25	110	498	498	14707	1161	43	2392	0
115.75	532	558	524	15002	1166	24	2257	78
116.25	351	486	537	15038	1301	0	1551	57
116.75	19	585	447	14405	1249	64	1672	0
117.25	342	539	515	13258	1412	20	3619	0
117.75	492	584	494	13356	1232	23	3567	216
118.25	644	547	518	14651	1207	0	3721	0
118.75	678	549	296	16051	1320	66	3425	138
119.25	351	536	566	13701	1258	33	2209	127
119.75	546	544	489	13129	1305	4	2165	122
120.25	300	320	401	9061	769	0	3253	129
120.75	20	193	130	4161	416	0	2078	70
121.25	81	186	136	2753	359	0	1550	0
121.75	0	134	147	2646	367	32	1455	122
122.25	327	332	241	5866	713	40	1714	0
122.75	237	468	444	12603	1145	28	2046	68
123.25	587	484	524	16128	1211	0	3743	87
123.75	324	507	536	20591	1156	18	3064	143
124.25	575	518	699	24564	1298	0	3850	0
124.75	433	493	598	24586	1184	0	2694	0
125.25	444	465	811	26170	1159	0	3077	221
125.75	574	475	553	24526	1107	0	3019	487
126.25	387	520	612	24211	1198	7	3183	77
126.75	267	556	541	25592	1254	0	2708	449
127.25	730	498	691	25781	1206	0	3319	199
127.75	434	595	351	24396	1194	0	4167	201
128.25	342	516	334	28282	1181	0	4341	280
128.75	531	547	518	38931	1266	0	3193	387
129.25	236	607	491	25733	1237	0	2161	281
129.75	415	550	729	19151	1260	0	2819	0
130.25	351	585	636	17829	1399	0	3815	0

Depth (cm)	Hg	I	Ir	K	La	Mg	Mn	Mo
130.75	370	596	529	17461	1422	36	1877	11
131.25	518	553	559	16471	1271	0	2218	0
131.75	307	478	178	15969	1244	8	2308	362
132.25	358	489	658	17673	1230	37	2823	172
132.75	248	502	417	17071	1250	0	3360	64
133.25	252	601	787	16744	1229	0	3907	0
133.75	447	537	343	17381	1202	0	2118	84
134.25	359	513	628	16757	1274	9	4434	0
134.75	463	560	454	12557	1202	0	2699	171
135.25	555	495	454	11323	1202	66	4107	216
135.75	281	565	449	11278	1205	27	4234	211
136.25	462	482	670	12440	1270	14	3239	6
136.75	371	655	526	12445	1195	0	2129	23
137.25	374	557	718	11113	1104	93	1967	0
137.75	771	513	466	10819	1179	0	3014	526
138.25	519	449	599	9774	1157	43	3795	0
138.75	471	522	656	9296	1312	0	2506	173
139.25	446	490	459	9174	1245	16	2073	0
139.75	232	398	452	9621	1220	49	3506	0
140.25	375	433	649	9625	1092	32	2470	183
140.75	713	418	592	11014	1119	21	1824	187
141.25	508	470	677	11667	1080	38	3218	0
141.75	481	462	542	12603	1088	65	2807	0
142.25	573	453	628	13467	1127	56	2648	382
142.75	349	433	585	15055	1078	0	3420	93
143.25	560	408	347	14724	1200	27	3066	44
143.75	416	625	320	13121	1220	8	1344	126
144.25	429	486	457	16406	1272	0	903	510
144.75	626	489	466	27914	1314	0	2211	285
145.25	831	457	67	48398	1213	0	844	147
145.75	709	336	397	87889	1187	0	2061	0
146.25	694	453	375	96968	1194	5	2334	99
146.75	699	403	367	108275	1071	0	1980	212
147.25	552	381	212	89072	1110	23	2334	305
147.75	421	365	337	48433	1068	0	2287	168
148.25	560	437	537	21491	1070	0	2081	0
148.75	278	526	638	16187	1216	26	3519	49
149.25	414	524	678	14304	1217	12	2412	153
149.75	437	466	500	14132	1328	60	3217	47

Depth (cm)	Hg	I	Ir	K	La	Mg	Mn	Mo
150.25	315	450	495	14604	1220	10	2224	0
150.75	374	527	466	16701	1178	0	2503	0
151.25	410	466	543	18127	1184	28	2213	484
151.75	551	421	498	19808	1281	12	2332	410
152.25	432	475	249	24369	1175	0	1849	148
152.75	412	481	479	27431	1138	36	2152	267
153.25	225	471	669	23061	1308	0	1559	151
153.75	500	493	561	22331	1047	64	1116	162
154.25	626	487	584	14739	1383	52	2177	483
154.75	447	413	440	13632	1137	18	3199	236
155.25	0	147	105	6312	458	38	3026	0
155.75	0	128	81	3182	287	0	2315	0
156.25	0	63	0	1475	195	0	2997	0
156.75	136	103	151	2321	257	34	1954	0
157.25	168	275	315	7386	796	0	2191	0
157.75	359	439	455	13549	1130	13	1986	40
158.25	148	413	349	12352	1330	0	2777	0
158.75	208	424	772	14191	1314	36	2900	0
159.25	425	348	629	12929	1251	27	3485	0
159.75	196	504	509	13931	1248	47	3895	176
160.25	346	487	579	14611	1216	0	1946	0
160.75	142	498	621	14000	1319	0	1497	0
161.25	408	464	408	12033	1232	4	1988	248
161.75	524	426	532	15202	1329	5	1746	312
162.25	315	415	508	12489	1329	27	3577	459
162.75	394	493	859	4327	1081	0	3659	310
163.25	695	429	626	2506	1144	11	3650	108
163.75	125	448	570	9193	1276	65	3579	165
164.25	273	461	400	5188	1093	37	2927	80
164.75	559	402	479	4212	1275	30	3970	0
165.25	173	373	342	2291	1064	61	3247	104
165.75	0	393	390	1496	1117	64	2644	101
166.25	0	141	108	316	352	0	1222	0
166.75	78	227	230	944	495	0	1876	0
167.25	328	441	650	4428	1141	30	2129	339
167.75	350	428	620	7769	1204	0	2280	165
168.25	293	462	324	15219	1190	46	1680	331
168.75	427	573	580	14289	1239	73	2964	513
169.25	364	476	676	15961	1301	31	2840	232

Depth (cm)	Hg	I	Ir	K	La	Mg	Mn	Mo
169.75	487	487	796	17462	1146	7	1846	14
170.25	534	446	414	15793	1174	86	3687	210
170.75	382	426	537	14436	1357	27	2764	50
171.25	106	411	719	14839	1224	11	1989	0
171.75	448	367	539	14635	1251	32	2928	6
172.25	59	388	248	13896	1174	0	2130	273
172.75	23	406	515	13380	1137	0	1838	0
173.25	173	319	129	11649	914	14	2284	0
173.75	72	295	114	6416	676	29	1864	0
174.25	362	339	415	8138	893	0	2143	126
174.75	279	392	255	11721	909	93	3309	36
175.25	518	441	431	14896	1273	43	2724	32
175.75	307	369	666	13797	1194	0	2699	0
176.25	508	335	467	13192	1335	0	1888	118
176.75	281	394	641	11341	1297	77	2967	184
177.25	570	464	666	11699	1299	54	1806	0
177.75	121	431	679	10240	1439	0	2816	31
178.25	342	376	538	11290	1206	32	2347	0
178.75	0	236	120	5337	521	37	2942	0
179.25	291	247	322	4940	461	0	2144	0
179.75	75	225	98	3793	334	15	1732	0
180.25	311	368	476	6623	1024	35	1403	65
180.75	396	368	368	12562	1352	80	2899	138
181.25	412	452	672	10594	1180	89	2396	390
181.75	260	439	843	5723	1266	51	2088	44
182.25	117	411	463	5386	1437	0	3992	15
182.75	366	489	603	5512	1234	18	2829	99
183.25	240	485	660	4386	1275	45	4223	349
183.75	294	453	626	4586	1195	0	2722	0
184.25	121	493	634	4337	1291	0	3378	0
184.75	345	421	882	3623	1299	38	3194	0
185.25	307	507	891	4570	1156	23	2460	0
185.75	233	415	732	5192	1224	0	3342	39
186.25	219	390	379	8886	1334	50	2350	114
186.75	509	347	769	10594	1261	29	2825	0
187.25	229	461	679	12383	1228	0	1857	111
187.75	317	414	596	10635	1371	11	2218	19
188.25	219	336	751	11234	1307	62	3222	239
188.75	531	427	680	12157	1343	0	2931	175

Depth (cm)	Hg	I	Ir	K	La	Mg	Mn	Mo
189.25	520	488	625	12254	1371	5	1730	0
189.75	140	455	530	11267	1306	35	2464	163
190.25	0	520	701	10921	1399	18	1449	0
190.75	486	402	481	11248	1338	18	2100	133
191.25	0	436	785	11856	1437	83	2258	0
191.75	294	444	527	11890	1198	0	1955	181
192.25	261	464	357	11204	1317	0	3092	101
192.75	354	449	356	11310	1291	38	1967	0
193.25	365	437	793	11455	1298	24	2243	0
193.75	126	401	518	12940	1377	0	3459	0
194.25	517	427	660	13610	1209	16	3164	0
194.75	198	477	514	13006	1251	22	2168	85
195.25	230	455	428	12387	1407	0	2615	195
195.75	261	432	676	9322	1280	0	2167	83
196.25	211	467	650	7312	1321	10	2811	144
196.75	410	400	662	7954	1295	72	3262	0
197.25	300	359	644	10494	1361	0	2745	0
197.75	322	400	659	9432	1197	10	2517	145
198.25	273	481	475	9887	1300	0	2670	0
198.75	248	382	534	9111	1317	12	1416	0
199.25	81	482	438	8818	1225	0	2597	278
199.75	114	447	694	10672	1373	0	3485	0
200.25	342	395	861	13060	1121	0	37	176
200.75	487	408	764	11126	1145	60	2686	329
201.25	385	460	780	12101	1320	14	1441	0
201.75	119	356	443	9633	915	46	2191	74
202.25	90	211	58	3296	358	0	2465	0
202.75	123	199	123	1204	281	0	2488	0
203.25	227	194	304	1335	361	0	2086	0
203.75	104	315	276	7515	915	0	1882	226
204.25	152	467	728	12277	1298	18	2639	163
204.75	512	504	366	12332	1402	51	1758	235
205.25	370	419	593	12295	1336	43	3637	223
205.75	477	471	649	13040	1225	13	3513	0
206.25	236	456	587	15126	1327	10	2389	192
206.75	461	382	479	11405	1349	0	3143	122
207.25	430	471	760	8977	1232	45	2623	118
207.75	35	442	555	11502	1304	76	1537	190
208.25	215	363	462	12372	1222	25	2324	0

Depth (cm)	Hg	I	Ir	K	La	Mg	Mn	Mo
208.75	302	435	404	10925	1222	45	3327	0
209.25	257	472	692	9516	1343	71	3495	0
209.75	191	508	610	11463	1363	61	3793	0
210.25	517	423	723	11069	1367	31	2043	142
210.75	245	403	500	11900	1375	16	1890	0
211.25	218	453	664	11084	1278	61	2761	28
211.75	0	392	617	12786	1145	30	2502	8
212.25	70	491	475	12662	1327	0	2091	123
212.75	71	415	351	12720	1323	0	1662	0
213.25	133	370	239	11163	1183	38	2616	454
213.75	193	377	444	10819	1144	0	2047	19
214.25	255	423	431	9634	1206	26	1587	121
214.75	77	419	731	6443	1251	28	2973	0
215.25	10	416	588	6565	1313	44	3897	21
215.75	485	427	502	4961	1254	0	3011	0
216.25	408	451	639	5860	1186	0	2545	0
216.75	479	393	713	4208	1301	38	3813	341
217.25	213	401	682	5609	1178	0	3130	0
217.75	359	477	713	6917	1289	0	3007	0
218.25	349	418	586	9577	1289	23	1984	84
218.75	242	394	566	12611	1155	0	2170	0
219.25	330	441	612	8446	1171	37	671	270
219.75	8	416	297	9767	1240	29	2713	422
220.25	467	400	616	8495	1192	0	1795	139
220.75	316	398	454	7129	1242	0	2349	495
221.25	0	480	240	8932	1314	113	1109	0
221.75	310	500	584	8436	1318	17	503	0
222.25	345	361	658	14351	1102	0	1575	25
222.75	534	443	618	16390	1283	0	1221	0
223.25	148	462	660	8976	1198	34	2238	221
223.75	0	384	656	5547	1122	12	2305	15
224.25	495	386	720	5399	1220	18	3899	229
224.75	253	405	545	11235	1136	0	1845	0
225.25	0	405	584	11939	1194	35	3066	170
225.75	295	467	342	8745	1142	22	2815	86
226.25	110	435	742	5531	1063	35	3039	453
226.75	0	451	803	6967	1278	37	3566	0
227.25	462	406	801	7854	1369	12	2219	171
227.75	190	452	679	8725	1183	37	2482	313

Depth (cm)	Hg	I	Ir	K	La	Mg	Mn	Mo
228.25	290	358	632	10911	1312	20	3139	175
228.75	465	430	752	18130	1435	26	1539	88
229.25	582	401	539	23908	1188	66	1216	0
229.75	521	359	660	18647	1238	25	1015	299
230.25	342	282	451	9378	727	17	2774	0
230.75	51	173	118	4768	429	0	2526	0
231.25	0	170	59	3114	308	0	1336	0
231.75	0	204	386	6575	679	0	1776	65
232.25	611	427	499	12290	1150	0	2277	0
232.75	424	489	552	12524	1237	14	2721	52
233.25	206	410	701	12503	1274	12	199	114
233.75	194	443	518	12990	1284	22	2135	0
234.25	0	536	681	11438	1415	0	1681	292
234.75	150	419	578	11627	1398	0	1284	196
235.25	207	404	406	17536	1192	0	2496	0
235.75	322	410	709	13738	1143	19	2785	0
236.25	227	441	367	13337	1167	0	3221	0
236.75	374	379	392	12711	1116	0	2459	0
237.25	100	431	666	16767	1275	33	2040	63
237.75	114	344	596	14811	1265	87	1986	0
238.25	241	402	563	10881	1269	0	3190	0
238.75	664	439	422	12881	1376	9	1095	0
239.25	483	366	387	11369	1249	0	2318	0
239.75	387	394	619	12842	1453	28	1868	327
240.25	412	349	409	13807	1139	9	1825	0
240.75	225	421	536	17233	1089	0	3055	8
241.25	430	433	713	9840	1047	38	3816	0
241.75	174	476	648	5897	1234	75	3832	0
242.25	250	352	322	5657	1171	0	3003	0
242.75	369	355	318	18049	1354	27	1208	318
243.25	380	339	604	15424	1348	28	951	48
243.75	254	331	515	16989	1446	0	2244	39
244.25	473	337	661	16866	1475	77	1815	536
244.75	310	368	668	19732	1472	0	812	300
245.25	375	276	129	18316	1415	54	1871	348
245.75	476	358	347	25157	1387	13	1849	325
246.25	226	382	505	15618	1588	35	2755	0
246.75	277	382	689	9059	1564	23	3972	277
247.25	493	388	329	12130	1521	0	2370	12

Depth (cm)	Hg	I	Ir	K	La	Mg	Mn	Mo
247.75	226	277	533	17421	1342	6	945	250
248.25	16	378	430	7706	1577	98	2816	0
248.75	396	353	584	9599	1454	20	1621	0
249.25	212	364	409	16407	1613	8	897	34
249.75	356	361	543	14179	1502	15	2304	105
250.25	364	273	620	18897	1394	11	2797	539
250.75	520	306	678	18006	1435	45	1813	108
251.25	330	245	473	21156	1525	83	2110	346
251.75	190	358	420	16324	1498	45	875	275
252.25	366	388	459	14926	1531	27	3254	0
252.75	535	422	381	13205	1566	50	712	359
253.25	44	367	460	13675	1599	18	1607	132
253.75	592	408	464	13137	1525	42	2312	536
254.25	268	340	412	12727	1515	14	715	638
254.75	316	338	700	12148	1447	25	2282	619
255.25	389	389	421	12607	1550	51	942	456
255.75	251	404	823	13455	1502	8	3518	619
256.25	478	346	825	11577	1532	17	1370	152
256.75	528	404	612	10137	1509	8	2090	322
257.25	215	391	253	14164	1341	31	896	237
257.75	306	361	267	16549	1261	47	1135	189
258.25	16	250	431	8899	1189	36	1385	104
258.75	467	385	523	7592	1317	23	2486	82
259.25	485	241	788	4971	1212	55	1841	58
259.75	469	325	472	5199	1083	8	2385	510
260.25	550	279	640	5917	1301	0	1248	341
260.75	294	405	673	13517	1489	21	2146	299
261.25	143	368	501	17455	1423	0	1755	0
261.75	472	288	413	20000	1402	41	1376	418
262.25	571	337	695	15654	1437	49	2345	0
262.75	473	382	493	12506	1366	34	3025	0
263.25	166	369	305	7504	1472	64	3172	424
263.75	341	377	620	8284	1464	45	2246	0
264.25	670	339	392	9399	1513	54	1586	742
264.75	307	403	703	11073	1534	41	2844	444
265.25	527	408	695	8851	1545	46	1869	59
265.75	326	441	384	9207	1596	50	1967	0
266.25	628	402	572	8622	1459	44	2615	0
266.75	482	395	681	13589	1450	0	2212	0

Depth (cm)	Hg	I	Ir	K	La	Mg	Mn	Mo
267.25	450	441	605	13810	1524	8	1816	0
267.75	439	438	525	12617	1545	55	2006	148
268.25	488	384	683	19406	1589	0	2591	32
268.75	498	441	429	18742	1462	0	2974	197
269.25	496	355	893	14096	1471	27	2791	349
269.75	237	295	213	20407	1363	9	1665	149
270.25	0	171	557	28100	1186	0	3281	497
270.75	341	119	1084	21009	1048	19	2159	258
271.25	0	0	1247	6697	630	12	2440	137
271.75	0	0	1296	6363	574	0	2492	171
272.25	117	0	1414	4329	720	0	3719	109
272.75	0	0	1474	4833	579	28	3699	0
273.25	0	0	1192	4946	769	0	3481	0
273.75	201	87	1228	4458	937	0	2550	0
274.25	212	204	1088	5704	1283	0	3860	0
274.75	336	196	659	2871	886	0	3034	0
275.25	102	80	427	1158	453	17	3798	0
275.75	13	96	319	1498	417	0	1903	0
276.25	0	96	572	1340	524	10	1987	0
276.75	376	206	493	2349	760	28	2904	0
277.25	378	368	356	3093	1315	6	2367	152
277.75	160	399	366	3113	1316	0	3042	1069
278.25	427	359	359	2479	1352	0	2466	1051
278.75	379	358	565	2969	1436	34	2738	1073
279.25	291	396	466	2984	1366	0	3096	645
279.75	279	400	652	2602	1244	0	3543	0
280.25	438	347	573	2566	1387	13	3412	80
280.75	380	374	345	2676	1297	0	1647	272
281.25	354	351	628	2452	1426	50	3350	467
281.75	571	385	649	2172	1285	0	2332	180
282.25	236	332	374	1770	1405	40	1793	73
282.75	296	440	653	1786	1419	52	3121	0
283.25	344	428	449	2555	1342	0	3326	0
283.75	376	497	511	3176	1384	71	3493	0
284.25	221	595	540	3301	1386	0	1638	0
284.75	435	473	688	3993	1401	50	2505	0
285.25	290	371	695	2716	1407	53	2528	654
285.75	708	365	588	2525	1383	77	3754	181
286.25	344	368	403	2513	1285	50	4060	142

Depth (cm)	Hg	I	Ir	K	La	Mg	Mn	Mo
286.75	369	422	831	3189	1392	46	3495	99
287.25	86	109	964	5193	1226	0	4604	297
287.75	0	0	1487	6158	430	0	2940	160
288.25	109	0	1025	12450	632	29	3137	23
288.75	407	217	569	36208	1446	43	1974	356
289.25	324	429	381	42800	1681	38	2162	277
289.75	508	361	346	45618	1606	57	0	397
290.25	536	317	551	42389	1439	30	1817	271
290.75	301	405	513	32875	1240	0	2487	135
291.25	451	277	377	33659	1469	0	2461	0
291.75	442	300	402	32426	1418	46	2306	233
292.25	248	307	143	32154	1321	18	2800	210
292.75	349	241	297	49610	1256	21	3286	82
293.25	331	185	566	41639	1247	0	2528	0
293.75	312	238	298	36859	1146	0	967	0

Table A 4.4 Galang Co XRF Geochemistry Ni – Sc

Depth (cm)	Ni	P	Pr	Pt	Rb	S	Sb	Sc
14.25	570	5	398	315	712	537	163	232
14.75	405	0	378	385	662	649	236	200
15.25	693	0	1073	833	1253	1197	230	375
15.75	619	39	1230	967	1189	1272	298	439
16.25	585	0	1361	1015	999	1543	427	417
16.75	506	0	1011	938	1069	1394	288	445
17.25	603	0	959	778	814	1149	297	367
17.75	649	0	1066	951	825	1192	291	397
18.25	604	0	1049	865	970	1081	276	381
18.75	497	0	1081	922	1013	1256	234	492
19.25	486	0	1038	1036	1047	1160	274	383
19.75	456	0	1220	914	1225	1284	154	452
20.25	366	40	1090	912	623	1204	312	403
20.75	519	0	1030	847	1195	1295	295	468
21.25	556	23	1172	951	1061	1295	195	529
21.75	493	0	1010	1020	793	1206	278	481
22.25	439	0	1084	872	558	1202	323	392
22.75	570	0	1016	849	1337	1150	242	468
23.25	455	0	1030	768	1003	1231	244	537
23.75	328	0	1205	859	809	1336	392	381
24.25	468	15	941	696	839	1224	405	423
24.75	583	0	883	860	1376	1350	404	286
25.25	545	18	1093	1050	811	1523	425	358
25.75	457	0	1064	1109	957	1436	350	579
26.25	559	0	954	904	1123	1294	341	426
26.75	550	7	999	951	984	1410	341	460
27.25	497	27	1014	866	978	1350	359	398
27.75	430	0	932	982	836	1348	404	462
28.25	480	0	1057	741	683	1388	326	519
28.75	677	0	1160	764	975	1224	334	504
29.25	600	0	953	1005	1326	1110	338	459
29.75	603	0	989	999	1072	1227	208	539
30.25	754	0	1050	853	1092	1144	338	424
30.75	669	0	932	777	1298	1141	350	534
31.25	679	0	1154	657	1254	1175	321	548
31.75	770	0	935	833	1052	1110	377	530
32.25	591	14	971	748	1287	1314	464	522
32.75	669	0	1179	1023	1100	1157	364	557

Depth (cm)	Ni	P	Pr	Pt	Rb	S	Sb	Sc
33.25	505	0	1256	683	1215	1286	291	395
33.75	579	0	1079	935	956	1428	317	490
34.25	709	0	1030	1094	947	1122	264	447
34.75	682	0	1321	991	932	1321	236	391
35.25	494	0	1241	1088	652	1341	303	391
35.75	690	10	1158	1076	919	1338	250	382
36.25	654	0	1064	685	915	1364	323	346
36.75	660	0	1109	975	1117	1484	229	497
37.25	595	0	974	952	905	1453	219	418
37.75	425	0	1174	1001	740	1549	219	562
38.25	457	0	1341	910	1187	1792	411	320
38.75	383	0	1092	996	974	1880	333	438
39.25	513	0	886	1093	1018	1586	295	385
39.75	326	0	1072	696	1042	1663	319	450
40.25	386	0	1251	668	1110	1612	428	445
40.75	513	0	999	891	1019	1346	480	571
41.25	516	0	953	699	1067	1358	316	478
41.75	560	0	1001	833	1069	1394	425	571
42.25	709	0	1067	984	1329	1352	398	466
42.75	637	0	1059	748	1221	1484	487	446
43.25	759	0	998	1069	924	1665	458	578
43.75	802	0	1088	837	1139	1513	393	536
44.25	799	14	1195	947	1277	1711	355	309
44.75	759	0	1161	997	939	1798	452	606
45.25	639	0	1386	670	1235	2052	424	485
45.75	772	37	1210	724	1244	1937	468	521
46.25	601	43	959	583	1357	1787	462	440
46.75	754	0	1077	602	1128	1629	506	410
47.25	616	14	915	703	1236	1816	536	683
47.75	686	0	1023	1015	1327	1791	490	469
48.25	670	10	1015	727	1527	1730	327	632
48.75	743	0	1035	1012	1278	1772	439	473
49.25	686	5	1326	769	1111	1792	383	496
49.75	647	26	1113	967	1259	1685	499	542
50.25	497	0	1142	708	1529	1679	450	587
50.75	769	0	958	972	1328	1986	478	401
51.25	582	0	1151	538	1218	1995	471	455
51.75	478	0	1151	658	1160	2207	560	665
52.25	678	6	1001	679	1357	2152	500	550

Depth (cm)	Ni	P	Pr	Pt	Rb	S	Sb	Sc
52.75	612	0	1070	854	1731	2042	759	717
53.25	641	20	1178	468	2486	1542	875	751
53.75	705	0	1115	658	2429	1538	785	648
54.25	809	0	989	748	2235	1374	796	749
54.75	674	0	1234	696	2628	1589	602	726
55.25	718	0	1270	778	1994	1686	730	631
55.75	828	0	1191	535	1546	1579	622	604
56.25	932	0	1069	1172	1531	1526	586	455
56.75	730	0	1055	1170	1166	1681	496	540
57.25	802	0	1069	657	1585	1563	438	482
57.75	823	12	1146	986	1277	1560	402	633
58.25	946	0	1096	900	1495	1597	336	512
58.75	790	0	1196	686	1764	1619	438	564
59.25	813	12	1189	829	1413	1542	308	460
59.75	791	41	1172	976	1407	1544	376	417
60.25	690	0	1002	700	1178	2170	175	323
60.75	667	0	1134	647	1439	2350	454	407
61.25	707	14	1293	750	1095	2389	387	688
61.75	556	0	1010	719	987	2206	348	470
62.25	691	0	1034	873	1003	2301	227	521
62.75	693	0	1004	813	1111	2388	381	528
63.25	624	0	1214	929	889	2225	346	504
63.75	597	0	1209	777	1068	2233	388	491
64.25	445	0	1214	716	1089	2066	261	470
64.75	584	0	1183	864	1226	1795	212	465
65.25	791	0	1153	486	846	2172	360	588
65.75	731	0	975	722	893	2143	353	455
66.25	606	6	1195	585	835	2143	194	399
66.75	668	0	1161	1026	815	2233	263	421
67.25	661	0	1111	825	804	2243	212	538
67.75	817	0	1098	802	665	2933	363	421
68.25	682	0	913	641	710	2351	332	639
68.75	831	0	1105	746	617	1908	219	437
69.25	788	0	1018	735	558	1921	180	371
69.75	798	13	1003	885	593	1879	257	355
70.25	739	0	869	927	594	2015	249	471
70.75	617	0	1048	859	565	1943	268	398
71.25	802	0	1183	845	555	2430	246	449
71.75	811	0	1124	926	606	2011	271	347

Depth (cm)	Ni	P	Pr	Pt	Rb	S	Sb	Sc
72.25	798	0	1052	963	879	2233	312	524
72.75	802	0	916	822	670	2646	371	477
73.25	751	0	984	778	795	2742	430	599
73.75	630	0	1121	964	1077	1968	231	416
74.25	725	0	1139	665	688	1574	307	470
74.75	910	19	1154	965	1117	1603	360	428
75.25	821	38	1203	915	1259	1473	254	399
75.75	643	0	1113	437	1518	1344	389	436
76.25	682	0	1046	785	1558	1350	344	512
76.75	756	0	1007	907	1671	1303	415	485
77.25	865	0	1181	669	1715	1376	556	542
77.75	813	0	1102	570	1459	1408	586	566
78.25	697	0	943	834	1501	1456	512	653
78.75	659	0	1091	633	1894	1433	626	635
79.25	570	0	1107	530	1394	926	476	754
79.75	810	0	1132	854	1085	892	382	585
80.25	585	13	991	706	1232	796	490	651
80.75	624	0	1011	470	1280	722	330	712
81.25	655	0	805	735	1225	744	333	465
81.75	711	33	963	759	1029	922	364	434
82.25	672	0	819	984	875	1021	294	506
82.75	594	0	1301	556	1116	1372	483	803
83.25	716	0	1195	1102	752	1506	313	591
83.75	623	0	1239	693	1146	1492	426	618
84.25	766	0	1145	841	1157	1484	462	792
84.75	594	17	1089	742	1231	1406	377	784
85.25	685	0	1185	687	1069	1425	337	689
85.75	614	0	1370	663	1331	1414	494	642
86.25	833	0	1117	901	1256	1439	482	703
86.75	807	27	1240	675	1309	1479	492	638
87.25	829	0	1220	724	1222	1475	318	764
87.75	641	15	1306	571	1038	1447	564	697
88.25	792	0	1092	962	952	1566	395	672
88.75	929	0	1254	801	831	1473	190	665
89.25	855	14	1108	1002	769	1463	348	529
89.75	800	15	1420	1055	1010	1848	276	256
90.25	666	0	1143	955	873	2947	341	465
90.75	693	0	1019	698	902	5553	463	874
91.25	757	0	1093	361	511	18468	1440	2336

Depth (cm)	Ni	P	Pr	Pt	Rb	S	Sb	Sc
91.75	719	0	886	280	684	21825	1538	3279
92.25	567	0	979	295	698	14677	1273	2004
92.75	684	0	1072	774	528	14812	1002	1673
93.25	530	0	1150	685	712	6885	608	1130
93.75	508	0	1088	603	670	4800	339	627
94.25	590	4	1119	911	639	2741	311	501
94.75	504	45	1217	866	915	1592	199	412
95.25	746	37	1222	849	597	1486	240	444
95.75	445	57	1106	718	981	1440	265	511
96.25	580	16	1036	789	614	1428	252	515
96.75	687	63	1157	744	1093	1383	377	567
97.25	685	46	1339	622	1139	1412	393	545
97.75	659	110	1309	791	1501	1557	408	471
98.25	566	67	1136	831	1223	1620	336	685
98.75	535	124	1074	727	1337	1519	489	749
99.25	548	50	1260	791	1013	1268	289	704
99.75	638	104	1330	719	966	1335	556	672
100.25	614	27	1052	874	1541	1422	369	605
100.75	602	41	1279	510	1433	1271	418	642
101.25	555	0	1270	907	1210	1375	593	767
101.75	686	0	1207	764	1208	1449	471	679
102.25	571	11	965	620	1180	1307	446	631
102.75	558	0	1041	733	1054	1373	408	731
103.25	645	0	1031	737	1389	1387	383	721
103.75	650	0	992	864	1270	1316	398	742
104.25	721	0	1341	880	1455	1219	431	767
104.75	633	0	1282	793	1310	1035	423	559
105.25	652	0	1113	893	1283	1135	388	605
105.75	719	16	1195	616	1312	1207	442	753
106.25	557	0	1138	824	1323	1062	348	585
106.75	753	0	1216	765	1435	1223	403	663
107.25	548	51	913	789	1035	1163	467	665
107.75	657	0	1220	747	983	1373	331	694
108.25	780	0	1235	1021	862	1420	495	752
108.75	825	0	899	1076	783	1212	449	624
109.25	837	0	1392	955	678	1207	436	729
109.75	603	0	1273	757	1273	1224	465	612
110.25	715	0	1002	1040	1195	1192	348	702
110.75	729	0	1204	825	1049	1164	371	586

Depth (cm)	Ni	P	Pr	Pt	Rb	S	Sb	Sc
111.25	876	0	1061	877	754	1128	386	631
111.75	655	0	1209	823	1140	1154	491	714
112.25	766	0	1154	762	1227	1044	346	664
112.75	671	0	1072	804	1444	1227	447	546
113.25	818	0	1199	1011	1289	1399	427	711
113.75	654	0	1183	719	1253	1314	394	684
114.25	695	0	1331	783	1027	1355	450	730
114.75	758	0	1204	846	1007	1341	406	698
115.25	892	0	1232	658	998	1436	439	553
115.75	784	0	1155	942	1135	1332	443	649
116.25	686	0	1037	725	1069	1253	347	664
116.75	652	0	1281	693	1111	1385	344	644
117.25	868	20	1025	865	948	1265	320	641
117.75	910	0	1087	742	1183	1413	313	656
118.25	797	0	1182	817	871	1298	458	702
118.75	635	0	1178	950	895	1243	300	569
119.25	778	0	1242	990	1151	1569	378	620
119.75	953	0	1077	749	967	1626	266	873
120.25	830	0	843	799	810	1132	300	419
120.75	769	15	340	541	317	609	176	244
121.25	730	0	348	286	387	359	188	216
121.75	592	0	358	446	410	385	136	179
122.25	793	42	723	709	602	823	170	305
122.75	651	0	1197	584	778	1777	374	566
123.25	764	15	1251	903	1141	1416	442	672
123.75	669	0	1127	739	1064	1272	396	492
124.25	658	0	1338	974	1403	1471	633	801
124.75	463	0	1044	630	1597	1414	655	896
125.25	586	6	1179	665	1274	1394	654	943
125.75	665	0	1119	829	1607	1317	517	780
126.25	684	0	1365	573	1434	1249	668	958
126.75	594	0	1189	516	1510	1469	622	1065
127.25	496	0	1329	707	1508	1723	584	729
127.75	574	0	1324	786	1353	1261	593	890
128.25	446	0	1036	672	1678	1132	474	673
128.75	627	0	1205	882	2206	1312	776	917
129.25	824	0	1151	704	1638	1436	685	724
129.75	833	0	949	582	928	1689	578	852
130.25	727	0	963	747	1169	1840	515	658

Depth (cm)	Ni	P	Pr	Pt	Rb	S	Sb	Sc
130.75	737	0	1009	686	924	1727	357	641
131.25	800	0	965	532	1049	1679	313	661
131.75	793	0	1078	603	1314	1512	388	590
132.25	810	0	1183	825	1005	1660	585	734
132.75	743	0	1094	724	1204	1813	435	399
133.25	843	0	1074	973	1391	1779	563	923
133.75	809	0	1161	737	1141	1723	464	711
134.25	866	0	1240	965	990	1543	353	620
134.75	746	0	1173	692	971	1813	413	693
135.25	740	0	1020	751	706	1824	466	628
135.75	687	13	1049	802	1034	1683	336	670
136.25	778	0	1029	1080	865	1651	411	668
136.75	772	0	1063	712	776	1623	212	667
137.25	773	0	1057	827	515	1824	309	584
137.75	795	52	956	1245	875	2075	313	598
138.25	757	0	1161	831	757	1890	308	582
138.75	887	0	1017	975	576	1646	303	481
139.25	734	0	1040	757	592	1511	263	452
139.75	630	0	900	932	405	1484	290	586
140.25	630	0	940	909	366	1756	227	327
140.75	693	0	1185	1100	580	1849	260	415
141.25	745	0	1029	917	834	1935	299	450
141.75	679	0	998	692	606	1677	265	622
142.25	754	0	1148	1042	720	1912	148	564
142.75	617	0	1017	782	1092	1646	379	645
143.25	852	0	887	605	840	1643	296	605
143.75	592	0	941	874	585	1713	228	422
144.25	553	0	1062	621	794	1557	301	477
144.75	443	0	1248	920	1231	1548	289	546
145.25	348	5	1184	544	2349	1175	394	831
145.75	500	8	1312	604	3608	995	733	745
146.25	500	0	1336	519	4080	826	698	787
146.75	565	0	1476	465	4593	611	749	865
147.25	641	12	1443	415	4324	812	720	797
147.75	810	53	1518	719	2555	1024	629	720
148.25	791	0	1313	962	1428	1308	299	495
148.75	778	0	1110	1017	927	1453	271	472
149.25	660	0	1150	931	887	1456	293	472
149.75	830	0	1187	978	871	1255	343	483

Depth (cm)	Ni	P	Pr	Pt	Rb	S	Sb	Sc
150.25	820	0	1165	874	1078	1243	114	422
150.75	755	8	1164	983	1189	1290	294	453
151.25	777	0	1288	821	988	1157	178	458
151.75	684	0	1316	760	1380	1264	320	518
152.25	702	63	1409	732	1583	1653	338	611
152.75	799	0	1204	837	1611	2353	431	623
153.25	655	0	965	858	1736	2023	363	451
153.75	814	0	1310	979	1735	1788	338	592
154.25	1001	0	1229	730	877	1612	148	497
154.75	969	0	1198	730	1096	1697	351	412
155.25	944	23	339	744	815	842	198	115
155.75	809	16	309	635	883	557	176	86
156.25	874	38	106	328	599	242	149	80
156.75	649	35	248	435	667	322	145	89
157.25	808	0	766	781	614	984	137	343
157.75	606	0	971	1014	1150	1667	186	464
158.25	689	29	1067	807	1326	1517	269	543
158.75	790	0	967	1024	922	1713	306	490
159.25	854	0	1233	1000	835	1764	274	467
159.75	689	0	1079	978	1119	1907	236	491
160.25	801	0	1052	1064	1054	1909	288	475
160.75	744	0	1263	989	1197	1758	264	504
161.25	771	0	1101	1014	1131	1517	288	628
161.75	656	0	1071	1082	1395	1639	251	495
162.25	887	0	1042	862	823	1456	183	443
162.75	845	0	1156	973	70	1457	270	440
163.25	913	0	1095	922	179	1266	193	409
163.75	889	6	1030	1325	469	1418	145	347
164.25	833	15	1139	1010	382	1242	150	311
164.75	1208	0	1060	1364	0	1322	256	433
165.25	1034	0	1198	1308	373	1301	224	342
165.75	931	0	1068	830	0	1372	218	287
166.25	448	42	99	270	0	374	59	154
166.75	797	0	427	581	0	444	80	183
167.25	866	0	1184	924	355	1087	95	372
167.75	859	0	1191	1202	396	1251	96	296
168.25	811	0	1287	966	934	1381	353	406
168.75	826	27	1124	1190	1293	1336	381	655
169.25	992	0	948	919	1033	1559	311	575

Depth (cm)	Ni	P	Pr	Pt	Rb	S	Sb	Sc
169.75	714	0	1053	825	1487	1379	362	546
170.25	824	0	1124	916	1105	1388	330	595
170.75	874	0	1072	1248	1291	1396	357	601
171.25	868	0	1238	936	1435	1320	334	584
171.75	789	0	937	812	1510	1390	289	429
172.25	704	0	1120	921	1325	1413	285	457
172.75	837	0	1017	742	1091	1234	277	650
173.25	848	0	862	723	1124	973	160	446
173.75	786	0	594	510	769	651	220	329
174.25	723	0	722	812	1020	742	107	370
174.75	760	31	860	659	929	1001	329	460
175.25	755	0	1132	833	1322	1311	256	433
175.75	836	0	1094	1058	898	1219	280	478
176.25	817	0	1158	871	1230	1491	375	441
176.75	683	0	1214	1093	1095	1181	214	572
177.25	721	0	1398	1081	1214	1336	329	480
177.75	824	37	1118	881	1110	1350	265	291
178.25	863	0	982	899	1194	1260	312	401
178.75	799	38	470	691	915	564	124	301
179.25	829	42	530	579	1007	562	192	245
179.75	588	11	376	443	484	353	160	151
180.25	832	0	1006	927	884	899	291	412
180.75	735	21	1171	947	1229	1553	269	438
181.25	821	0	1247	946	997	1718	232	510
181.75	976	0	1361	1127	523	1662	199	538
182.25	1089	0	1067	1216	288	1727	135	486
182.75	974	20	1319	1176	402	2330	184	478
183.25	888	0	1067	1428	527	1639	244	326
183.75	854	21	1295	936	161	1826	199	346
184.25	932	0	1243	945	319	1801	151	271
184.75	945	0	1254	1193	249	1664	169	437
185.25	937	7	1240	1144	208	1663	215	315
185.75	961	9	1152	1254	489	1726	286	309
186.25	755	0	1220	1200	747	1741	309	391
186.75	930	0	1154	1328	751	1689	204	501
187.25	908	0	1061	886	1084	1659	327	523
187.75	935	0	1276	1114	1161	1635	321	757
188.25	892	0	1288	957	777	1693	418	426
188.75	836	0	1068	883	1034	1688	230	460

Depth (cm)	Ni	P	Pr	Pt	Rb	S	Sb	Sc
189.25	711	0	1208	878	980	1454	329	574
189.75	827	0	1258	877	670	1712	207	594
190.25	870	0	1017	768	995	1581	113	537
190.75	910	0	1195	1161	954	1449	203	447
191.25	914	0	1130	1181	1112	1533	336	546
191.75	812	0	1093	1146	982	1588	204	467
192.25	788	0	1174	1068	1369	1471	179	468
192.75	879	0	1277	975	731	1350	313	448
193.25	812	0	1218	919	1134	1391	348	405
193.75	960	0	1056	743	844	1591	464	524
194.25	885	6	1200	1121	926	1429	360	464
194.75	864	0	1096	1089	1439	1479	155	574
195.25	828	0	1006	840	1163	1529	265	642
195.75	757	0	1129	1124	967	1219	280	336
196.25	937	0	1053	909	408	1426	207	356
196.75	904	0	1289	1197	867	1268	331	508
197.25	955	0	1094	961	688	1323	245	644
197.75	692	0	1441	920	692	1231	386	473
198.25	930	0	1276	1035	882	1357	207	516
198.75	756	0	1011	1101	826	1246	233	383
199.25	727	0	994	928	760	1191	172	462
199.75	902	0	1055	745	1310	1211	215	509
200.25	721	13	1162	753	992	1252	374	525
200.75	739	0	1204	786	1274	1170	271	460
201.25	914	0	1034	949	1013	1212	334	640
201.75	963	31	849	739	829	890	173	316
202.25	735	27	322	361	832	316	225	167
202.75	810	19	206	477	736	207	190	130
203.25	690	39	324	631	415	294	157	203
203.75	814	0	874	946	835	842	219	406
204.25	833	0	1354	673	1203	1366	297	519
204.75	648	0	1177	796	1423	1357	347	598
205.25	722	0	1173	1135	1183	1407	330	484
205.75	912	0	1041	1001	1167	1399	199	719
206.25	754	0	1283	976	1394	1342	285	402
206.75	978	0	1137	967	1254	1144	337	716
207.25	890	0	1395	1003	1008	1168	343	609
207.75	737	0	1132	683	1103	1199	325	476
208.25	886	0	1058	699	1177	1024	237	437

Depth (cm)	Ni	P	Pr	Pt	Rb	S	Sb	Sc
208.75	858	0	976	1116	934	1201	266	512
209.25	905	0	1171	1249	1133	1313	218	582
209.75	809	0	1162	1061	989	1376	281	471
210.25	921	0	1060	1050	812	1366	314	325
210.75	873	0	1126	1198	923	1304	293	510
211.25	751	0	1082	1062	907	1206	253	569
211.75	813	0	991	658	679	1213	240	416
212.25	697	0	1107	785	1312	1269	409	633
212.75	873	0	1055	869	1328	1357	245	615
213.25	893	0	1335	1015	1240	1370	351	529
213.75	717	0	1128	746	323	1246	362	400
214.25	923	0	1273	863	687	1300	96	366
214.75	1017	0	993	1101	220	1414	126	215
215.25	1039	0	1001	1088	207	1440	150	317
215.75	1159	0	1125	1249	337	1425	161	452
216.25	1070	0	1225	1293	132	1465	157	367
216.75	996	0	1158	1214	655	1390	111	346
217.25	986	0	1354	1135	229	1377	288	391
217.75	908	0	1289	984	499	1516	254	587
218.25	874	0	1155	1058	1096	1481	235	314
218.75	708	0	1110	816	1384	1304	246	350
219.25	763	32	1343	1189	483	1281	132	369
219.75	782	0	886	1039	622	1432	260	381
220.25	817	5	1090	1023	660	1453	246	516
220.75	1017	0	1049	1192	377	1554	181	434
221.25	934	0	1177	775	496	1566	229	397
221.75	833	0	1140	870	844	1818	183	361
222.25	757	0	1095	760	1325	2470	315	530
222.75	795	0	1142	679	1446	1952	328	494
223.25	835	0	1057	749	727	2116	377	444
223.75	734	0	1056	835	260	2319	228	306
224.25	834	0	1017	1029	678	2119	244	407
224.75	665	0	1201	904	1175	1972	448	525
225.25	532	0	1300	989	1247	1633	215	422
225.75	857	5	1077	888	985	2527	386	424
226.25	850	0	1115	935	516	1964	243	356
226.75	944	0	1062	1369	316	1689	230	413
227.25	1088	0	1232	1037	418	1826	207	433
227.75	923	0	1359	1098	666	1901	330	491

Depth (cm)	Ni	P	Pr	Pt	Rb	S	Sb	Sc
228.25	1010	0	1203	1175	1017	1977	342	508
228.75	802	18	1134	941	1071	1604	315	565
229.25	812	0	1331	1173	1712	1733	522	695
229.75	730	0	1358	855	1607	2009	506	528
230.25	908	0	831	683	1238	1180	187	244
230.75	802	10	266	548	815	569	176	212
231.25	727	33	326	427	322	284	163	192
231.75	522	0	572	613	488	828	191	240
232.25	655	0	1340	835	995	1633	343	484
232.75	933	0	839	918	947	1266	348	470
233.25	744	0	1275	754	1415	1405	467	593
233.75	710	0	1090	672	1377	1479	283	605
234.25	859	0	1092	771	872	1995	227	505
234.75	787	0	1214	924	1194	2691	430	606
235.25	754	0	1269	774	1302	1745	437	645
235.75	726	0	1024	912	926	1578	496	530
236.25	725	0	1122	964	870	1398	381	553
236.75	690	0	1037	830	1224	1623	247	433
237.25	648	0	1022	811	1503	1458	264	759
237.75	617	0	1269	798	1436	1395	317	674
238.25	941	0	1096	1088	1057	1365	437	639
238.75	812	0	1099	1038	970	1488	249	545
239.25	648	0	1357	883	1199	1173	268	513
239.75	857	0	1074	1236	1615	1479	247	491
240.25	811	0	1280	867	1352	1446	344	454
240.75	726	0	1175	583	1247	1382	408	617
241.25	665	0	1096	891	945	1437	208	498
241.75	814	0	1115	1412	453	1832	279	536
242.25	930	0	1188	1353	324	1530	119	378
242.75	942	0	536	712	1453	1464	831	578
243.25	911	0	633	768	1159	1328	674	695
243.75	949	0	780	764	1466	1381	691	691
244.25	935	0	627	642	1228	1501	742	513
244.75	866	0	618	649	1314	1779	630	580
245.25	930	0	493	645	1557	1476	900	701
245.75	807	0	451	650	1919	1674	916	714
246.25	1067	0	328	783	1386	1437	655	605
246.75	1231	0	472	829	356	1599	531	498
247.25	1169	0	554	724	736	1557	407	520

Depth (cm)	Ni	P	Pr	Pt	Rb	S	Sb	Sc
247.75	991	0	276	1047	762	1207	608	426
248.25	1223	0	468	693	532	1307	459	462
248.75	986	0	622	607	1159	1582	508	441
249.25	860	0	419	819	1682	1826	648	546
249.75	951	0	587	760	1332	1746	630	604
250.25	856	0	699	706	1423	1673	651	641
250.75	984	0	596	855	1557	1754	743	587
251.25	1101	0	612	711	1312	1732	893	534
251.75	965	0	732	783	1348	1635	453	409
252.25	986	0	510	870	1096	1808	273	351
252.75	986	9	549	919	1267	1928	426	221
253.25	932	0	411	686	1087	1922	352	382
253.75	1059	0	612	641	1335	1921	334	332
254.25	1022	0	457	848	1153	1849	377	422
254.75	953	0	518	639	1168	1820	366	420
255.25	853	0	650	772	1422	1858	276	447
255.75	1145	0	725	893	1134	1913	325	336
256.25	976	0	549	868	1231	1876	315	448
256.75	1118	0	620	909	1345	1745	345	448
257.25	926	0	444	859	1348	1778	406	202
257.75	759	0	475	705	1347	1779	519	482
258.25	825	0	527	347	600	1841	667	557
258.75	1052	0	449	739	512	2500	917	652
259.25	946	0	273	1002	433	1701	570	366
259.75	906	0	276	746	324	1430	451	446
260.25	959	0	510	1002	880	1965	655	519
260.75	1080	0	422	484	728	1774	535	704
261.25	921	11	598	427	1424	1903	739	593
261.75	934	0	558	838	1373	1591	494	462
262.25	1125	0	455	864	1269	1790	673	399
262.75	1066	0	388	1008	804	1641	481	440
263.25	1172	0	488	949	244	1732	361	413
263.75	1096	0	650	770	1042	1695	330	409
264.25	1197	0	671	715	1070	1654	467	392
264.75	1201	0	599	920	1318	1691	409	459
265.25	1206	0	643	559	840	1678	461	373
265.75	1237	0	417	850	1079	1757	397	484
266.25	1049	0	484	921	922	1722	608	517
266.75	1152	0	555	865	1150	1717	482	531

Depth (cm)	Ni	P	Pr	Pt	Rb	S	Sb	Sc
267.25	1044	0	486	997	1574	1810	499	571
267.75	1017	0	511	943	974	2012	421	629
268.25	1034	0	474	609	1280	2695	689	416
268.75	905	0	722	602	1633	1803	766	683
269.25	945	0	367	796	1034	1752	1265	712
269.75	813	0	550	120	1340	1854	1402	887
270.25	801	0	722	186	1810	1849	2582	1305
270.75	1022	0	505	400	1005	1971	4874	2490
271.25	1937	0	607	266	147	1717	7783	4309
271.75	1851	0	542	440	0	1583	8610	4175
272.25	1878	0	406	233	0	1452	8168	4408
272.75	2292	0	500	475	0	1450	9271	5440
273.25	1664	0	471	448	281	1535	7539	3921
273.75	1090	0	663	960	532	1602	4345	1925
274.25	1069	0	498	964	520	2387	2040	942
274.75	853	0	132	878	0	1570	805	481
275.25	636	0	179	417	0	1086	499	314
275.75	774	0	219	465	217	853	401	254
276.25	787	0	173	655	336	898	317	223
276.75	855	0	298	610	424	1281	528	416
277.25	920	0	537	976	817	1805	543	486
277.75	1061	0	506	1070	992	1878	605	505
278.25	1083	0	539	735	835	1959	570	611
278.75	1231	0	473	788	544	1806	576	417
279.25	1179	0	777	903	451	1950	511	467
279.75	1199	0	648	905	253	1789	461	493
280.25	1209	0	513	1141	221	1942	506	346
280.75	918	0	712	826	341	1971	583	503
281.25	1386	0	468	912	613	1918	465	433
281.75	1150	0	575	1252	633	1750	423	380
282.25	1073	0	536	696	6	1640	440	399
282.75	1095	0	342	1014	485	1546	448	363
283.25	1091	0	620	1146	1068	1869	578	586
283.75	1162	16	487	650	1062	1810	638	500
284.25	1072	0	706	1090	1294	1736	471	463
284.75	1009	0	601	1140	1330	1845	647	673
285.25	1175	0	613	925	267	2196	644	449
285.75	1206	0	428	886	304	1848	649	471
286.25	1307	0	477	597	247	2046	871	669

Depth (cm)	Ni	P	Pr	Pt	Rb	S	Sb	Sc
286.75	1051	0	594	1076	379	1862	762	728
287.25	1213	0	513	633	478	1977	3591	1936
287.75	2102	0	641	246	406	1836	9535	5039
288.25	1624	0	526	140	1036	1550	6569	2603
288.75	649	0	710	419	2527	2574	1304	841
289.25	894	0	586	739	2639	3318	929	583
289.75	775	0	557	617	2710	3685	813	529
290.25	799	0	576	660	2212	3436	702	758
290.75	834	8	587	867	2462	2352	620	564
291.25	785	0	560	734	2203	2423	786	572
291.75	899	0	565	496	2099	2672	1148	796
292.25	828	0	592	358	2209	2133	974	833
292.75	714	0	731	560	2022	2681	943	649
293.25	659	0	530	444	2097	2267	1095	920
293.75	570	0	549	387	2035	2516	1200	888

Table A 4.5 Galang Co XRF Geochemistry Se – U

Depth (cm)	Se	Si	Sr	Ta	Tb	Te	Tm	U
14.25	0	260	1080	783	662	50	98	
14.75	176	254	1104	655	791	407	316	
15.25	318	647	1407	1479	1657	553	575	
15.75	143	738	1423	1680	2123	606	612	
16.25	180	743	1503	1612	2246	535	576	
16.75	101	606	828	1441	1869	622	752	
17.25	183	584	1303	1305	1654	632	684	
17.75	331	598	897	1325	1939	516	702	
18.25	217	660	782	1392	1676	426	528	
18.75	410	697	979	1401	1918	685	684	
19.25	226	655	1227	1436	1872	526	686	
19.75	242	655	1167	1439	2012	523	482	
20.25	10	633	965	1505	2004	576	628	
20.75	401	727	999	1444	2144	504	789	
21.25	287	671	1169	1497	2110	367	792	
21.75	25	676	942	1515	2130	475	650	
22.25	85	613	1055	1505	2300	434	598	
22.75	169	547	959	1376	1947	490	671	
23.25	203	623	1115	1462	1976	395	630	
23.75	61	578	764	1463	2445	604	803	
24.25	253	519	1158	1330	2374	522	827	
24.75	277	558	1157	1297	2230	752	841	
25.25	34	623	1236	1468	2252	733	739	
25.75	0	618	1328	1262	2101	343	635	
26.25	140	606	1239	1436	2359	517	658	
26.75	0	698	1519	1277	2304	555	803	
27.25	421	762	1092	1401	2012	396	562	
27.75	378	711	1258	1503	2419	589	666	
28.25	280	868	1043	1700	2299	491	465	
28.75	377	753	1146	1737	1573	521	500	
29.25	112	910	1501	1626	1498	527	532	
29.75	121	1030	1565	1607	1479	523	446	
30.25	430	880	1461	1483	1795	531	569	
30.75	472	913	1353	1557	1809	406	618	
31.25	363	954	1375	1554	1822	521	531	
31.75	296	772	1922	1463	1680	471	536	
32.25	198	864	1404	1485	1730	432	637	
32.75	34	988	1410	1610	1858	491	509	

Depth (cm)	Se	Si	Sr	Ta	Tb	Te	Tm	U
33.25	89	1150	1372	1735	1878	531	645	
33.75	78	1181	1043	1583	1801	651	570	
34.25	0	963	1054	1702	1573	449	523	
34.75	420	1182	1161	1489	1508	474	543	
35.25	301	1329	733	1866	1639	381	444	
35.75	152	1348	883	1689	1419	360	474	
36.25	13	1429	1109	1543	1595	398	556	
36.75	298	1326	1263	1921	1627	388	590	
37.25	84	1158	1144	1780	1902	534	586	
37.75	283	964	1149	1716	1990	331	783	
38.25	122	872	998	1712	2413	623	556	
38.75	257	873	1394	1388	2550	587	716	
39.25	229	693	1347	1251	1952	705	718	
39.75	0	775	1300	1666	2538	563	517	
40.25	0	785	1235	1449	2510	588	607	
40.75	0	763	1048	1297	2092	381	885	
41.25	319	741	1119	1379	1995	596	543	
41.75	207	795	1301	1658	2219	450	460	
42.25	213	737	992	1709	2036	674	560	
42.75	379	801	1556	1727	1854	592	666	
43.25	284	710	1362	1616	1846	312	392	
43.75	540	799	1562	1583	1680	486	585	
44.25	713	1041	1160	1791	1371	697	508	
44.75	400	949	1567	1752	1976	378	613	
45.25	0	983	1386	1660	1879	597	629	
45.75	381	1099	1497	1622	1789	653	684	
46.25	196	1018	1283	1902	2235	405	576	
46.75	413	979	1618	1753	1921	561	539	
47.25	261	859	1551	1587	2306	473	494	
47.75	0	803	1672	1510	2325	532	568	
48.25	172	787	1498	1386	2223	488	593	
48.75	72	809	1334	1393	2023	586	628	
49.25	291	735	1748	1662	2147	656	558	
49.75	330	731	1409	1453	1934	579	706	
50.25	523	731	1747	1707	2121	463	494	
50.75	271	744	1533	1653	2010	726	480	
51.25	118	938	1630	1474	2035	526	639	
51.75	100	991	1515	1508	2216	486	529	
52.25	82	1046	1883	1568	1892	500	691	

Depth (cm)	Se	Si	Sr	Ta	Tb	Te	Tm	U
52.75	163	1648	2472	1362	1859	399	572	
53.25	140	2521	3558	1264	1515	421	441	
53.75	273	2186	2874	1279	1569	447	422	
54.25	157	2192	3003	1284	1420	695	532	
54.75	0	1721	3031	1374	1618	716	519	
55.25	0	1510	2733	1435	1657	809	508	
55.75	328	1291	2399	1787	1345	534	368	
56.25	116	940	1771	1524	1532	624	542	
56.75	30	905	1909	1822	1420	437	481	
57.25	441	1244	2424	1663	1320	442	472	
57.75	61	958	1431	1763	1356	259	436	
58.25	305	947	1817	1745	1377	337	716	
58.75	35	983	1734	1993	1740	303	460	
59.25	340	1083	1554	1661	1559	288	639	
59.75	447	786	1669	1588	1367	140	520	
60.25	129	813	1303	1737	1592	616	737	
60.75	32	489	1228	1490	1956	603	646	
61.25	254	628	1253	1717	1873	458	575	
61.75	381	545	1410	1485	2381	472	679	
62.25	135	502	1105	1469	2217	580	841	
62.75	222	490	1183	1422	2228	400	704	
63.25	10	703	1585	1295	2115	512	749	
63.75	355	615	1271	1545	2028	528	589	
64.25	0	614	1423	1591	2160	270	821	
64.75	150	473	1157	1591	1948	390	662	
65.25	297	785	1232	1672	1656	316	644	
65.75	34	573	1305	1690	2007	367	804	
66.25	152	524	645	1726	2064	282	600	
66.75	15	499	967	1444	2232	605	713	
67.25	321	570	1073	1625	1972	521	729	
67.75	184	579	973	1682	1782	1008	681	
68.25	136	593	1040	1575	2044	540	736	
68.75	46	632	656	1626	1794	426	594	
69.25	224	639	362	1605	2243	354	762	
69.75	435	637	890	1546	1814	440	648	
70.25	455	679	799	1580	1645	185	633	
70.75	185	734	584	1689	2024	435	766	
71.25	187	740	906	1604	2012	536	802	
71.75	367	810	542	1467	1569	477	532	

Depth (cm)	Se	Si	Sr	Ta	Tb	Te	Tm	U
72.25	144	750	925	1596	1639	758	700	
72.75	350	663	905	1601	1526	1138	727	
73.25	130	747	970	1711	1274	696	523	
73.75	326	825	865	1549	1603	643	657	
74.25	120	741	1266	1671	1531	260	505	
74.75	348	792	1307	1738	1301	413	560	
75.25	405	886	979	1675	1296	398	452	
75.75	73	895	1842	1517	1656	441	428	
76.25	181	1025	1604	1371	1548	443	649	
76.75	154	919	2096	1369	1543	380	615	
77.25	122	1160	2092	1455	1653	658	566	
77.75	233	1230	2017	1630	1453	768	611	
78.25	181	1124	1996	1493	1512	781	580	
78.75	0	1224	2496	1486	1385	896	515	
79.25	317	561	1853	1320	1412	595	602	129
79.75	176	444	1554	1416	1390	658	604	9
80.25	260	186	1633	1373	1293	335	430	31
80.75	200	295	1704	1528	1349	343	540	62
81.25	164	290	1558	1146	1304	364	524	106
81.75	184	416	1245	1109	1323	374	476	47
82.25	0	506	1597	1106	1107	433	560	201
82.75	220	677	1521	1767	1681	345	543	0
83.25	0	562	1177	1643	1607	653	898	207
83.75	601	710	1688	1595	1910	491	616	64
84.25	354	937	1784	1650	1264	278	581	344
84.75	432	808	1655	1612	1265	367	627	17
85.25	264	763	1762	1639	1557	482	636	251
85.75	241	853	1780	1379	1202	620	583	200
86.25	223	746	1358	1467	1519	367	533	0
86.75	186	845	1530	1961	1212	426	469	133
87.25	448	868	1666	1944	938	445	437	145
87.75	358	775	1638	1752	1425	247	594	23
88.25	38	737	1429	1696	1440	459	401	184
88.75	362	741	1188	1797	1357	428	567	0
89.25	203	634	1379	2020	1629	228	442	31
89.75	427	568	995	1487	1584	308	715	0
90.25	159	584	635	1960	1460	450	528	182
90.75	481	375	560	1471	1383	1216	538	323
91.25	0	376	1176	1059	1115	3341	713	462

Depth (cm)	Se	Si	Sr	Ta	Tb	Te	Tm	U
91.75	0	343	944	759	1109	3113	602	239
92.25	137	438	666	880	1666	2395	631	208
92.75	0	555	842	1131	1912	2184	813	17
93.25	45	443	673	1301	2506	892	633	105
93.75	28	376	305	1471	2983	740	727	53
94.25	0	355	658	1228	3086	537	753	239
94.75	0	525	765	1283	2361	265	756	17
95.25	515	509	694	1456	2121	222	821	253
95.75	211	579	727	1291	2405	130	814	26
96.25	425	602	1005	1438	2271	376	719	0
96.75	330	787	1066	1334	2445	454	708	8
97.25	477	784	1136	1420	2210	393	446	189
97.75	321	857	1571	1605	1901	499	721	0
98.25	0	985	1325	1299	1983	371	766	132
98.75	159	854	1253	1286	1949	207	820	0
99.25	0	677	1217	1471	1989	367	648	76
99.75	412	800	1463	1389	2279	136	640	36
100.25	146	959	1596	1395	1895	347	609	57
100.75	165	846	1470	1325	1995	168	452	0
101.25	331	697	1252	1441	2261	116	795	0
101.75	326	741	1206	1532	1782	501	660	102
102.25	62	820	1107	1634	1895	377	492	0
102.75	319	868	1376	1515	1573	469	507	0
103.25	526	993	1507	1420	2067	667	754	170
103.75	21	954	1588	1316	1832	582	586	75
104.25	364	980	1310	1560	1697	461	462	0
104.75	129	1087	1610	1568	1501	556	575	0
105.25	18	1168	1312	1578	1692	402	500	79
105.75	135	940	1459	1409	1948	472	741	206
106.25	124	1079	1238	1315	1568	435	732	0
106.75	0	973	1454	1519	1750	423	699	67
107.25	215	759	1407	1546	1670	309	585	117
107.75	394	709	1472	1535	1560	518	651	0
108.25	132	747	1505	1592	1662	262	521	0
108.75	132	732	1194	1536	1459	179	604	0
109.25	0	738	1235	1747	1508	310	497	21
109.75	139	902	1344	1686	1351	317	606	0
110.25	9	1011	1446	1683	1090	402	610	0
110.75	257	901	1286	1978	1379	395	372	0

Depth (cm)	Se	Si	Sr	Ta	Tb	Te	Tm	U
111.25	219	859	1358	1782	1572	185	594	147
111.75	0	829	1541	1763	1653	312	456	173
112.25	248	891	1661	1569	1654	387	642	164
112.75	208	1204	1555	1505	1451	305	629	0
113.25	122	1056	1221	1471	1649	343	698	96
113.75	179	838	1462	1384	1442	581	498	126
114.25	335	833	1814	1778	1324	468	570	70
114.75	318	740	1667	1692	1525	449	591	77
115.25	176	556	1350	1722	1481	498	600	0
115.75	0	516	1200	1879	1554	279	549	103
116.25	305	543	1406	1667	1531	347	594	87
116.75	205	631	1239	1359	1592	396	485	297
117.25	441	511	1474	1682	1637	324	687	208
117.75	231	500	1557	1637	1574	330	519	322
118.25	169	595	1119	1937	1583	207	415	143
118.75	122	606	1316	1562	1421	543	669	110
119.25	58	498	1243	1679	1818	545	508	245
119.75	203	488	1149	1988	1481	229	598	247
120.25	299	384	1208	1498	1372	149	367	0
120.75	0	230	773	799	689	63	173	147
121.25	53	87	1038	716	467	35	109	196
121.75	41	152	563	620	493	73	93	66
122.25	154	339	561	1372	720	158	348	157
122.75	300	777	1296	1782	1664	635	465	0
123.25	171	938	1051	1399	1736	403	501	0
123.75	82	1356	1772	1361	1600	289	501	14
124.25	209	1175	2088	1281	1626	436	806	119
124.75	181	1258	2317	1465	1421	404	576	176
125.25	407	1342	2146	1545	1416	453	461	163
125.75	156	1203	2252	1583	1386	559	433	8
126.25	339	1369	2040	1673	1522	195	442	80
126.75	154	1276	2286	1352	1565	337	526	116
127.25	172	1144	1854	1371	1837	460	403	0
127.75	229	1392	1866	1063	1776	0	545	0
128.25	69	1566	1554	1080	2345	362	720	0
128.75	0	1669	2064	1036	1115	0	474	0
129.25	285	990	2131	1215	1763	409	585	9
129.75	255	933	1803	1622	1577	436	542	46
130.25	161	833	1776	1648	1328	386	555	224

Depth (cm)	Se	Si	Sr	Ta	Tb	Te	Tm	U
130.75	128	921	1571	1734	1353	287	485	0
131.25	258	841	1543	1590	1570	562	474	235
131.75	302	949	1608	1883	1513	528	606	92
132.25	134	1258	1369	1599	1575	58	503	298
132.75	179	1260	1529	1669	1463	480	272	50
133.25	103	1025	1589	1538	1498	243	586	215
133.75	475	760	1320	1610	1404	396	536	0
134.25	0	599	1205	1789	1119	646	583	0
134.75	412	433	1116	1699	1152	320	608	22
135.25	483	482	1024	1727	1469	218	563	87
135.75	83	519	1114	1675	1390	423	529	638
136.25	197	541	1285	1636	1641	492	661	148
136.75	228	365	1120	1827	1588	414	513	291
137.25	239	455	1271	1691	1442	166	606	346
137.75	135	419	799	1314	1607	428	755	270
138.25	170	328	586	1833	1900	516	398	255
138.75	91	351	842	1732	1961	304	695	291
139.25	110	413	723	1569	1782	444	642	162
139.75	37	361	699	1785	1326	389	572	387
140.25	229	361	855	1511	1774	578	495	278
140.75	114	419	908	1431	1788	329	671	125
141.25	140	430	814	1522	1913	324	611	125
141.75	246	530	1325	1557	1723	373	583	362
142.25	206	587	1116	1418	1994	408	649	0
142.75	0	685	1374	1427	1913	232	553	192
143.25	246	638	1275	1546	1910	205	636	249
143.75	0	484	683	1308	1861	129	614	306
144.25	4	710	556	1159	2426	96	793	0
144.75	45	967	577	1063	2558	125	593	96
145.25	23	1913	970	982	2069	0	736	105
145.75	15	4100	1507	594	1596	0	547	0
146.25	150	4760	2053	679	1348	0	307	0
146.75	208	5479	1944	955	1309	0	416	92
147.25	180	4143	1895	851	1660	0	626	102
147.75	329	1985	1524	1065	1697	0	655	69
148.25	0	747	864	1729	1575	303	577	25
148.75	274	506	1141	1745	1246	323	612	92
149.25	169	497	722	1763	1766	301	473	31
149.75	175	510	969	1585	1851	0	779	41

Depth (cm)	Se	Si	Sr	Ta	Tb	Te	Tm	U
150.25	257	507	1162	1647	1822	463	666	197
150.75	86	596	1238	1516	1983	276	725	178
151.25	347	590	919	1743	1879	283	750	84
151.75	254	767	942	1547	1819	235	526	123
152.25	409	997	966	1666	1720	411	635	328
152.75	131	991	1021	1522	1893	370	554	318
153.25	83	825	1193	1376	1675	382	679	166
153.75	283	815	919	1731	1632	205	626	182
154.25	284	587	710	2102	1496	351	374	614
154.75	0	643	917	1905	1343	84	416	762
155.25	118	291	1024	928	710	72	75	701
155.75	58	105	790	719	332	0	89	614
156.25	203	110	866	590	329	0	0	620
156.75	175	122	448	586	369	18	92	457
157.25	35	375	663	1672	944	184	215	850
157.75	140	527	890	1757	1330	290	510	599
158.25	622	431	818	1866	1181	225	448	689
158.75	352	731	563	1734	1596	256	489	499
159.25	374	560	577	2133	1437	391	441	802
159.75	246	673	791	1934	1384	294	548	721
160.25	500	642	836	1678	1340	383	543	700
160.75	532	586	715	1848	1366	336	530	927
161.25	106	582	1187	1869	1237	336	524	878
161.75	179	744	1093	1955	1471	628	484	784
162.25	457	492	1112	2098	1397	574	379	834
162.75	635	241	35	2293	1148	224	505	1009
163.25	709	157	400	2516	1133	213	399	892
163.75	549	383	636	2067	1357	389	422	947
164.25	372	184	681	2031	1179	196	437	746
164.75	67	146	146	2234	891	253	560	697
165.25	455	121	356	2139	910	170	393	550
165.75	615	101	158	2458	844	257	316	722
166.25	95	50	210	554	207	0	101	182
166.75	138	5	242	967	463	219	131	413
167.25	716	158	398	2120	1070	398	344	703
167.75	323	283	553	2221	1288	476	472	770
168.25	288	728	542	1939	1395	213	481	612
168.75	176	694	898	1818	1180	141	531	959
169.25	443	718	888	1947	1142	214	370	865

Depth (cm)	Se	Si	Sr	Ta	Tb	Te	Tm	U
169.75	339	780	1117	1721	1518	229	658	834
170.25	351	674	1074	1642	1341	58	635	897
170.75	278	586	853	1666	1385	292	543	875
171.25	96	614	1140	1826	1313	165	386	818
171.75	266	710	920	1891	1371	384	364	888
172.25	457	583	905	1637	1385	220	320	737
172.75	182	536	1122	1749	1356	239	510	510
173.25	385	405	1035	1507	1019	297	390	554
173.75	171	292	695	1140	859	16	323	458
174.25	0	299	1062	1162	908	171	344	516
174.75	259	534	923	1630	878	172	382	610
175.25	291	734	1021	1921	1411	460	393	
175.75	161	653	1045	1726	1190	394	554	
176.25	445	577	853	2043	1291	468	482	
176.75	412	453	756	2085	1421	376	555	
177.25	36	467	900	1978	1409	372	530	
177.75	400	459	576	2013	1310	733	545	
178.25	299	547	801	1829	1152	498	485	
178.75	87	244	972	1019	202	250	146	
179.25	203	237	882	1127	159	169	227	
179.75	213	223	630	653	169	135	106	
180.25	452	275	736	1467	922	374	555	
180.75	557	454	1133	1878	1289	621	509	
181.25	194	448	995	2010	1366	469	465	
181.75	269	254	486	2331	1223	440	629	
182.25	403	225	747	2204	1143	505	496	
182.75	572	185	533	2401	1116	602	560	
183.25	399	117	45	2167	1138	628	452	
183.75	552	169	772	2336	1197	681	474	
184.25	251	146	158	2415	1171	800	430	
184.75	630	101	637	2344	1099	605	356	
185.25	671	218	617	1976	1192	497	393	
185.75	654	185	431	2209	1014	795	423	
186.25	389	336	954	1874	1291	815	605	
186.75	365	476	981	1921	1106	757	574	
187.25	239	524	1103	1876	1248	548	507	
187.75	633	380	733	1997	1317	516	512	
188.25	31	515	654	2146	1338	674	564	
188.75	526	561	1210	2173	1213	618	490	

Depth (cm)	Se	Si	Sr	Ta	Tb	Te	Tm	U
189.25	549	582	865	2050	1194	338	416	
189.75	428	335	1344	2024	1268	459	437	
190.25	279	431	1140	1925	1449	661	627	
190.75	315	436	808	1739	1268	638	594	
191.25	276	514	1302	1844	1408	615	709	
191.75	261	447	1200	1837	1386	711	435	
192.25	0	474	1249	1878	1292	631	580	
192.75	511	458	1127	1916	1388	670	517	
193.25	374	537	1076	1943	1236	722	543	
193.75	516	689	781	2193	1574	509	422	
194.25	306	625	906	2048	1248	531	566	
194.75	380	601	1002	1910	1332	683	393	
195.25	148	490	866	1917	1505	612	666	
195.75	440	296	872	2119	1152	564	443	
196.25	814	254	309	2421	1262	658	465	
196.75	451	363	764	2153	1072	646	461	
197.25	500	508	736	2151	1218	695	526	
197.75	725	439	786	2209	1239	585	359	
198.25	716	401	1122	2107	1283	652	641	
198.75	268	492	1084	1746	1152	742	631	
199.25	431	353	1045	1877	1279	600	496	
199.75	355	474	1148	1885	1152	573	511	
200.25	766	613	1040	1924	1250	579	386	
200.75	420	403	1385	2016	1395	692	518	
201.25	71	555	1498	1667	1305	594	586	
201.75	259	458	1418	1535	570	443	276	
202.25	64	221	1223	715	0	95	37	
202.75	0	64	1243	613	0	119	0	
203.25	408	88	447	875	74	126	68	
203.75	458	322	960	1661	767	507	262	
204.25	681	604	1000	2050	1307	514	261	
204.75	591	583	1277	2053	1349	644	530	
205.25	0	589	1361	2014	1396	648	330	
205.75	671	567	1060	1781	1488	521	621	
206.25	490	660	1201	1729	1337	658	469	
206.75	298	462	1279	1997	1232	470	465	
207.25	461	404	928	2248	1176	632	423	
207.75	224	580	1046	2124	1129	527	495	
208.25	330	453	1233	1787	1290	585	550	

Depth (cm)	Se	Si	Sr	Ta	Tb	Te	Tm	U
208.75	382	497	756	1594	1067	582	641	
209.25	613	487	1014	2083	1247	587	426	
209.75	324	538	957	1889	1458	750	634	
210.25	401	632	971	2114	1367	635	505	
210.75	476	669	986	1985	1236	717	532	
211.25	393	645	647	1800	1207	562	542	
211.75	204	686	956	1917	1189	484	363	
212.25	356	556	1427	1819	1317	552	613	
212.75	461	626	973	1864	1349	738	654	
213.25	409	479	1279	1818	1077	707	313	
213.75	366	612	772	2210	1099	630	356	
214.25	781	392	1079	1979	928	896	485	
214.75	644	283	630	2420	868	818	303	
215.25	422	365	95	2250	964	770	425	
215.75	377	186	642	2348	860	643	280	
216.25	405	181	683	2164	972	724	428	
216.75	776	164	1012	2080	947	859	518	
217.25	427	198	630	2236	971	760	435	
217.75	369	265	857	2138	1092	524	503	
218.25	379	348	1038	2138	1208	768	516	
218.75	333	823	1658	1773	1200	617	479	
219.25	483	326	777	2095	1275	602	427	
219.75	448	468	580	2016	1229	484	431	
220.25	868	338	430	2022	1161	410	485	
220.75	243	238	145	2133	1264	482	568	
221.25	832	289	481	1900	1147	310	574	
221.75	432	325	704	2076	1387	424	572	
222.25	459	736	1036	1797	1026	792	417	
222.75	507	928	1925	1845	1345	493	578	
223.25	538	517	1004	2030	1292	539	505	
223.75	584	302	230	2337	1281	842	401	
224.25	391	192	574	1944	1218	537	428	
224.75	454	636	785	1685	1176	595	413	
225.25	230	540	1121	1558	1103	643	379	
225.75	532	295	680	1810	1101	911	586	
226.25	532	201	618	2152	997	732	397	
226.75	378	260	391	2002	1050	354	374	
227.25	719	246	283	2184	1089	705	383	
227.75	683	301	402	2163	1262	368	561	

Depth (cm)	Se	Si	Sr	Ta	Tb	Te	Tm	U
228.25	248	356	618	2064	1201	595	451	
228.75	680	513	765	2041	1518	378	533	
229.25	100	746	922	1631	1249	191	602	
229.75	235	573	1089	1891	1357	281	669	
230.25	74	478	872	1327	505	454	386	
230.75	0	378	908	785	72	209	43	
231.25	0	251	863	519	15	49	46	
231.75	311	310	840	1291	499	362	54	
232.25	293	674	936	1751	1167	713	430	
232.75	252	567	1109	1826	1103	586	454	
233.25	488	600	1373	2019	1337	676	466	
233.75	553	534	1498	1801	1363	683	679	
234.25	344	480	1324	2016	1527	860	533	
234.75	665	669	1360	1676	1420	841	714	
235.25	364	1129	1456	1891	1192	894	510	
235.75	352	769	931	1900	1111	781	449	
236.25	451	749	1007	2012	1339	592	465	
236.75	424	658	1081	1796	1215	1050	502	
237.25	125	936	1569	1475	1469	681	601	
237.75	299	652	1580	1896	1409	517	550	
238.25	653	594	1122	1988	1068	661	343	
238.75	416	669	1263	1987	1076	846	494	
239.25	765	463	1010	2033	1099	647	419	
239.75	880	435	897	1884	1236	538	605	
240.25	383	731	1312	1724	1165	823	397	
240.75	567	1099	1678	1699	1199	576	477	
241.25	412	366	1028	1964	1216	650	577	
241.75	322	191	775	2178	1072	593	435	
242.25	661	183	834	2054	1143	512	415	
242.75	557	1002	1434	1619	1705	450	756	233
243.25	0	762	1777	1383	1603	543	886	162
243.75	206	688	1322	1497	1434	804	659	335
244.25	655	825	1458	1834	1702	687	672	529
244.75	285	1001	1551	1837	1676	990	816	257
245.25	0	1075	1605	1487	1444	574	764	779
245.75	0	1391	2455	1387	1582	651	812	81
246.25	0	802	1790	1995	1500	618	642	650
246.75	326	392	394	2282	1230	491	684	520
247.25	365	473	1610	2060	1467	709	806	257

Depth (cm)	Se	Si	Sr	Ta	Tb	Te	Tm	U
247.75	303	1032	1440	1671	1418	560	771	95
248.25	123	234	867	2087	1203	545	833	0
248.75	496	419	1000	1902	1606	581	846	10
249.25	0	691	1542	1757	1916	389	882	352
249.75	305	734	1473	1767	1774	527	720	677
250.25	218	990	1509	1661	1847	393	727	151
250.75	0	968	1785	1810	1822	494	814	807
251.25	0	1163	1588	1849	1860	577	911	776
251.75	150	727	1239	1833	1784	562	812	1531
252.25	467	590	901	2163	1795	514	669	2571
252.75	387	602	855	1883	2055	504	977	2248
253.25	271	500	781	2076	1781	493	642	2811
253.75	393	486	913	2205	1615	400	875	2520
254.25	17	486	726	1694	1844	402	801	2223
254.75	280	357	645	2087	1908	353	1026	2888
255.25	284	366	687	1952	1798	200	882	2474
255.75	179	416	499	1884	1712	478	692	2646
256.25	520	417	843	1948	1762	436	838	2280
256.75	181	342	995	1888	1578	467	864	2741
257.25	65	818	1377	1337	1525	464	901	1037
257.75	201	945	1312	1241	1391	332	651	430
258.25	158	570	1076	1743	1362	279	486	226
258.75	403	398	743	2092	1400	414	615	70
259.25	262	360	923	1605	915	387	647	8
259.75	246	247	410	1914	1039	621	548	0
260.25	193	317	891	1945	1219	633	793	715
260.75	327	572	923	1865	1592	350	942	657
261.25	165	828	1394	1812	2012	262	894	944
261.75	0	968	1137	1624	1820	709	752	1153
262.25	285	717	787	2062	1871	413	665	1633
262.75	456	581	622	2014	1306	108	675	1849
263.25	385	259	704	2193	1323	408	741	1856
263.75	510	249	658	2114	1449	621	768	1989
264.25	35	290	671	2273	1774	465	767	2479
264.75	552	362	1244	2166	1757	508	812	1797
265.25	236	296	904	2460	1479	440	704	1754
265.75	402	285	460	2097	1531	374	915	1793
266.25	356	252	598	2357	1524	356	798	2212
266.75	41	411	733	2179	1840	436	764	2574

Depth (cm)	Se	Si	Sr	Ta	Tb	Te	Tm	U
267.25	180	409	1034	2010	1879	365	852	1480
267.75	542	436	592	1860	1746	255	951	1588
268.25	547	842	941	1807	1940	659	802	1377
268.75	0	825	1563	1727	1944	412	715	719
269.25	346	636	1251	1812	1478	791	763	443
269.75	207	1318	1958	1446	1718	641	798	92
270.25	0	2022	2429	1378	1587	735	761	0
270.75	106	988	2478	1017	1177	1289	722	305
271.25	0	375	2010	752	546	1629	818	173
271.75	0	346	1664	856	506	1164	887	144
272.25	6	185	1737	1028	575	1774	747	0
272.75	0	202	2052	828	319	1432	912	324
273.25	0	173	1804	919	713	1006	753	346
273.75	63	168	1355	1773	943	1051	682	980
274.25	553	272	1060	2130	1119	923	670	2069
274.75	131	122	882	1440	557	154	254	1531
275.25	0	50	625	1131	102	120	42	1860
275.75	0	46	307	937	184	190	55	2893
276.25	77	71	530	1119	288	167	187	3007
276.75	366	91	76	1403	510	215	370	2442
277.25	0	70	874	1860	1213	500	723	3742
277.75	56	89	152	2106	1110	549	606	5491
278.25	465	136	595	2268	1340	266	679	4190
278.75	711	18	565	2269	1429	574	935	2120
279.25	403	61	353	2238	1374	682	842	879
279.75	479	63	524	2076	1518	385	820	1006
280.25	175	63	704	2310	1207	407	658	1230
280.75	362	77	101	2272	1421	309	694	1363
281.25	318	70	158	2370	1092	392	807	1713
281.75	67	24	407	2085	1274	375	799	1407
282.25	583	33	230	2233	1419	398	760	2155
282.75	158	92	524	2283	1409	479	775	3363
283.25	186	76	556	2284	1368	397	769	5789
283.75	400	107	502	2298	1413	380	739	6239
284.25	173	116	401	2100	1359	494	920	8290
284.75	250	143	395	2286	1247	438	781	7267
285.25	286	104	452	2221	1477	609	827	3265
285.75	374	80	369	2305	1055	713	743	2155
286.25	384	49	398	2308	1057	743	655	1315

Depth (cm)	Se	Si	Sr	Ta	Tb	Te	Tm	U
286.75	182	127	474	2156	1212	663	793	1112
287.25	91	148	1547	1599	1213	1952	705	905
287.75	0	317	1994	552	515	1326	1017	218
288.25	81	572	1731	1071	612	757	559	143
288.75	266	1299	1852	1423	2022	677	872	455
289.25	221	1610	1737	1359	2446	65	941	477
289.75	0	1750	1859	1346	2522	427	719	716
290.25	108	1877	1776	1451	2035	0	626	500
290.75	171	1331	1797	1239	1905	198	733	136
291.25	304	1302	1538	1512	1874	526	753	148
291.75	0	1678	1837	1386	1886	616	834	206
292.25	0	1371	2154	1379	1803	501	768	326
292.75	24	2550	2265	1310	1822	466	487	251
293.25	223	2225	2204	1259	1678	320	498	495
293.75	169	2100	2042	1121	1631	259	380	473

Table A 4.6 Galang Co XRF Geochemistry V – Zn

Depth (cm)	V	W	Y	Zn
14.25	787	1157	541	314
14.75	1022	1402	638	243
15.25	1809	2542	608	395
15.75	1950	2672	484	304
16.25	1910	2728	169	257
16.75	1946	2352	341	141
17.25	1742	2391	307	433
17.75	1818	2385	44	283
18.25	1671	2494	139	382
18.75	1889	2747	81	495
19.25	1767	2419	256	462
19.75	1547	2678	208	292
20.25	1818	2443	0	398
20.75	2186	2611	194	409
21.25	1775	2679	0	403
21.75	2021	2657	262	396
22.25	1861	2477	249	451
22.75	1998	2589	90	510
23.25	1924	2553	206	315
23.75	1838	2569	0	333
24.25	2033	2599	406	402
24.75	2096	2633	397	399
25.25	1985	2400	0	405
25.75	1886	2358	208	171
26.25	2129	2605	324	435
26.75	2087	2694	128	308
27.25	1947	2500	0	450
27.75	2159	2551	240	394
28.25	2189	2449	39	315
28.75	1837	2617	299	293
29.25	1967	2838	387	307
29.75	1950	2753	492	215
30.25	2101	2780	419	490
30.75	2008	2758	238	533
31.25	1915	2795	283	318
31.75	2182	2657	452	402
32.25	1911	2720	140	337
32.75	1979	2869	310	349

Depth (cm)	V	W	Y	Zn
33.25	1772	2848	200	340
33.75	2131	2900	220	268
34.25	1891	2987	87	490
34.75	1667	2850	238	360
35.25	1791	2918	0	85
35.75	1841	3099	179	481
36.25	1888	2885	327	341
36.75	2150	2927	0	377
37.25	2246	2723	91	452
37.75	2010	2682	425	321
38.25	2040	2763	37	288
38.75	2233	2619	542	211
39.25	2121	2565	206	283
39.75	2223	2596	177	464
40.25	2015	2531	200	338
40.75	2164	2423	16	380
41.25	2444	2698	72	468
41.75	2199	2688	0	346
42.25	2186	2747	0	387
42.75	2160	2662	36	437
43.25	2161	2979	219	722
43.75	2002	2771	130	497
44.25	1991	2864	0	413
44.75	2207	2773	88	456
45.25	1756	2852	258	289
45.75	2104	2836	0	530
46.25	2346	2853	280	503
46.75	2192	2615	456	444
47.25	2534	2845	276	458
47.75	2631	2923	0	525
48.25	2246	2697	219	480
48.75	2240	2705	0	507
49.25	2005	2616	0	336
49.75	2234	2867	113	383
50.25	2154	2799	219	375
50.75	2361	2847	348	358
51.25	2009	2613	0	461
51.75	2203	2778	197	365
52.25	2322	2789	329	644

Depth (cm)	V	W	Y	Zn
52.75	2056	3042	151	527
53.25	1958	2979	189	692
53.75	1978	2695	51	729
54.25	2195	3126	447	640
54.75	1902	2905	85	602
55.25	1875	2954	291	741
55.75	1721	2944	473	1139
56.25	1959	3207	384	1107
56.75	1986	3011	188	526
57.25	2102	2910	86	392
57.75	2044	3048	526	308
58.25	2165	2880	573	449
58.75	2223	3079	153	200
59.25	1907	2894	297	371
59.75	1863	2910	401	345
60.25	2268	2984	331	328
60.75	2024	2648	266	0
61.25	1785	2732	276	146
61.75	2181	2533	396	418
62.25	2276	2662	172	331
62.75	2341	2672	17	285
63.25	2080	2596	178	204
63.75	2166	2606	290	59
64.25	2520	2427	265	146
64.75	2213	2491	257	250
65.25	2240	2787	334	174
65.75	2605	2755	116	333
66.25	2427	2648	300	64
66.75	2948	2537	208	88
67.25	2611	2777	118	247
67.75	2647	2786	396	251
68.25	2444	2616	688	0
68.75	2350	2601	423	242
69.25	2387	2728	335	248
69.75	2782	2618	136	99
70.25	2431	2633	424	0
70.75	2392	2542	310	91
71.25	2351	2642	99	273
71.75	2040	2770	481	64

Depth (cm)	V	W	Y	Zn
72.25	2247	2709	28	4
72.75	2609	2770	950	126
73.25	2178	2806	263	70
73.75	2124	2696	166	139
74.25	2146	2525	434	94
74.75	1978	2969	428	228
75.25	1691	2584	214	425
75.75	2080	2731	241	202
76.25	2170	2644	551	466
76.75	2430	2722	351	736
77.25	1781	2606	438	948
77.75	1768	2702	358	1349
78.25	2398	2740	241	1105
78.75	2063	2742	293	891
79.25	2233	2477		365
79.75	1998	2670		258
80.25	1967	2199		410
80.75	1870	2446		412
81.25	1768	2140		342
81.75	1743	2365		303
82.25	1999	2210		360
82.75	2443	2861		436
83.25	2435	2754		375
83.75	2625	2616		138
84.25	2571	2760		394
84.75	2593	2758		172
85.25	2635	2698		546
85.75	2409	3014		501
86.25	2163	2945		368
86.75	2343	2938		274
87.25	2173	2880		496
87.75	2406	2740		500
88.25	2388	2692		555
88.75	2208	2790		551
89.25	2441	2879		352
89.75	2524	2602		225
90.25	2900	2810		86
90.75	2494	2433		0
91.25	1833	2030		0

Depth (cm)	V	W	Y	Zn
91.75	1667	1828		0
92.25	2118	1923		0
92.75	2359	2024		0
93.25	2739	2252		0
93.75	3134	2359		0
94.25	3030	2401		276
94.75	2873	2376		379
95.25	2488	2622		262
95.75	2780	2370		465
96.25	2890	2431		440
96.75	2508	2526		459
97.25	2530	2511		590
97.75	2305	2526		554
98.25	2312	2367		599
98.75	2247	2318		345
99.25	2187	2477		568
99.75	1924	2471		522
100.25	2486	2643		709
100.75	1989	2399		472
101.25	2092	2462		537
101.75	2085	2368		508
102.25	2241	2487		220
102.75	2388	2573		509
103.25	2562	2809		358
103.75	2188	2689		509
104.25	2306	2603		547
104.75	2224	2679		427
105.25	2240	2854		648
105.75	2247	2669		346
106.25	2533	2707		443
106.75	2267	2878		387
107.25	2438	2520		593
107.75	2084	2644		457
108.25	2213	2726		609
108.75	2319	2652		291
109.25	2219	2822		460
109.75	2163	2747		305
110.25	2306	2861		344
110.75	2025	2926		249

Depth (cm)	V	W	Y	Zn
111.25	2248	2719		490
111.75	2368	2869		286
112.25	2225	2661		526
112.75	2265	2735		521
113.25	2253	2810		549
113.75	2176	2735		433
114.25	2200	2859		317
114.75	2049	2733		557
115.25	2430	2698		490
115.75	2060	2800		272
116.25	2245	2715		474
116.75	2339	2487		249
117.25	2437	2871		444
117.75	2295	2664		195
118.25	2215	2822		317
118.75	2261	2610		472
119.25	2252	2663		463
119.75	2468	2812		328
120.25	1577	2147		428
120.75	897	1200		281
121.25	630	1198		329
121.75	644	962		233
122.25	1287	2295		486
122.75	2149	2598		337
123.25	2215	2459		406
123.75	2209	2639		567
124.25	2366	2817		761
124.75	2486	2581		505
125.25	2553	2616		594
125.75	2538	2780		493
126.25	2118	2694		450
126.75	2149	2797		501
127.25	2213	2598		522
127.75	2034	2510		534
128.25	2412	2419		468
128.75	2388	2436		802
129.25	2290	2578		645
129.75	2456	2842		531
130.25	2671	2819		478

Depth (cm)	V	W	Y	Zn
130.75	2379	2769		453
131.25	2730	2754		375
131.75	2485	2768		428
132.25	2313	2756		470
132.75	2388	2648		417
133.25	2195	2956		534
133.75	2262	2742		577
134.25	2342	2757		612
134.75	2377	2506		355
135.25	2429	2521		456
135.75	2565	2622		384
136.25	2587	2487		462
136.75	2419	2614		369
137.25	2408	2608		435
137.75	2676	2561		319
138.25	2708	2566		395
138.75	2495	2594		395
139.25	2307	2483		167
139.75	2504	2675		226
140.25	2532	2435		326
140.75	2485	2325		277
141.25	2536	2406		504
141.75	2436	2354		226
142.25	2155	2421		640
142.75	2365	2418		414
143.25	2434	2458		433
143.75	2817	2177		268
144.25	2653	2102		300
144.75	2325	2253		576
145.25	2603	1846		796
145.75	2702	2030		1234
146.25	2466	2079		1658
146.75	2750	2499		1699
147.25	2396	2182		1678
147.75	1746	2434		988
148.25	2029	2704		379
148.75	2141	2802		351
149.25	2492	2563		318
149.75	2357	2816		481

Depth (cm)	V	W	Y	Zn
150.25	2124	2353		403
150.75	2312	2660		356
151.25	2430	2518		336
151.75	2230	2675		546
152.25	2065	2576		792
152.75	2049	2381		662
153.25	2534	2394		446
153.75	2121	2720		426
154.25	2206	2597		272
154.75	1861	2590		242
155.25	968	1529		475
155.75	567	1222		285
156.25	446	922		275
156.75	473	868		228
157.25	1318	2243		76
157.75	2595	2783		234
158.25	2021	2764		299
158.75	2223	2760		85
159.25	2426	2812		286
159.75	2214	2708		257
160.25	2115	2842		220
160.75	1954	2973		317
161.25	2204	2824		193
161.75	2284	2984		342
162.25	2156	3039		247
162.75	2178	3162		0
163.25	2193	3423		0
163.75	2422	3205		66
164.25	2206	3132		0
164.75	2102	3307		0
165.25	1924	3244		0
165.75	2018	3486		111
166.25	663	799		9
166.75	894	1395		54
167.25	1903	2792		18
167.75	1854	2985		0
168.25	1949	2900		439
168.75	2004	2856		337
169.25	2513	2807		371

Depth (cm)	V	W	Y	Zn
169.75	2486	2712		323
170.25	2315	2753		345
170.75	2355	2978		438
171.25	1841	2597		320
171.75	2261	2793		325
172.25	1937	2559		257
172.75	1888	2665		256
173.25	1785	2317		247
173.75	1353	1694		140
174.25	1561	2006		521
174.75	1719	2368		164
175.25	2291	2970	176	195
175.75	2218	2764	0	295
176.25	2241	2907	199	340
176.75	2128	2916	228	350
177.25	1990	2870	254	480
177.75	2397	2966	66	97
178.25	2050	2905	472	86
178.75	1003	1587	727	144
179.25	924	1733	431	235
179.75	500	998	525	162
180.25	1288	2417	13	324
180.75	2332	2771	168	143
181.25	2510	3023	61	40
181.75	1809	2914	351	0
182.25	2014	2913	281	12
182.75	1824	3032	166	145
183.25	2006	3044	0	0
183.75	2058	2858	259	0
184.25	1721	2952	139	28
184.75	1903	3003	177	51
185.25	1832	3009	256	0
185.75	2086	3073	0	40
186.25	2137	2683	61	0
186.75	1954	3065	245	135
187.25	2542	2916	169	353
187.75	2200	3162	444	75
188.25	2198	2877	293	79
188.75	2262	2795	155	26

Depth (cm)	V	W	Y	Zn
189.25	2044	2937	228	105
189.75	1932	2827	332	232
190.25	2257	2918	141	181
190.75	2224	2993	293	198
191.25	2100	2985	362	169
191.75	2315	2975	0	327
192.25	2245	2886	417	206
192.75	2115	2832	411	61
193.25	2136	3008	302	333
193.75	2407	2990	128	94
194.25	2080	2811	0	341
194.75	2169	2808	0	212
195.25	2287	2955	375	325
195.75	2071	2960	0	137
196.25	2295	3089	0	36
196.75	2183	3026	0	99
197.25	2206	2891	0	153
197.75	2079	3081	49	86
198.25	2089	3163	287	5
198.75	2033	2938	0	0
199.25	2229	2814	95	9
199.75	2205	2827	477	247
200.25	2070	2818	361	100
200.75	2249	2934	251	433
201.25	2310	2694	228	133
201.75	1674	2299	584	333
202.25	408	1025	1114	134
202.75	366	976	808	166
203.25	679	1180	416	156
203.75	1479	2472	180	0
204.25	1980	2929	298	175
204.75	2286	2929	0	317
205.25	2147	2778	155	52
205.75	2369	3006	0	144
206.25	1963	2818	0	246
206.75	1995	2763	0	281
207.25	1970	3034	63	93
207.75	2148	2822	250	149
208.25	2143	2814	414	181

Depth (cm)	V	W	Y	Zn
208.75	2205	2740	88	98
209.25	1907	2972	0	286
209.75	2244	2818	22	223
210.25	2089	3110	93	66
210.75	2372	2770	141	298
211.25	2035	2915	168	69
211.75	1949	2502	234	164
212.25	2053	2546	333	118
212.75	2126	2899	95	74
213.25	1850	2744	233	112
213.75	2155	2755	419	103
214.25	1932	2765	493	18
214.75	1800	3082	439	35
215.25	1765	3117	431	76
215.75	1773	2970	161	73
216.25	1673	2931	140	0
216.75	1819	3220	390	8
217.25	1791	3119	0	104
217.75	2126	2945	60	44
218.25	2080	3011	0	0
218.75	2288	2930	126	147
219.25	1794	2980	404	32
219.75	2058	2979	0	0
220.25	1779	2714	0	42
220.75	1995	2897	219	165
221.25	1981	2851	301	55
221.75	1769	2896	0	0
222.25	2037	2524	520	219
222.75	2258	2810	425	311
223.25	2062	2962	357	14
223.75	1730	2852	0	0
224.25	1756	2930	162	0
224.75	1967	2663	150	50
225.25	2033	2770	168	244
225.75	1783	2817	139	142
226.25	1928	2836	69	0
226.75	2043	2973	22	0
227.25	2139	3029	0	170
227.75	1853	2909	0	157

Depth (cm)	V	W	Y	Zn
228.25	2248	2936	238	187
228.75	2655	2845	222	298
229.25	2261	2738	598	603
229.75	2293	2611	177	341
230.25	1369	1968	476	269
230.75	737	1176	704	218
231.25	538	940	674	187
231.75	1109	1872	348	0
232.25	1879	2560	50	96
232.75	2311	2821	48	200
233.25	2126	2755	583	0
233.75	2143	2697	316	53
234.25	2375	3083	528	162
234.75	2073	2666	0	232
235.25	1976	2920	0	196
235.75	1998	3065	175	140
236.25	2190	3143	34	74
236.75	2249	2640	0	0
237.25	2218	2740	164	66
237.75	2378	2787	137	0
238.25	2171	2923	178	302
238.75	2049	2675	0	263
239.25	1755	2978	69	159
239.75	1988	2886	0	174
240.25	1814	2800	183	286
240.75	1782	2682	0	68
241.25	2171	2792	306	200
241.75	1860	2869	0	0
242.25	1757	2942	114	34
242.75	3055	2888		408
243.25	3117	2773		731
243.75	2931	2996		522
244.25	2610	3107		580
244.75	3043	2856		344
245.25	3001	3108		446
245.75	2720	2790		379
246.25	2760	3053		282
246.75	2561	3307		198
247.25	2790	3215		351

Depth (cm)	V	W	Y	Zn
247.75	2248	2991		300
248.25	2395	3508		216
248.75	2654	3061		321
249.25	3147	3267		424
249.75	2846	3203		393
250.25	2859	2764		366
250.75	3046	3155		592
251.25	3007	3132		564
251.75	2918	2996		313
252.25	2921	3011		405
252.75	2575	3118		281
253.25	2729	3086		198
253.75	2727	3223		373
254.25	2833	2811		79
254.75	2620	2994		160
255.25	2605	2951		266
255.75	2563	2861		257
256.25	2860	3010		495
256.75	2707	2927		252
257.25	2662	2859		98
257.75	2445	2455		303
258.25	2077	2435		120
258.75	2382	2846		143
259.25	2178	2590		290
259.75	2325	2530		194
260.25	2655	2870		434
260.75	2913	2995		408
261.25	2943	3145		546
261.75	2804	2818		446
262.25	3181	3163		647
262.75	2799	2847		382
263.25	2402	3010		119
263.75	2383	3212		198
264.25	2727	2898		292
264.75	3032	3236		562
265.25	2506	3175		332
265.75	2788	3172		396
266.25	2540	3347		267
266.75	2767	2924		498

Depth (cm)	V	W	Y	Zn
267.25	2684	3035		503
267.75	2882	3045		494
268.25	3032	2852		551
268.75	2846	2915		433
269.25	2841	2801		242
269.75	2915	2691		201
270.25	2418	2722		142
270.75	2493	2185		0
271.25	1907	2004		0
271.75	2005	2111		0
272.25	2163	2082		0
272.75	1989	1847		0
273.25	2221	2188		0
273.75	2568	2579		0
274.25	3433	3152		182
274.75	2139	2109		12
275.25	1291	1403		0
275.75	1126	1358		0
276.25	1274	1552		182
276.75	1685	2302		43
277.25	2646	3373		0
277.75	2772	3300		49
278.25	2883	3323		0
278.75	2907	3192		71
279.25	2640	3138		24
279.75	2596	3093		7
280.25	2648	3196		0
280.75	2742	3236		0
281.25	3050	3406		29
281.75	2886	3186		29
282.25	3215	3261		0
282.75	3531	3016		149
283.25	4243	3258		0
283.75	4597	3245		59
284.25	4876	3276		0
284.75	5532	3181		86
285.25	4911	3166		155
285.75	4226	3320		82
286.25	3734	3105		298

Depth (cm)	V	W	Y	Zn
286.75	3265	2882		372
287.25	3317	2611		0
287.75	2032	1696		0
288.25	1838	1840		0
288.75	3301	2819		865
289.25	3122	2957		1155
289.75	3195	2782		962
290.25	2860	2879		1201
290.75	2683	2667		1139
291.25	2811	2776		1215
291.75	2486	2560		898
292.25	2658	2739		554
292.75	2419	2540		759
293.25	2265	2263		576
293.75	1904	2257		533

CURRICULUM VITAE

Melanie Marie Perello

Education

December 2020 Doctor of Philosophy in **Applied Earth Sciences**
Indiana University degree, earned at Indiana University-Purdue University Indianapolis (IUPUI), Indianapolis, IN
Dissertation: Reconstructing Holocene Indian Summer Monsoon Variability using High Resolution Sediments from the Southeastern Tibet
Ph.D. Minor: Geographic Information Science
Advisor: Dr. Broxton Bird

June 2016 Master of Science in **Environmental Science and Policy**
Center for the Environment, Plymouth State University (PSU), NH
Master's Thesis: Linking the Effects of Land Use vs Climate Change on Water Quality in Northern New England lakes (Defended May 2015)
Advisor: Dr. Lisa Doner

May 2013 Bachelor of Science in **Biology** with All-College Honors
Westminster College, New Wilmington, PA
Thesis: The Behavior of Silver Nanoparticles in a Freshwater Tritrophic System
Advisor: Dr. Ann Throckmorton

Publications

Perello MM, Kane DD, Golnick P, Hughes MC, Thomas MA, Conroy JD. 2017. Effects of local weather variation on water-column stratification and hypoxia in the western, Sandusky and central basins of Lake Erie. Water 9(4): 279.

Bird B, Lei Y, **Perello M**, Polissar PJ, Yao T, Finney B, Bain D, Pompeani D, Thompson LG. 2017. Late Holocene Indian summer monsoon variability revealed from a

3,300-year-long lake sediment record from Nir'pa Co, southeastern Tibet. The Holocene 27(4): 541-552.

Perello M, Simon TP, Thompson H, Kane D. 2014. Feeding ecology the invasive round goby, *Appolonia melanostomus* (Pallas 1811), in the Western basin of Lake Erie. Journal of Aquatic Invasions 10(4): 463-474.

Middleton S, **Perello M**, Simon TP 2013. Length-weight relationships of the Mimic Shiner *Notropis volucellus* (Cope 1865) in the Western Basin of Lake Erie. The Ohio Journal of Science, 112 (2): 44-50.

Perello M, Throckmorton A. 2013. Effects of direct and dietary exposure to silver nanoparticles on a tritrophic system. Proceedings of the National Conference for Undergraduate Research 2013: 117-124.

Relevant Research & Work Experience

2019 – pres.	**NOAA Coastal Management Fellow**, Minnesota's Lake Superior Coastal Program, Minnesota Department of Natural Resources
2015 – 2019	**Graduate Research Assistant**, Department of Earth Sciences, IUPUI
2014- 2015	**Student Lab Supervisor,** Watershed Sensing Lab, PSU
2014 - 2015	**Graduate Assistant,** Pathways Project, PSU
2013 - 2015	**Graduate Research Assistant**, Center for the Environment, PSU
2013	**Field Technician**, Westminster College Field Station
2011 - 2013	**All-College Honors Program Honors Program**, Westminster College
2012	**Undergraduate Researcher**, F.T. Stone Laboratory, The Ohio State University

Teaching Experience

2018-2019	**Lab Instructor, Environmental Geology**, Department of Earth Sciences, IUPUI
2018	**Teacher's Assistant, Earth Materials**, Department of Earth Sciences, IUPUI

2015	**Graduate Co-Instructor, Environmental Science & Policy Capstone**, Environmental Science & Policy Department, PSU
2013	**Teacher's Assistant, Molecular Genetics & Heredity Lab**, Biology Department, Westminster College
2012	**Teacher's Assistant, Recombinant DNA & Biotechnology Lab**, Biology Department, Westminster College

Community Involvement & Outreach Experience

2019	**Mentor**, Center for Earth and Environmental Science, IUPUI
2018	**Mentor**, Multidisciplinary Undergraduate Research Institute, IUPUI
2018 - 2019	**Earth Sciences Representative**, School of Science Multidisciplinary Committee, IUPUI
2017 - 2020	**Graduate Student Representative**, Global Environmental Change Section, American Geophysical Union
2015	**Student Researcher**, U.S. State Department Diplomacy Lab, Department of Earth Sciences, IUPUI
2015	**Mentor**, K-12 Science Education Outreach, Environmental Science & Policy Department, PSU
2015	**Workshop Assistant**, K-12 Science Education, Outreach, Center for the Environment, PSU
2014	**Researcher**, Environmental Economics, Environmental Science & Policy Department, PSU & The Nature Conservancy
2014	**Researcher**, Community Reports on Water Resources, Environmental Science & Policy Department, PSU
2014	**Web Designer**, Community Outreach, Environmental Science & Policy Department, PSU
2014	**Facilitator**, Community Forum, Plymouth NH
2011-2012	**Youth Mentor**, Transformers Robotics Program, Westminster College
2011-2013	**Scholar-in-Service to Pennsylvania**, AmeriCorps

Presentations

Perello, M, Bird, B, Lei, Y, Pollisar P, Thompson, L, Yao, T. 2018. Holocene Indian Summer Monsoon Across a Transect of Lakes in Southeastern Tibet. American Geophysical Union Fall Meeting, Washington DC.

Perello, M, Bird, B, Lei, Y, Pollisar P, Thompson, L, Yao, T. 2018. Holocene Monsoon Rainfall and Lake Levels in Galang Co, Southeastern Tibet. Geological Society of America Annual Meeting, Indianapolis IN.

Perello, M, Bird, B, Lei, Y, Pollisar P, Thompson, L, Yao, T. 2018. Inferred Holocene Monsoon Rainfall and Lake Levels in Eastern Tibet. Geological Society of America North-Central Section Meeting, Ames IA.

Perello, M, Bird, B, Lei, Y, Pollisar P, Thompson, L, Yao, T. 2017. Measuring Holocene Indian Summer Monsoon Precipitation through Lake Sedimentary Proxies, Eastern Tibet. American Geophysical Union Fall Meeting, New Orleans LA.

Perello, M, Smythe, R, Borre, L, Baumert, K, Weirich, C, Bartlett, S, Klug, J, Johnson, D, Kimirei, I, and Perillo, G. 2017. Differences and similarities in perceived threats to North American lakes by scientists, managers, and stakeholders. GLEON 19, Lake Mohonk NY.

Perello, M, Bird, B, Lei, Y, Pollisar P, Thompson, L, Yao, T. 2017. Changing Indian Summer Monsoon Intensity throughout the Holocene at Galang Co, Southeastern Tibet. GLEON 19, Lake Mohonk NY.

Perello, M, Bird, B, Lei Y, Pollisar, P, Thompson, L, Yao, T. 2017. Tracking Changes in Indian Summer Monsoon Intensity using Precipitation and Lake Level Proxies from Eastern Tibet. GSA North-East and North-Central Joint Meeting, Pittsburgh PA.

Perello, M, Bird, B, Lei Y, Yao T, Thompson, L. 2015. Monitoring the Indian Summer Monsoon using lake sediments in the Eastern Tibetan Plateau. GLEON 17, Chuncheon South Korea.

Professional Societies

2019-20 American Meteorological Society

2017-18 North American Lake Management Society

2016-20	American Geophysical Union
2016-20	International Paleolimnological Association
2014-20	Global Lakes Ecological Observation Network
2014-20	Geological Society of America
2014-15	International Phycological Society
2014-17	Phycological Society of America
2013-14	Ohio Academy of Science
2012-14	Association for the Sciences of Limnology and Oceanography

Academic Societies

2018-19	**Earth Sciences Representative,** School of Science Multidisciplinary Committee, IUPUI
2017-19	Preparing Future Faculty and Professionals (PFFP), IUPUI
2017-19	**Earth Sciences Representative,** Graduate Student Council, School of Science
2016-17	**Representative,** Graduate and Professional Student Government, IUPUI
2014-15	Graduate Research Society, PSU
2012-13	Member, Pi Sigma Pi, Westminster College
2010-13	**President**, Beta Beta Beta, Westminster College
2010-11	Member, Lambda Sigma, Westminster College
2009-13	**Vice-President**, **Secretary**, Omicron Kappa Sigma, Westminster College

Honors & Awards

2016	GSA NC Section Graduate Student Poster (Honorable Mention)
2013, 2014	Pamela Marrapese Keep NH Lakes Clear Scholarship, PSU
2012	Thomas V. and Margaret Mansell Scholarship, Westminster College
2012	Allen P. Splete Leadership and Service Award, Westminster College
2011, 2012	Nathan & E. Lucille Beerbower Frey Scholarship Biology Department Award, Westminster College
2010-2013	Dean's List, seven semesters, Westminster College
2009	Vance Honors Scholarship, Westminster College

Research Grants

2015	Sigma XI Grants in Aid of Research Grant
2015	GSA Graduate Student Research Grant
2015	Paul C. Silva Student Grant, International Phycological Society
2014	Student Research Advisory Council (SRAC) Student Research Grant, PSU
2012	Undergraduate Research Grant - Drinko Center for Experiential Learning, Westminster College